The Pennsylvania State University

The Graduate School

Department of Veterinary and Biomedical Sciences

MACROPHAGE POLARIZATION: A DUAL ROLE BETWEEN INTERLEUKIN-4 SIGNALING AND SELENOPROTEIN BIOSYNTHESIS

A Dissertation in

Molecular Medicine

by

Ashley Elizabeth Shay

Submitted in Partial Fulfillment
of the Requirements
for the Degree of

Doctor of Philosophy

December 2017

The dissertation of Ashley Elizabeth Shay was reviewed and approved* by the following:

K. Sandeep Prabhu
Professor of Immunology and Molecular Toxicology
Advisor of Dissertation
Chair of Dissertation Committee

Margherita T. Cantorna
Distinguished Professor of Molecular Immunology

Connie J. Rogers
Associate Professor of Nutrition

Girish S. Kirimanjeswara
Assistant Professor of Veterinary and Biomedical Sciences

Pamela A. Hankey Giblin
Professor of Immunology

Adam B. Glick
Professor of Veterinary and Biomedical Sciences
Chair of Molecular Medicine Graduate Program

*Signatures are on file in the Graduate School

ABSTRACT

Selenium (Se) is an essential micronutrient that utilizes a unique mechanism to be chemically converted and charged to the 21st amino acid, selenocysteine (Sec), which is incorporated into proteins at a UGA codon. Sequence analysis has revealed 25 known selenoproteins in humans and 24 in mice based on a specific 3' untranslated region element termed the Sec insertion sequence present in mRNA that forms a distinct stem-loop structure necessary for the recruitment of Sec to the actively translating ribosome. Studies have shown that either dietary Se deficiency or genetic mutations in individual selenoproteins or proteins involved in selenoprotein biosynthesis cause detrimental effects on human health. Selenoproteins have been shown to have a variety of functions, including redox homeostasis, thyroid metabolism, and protein folding. Many selenoproteins remain uncharacterized with new functions being unraveled. The goal of these studies is to identify new, uncharacterized selenoprotein functions involved in IL-4-dependent M2 macrophage polarization.

An *in vivo* model of parasitic infection was used to induce a T-helper type-2 (Th2) response characterized by an IL-4 release in order to mimic IL-4 stimulation in *in vitro* studies. Mice were kept on three custom Se diets and infected with the murine helminth *Nippostrongylus brasiliensis*. Wild-type mice kept on Se deficient diet (Se-Def; sodium selenite $\leq$ 0.01 ppm) had a significantly higher parasite burden compared to mice fed Se adequate (Se-Ade; sodium selenite = 0.08 ppm) or Se supplemented (Se-Supp; sodium selenite = 0.4ppm) diets. Additionally, jejunal macrophages from wild-type mice fed Se-Def diet had higher M1 macrophage gene expression and lower M2 macrophage gene

expression compared to mice fed Se-Ade or Se-Supp diets. Macrophage-specific Sec tRNA deficient mice had similar results to wild-type mice fed Se-Def diet despite being fed Se-Supp diet. These Se dependent effects appear to be mediated through arachidonic acid metabolism and peroxisome proliferator-activated receptor gamma signaling since inhibition of either pathway led to increased parasite burden, increased M1 macrophage gene expression, and decreased M2 macrophage gene expression despite being fed Se-Ade or Se-Supp diet and was rescued by exogenous administration of 15-deoxy-$\Delta^{12,14}$-prostaglandin J_2 (15d-PGJ_2).

In order to examine the mechanism by which IL-4 stimulation increases the production of 15d-PGJ_2 to drive M2 macrophage polarization, the two isoforms important for the production of 15d-PGJ_2, cyclooxygenase (*Ptgs*; Cox)-1 and Cox-2, were examined. Interestingly, *Ptgs-2*, which is a highly inducible gene regulated by diverse stimuli via mechanisms involving transcriptional and translational control of expression, was significantly downregulated by IL-4 in bone marrow-derived macrophages (BMDMs), highlighting the importance of Cox-1 in a Th2 environment. This phenomenon not only challenges the dogma that Cox-1 is only developmentally regulated, but also demonstrates a novel mechanism in which IL-4–dependent regulation of Cox-1 involves the activation of the feline sarcoma oncogene kinase-Akt-mechanistic target of rapamycin complex (mTORC) axis. The presence of terminal oligopyrimidine sequences in the vicinity of the transcription start site in the 5’ untranslated region of both murine and human *PTGS-1* mRNA further supported the involvement of mTORC. Since Cox-1 does not behave as a *bona fide* terminal oligopyrimidine sequence with regard to polysome-dependent control, it is likely that mTORC2 may affect Cox-1 protein

expression. Downstream targets of mTORC2 are unknown and further work is needed to delineate the functional differences between mTORC1 and mTORC2 in regulating Cox-1 protein expression. That being said mTORC signaling appears to play a role in the accumulation of Cox-1 protein over the course of IL-4 stimulation potentially through either increased abundance of or increased interaction with heat shock protein chaperones. Activation of AMP-activated protein kinase (Ampk) by metformin, inhibition of mTORC by torin 1, or CRISPR/Cas9-mediated genetic knockout of tuberous sclerosis complex-2 blocked the IL-4-dependent expression of Cox-1 and the ability of macrophages to polarize to M2. However, use of 15d-PGJ_2 partially rescued the effects of Ampk activation *in-vivo*, suggesting the importance of Cox-1 in macrophage polarization as well as *N.brasiliensis* clearance. In summary, these findings suggest a new paradigm where IL-4–dependent upregulation of Cox-1 expression may play a key role in tissue homeostasis and wound healing during Th2-mediated immune responses, as seen during helminth infections.

To examine the Se-dependent requirement for prostaglandin J_2 production and M2 macrophage polarization during IL-4 stimulation, macrophage specific Cre-Lox mouse models were utilized to knockout various components of the selenoprotein biosynthesis machinery. While loss of Sec-$tRNA^{[Ser]Sec}$ (*Trsp*) in macrophages significantly reduced the expression of the entire selenoproteome, loss of Sec insertion sequence binding protein-2 (*Sbp2*) led to only a partial loss of the selenoproteome, reminiscent of a hierarchical control of selenoprotein expression. Complete selenoproteome loss in the *TrspLysM*^{Cre} model lead to decrease in the production of Δ^{12}-PGJ_2, M2 macrophage polarization, and the ability to efficiently clear *N.brasiliensis* despite Se-supplementation.

Sbp2LysM^{Cre} BMDMs, with a select few selenoproteins upregulated by IL-4 stimulation (*Seleno-I, Seleno-K, Txnrd-1,* and *Gpx-2*), were able to produce Δ^{12}-PGJ_2 at levels similar to those in *Sbp2LysM*^{WT} BMDMs. Normal production of Δ^{12}-PGJ_2 led to unaltered M2 macrophage polarization and efficient *N.brasiliensis* clearance in the *Sbp2LysM*^{Cre}model. These results suggest that these select few selenoproteins may regulate eicosanoid class switching upon IL-4 stimulation to increase M2 macrophages and effectively clear *N.brasiliensis* infection. Further work needs to be performed to narrow in on which selenoprotein(s) is playing a role in polarization and determining its exact function.

This dissertation demonstrates for the first time how IL-4 and Se function in an additive manner to upregulate Cox-1 expression as well as a specific set of selenoproteins, respectively, to enhance eicosanoid class switching to produce the peroxisome proliferator-activated receptor gamma ligands Δ^{12}-PGJ_2 and 15d-PGJ_2. Enhanced peroxisome proliferator-activated receptor gamma signaling increases the expression of M2 macrophages, which are required to efficiently clear helminth *N.brasiliensis*.

TABLE OF CONTENTS

LIST OF FIGURES

LIST OF TABLES

LIST OF ABBREVIATIONS

15d-PGJ_2: 15-deoxy-$\Delta^{12,14}$-prostaglandin J_2
AA: Arachidonic Acid
BMDM: Bone marrow-derived macrophages
Cox: Cyclooxygenase
CyPG: Cyclopentenone prostaglandins
Dio: Deiodinase
ER: Endoplasmic reticulum
Fes: Feline sarcoma oncogene kinase
Gpx: Glutathione peroxidase
Hpgds: Hematopoietic type prostaglandin D synthase
IL: Interleukin
Jak: Janus kinase
M1: Classically-activated macrophages
M2: Alternatively-activated macrophages
Mrc-1: Mannose receptor C-type 1
mTORC: Mechanistic target of rapamycin complex
NTC: Non-targeting control
PBMC: Peripheral blood mononuclear cells
PG: Prostaglandin
PPAR: Peroxisome proliferator-activated receptor
Ppm: Parts per million
Ptgs: Prostaglandin-endoperoxide synthase
Sbp2: Selenocysteine insertion sequence binding protein-2
Se: Selenium
Se-Ade (Se-A): Selenium adequate
Sec: Selenocysteine
SECIS: Selenocysteine insertion sequence
Se-Def (Se-D): Selenium deficient
Seleno: Selenoprotein
Se-Supp (Se-S): Selenium supplemented
SNP: Single nucleotide polymorphism
SRE: Selenocysteine redefinition element
Stat: Signal transducer and activator of transcription
STH: Soil-transmitted helminth
Th: T-helper
Trsp: Selenocysteine $tRNA^{[Ser]Sec}$
Tsc: Tuberous sclerosis protein
TX: Thromboxane
Txnrd: Thioredoxin reductase
WT: Wild-type
Δ^{12}-PGJ_2: Δ^{12}-prostaglandin J_2

ACKNOWLEDGEMENTS

There are many people in my life that have helped me achieve this moment. My parents, Terry and Suzanne Shay, have always been and always will be my greatest source of inspiration, motivation, and support for everything I have ever accomplished in my life. They both have struggled in life and have sacrificed a lot in order for me to have a better life than they did. Everything they have done for me has allowed me to grow as a person and encouraged me to become who I am today. I will never be able to thank them enough.

Throughout my years in school I have had a few teachers that have had a positive impact on my studies as well as my life. Mr. Rob Naylor is the largest contributor to why I fell in love with molecular biology and genetics. He was straight out of college and we were his first group of students he had ever taught. His enthusiasm, involvement, devotion, and artistic and hands-on techniques for teaching science is stuck in my mind even to this day. I like to blame him for Graduate school, but hopefully now I will be able to afford that Porsche.

Dr. Vicky Funanage, my undergraduate research advisor, gave me a fantastic opportunity when she agreed to allow me to do research in her laboratory at Nemours Alfred I. duPont Hospital for Children. I was able to work at the interface of clinical and experimental research through interactions with both surgeons and scientists. That experience really solidified my desire to continue a career in medical research and strive to earn my PhD.

Dr. Sandeep Prabhu and I first met when I interviewed for admittance into the Molecular Medicine program here at Penn State. I can still vividly remember that day, sitting in his office, going over the details of my undergraduate research poster with him on a printout I had brought. It's hard to believe how quickly time has flown by. I joined his laboratory with absolutely no idea what selenoproteins or prostaglandins were but now I will leave here knowing they are responsible for doing everything. Despite the steep learning curve and the occasional head butting we did with each other, I really appreciate everything he has done for me and how much he has helped me get to this point. Being in his laboratory has really developed me a lot both as a person overall and as a scientist.

Over the years in this laboratory I have met and worked with many talented individuals that have not only helped me develop my research but survive this process (Dr. Shakira Nelson, Chang Liao, Dr. Emily Finch, Dr. Naveen Kaushal, Dr. Avinash Kudva, Dr. Vivek Narayan, Dr. Arvind Korwar, Dr. Ashok Kumar, Dr. Bastihalli Diwakar, Shaneice Nettleford, and Fenghua Qian). Shakira established the project that I continued working on and taught me many of the techniques I needed in order to have a strong start. Even years after she graduated I could still contact her with my many questions and she always had time to talk to me. Chang and I rotated and joined the laboratory together at the same time. We have endured many stressful situations together and my experience here would not have been the same without her. She is truly a gifted scientist and a dear friend. Emily was definitely the smile and the laughter of this laboratory during my time here. I worked with her for the beginning of graduate career and learned a great deal from her. Even outside of the laboratory there were many people

in the department always willing to help both with research and with life (Mike Quickel, Dr. Laura Bennett, Dr. Laura Goodfield, and Kristin Cox). All of these people have taught me and helped me get through graduate school and receive my PhD.

My committee members (Dr. Girish Kirimanjeswara, Dr. Connie Rogers, Dr. Pamela Hankey Giblin, and Dr. Margherita Cantorna) have provided me guidance throughout my time here as well as ideas and helpful discussions about experimental designs and troubleshooting. Additionally, without the assistance and collaboration with the following people aspects of this work would have been challenging to complete: Dr. Joseph F. Urban Jr., Dr. Bo-Jhih Guan, Dr. Paul Copeland, Dr. Mary Kennett, Dr. Dolph Hatfield, Brad Carlson, Dr. Ulrich Schweizer, and Dr. Venkatesha Basrur. As well as the facility and staff support from the Huck Institutes of the Life Sciences, the College of Agricultural Sciences, the Department of Veterinary and Biomedical Sciences, the Animal Diagnostics Laboratory, and the Animal Resource Program.

Finally, this dissertation would not have been possible without funding from the National Institutes of Health (R01 Grants: DK077152, CA175576, CA162665; T32 Training Grant: 5T32AI074551-05), the United States Department of Agriculture Hatch Funds (project numbers 4475, 4605) and an United States Department of Agriculture intramural grant awarded to Dr. Joseph F. Urban Jr. (1235-5100-058). [Disclaimer: The findings and conclusions in this dissertation do not necessarily reflect the view of these funding agencies.]

Chapter 1

Literature Review

Select passages have been published in two publications:

Selenium and inflammatory bowel disease.

Published in The American Journal of Physiology-Gastrointestinal and Liver Physiology.

Am J Physiol Gastrointest Liver Physiol. 2015 Jul 15;309(2):G71-7. Doi: 10.1152/ajpgi.00379.2014 [Epub 2015 Jun 4.]

Avinash K. Kudva[1*], Ashley E. Shay[1*], and K. Sandeep Prabhu[2].

* Both authors contributed equally.

Affiliations: [1]Center for Molecular Immunology and Infectious Disease and Center for Molecular Toxicology and Carcinogenesis, Department of Veterinary and Biomedical Sciences, The Pennsylvania State University, University Park, Pennsylvania. [2]Center for Molecular Immunology and Infectious Disease and Center for Molecular Toxicology and Carcinogenesis, Department of Veterinary and Biomedical Sciences, The Pennsylvania State University, University Park, Pennsylvania

The role of selenoproteins in resolution of inflammation.

Published in Selenium: Its Molecular Biology and Role in Human Health

Textbook 4th Ed. pp. 499-510 *[Epub 2016 Sep 16.]*

Bastihalli T. Diwakar[1*], Emily R. Finch[1*], Chang Liao[1*], Ashley E. Shay[1*], and K. Sandeep Prabhu[1].

* All authors contributed equally.

Affiliations: [1]Department of Veterinary and Biomedical Science, Center for Molecular Immunology and Infectious Disease and Center for Molecular Toxicology and Carcinogenesis The Pennsylvania State University, University Park, PA, USA.

Selenium Chemical Properties and Forms

Selenium (Se) is an essential trace element first discovered in 1817, 200 years ago, by Swedish chemist Jöns Jacob Berzelius (1). As a member of the metalloid family as well as belonging to the same group as oxygen, sulfur, and tellurium, Se has many unique properties upon incorporation into proteins, which will be discussed in more detail below. Although Se containing compounds, such as selenols, are structurally similar to sulfur containing compounds, such as thiols, there are a few key differences which account for selenols being better nucleophiles. The bond between carbon and Se is longer than carbon and sulfur and the bond energy between Se and hydrogen is weaker than that of sulfur and hydrogen (2). Therefore, selenols have a lower reduction potential and are therefore easily oxidized upon air exposure and resistant to reduction (3). Additionally, selenols (pK_a=5.3) are stronger acids than thiols (pK_a=8.3) leading to deprotonation and generation of a selenolate anion which is highly nucleophilic (3,4). Finally, Se can enhance the formation of thiol-disulfide like bonds and help reduce the disulfide bonds, which are essential for proper protein folding (5,6).

Selenium exists in both organic and inorganic forms. The inorganic forms, selenite and selenate, are derived from sandstone, limestone, and volcanoes, and are found in soil as well as food (7). While inorganic forms of Se (selenite and selenate) are easily absorbed in the intestine, they are less retained in the body than organic forms of Se (8). The organic forms of Se, selenocysteine (Sec) and selenomethionine, are derived from food, both plant and animal in origin. Selenomethionine is the most abundant form of Se consisting of 90% of the total Se found in plants, due to the fact that when in excess

it can replace methionine in protein synthesis (9). Sec is considered the 21st amino acid due to its structural similarity to cysteine, where Se replaces sulfur, and uses its own unique machinery for incorporation into polypeptide chains in a co-translational manner (10). Sec is found in animals, but rarely in its free form. Sec first needs to be released from proteins through proteolytic digestion in order to be utilized for incorporation into proteins (11).

Selenoprotein Biosynthesis

Both inorganic and organic forms of Se are first converted to hydrogen selenide (H_2Se) for it to be used in selenoprotein biosynthesis. Selenate is directly reduced to selenite (12). Selenite is reduced to H_2Se by glutathione as well as thioredoxin and glutaredoxin reductase (13). H_2Se can also be derived from Sec by the action of β-lyase; while selenomethionine is metabolized to methylselenol (CH_3SeH) by γ-lyase and subsequently converted to H_2Se. Excess H_2Se and selenomethionine are excreted in the urine as either trimethylselenide, dimethylselenide, or selenosugars (**Fig 1.1**) (14).

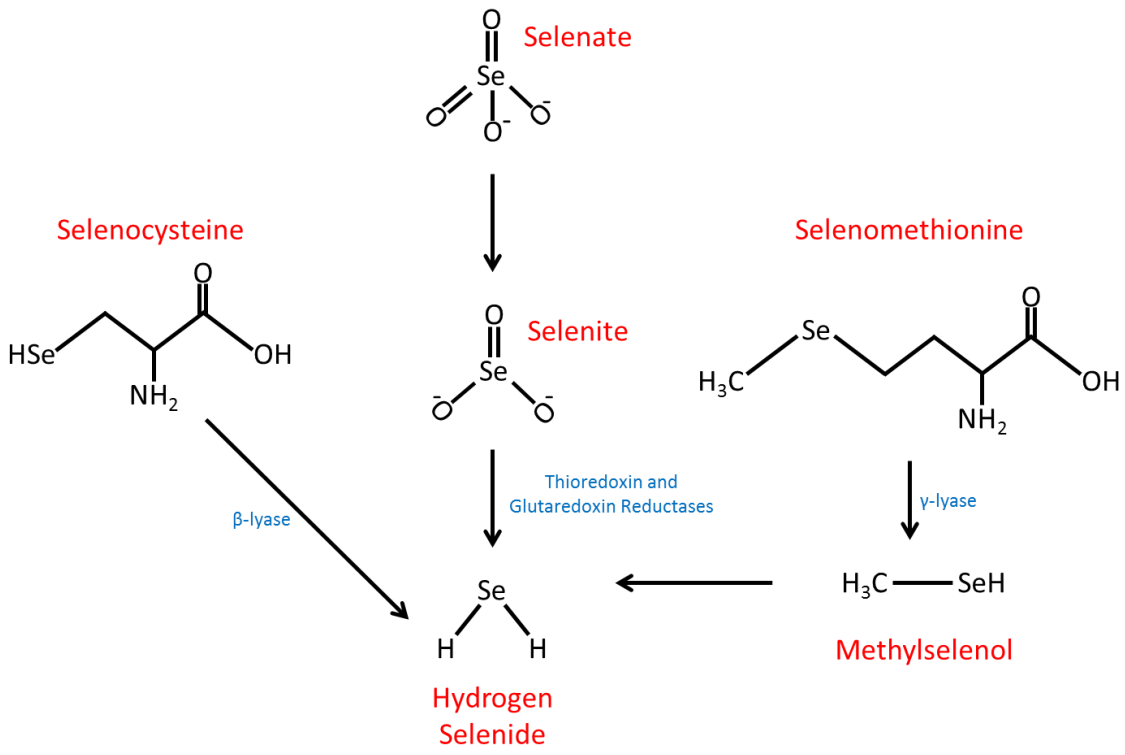

Figure 1.1: Generation of hydrogen selenide

Hydrogen selenide is the key molecule needed for the synthesis of selenocysteine charged tRNA. Hydrogen selenide can be derived from either selenate, selenite, selenocysteine, or selenomethionine. Selenate is first reduced to selenite and then selenite is directly metabolized into hydrogen selenide through the action of thioredoxin or glutaredoxin reductases. Selenocysteine and selenomethionine are acted upon by β- or γ- lyase, respectively to generate hydrogen selenide.

There are five steps required to charge Sec $tRNA^{[Ser]Sec}$. First, seryl-tRNA synthetase charges $tRNA^{[Ser]Sec}$ with serine to become serine $tRNA^{[Ser]Sec}$. The serine $tRNA^{[Ser]Sec}$ is then phosphorylated by 0-phosphoseryl $tRNA^{[Ser]Sec}$ kinase to become phospho-serine $tRNA^{[Ser]Sec}$. Thirdly, H_2Se is converted to selenophosphate by the selenoprotein, selenophosphate synthetase-2 and ATP (15). The fourth and fifth steps occur simultaneously. Sec synthase acts on phospho-serine $tRNA^{[Ser]Sec}$ and selenophosphate to generate Sec $tRNA^{[Ser]Sec}$ (**Fig 1.2**). At low Se levels this mechanism

can convert sulfide into thiophosphate and generate Cys $tRNA^{[Ser]Sec}$ (16). Sec $tRNA^{[Ser]Sec}$ exists as two isoforms based on the methylation of the ribosyl moiety at position 34 of the tRNA (Um34). The methylated Um34 isoform is considered a Se-dependent isoform and supports the synthesis of "stress"-related selenoproteins. The non-methylated Um34 isoform is mainly responsible for the synthesis of "housekeeping" selenoproteins (17). The gene responsible for Sec $tRNA^{[Ser]Sec}$, *Trsp*, is a single copy gene in all organisms with the exception of zebrafish and is the longest tRNA sequenced in higher vertebrates consisting of 90 nucleotides (18).

Selenium is incorporated into proteins as Sec, recognized as the 21^{st} amino acid, and decoded by the UGA codon, normally a termination codon (15). While most selenoproteins only contain one UGA codon, selenoprotein P (Seleno-P) has anywhere between ten and 18 UGA codons depending on the species (19). The selenoprotein synthesis machinery is comprised of various trans- and cis-acting regulatory elements necessary for the proper incorporation of selenocysteine into growing polypeptide chains, the main components are briefly described below (20,21). Elongation factor specific to Sec (EFSec) is a GTP binding protein with no GEF activity and can only bind Sec (22). The other functions of EFSec remain unknown. Selenocysteine insertion sequence (SECIS) binding protein-2 (Sbp2) can bind SECIS, ribosomes and to some extent, EFSec (23). It is comprised of 3 domains: the N-terminal: function unknown, the central domain: Sec incorporation, and the C-terminal: which is a conserved L7Ae RNA binding domain (23). The other trans-acting components of the selenoprotein synthesis machinery include SECp43, SPS1, SLA, eIF4A3, and ribosomal protein L30 (18). The SECIS element is the only required cis-acting component and, among the different selenoprotein

transcripts, is composed of highly variable sequences. However, they form a similar secondary structure consisting of an internal loop (AUGA and UGR residues) and an apical loop (AAR residues) (18). There are two forms of the SECIS element based on the helices and loops formed from non-Watson and Crick base pairing that causes kinks and turns (18). Finally, a Sec redefinition element has been identified to reside adjacent to a subset of UGA codons in various selenoprotein transcripts (**Fig 1.2**) (24). The components of the selenoprotein biosynthesis machinery have been shown in all branches of life (25).

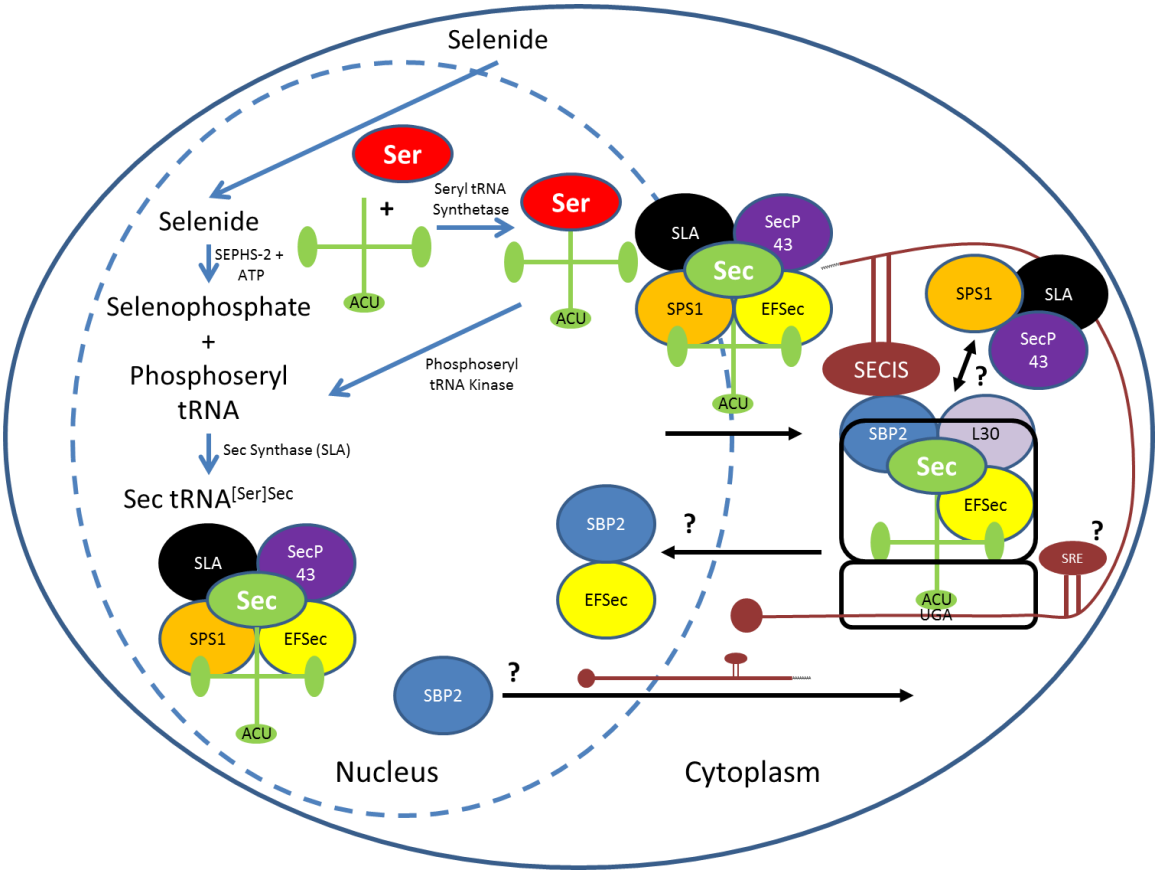

Figure 1.2: Conversion of hydrogen selenide into selenocysteine charged tRNA and co-translational incorporation

The selenocysteine incorporation machinery relies on two unique parts, the charging of selenocysteine (Sec) to its tRNA and the incorporation into the polypeptide chain.

Selenophosphate synthetase-2 (SEPHS-2) phosphorylates hydrogen selenide into selenophosphate. Selenocysteine synthase (SLA) uses selenophosphate and an ACU anticodon that has been charged with serine (Ser) and phosphorylated to generate the selenocysteine charged tRNA. The Sec tRNA interacts with a variety of proteins to shuttle it out of the nucleus and to the activating translating ribosome including selenophosphate synthetase-1 (Sephs-1), 60S ribosomal protein L30 (L30), and tRNA selenocysteine-1-associated protein-1 (SecP43). Selenoprotein mRNA have a unique 3' untranslated region stem-loop structure, termed the selenocysteine insertion sequence (SECIS), that is bound to by SECIS binding protein-2 (SBP2), which helps recruit the Sec tRNA to the ribosome at UGA sequence, along with a unique Sec tRNA elongation factor (EFSec). A subset of selenoprotein mRNAs also include a selenocysteine redefinition element (SRE) located adjacent to the UGA codon. Question mark: Exact mechanism and role is currently unclear but evidence suggests depicted function.

Selenoproteins were first identified through sequence analyses using various bioinformatic tools. Potential selenoproteins were predicted in small nucleotide sequence and whole genome database searches based on candidate SECIS elements. After predicting a potential SECIS element, the identity of the protein upstream the SECIS element was determined. These potential selenoprotein candidates were tested for insertion of Sec using ^{75}Se radiolabeling (21,26). Additionally, groups of closely related genomes were analyzed in order to identify conserved SECIS elements that belong to selenoprotein orthologs. Finally, sequences are examined upstream of the SECIS element for UGA codons and other potentially conserved coding sequences (21,26). Prediction of candidate SECIS elements and confirmation of Sec insertion through ^{75}Se radiolabeling has led to the identification of 25 selenoproteins in humans and 24 selenoproteins in mice (21,26) (**Tables 1.1 and 1.2**).

Symbol	Name	Synonyms
SELENO F	Selenoprotein F	selenoprotein 15, SEP15
SELENO H	Selenoprotein H	SELH, C11orf31*
SELENO I	Selenoprotein I	SELI, EPT1
SELENO K	Selenoprotein K	SELK
SELENO M	Selenoprotein M	SELM, SEPM
SELENO N	Selenoprotein N	SEPN1* SELN
SELENO O	Selenoprotein O	SELO
SELENO P	Selenoprotein P	SEPP1*, SeP, SELP, SEPP
SELENO S	Selenoprotein S	SELS, SEPS1, VIMP*
SELENO T	Selenoprotein T	SELT
SELENO V	Selenoprotein V	SELV
SELENO W	Selenoprotein W	SELW, SEPW1*

Table 1.1: Selenoprotein gene nomenclature

*New HGNC selenoprotein gene nomenclature is indicated in the column "symbol". Previous HGNC symbols (shown with *) will become synonyms, along with other previously used designations (Adapted and modified from Gladyshev et. al, J Biol Chem 2016).*

Symbol	Name	Synonyms
TXNRD1	Thioredoxin reductase 1	TR1, TRXR1
TXNRD2	Thioredoxin reductase 2	TRXR2, TR3, mitochondrial Thioredoxin reductase
TXNRD3	Thioredoxin-glutathione reductase	TGR, TRXR3, TR2
GPX1	Glutathione peroxidase 1	Cytosolic glutathione Peroxidase, GSHPX1
GPX2	Glutathione peroxidase 2	GSHPX-GI
GPX3	Glutathione peroxidase 3	Plasma glutathione peroxidase
GPX4	Glutathione peroxidase 4	Phophoslipid hydrpperoxidase glutathione peroxidase, PHGPX
GPX6	Glutathione peroxidase 6	
DIO1	Iodothyronine diodinase 1	D1
DIO2	Iodothyronine diodinase 2	D2
DIO3	Iodothyronine diodinase 3	D3
MSRB1	Methionine-R-sulfoxide reductase 1	SELR, SELX, SEPX1
SEPHS2	Selenophosphate synthetase 2	SPS2

Table 1.2: Selenoprotein gene nomenclature based on enzymatic activity

The nomenclature of these genes will not be changing to use the SELENO root. (Adapted and modified from Gladyshev et. al, J Biol Chem 2016).

Selenoprotein Function and Health

Selenoproteins have a variety of functions and activities including redox homeostasis, thyroid metabolism, and protein folding. The four most commonly studied classes are the glutathione peroxidase (Gpx) family, the thioredoxin reductase (Txnrd) family, the iodothyronine deiodinase (Dio) family and endoplasmic reticulum (ER) resident selenoproteins. Gpx has five isoforms in humans, four in mice, which vary in cellular location and disease association. The Gpx family uses glutathione as a reductant to reduce hydrogen peroxide into water and lipid peroxides into alcohols. Gpx-1 is ubiquitously expressed in the cytoplasm as well as the mitochondria as a homotetramer (27,28). Gpx-1 also has the capability to metabolize cholesterol and long chain fatty acid peroxides if they are first released from phospholipids through the action of phospholipase A_2, such as during arachidonic acid metabolism (29,30). Gpx-2 is predominately expressed in the gastrointestinal tract as well as liver and is localized to the cytoplasm (31). Overexpression of Gpx-2 is associated with increased cellular differentiation and proliferation in patients with colorectal cancer (32,33). Gpx-3 is the secreted isoform and found abundantly in the plasma (34). Downregulation of Gpx-3 has been observed in patients with thyroid cancer, heptacellular carcinoma, and chronic myeloid leukemia (35). Gpx-4's cellular location can vary based on alternative splicing to be in the cytoplasm, mitochondria, or nucleus. Unlike the other Gpx isoforms it is functional as a monomer, has phospholipid hydroperoxidase activity, and a less restricted dependence on glutathione as a reductant (27). Studies have shown that Gpx-4 is required for normal sperm development and mutations in Gpx-4 are associated with Sedaghatian

type of spondylometaphyseal dysplasia (36,37). The last selenocysteine-containing member of the Gpx family, Gpx-6, contains a selenocysteine in humans but a cysteine residue in mice (38). It is found in the Bowman's gland of the olfactory system however, its function remains unknown (29).

The three members of the Txnrd family have evolved from glutathione reductases. The C-terminal Sec of Txnrds interacts with the N-terminal active site of pyridine nucleotide disulfide oxidoreductase family members (31). Txnrds function as homodimers containing a FAD prosthetic group and a NADPH binding domain to reduce thioredoxin which in turn reduces hydrogen peroxide, and lipid hydroperoxides (31). Txnrd-1 is ubiquitously expressed and can be found in both the cytosol as well as the nucleus (31). Txnrd-2 is present in the mitochondria of cells (31). Txnrd-1's main function is to reduce the disulfide bonds in thioredoxin-1 in an NAPDH-dependent manner (31). Genetic knockout studies have found that loss of Txnrd-1 or Txnrd-2 is embryonic lethal (39,40). Txnrd-3 is highly expressed in the testes and contains an additional N-terminal glutaredoxin domain not present in the other two isozymes (41). This additional domain allows Txnrd-3 to reduce both thioredoxin and glutathione.

Unlike the Gpx and Txnrd families which serve as potent enzymes for maintaining redox homeostasis within the cell, members of the Dio family are important for regulating thyroid hormone metabolism. Dio-1 (expressed in liver and kidney) and Dio-2 (expressed in thyroid, placenta, pituitary, and brain) cleave the iodine-carbon bond of the prohormone 3,5,3',5'-tetraiodothyronine (T4), which is secreted by the thyroid gland, into the active metabolite 3,5,3'-triiodothyronine (T3) by 5'-deiodination (31). Maintaining proper levels of T3 are essential for growth, differentiation, and metabolism

(31). While Dio-1 is thought to provide the majority of the circulating T3, Dio-2 appears to be more important for local thyroid production of T3 (42,43). Additionally, a high level of Dio-2 expression has been reported in patients with Graves' disease and in follicular adenomas (44). Dio-3 (expressed in pregnant uterus, placenta, fetal and neonatal tissues) is responsible for the inactivation of T4 and T3 (31). The inactivation reaction involves the conversion of T4 and T3 into the inactive metabolites, 3,3',5'-triiodothyronine and 3,3'-diiodothyronine, respectively (31). Inactivation of these thyroid hormones prevents premature exposure of fetal and neonatal tissues to adult levels of T3, which could lead to improper growth (45).

Researchers in the selenoprotein field have begun to characterize and investigate a group of selenoproteins that reside in the ER. This includes Seleno-K, Seleno-S, Seleno-F, Dio-2, Seleno-M, Seleno-N, and Seleno-T. Although much is still unknown about the exact functions of these specific selenoproteins, some information has been discovered. Seleno-K is a 11kDa selenoprotein with a single transmembrane helix in its N-terminus that targets it to the ER membrane and the Sec located in its C-terminus (46). Seleno-K associates with the protein acetyltransferase, DHHC6, to palmitoylate cysteine residues on target proteins including inositol-1,4,5-triphosphate receptor and CD36 (47,48). Inositol-1,4,5-triphosphate receptor plays an important role for the influx of calcium during macrophage Fc_{γ} receptor activation (48,49). CD36 is a fatty acid translocase and plays an important role in the alternative activation of macrophages (50). Therefore, deletion of Seleno-K leads to impaired immune responses particularly the activation of M2 macrophages.

Dr. Vadim Gladyshev's laboratory has also shown that both Seleno-K and Seleno-S bind derlin-1 and -2, respectively, and play a role in ER homeostasis (46). Derlins are a part of a complex that mediates ER-associated degradation by detecting misfolded proteins and targeting them for degradation (46). Seleno-K co-precipitates with soluble glycosylated ER-associated degradation substrates and plays a role in their degradation (46). Finally, Seleno-K's gene contains an ER stress response element, which leads to an increase in its expression when misfolded proteins have accumulated in the ER (46).

The remaining ER resident selenoproteins' functions are still largely unknown. Seleno-F has been shown to associate with UDP-glycoprotein glucosyltransferase, an ER-resident protein, which is involved in the quality control of protein folding (51). It is this association which appears to be what keeps Seleno-F in the ER but the exact function of Seleno-F is unknown (51). Seleno-M is expressed in the brain, heart, lung and kidneys and may be involved in neurodegenerative disorders and cytosolic calcium regulation (52). Seleno-N mutations have been associated with four autosomal recessive muscle disorders: rigid spine muscular dystrophy, the classical form of multiminicore disease, desmin related myopathy with Mallory-body like inclusions, and congenital fiber-type disproportion (53).

Seleno-W, Seleno-H, Seleno-V and Seleno-T all contain a thioredoxin-like fold with a CXXU motif suggesting potential oxidoreductase activity (54). Seleno-W is highly expressed in skeletal muscle, heart and brain (55). Studies in mouse show that this selenoprotein is involved in muscle growth and differentiation, and in the protection of neurons from oxidative stress during neuronal development (56-58). Seleno-H functions as an oxidoreductase, and has been shown to protect neurons against UVB-induced

damage by inhibiting apoptotic cell death pathways, promote mitochondrial biogenesis and mitochondrial function, and suppress cellular senescence through genome maintenance and redox regulation (59-61). Seleno-V is specifically expressed in the testis and its function is unknown. Finally studies in mice to determine Seleno-T function indicate a crucial role for this gene in the protection of dopaminergic neurons against oxidative stress in Parkinson's disease, and in the control of glucose homeostasis in pancreatic beta-cells (62,63).

Seleno-P is the major selenoproteins in plasma and consists of up to ten Sec residues, hence making it sensitive to changes in selenium levels (31). The main function of Seleno-P is to deliver selenium to various tissues throughout the body (31). Seleno-P has been reported to have two additional activities in the form of a phospholipid hydroperoxide glutathione peroxidase and a peroxynitrite reductase (31). However, its phospholipid hydroperoxide glutathione peroxidase activity is ~100-fold lower than that of GPX-4 (64). Seleno-I, also referred to as ethanolamine phosphotransferase-1, is a member of the CDP-alcohol phosphatidyltransferase class-I family (18). It catalyzes the transfer of phosphoethanolamine from CDP-ethanolamine to diacylglycerol to produce phosphatidylethanolamine, which is involved in the formation and maintenance of vesicular membranes, regulation of lipid metabolism, and protein folding (65). Seleno-R is the only Sec containing member of the methionine-R-sulfoxide reductase B family and has the highest activity compared to its cysteine containing family members (66). This family of proteins reduces oxidative stress by reducing methionine-R-sulfoxides into methionine. This protein is highly expressed in liver and kidney, and is localized to the

nucleus and cytosol (67). Seleno-O is the largest selenoprotein and is located in the mitochondria but its exact function remains unknown (68).

Selenoprotein Hierarchy

Sec is only utilized when it is essential for protein function. Additionally, not all selenoproteins are expressed equally. Sec incorporation efficiency leads to a selenoprotein hierarchy wherein which selenoprotein is synthesized depends on a variety of factors including Se status, SECIS element present, and the presence of any genomic mutations in either the selenoprotein of interest or the selenoprotein biosynthesis machinery (69-72). Limiting the Se supply leads to competition between selenoprotein mRNAs due to the fact that they all share the same tRNA and incorporation machinery. At the gene level, expression of certain selenoproteins are resistant to changes in Se status, such as *Gpx-4* and *Txnrd-1*, while others are highly responsive to changes in Se status, such as *Gpx-1*, *Msrb-1*, and *Seleno-W* (73). Selenoproteins therefore be classified as either house-keeping or stress-induced selenoproteins based on response to changes in Se status as well as stimulation (73). Interestingly, the syntheses of selenoproteins that are sensitive to changes in Se status have been shown to have an abundance of ribosome pausing (74). The more Se present, the more ribosomal pausing that is occurring. However, there is an increase in translation past the UGA codon particularly for stress-related selenoproteins and this is more dramatic than regulation of mRNA levels suggesting the primary regulation of selenoprotein biosynthesis is at a translational level by dietary Se (74). In addition to Se status, the 3’ untranslated region plays an important

role in determining selenoprotein biosynthesis (75). Sbp2 has various binding affinities based on the SECIS element of individual selenoprotein mRNAs (76). Finally, genetic variants in either the SECIS element of an individual selenoprotein or an incorporation factor can affect the competition and balance of the synthesis of the whole selenoproteome (77).

Selenium Deficiency, Genetics, and Health

Dietary Se status not only affects the transcription and translation of various selenoproteins but also effects genetics and disease outcome. Soil Se levels not only vary around the world, but also vary in the 48 contiguous states of the United States of America (**Fig 1.3**).

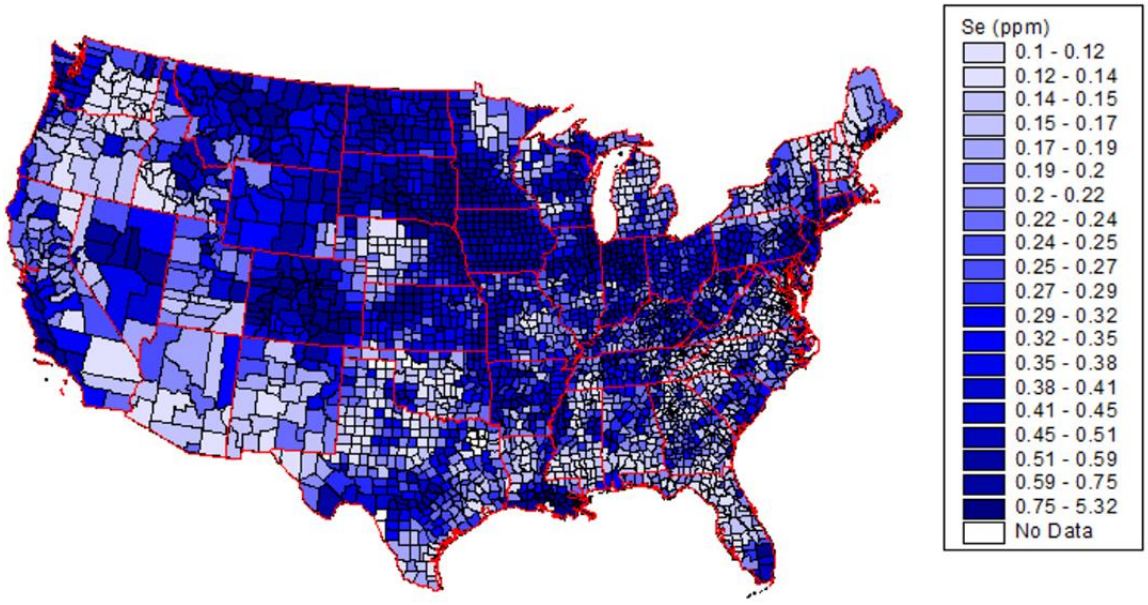

Figure 1.3: Selenium content in counties of the contiguous United States of America

Geological survey representing the soil selenium content (parts per million) in individual counties of the 48 contiguous states of the United States of America (Adapted and modified from the United States Geological Survey Agency).

There is an estimated 1 billion people worldwide that are Se deficient (78,79). The recommended dietary allowance for Se for various age groups is as follows: children ages 1-3 is 20 µg/day, children ages 4-8 is 30 µg/day, children ages 9-13 is 40 µg/day, adults and children 14 and up is 55 µg/day, pregnant women is 60 µg/day, and breastfeeding women is 70 µg/day (80). There are two documented diseases that have been associated with Se deficiency. Keshan disease is an often fatal congestive cardiomyopathy caused by both Se deficiency and a mutated strain of coxsackievirus (81,82). Keshan disease received its name based on the location of the first reported case in Keshan County, Heilongjiang province, China. Keshan disease has also been reported in New Zealand and Finland where soil Se levels are also low (83,84). The second is Kashin–Beck disease which is a chronic, endemic type of osteochondropathy that has been highly associated with Se and iodine deficiency and mainly afflicting China, Siberia, and North Korea (85,86). Other contributing factors to the onset of this disease include mycotoxins and high levels of fulvic acid (87). Interestingly, China has both the highest and lowest Se soil levels in the world (88,89). Se deficiency is also known to exacerbate other diseases and infections including ulcerative colitis, Crohn's disease, HIV, influenza, and helminth infections (90-92).

In addition to either directly contributing to disease onset or exacerbating a preexisting disease or infection, several studies have suggested that there is local adaptation pressure leading to genetic mutations in selenoprotein genes in populations

residing in Se deficient areas (93,94). Currently, the selenoprotein database, SelenoDB 2.0, contains single nucleotide polymorphisms (SNPs) data for 928 individuals with approximately 8,000 SNPs in either selenoproteins or selenoprotein related genes, such as the selenoprotein biosynthesis machinery (95). SNPs have been documented in the following selenoproteins: *GPX-1*, *GPX-2*, *GPX-3*, *SELENO-P*, *SBP-1*, *SELENO-K*, *TXNRD-1*, *TXNRD-2*, and *SELENO-O* (96,97). There is one SNP in *GPX-2* in a US population that is significantly associated with the development of rectal cancer (98). In a German population with low Se intake, SNPs in *SELENO-K*, *TXNRD-1*, and *TXNRD-2* were found to interact with plasma Se or *SELENO-P* status to modulate risk or advanced disease (99,100). Several SNPs in *SELENO-P* are associated with risk for several cancers and cognitive impairment as well as affect body mass index, blood pressure, peripheral arterial disease occurrence, and abdominal aortic aneurysm development in overweight and obese individuals (96,101,102). In the selenoprotein biosynthesis machinery, SNPs in Sec tRNA$^{[Ser]Sec}$ and *SEPHS-2* have been linked to an area with low Se intake and high prevalence of Crohn's disease (103). Additionally, missense mutations in *SBP2* cause poor Sec incorporation and low expression of most of the 25 known human selenoproteins. Low selenoprotein expression caused increased sensitivity to oxidative stress, poor thyroid function, and the development of an axial muscular dystrophy with a similar phenotype to rigid spine muscular dystrophy that has been associated with mutations in the *SELENO-N* gene (104). Finally, mice with genetic deletion of the Sec tRNA$^{[Ser]Sec}$ gene in macrophages are more susceptible to symptoms of dextran sulfate sodium-induced experimental colitis despite being fed a Se-supplemented diet (113). Worsened symptoms of colitis in Sec tRNA$^{[Ser]Sec}$ macrophage-specific deficient mice is

due to both a decreased expression and activity of 15-hydroxy-prostaglandin dehydrogenase, which is responsible for the catabolism of the pro-inflammatory arachidonic acid metabolite, prostaglandin E_2 (113).

Arachidonic Acid Metabolism

Macrophages express various receptors, not necessarily exclusive to this cell type, including Fc, mannose, and toll-like receptors, for the detection of pathogens in the environment through the recognition of pathogen-associated molecular pattern (PAMP) molecules and for the detection of cellular stress through the recognition of damage-associated molecular pattern (DAMP) molecules. Activation of these receptors leads to the production of lipid mediators, specifically eicosanoids, through the mobilization of arachidonic acid from the phospholipid bilayer (105). In a resting cell, arachidonic acid is rarely found as a free fatty acid. Therefore, during an immune response, arachidonic acid is first mobilized by phospholipase A_2 and then acted upon by a variety of enzymes including lipoxygenases, cyclooxygenases, and cytochrome P450 epoxygenase (**Fig 1.4**).

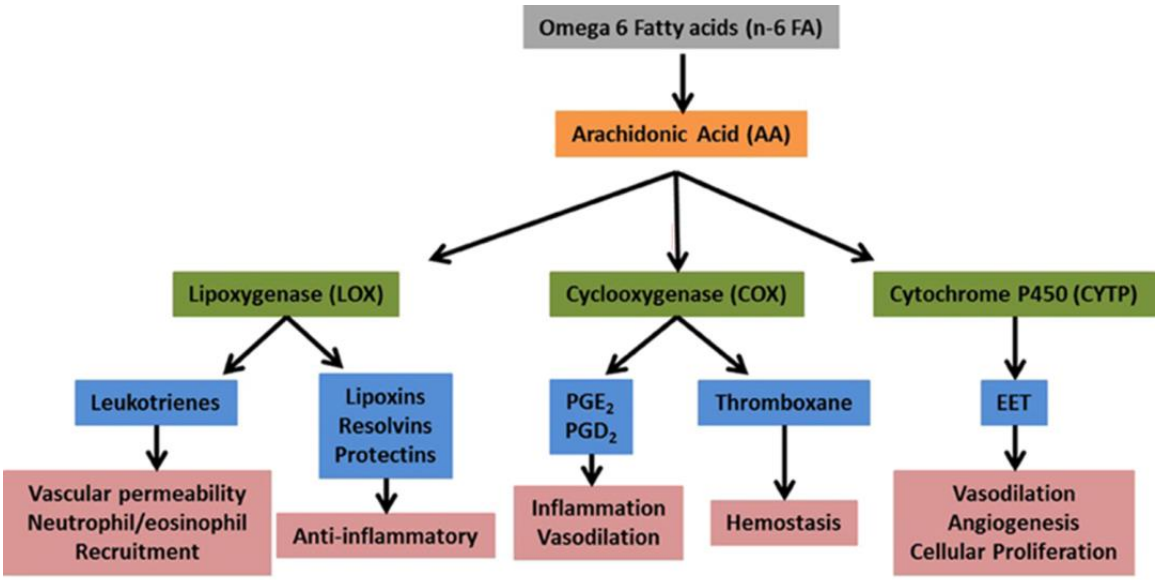

Figure 1.4: Arachidonic acid metabolized into different lipid mediators by various enzymes

Once released from the phospholipid membrane by phospholipase A_2, arachidonic acid is an available substrate for either lipoxygenases, cyclooxygenases, or cytochrome P450 epoxygenase. Lipoxygenases generate leukotrienes, lipoxins, resolvins, and protectins. Cyclooxygenases produce prostaglandins and thromboxanes. Cytochrome P450 epoxygenase creates epoxyeicosatrienoic acids. The exact lipid mediator produced and physiological effect depends on which synthase acts on the metabolized arachidonic acid product from these three enzymes (Adapted and modified from Pratt et. al, Front Cell Infect Microbiol 2014).

There are two isoforms of Cox: Cox-1, which has historically been considered as the constitutively expressed isoform, while Cox-2 is considered the inducible isoform by diverse stimuli. Differences between the regulation and activity of these two isoforms will be discussed in further detail below. Cox enzymes convert arachidonic acid into prostaglandin (PG) G_2, an unstable hydroperoxide that is reduced to PGH_2. The first reaction is catalyzed by the cyclooxygenase activity, while the second reaction is catalyzed by the peroxidase activity within the Cox enzymes. Certain glutathione S-transferases and Gpxs have been shown to catalyze this reaction in a non-heme dependent

mechanism (29). Regardless of which peroxidase acts on PGG_2, PGH_2 is a substrate for a variety of synthases to form specific prostanoids that impart diverse biological activities. For instance, selenium, in the form of selenoproteins, has been shown to up-regulate the expression of hematopoietic PGD_2 synthase (Hpgds), a sigma-class glutathione S-transferase (106). The increased expression of Hpgds effects the production of PGD_2 in immune cells, such as macrophages and T-cells. PGD_2 undergoes spontaneous dehydration followed by an isomerization to form prostaglandin J_2 (Δ^{13}-PGJ_2) and Δ^{12}-PGJ_2, respectively. A second thermodynamically less favored dehydration converts Δ^{12}-PGJ_2 to 15-deoxy-$\Delta^{12,14}$-prostaglandin J_2 (15d-PGJ_2) (**Fig 1.5**).

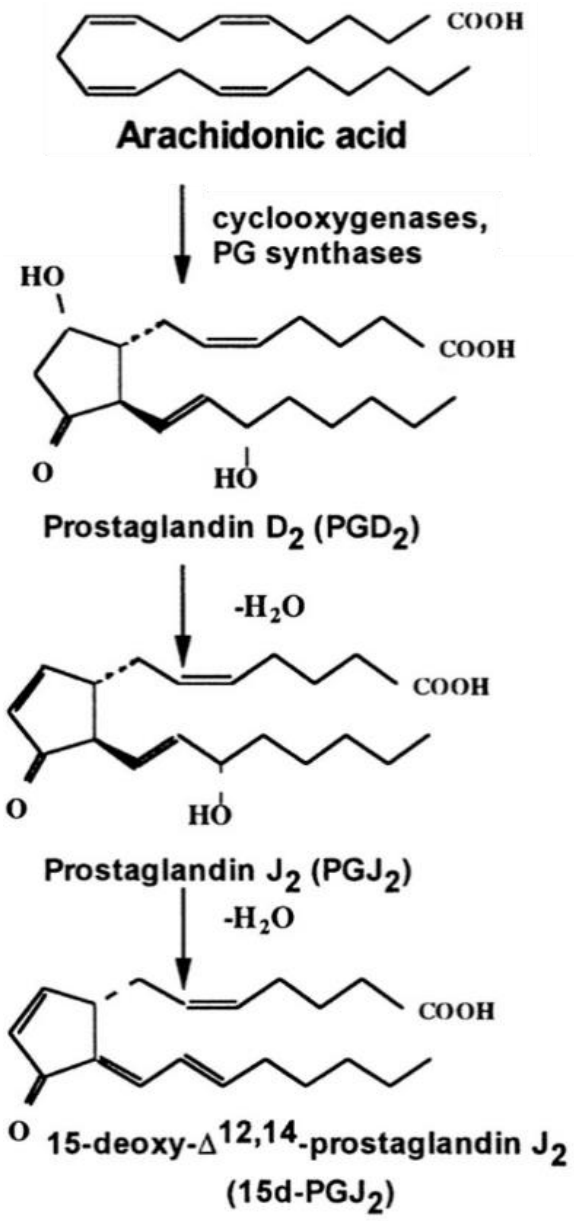

Figure 1.5: Arachidonic acid metabolism via the Cox/Hpgds pathway to 15-deoxy-$\Delta^{12,14}$-prostaglandin J_2

Cyclooxygenase-1 and -2 metabolize arachidonic acid into PGH_2 through their cyclooxygenase and peroxidase activity. PGH_2 is further metabolized into PGD_2 by hematopoietic prostaglandin D synthase (Hpgds). PGD_2 undergoes spontaneous dehydration followed by an isomerization to form Δ^{13}-prostaglandin J_2 and Δ^{12}-prostaglandin J_2, respectively. A second thermodynamically less favored dehydration converts Δ^{12}-prostaglandin J_2 to 15-deoxy-$\Delta^{12,14}$-prostaglandin J_2 (Adapted and modified from Petrova et. al, Proc Natl Acad Sci 1999).

Selenium-driven Eicosanoid Class Switching

Our long-standing hypothesis is that, there exists a selenoprotein or a group of selenoproteins that can metabolize PGH_2 to PGD_2 or CyPGs to activate Ppar-γ-dependent expression of *Hpgds*, while inhibiting NF-κB, to create a feed-forward loop. Studies are currently underway to identify these selenoproteins. The ability of selenium to down regulate nuclear factor-κB (NF-κB)-dependent pathways, including microsomal PGE_2 synthase (mPges-1) and thromboxane synthase (Txas), which catalyze the conversion of PGH_2 to PGE_2 and PGH_2 to TXA_2, respectively, also aids in the eicosanoid class switching phenomenon to differentially regulate pathways of inflammation and resolution (106). The chemically reactive electrophilic nature of CyPGs enables these bioactive molecules to form covalent complexes, termed Michael adducts, involving specific protein thiols and electrophilic carbon to impact various pathways of inflammation, including the NF-κB pathway. Previous studies in our laboratory have demonstrated such a covalent adduct formation of Ikappa kinase-2 with 15d-PGJ_2 to inhibit the NF-κB pathway was dependent on selenium and selenoprotein expression in macrophages (107). A recent report from our laboratory demonstrated the ability of selenium to inhibit the acetylation of non-histone and histone proteins by histone acetyltransferase p300 and therefore affect the expression of pro-inflammatory genes, including NF-κB member p65, in macrophages (108,109). Such an epigenetic modulation of inflammatory gene expression was, in part, dependent on the selenoprotein-mediated shunting of arachidonic acid (108,109). Taken together, the ability of selenoproteins to effectively shunt the

eicosanoid pathway may represent one of the many anti-inflammatory and pro-resolving functions of selenium (**Fig 1.6**).

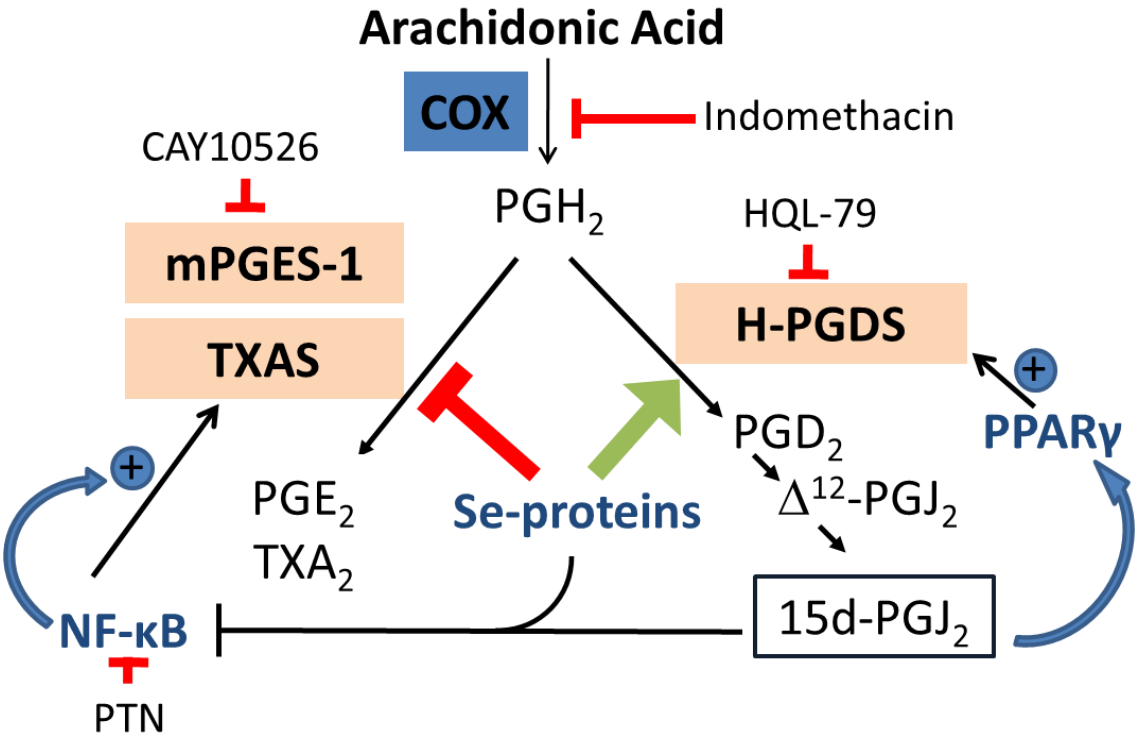

Figure 1.6: Selenium-driven eicosanoid class switching

Selenoprotein(s) are able to create a regulatory loop between the expression of Hpgds and the inhibition of NF-κB signaling. Selenium supplementation leads to the increased expression of Hpgds and decreased expression of mPges-1 and Txas. This shunting toward Hpgds leads to an increased production of 15-deoxy-$\Delta^{12,14}$-prostaglandin J_2 (15d-PGJ_2). Ppar-γ activation by 15d-PGJ_2 further increases Hpgds expression. 15d-PGJ_2 also inhibits NF-κB, additionally decreasing mPGES-1 and TXAS expression (Adapted from Gandhi et. al, J Biol Chem 2011).

CyPGs have been shown to have multiple anti-inflammatory effects *in-vitro* and *in-vivo*. First, the utilization of PGH_2 for the production of PGD_2 leaves little to no substrate for the production of PGE_2 and TXA_2, which are essential for initiation of inflammation (110,111). Second, PGD_2 and its cyclopentenone derivatives, Δ^{12}-PGJ_2 and

15d-PGJ_2 resolve inflammation by controlling leukocyte trafficking and macrophage efflux to draining lymphatics (110). Third, recent studies from our laboratory have shown that selenoprotein expression is required to up-regulate the expression of 15-prostaglandin dehydrogenase (15-Pgdh), an enzyme that oxidizes lipid mediators with an enhanced preference towards PGE_2, specifically in the gut (111-113). Preliminary studies in our laboratory suggest that Ppar-γ mediates this process. Furthermore, our studies also suggest a positive correlation between selenoprotein status and increased oxidation of PGE_2 to 15-keto-PGE_2, which has been reported to lack pro-inflammatory activity (113). 15-keto-PGE_2 can be further converted to 13,14-dihydro-15-keto-PGE_2 and subsequently to 13,14-dihydro-15-keto-PGA_2 that could potentially serve as a ligand for Ppar-γ activation (113) (**Fig 1.7**).

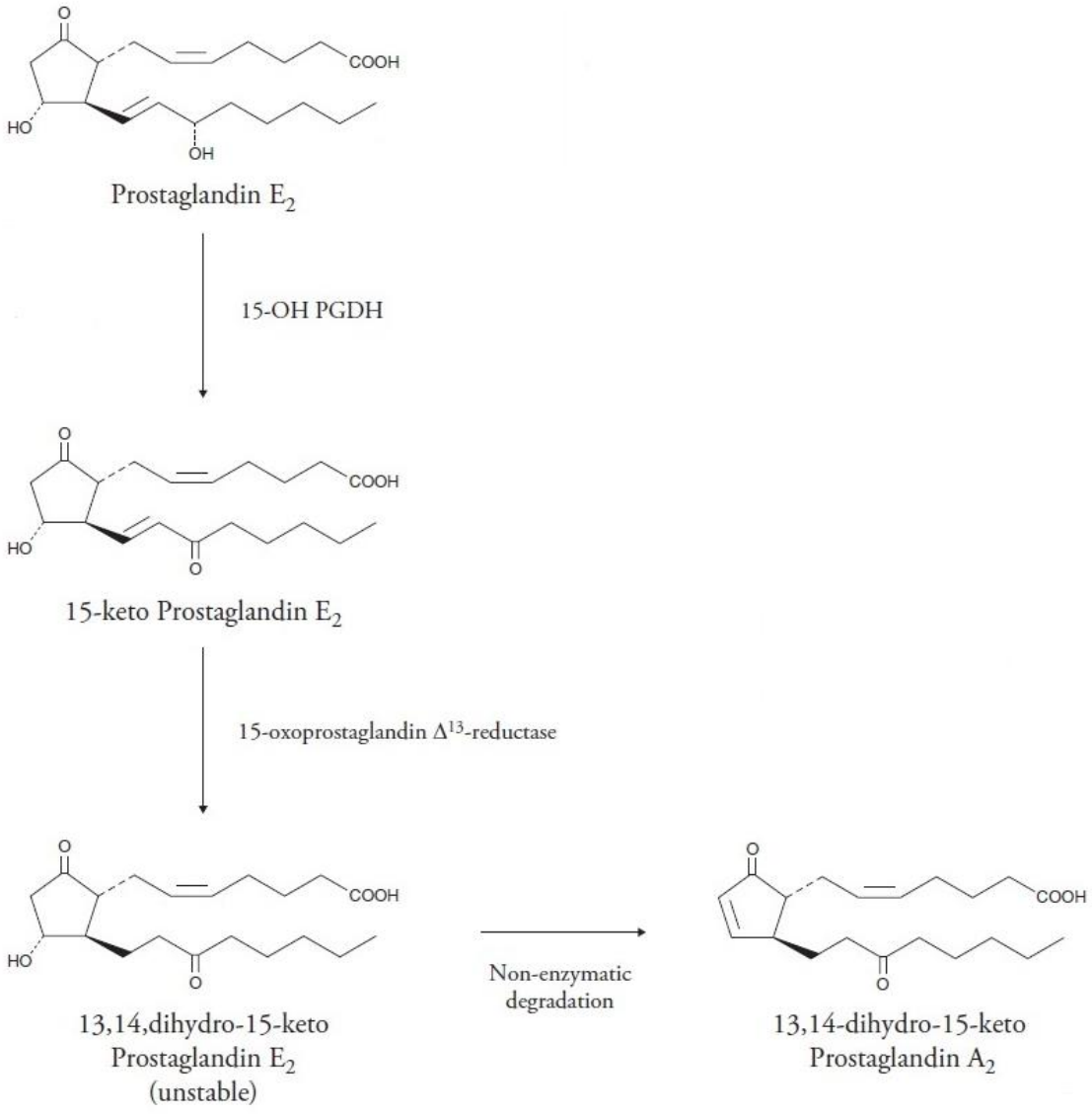

Figure 1.7: Prostaglandin E_2 metabolism

Prostaglandin E_2 is metabolized to 15-keto prostaglandin E_2 by 15-hydroxy prostaglandin dehydrogenase (15-OH PGDH). 15-oxoprostaglandin Δ^{13}-reductase converts 15-keto prostaglandin E_2 into the unstable metabolite, 13,14,dihydro-15-keto prostaglandin E_2. A final non-enzymatic degradation leads to the production of 13,14-dihydro-15-keto prostaglandin A_2 (Adapted and modified from Cayman Chemical).

Cyclooxygenase Regulation

Even though Cox-1 (*Ptgs-1*) and Cox-2 (*Ptgs-2*) have a high-degree of sequence homology (~ 63%), they differ in many respects from gene structure to enzymatic activity. Cox-1 has been generally considered as a constitutive enzyme, with some exceptions such as upregulation of transcription in fibroblasts by TGFβ and IL-1β and during cellular differentiation of transcription in fibroblasts by TGFβ and IL-1β and during cellular differentiation of monocytes with phorbol ester in THP-1 cells (114). Cox-2 is subjected to transcriptional and post-translational regulation by diverse stimuli (115-118). While *Ptgs-2* promoter contains many regulatory elements present in "early immediate genes", the *Ptgs-1* promoter is more reminiscent of "house-keeping" genes lacking TATA and CAAT boxes, high GC content, and multiple transcriptional start sites (115-118). Additionally, *Ptgs*-2 mRNA, as well as protein, has a short half-life of two to seven hours, while *Ptgs*-1 mRNA and protein is relatively stable (117). The instability of Cox-2 protein is due to a 27 amino acid cassette at the C-terminus, not present in Cox-1, which targets it for degradation through the endoplasmic-reticulum-associated protein degradation system followed by ubiquitination and proteolysis by 26S proteasome (117,119).

Interleukin-4 Signaling Pathways

Janus Kinase, Signal Transducer and Activator of Transcription, and Feline Sarcoma Oncogene Kinase Signaling Pathway

Binding of IL-4 to its receptor leads to the recruitment of various tyrosine kinases, such as Janus kinases (Jak1-3) and Feline sarcoma oncogene kinase (Fes). Recruitment of Jak-1 and Jak-3 leads to the activation of Signal Transducer and Activator of Transcription-6 followed by nuclear translocation and transcriptional activation of M2 macrophage genes including peroxisome proliferator-activated receptor gamma (*Ppar-γ*), arginase-1, mannose receptor-1 (*Mrc-1*; *Cd206*), and *Il-10* (120,121) (**Fig 1.8**). IL-4 receptor engagement can also recruit Fes and lead to an increase in signaling pathways that regulate protein translation (122). Fes activates phosphatidylinositide 3-kinase leading to the generation of phosphatidylinositol (3,4,5)-triphosphate. 3-phosphoinositide-dependent protein kinase-1 is activated by membrane phospholipids and is a major regulator of protein kinase B/Akt signaling (123,124).

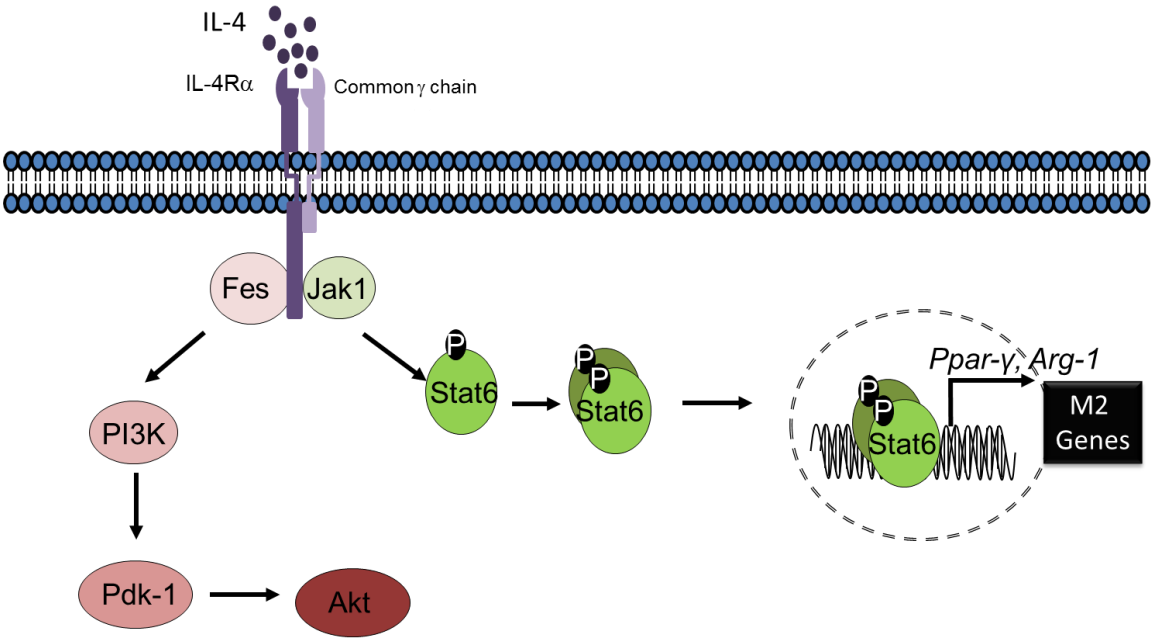

Figure 1.8: Janus kinase and feline sarcoma oncogene kinase signaling pathway

Engagement of the IL-4 receptor leads to the activation and recruitment of a variety of kinases and adaptor proteins including Janus kinase-1 (Jak-1), feline sarcoma oncogene kinase (Fes), and Signal transducer and activator of transcription 6 (Stat6). Ligand binding of the IL-4 receptor leads to phosphorylation and activation of Jak-1 associated with the receptor. Activated Jak1 phosphorylates tyrosine residues on the cytoplasmic tail of the receptor creating SH2 binding sites. The SH2 domain of Stat6 allows it to bind the IL-4 receptor in order to be phosphorylated by Jak-1. Phosphorylated Stat6 forms homodimers and translocate into the nucleus to promote transcription of various M2 macrophage genes. Fes activates phosphoinositide 3-kinase (PI3K), which is responsible for the generation of the secondary messenger, phosphatidylinositol (3,4,5)-triphosphate. 3-phosphoinositide-dependent protein kinase-1 (Pdk-1) is activated by membrane phospholipids and is a major regulator of protein kinase B/Akt signaling.

Mechanistic Target of Rapamycin Complex Signaling Pathway

mTORC activity increases the phosphorylation of Akt. Akt inhibits tuberous sclerosis complex (Tsc), activating mTORC. mTORC increases translation by activating ribosomal protein S6 kinase β-1 (p70S6K) and releasing elongation factor eIF4E from its inhibitor 4EBP. S6 kinase negatively feeds back to inhibit phosphatidylinositide 3-kinase

activity (125). Therefore Akt is both regulated and regulates mTOR signaling pathways (**Fig 1.9**). Finally, mTOR has been shown to play a critical role in M2 macrophage polarization in both peritoneal macrophages and BMDMs with IL-4 stimulation increasing the expression of Tsc1 and Tsc2 protein in stimulated macrophages (126).

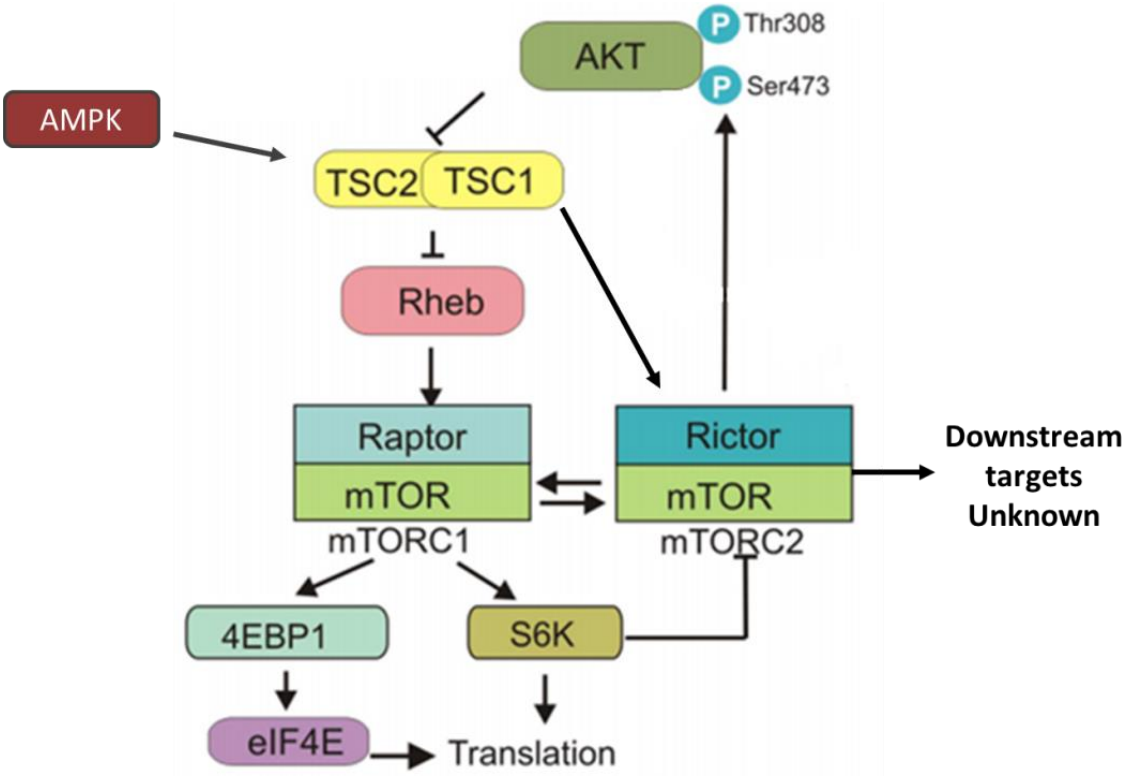

Figure 1.9: Mechanistic target of rapamycin complex signaling pathway

Akt activation inhibits tuberous sclerosis complex-1 and -2 (Tsc1/Tsc2) leading to the exchange of GDP for GTP in Rheb and subsequent activation of mechanistic target of rapamycin complex 1 (mTORC1). mTORC1 consists of the proteins mTOR, raptor, mLST, deptor, and PRAS40. It is responsible for increasing cell growth by upregulating cellular translation through the phosphorylation of 4EBP1 and ribosomal S6 kinase. mTORC2 consists of mTOR, rictor, mLST8, deptor, sin1, and protor 1/2. mTORC2 has been shown to regulate Akt, SGK1, and PKCα, however much remains unknown about downstream targets of mTORC2 (Adapted and modified from Jozwiak et. al, Front Endocrinol 2014).

Peroxisome Proliferator-Activated Receptor Signaling Pathway

Peroxisome proliferator-activated receptor (Ppar) is a member of the nuclear receptor family and exists in three forms, Ppar-α, Ppar-β/δ, and Ppar-γ. The expression level of each isoform varies depending on tissue of interest (127). The formation of heterodimers with various protein binding partners dictates whether Ppars are in their active or inactive state. When Ppars are inactive in the cytoplasm, ligands compete with co-repressors bound to Ppars and recruit co-activators, with retinoid-X-receptor being the most characterized Ppar co-activator leading to the translocation of the active Ppar and co-activator into the nucleus (127). Once in the nucleus the active heterodimer binds to peroxisome proliferator response elements in target genes or binds directly to transcription factors, such as NF-kB, and suppress signaling through that target pathway. Target genes include those important for inflammation, lipid metabolism, and cellular proliferation (127) (**Fig 1.10**). Ppar-α is expressed primarily in the heart, liver, and muscle tissues and plays an important role in fatty acid catabolism (127). Ppar-β/δ is ubiquitously expressed in most tissues. Therefore, this receptor is involved in many important processes including glucose homeostasis, cholesterol management, fatty acid catabolism, cell proliferation, and anti-inflammation (127). Finally Ppar-γ is expressed in immune cells and adipose tissue and plays an important role in inflammation (127). The metabolites of PGD_2, Δ^{12}-PGJ_2 and 15d-PGJ_2, serve as ligands for Ppar-γ which in turn binds to the peroxisome proliferator response element present in the *Hpgds* promoter and up-regulate its expression (106). Ppars are present in macrophages, T-cells, fibroblasts, neutrophils, and bone marrow precursor cells.

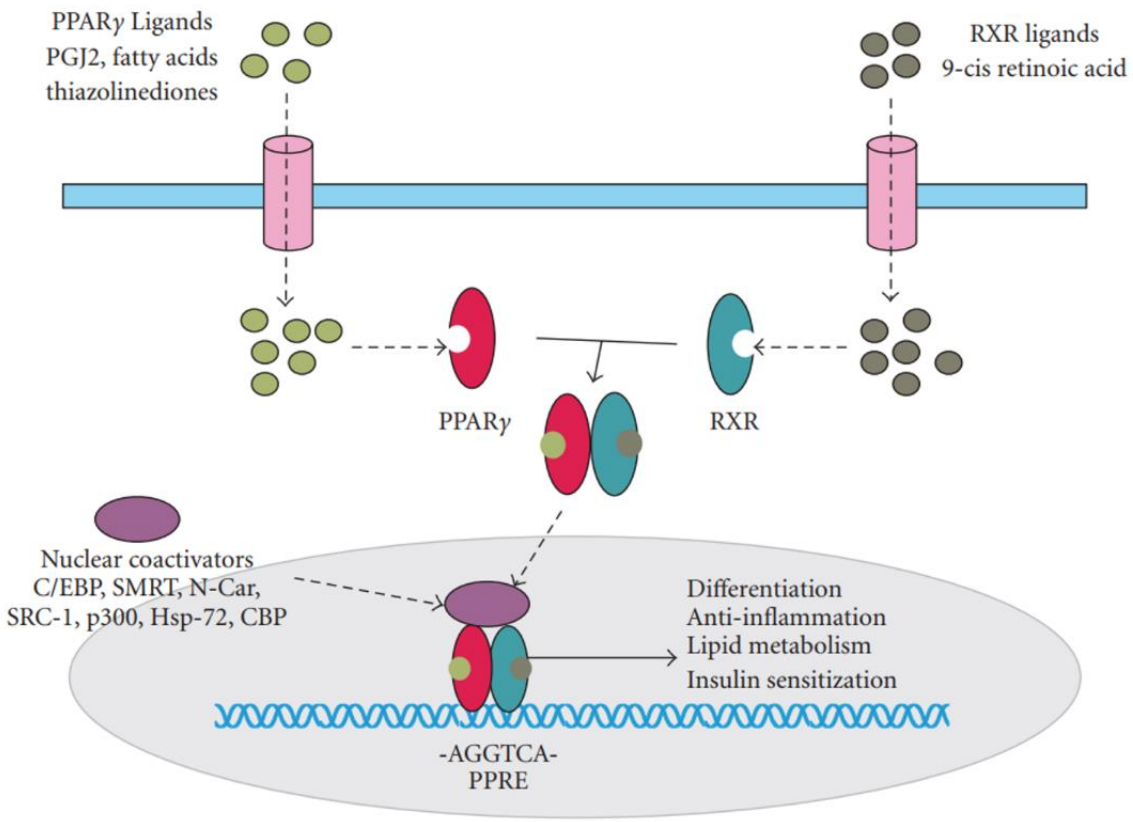

Figure 1.10: Mode of action for peroxisome proliferator-activated receptor gamma

Ppar-γ and RXR are activated by fatty acids/thiazolinediones and 9-cis retinoic acid, respectively and form a heterodimer. The activated Ppar-γ/RXR heterodimer translocates into nucleus and form a complex with other nuclear co-activators to regulate downstream target genes containing a Ppar response element in their promoter (Adapted from Wagner et. al, PPAR Res 2010).

Macrophages

Infiltrating versus Tissue Resident Macrophages

Macrophages are phagocytic innate immune cells responsible for responding to infections, removing debris, and aiding in wound healing (128). They can be found in circulation as well as stationary within tissues with current research defining these

macrophages as two different populations varying in both origin and activation. Infiltrating macrophages are differentiated from bone marrow-derived Ly6C^{hi} monocytes (129). During an event like infection or tissue damage signals lead to rapid monocyte mobilization and differentiation. These macrophages play an important role in tissue healing, clearance of pathogens and cellular debris, the initiation of the adaptive immune response, and have the typical polarization phenotypes as described in the following section (128,130).

Tissue-resident macrophages were initially thought to be terminally differentiated from bone marrow-derived monocytes and are primarily involved with tissue homeostasis (131,132). Recent fate-mapping studies have shown that they arise from three potential sources, yolk sac-derived erythro-myeloid progenitors, fetal liver-derived monocytes, or bone marrow-derived monocytes (133). During embryogenesis, two waves of macrophages are generated from erythro-myeloid progenitors that are the first to seed tissues and as development continues a majority of these macrophages, but not all, are replaced by fetal liver-derived monocytes which migrate into tissues and differentiate into macrophages (131,132,134-136). Tissue-resident macrophages not only play a role in maintaining tissue homeostasis but are also the first to respond to infection or damage and initiate the immune response through antigen presentation and cytokine production (131,132,137,138). In the liver, lung, skin, spleen, and peritoneum, fetal liver-derived macrophages maintain the ability to self-renew throughout adulthood (134-136). Therefore, tissue-resident macrophages may exist both at the beginning and after an inflammatory event. Tissue-resident macrophages have the ability to be activated and then return to homeostasis (135). In some other tissues, such as the gut and the dermis,

which are large immune sites, fetal liver-derived monocytes are gradually replaced by bone marrow-derived monocytes generated by adult hematopoiesis (131,132,135,136,138). During or after severe inflammation a majority of tissue resident macrophages are replaced by monocyte-derived macrophages but slowly recover over time (136). Interestingly tissue-resident macrophages may not polarize in the same manner as infiltrating/bone marrow-derived macrophages (139). While tissue-resident macrophages appear to have a similar classically activated phenotype as infiltrating/bone marrow-derived macrophages, their alternatively activated phenotype are quite distinct based on gene expression profiles (139). Upon IL-4 stimulation, tissue-resident macrophages increase the M2 markers *Arg-1*, *Fizz-1*, and *Ym-1*, however, when compared to monocyte-derived macrophages by whole genome microarray, there are vast global differences in gene expression profiles (139). Due to both the differences in phenotypes between tissue-resident macrophages and infiltrating macrophages and the main tissues (dermis, lungs, and intestinal tract) affected by helminth infection, which are large immune sites, the studies presented below focus on infiltrating bone marrow-derived macrophages.

Polarization

Macrophages are versatile innate immune cells endowed with the ability to enhance either inflammation or resolution based on various stimuli. A common system of classification divides macrophages into two groups: M1, classically activated macrophages and M2, alternatively activated macrophages, which represents two ends of

a spectrum comprising intermediary phenotypes that are poorly described (140). M0 macrophages are activated by IFN-γ, TNF-α, GM-CSF, LPS, and other TLR ligands to become M1 macrophages (130). Upon activation, M1 macrophages phagocytize pathogens and release nitric oxide, TNF-α, IL-1β, IL-6, and IL-12 (130,140-142). While M1 macrophages are necessary to facilitate a potent immune response, excess activation or prolonged exposure can lead to tissue damage and potentially tumor development (143). M0 macrophages are activated by IL-4, IL-13, IL-10, TGFβ, IL-6, glucocorticoids, immune complexes, leukocyte inhibitory factor, and IL-1R activation to become a spectrum of M2 (a-d) macrophages (130,144) (**Fig 1.11**). M2 macrophages are anti-inflammatory due to their increased expression of arginase-1, which competes for L-arginine, a substrate for iNOS, to produce L-ornithine and urea instead of nitric oxide (144). In addition to dampening the M1 response by limiting the production of nitric oxide, L-ornithine is converted into prolines and polyamines, which play an important role during wound healing and fibrosis (130,140-142). M2 macrophages are identified by the expression of Arg-1, Mrc-1, Ym-1, and Fizz-1 (130,140-142). Studies from our laboratory have shown that selenium supplementation increases the polarization of macrophages from a M1 to M2-like phenotype thereby decreasing inflammation and increasing resolution (113,144).

Selenoproteins act synergistically with IL-4, *in vitro*, to decrease expression of prototypical markers of pro-inflammatory M1 macrophages such as iNOS, IL-1β, and TNFα (144), while increasing the expression of Arg-1, Ym-1, and Fizz-1, characteristic of pro-resolution and reparative M2 macrophages (144). Treatment of bone marrow-derived macrophages harvested from Se-deficient and Se-adequate mice treated with the

hematopoietic PGD_2 synthase inhibitor, HQL-79, significantly reduced the effect of Se on Arg-1 activity (144). Additionally, treatment of these cells with either GW9662, a Ppar-γ antagonist, or leflunomide, a Stat6 antagonist, led to a significant decrease in M2 macrophage genes (144). This provided further evidence for the synergistic effect of Se supplementation and IL-4 signaling to increase M2 macrophages.

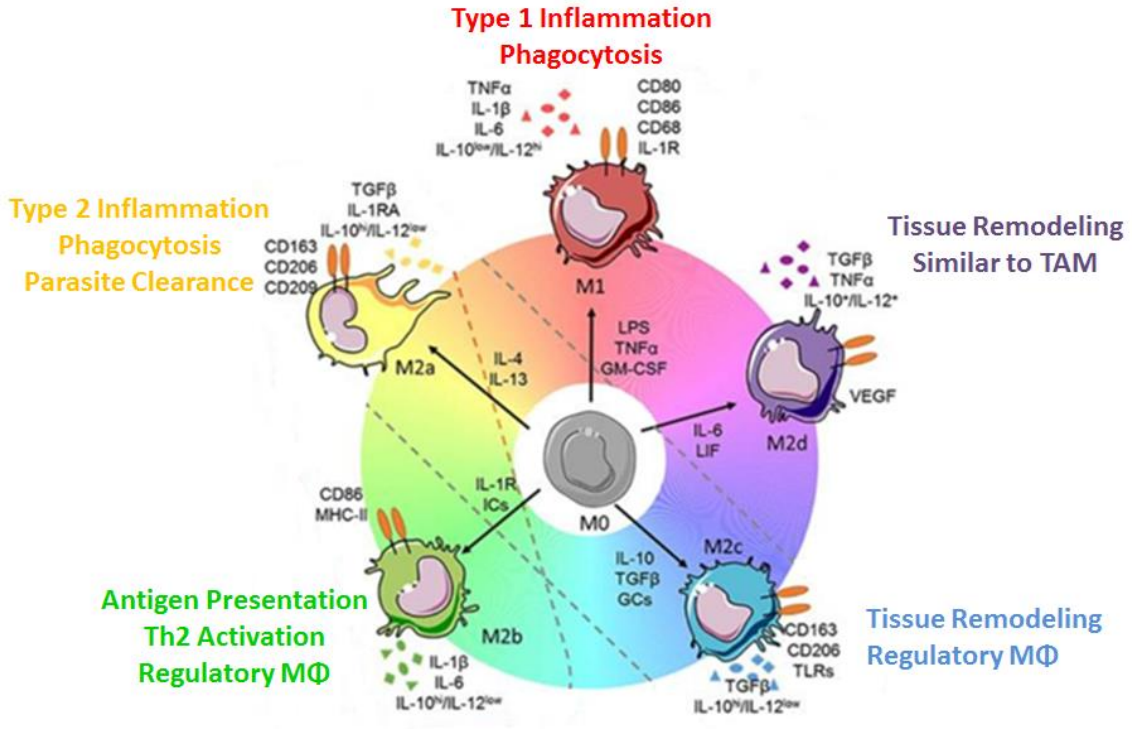

Figure 1.11: Macrophage polarization

Schematic depicting differences in stimulation, cytokine/chemokine secretion, and cell surface receptor expression between M1, M2a, M2b, M2c, and M2d macrophages. Abbreviations: GC: Glucocorticoids, IC: Immune Complexes, LIF: Leukocyte Inhibitory Factor (Adapted from Schliefsteiner et. al, Front Immunol 2017).

Inflammation

The stimulation present from infection which drives macrophage polarization determines the type of inflammatory response elicited. In general, M1 macrophages elicit

type 1 inflammation which phagocytizes pathogens and clears infection. While the spectrum of M2 macrophages elicit type 2 inflammation which assists with the resolution of cell-mediated inflammation. Inflammation has been a known biological process since the Roman scholar Aulus Cornelius Celsus first described the five cardinal symptoms (*rubor*, *calor*, *tumor*, *dolor*, and *functio laesa*) in *De Medicina* in the first century AD. During an acute inflammatory event in response to harmful stimuli such as pathogens, cellular debris, or irritants, tissue resident innate immune cells (macrophages, dendritic cells, and mast cells) become activated through their PAMP receptors and DAMP receptors (145). These activated tissue resident immune cells then release mediators that propagate the clinical signs of inflammation. First, there is vasodilation to increase blood flow to the site of injury to recruit additional immune cells. This increased blood flow leads to both *rubor* (redness) and *calor* (heat) (137,146). Then increased vascular permeability allows infiltrating immune cells to reach the site of injury, leading to *tumor* (swelling) (137,146). In addition to the recruitment of additional immune cells to the site of injury, mediators such as bradykinin, are responsible to eliciting *dolor* (pain) (137,146). The final cardinal sign of inflammation, *functio laesa* (loss of function), is likely the result of a neurological response to the pain (137,146). Inflammation is a critical biological process needed for responding to infection or injury; however prolonged inflammation can become pathogenic.

The resolution of acute inflammation is just as important as the onset. Resolution is an active process and is not complete until all inflammatory cells are removed from the site of injury. Failure to resolve due to persistent infection or cellular destruction leads to chronic inflammation causing scarring, fibrosis, and incomplete wound healing. In order

for resolution to occur properly macrophages are recruited to the site of injury in order to remove apoptotic polymorphonuclear neutrophils and any remaining microorganisms (147,148). The process of resolution is distinct from anti-inflammation, which is the downregulation of inflammation or pharmacological blocking of pro-inflammatory lipid mediators such as PGE_2 and LTB_4. Drugs such as ibuprofen block lipid mediators and dampen the cardinal signs of inflammation but they do not promote the recruitment of macrophages to promote tissue resolution and the ability to return to homeostasis (149). Resolution of acute inflammation is an important process needed for the clearance and subsequent tissue repair of soil-transmitted helminths. Failure to properly resolve helminth-induced inflammation will lead to permanent tissue damage and life-long health complications.

Soil-transmitted Helminth Infections

Soil-transmitted helminth (STH) infections are considered a neglected tropical disease and affect approximately 1.5 billion people worldwide according to the World Health Organization (**Fig 1.12**).

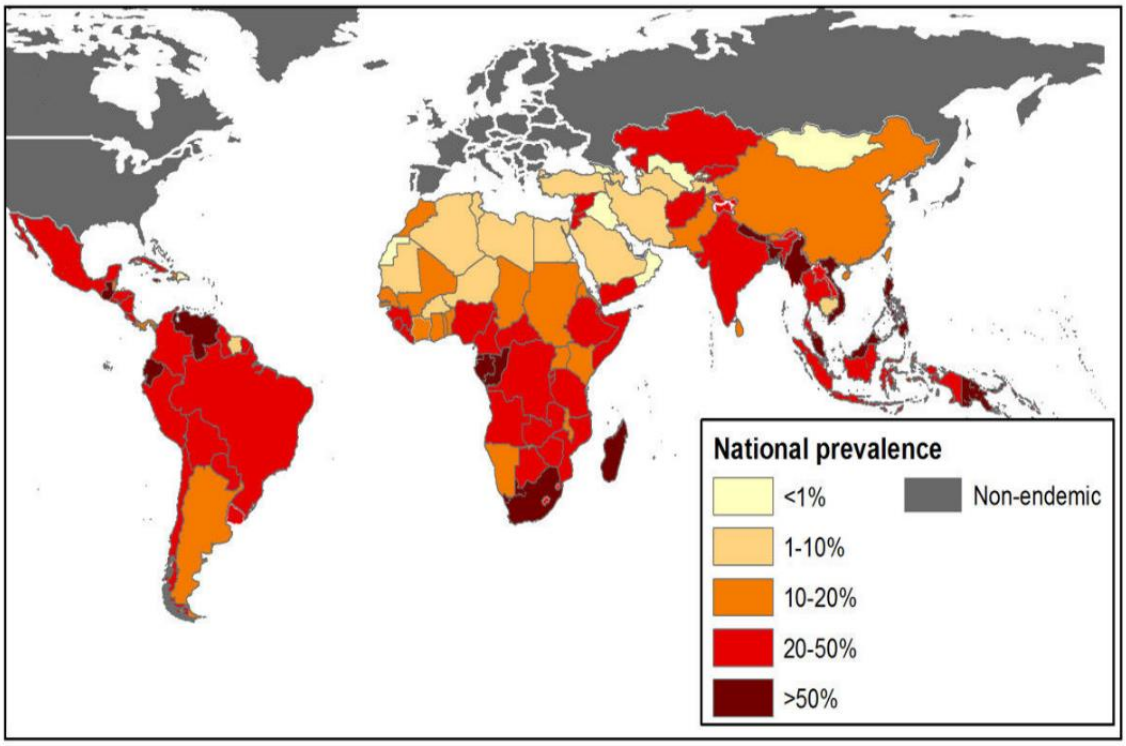

Figure 1.12: Global distribution of soil-transmitted helminths from the Global Atlas of Helminth Infection in 2010

Global estimates of soil-transmitted helminth infections from the following parasites: Ascaris lumbricoides, Trichuris trichiura, Necator americanus, and Ancylostoma duodenale. (Adapted from Campbell et. al, Trends Parasitol 2016).

Infections are most common in underdeveloped tropical and sub-tropical countries where sanitation is poor (150). STHs are blood feeding gastrointestinal parasites that hinder proper nourishment through depleting iron and protein from the blood, competing with the host for key nutrients and causing a decrease in appetite. Individuals with STH infections develop acute inflammation, which can either be resolved or lead to chronic inflammation due to persistent or recurrent infections leading to serious life threatening complications. Symptoms of infection can range from abdominal pain and diarrhea to anemia and protein deficiency to death depending on the

number of worms harbored (150). The most widely implemented method for controlling STH infections is through periodic administration of anthelmintic drugs. However, current treatments focus on reducing severity of infection and transmission rather than curing. This is due to a combination of compliance, the accessibility/availability of medication, and the self-clearing nature of the infection. Overuse of anthelmintic drugs in livestock has led to such a high degree of drug resistance in some geographical locations that raising livestock is no longer a viable option as the livestock succumb to helminth infection (151). Therefore there is an increasing concern for anthelmintic drug resistance in humans due to animal evidence and current treatments reducing severity of infection instead of eradication (151).

Nippostrongylus brasiliensis is a rodent helminth that has a similar life cycle to the human hookworms *Ancylostoma duodenale* (Old World Hookworm) and *Necator americanus* (New World Hookworm) and are classified as STHs. STHs enter the body by penetrating the skin or via the ingestion of contaminated water or food. Once in the body, the larvae travel through the circulatory system to the lungs where they burrow through pulmonary alveoli and migrate up the trachea. The larvae then travel to the small intestine where they mature into adults and reproduce. Eggs are passed through the feces of the infected individual to complete the cycle (152) (**Fig 1.13**).

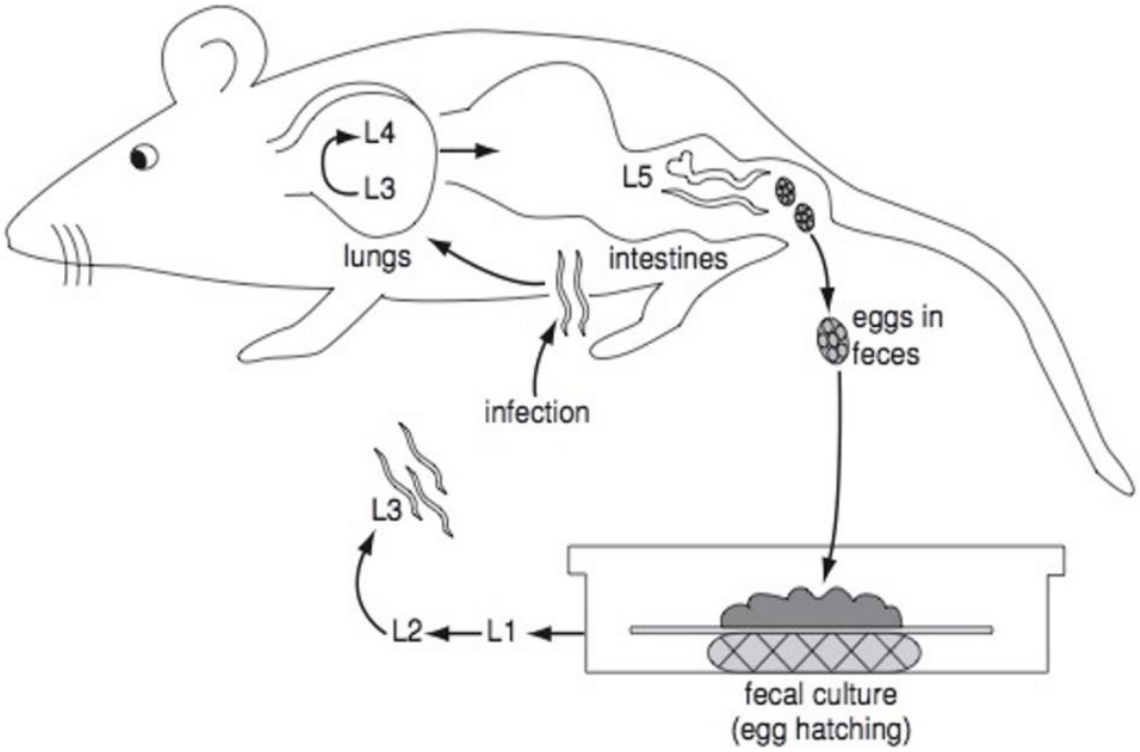

Figure 1.13: *Nippostrongylus brasiliensis* life cycle

Nippostrongylus brasiliensis is a murine soil-transmitted helminth which can be contracted through skin contact or ingestion of contaminated water or food. Its life cycle resembles that of human soil-transmitted helminthes. Eggs present in the feces of an infected individual hatch in soil and mature into three stages of larvae, with the third stage (L3) being the infective stage. Once through the skin the L3 larvae utilize the circulatory system of the host to reach the lungs, where they burrow through the pulmonary alveoli causing massive tissue damage. The larvae then mature into a fourth stage and migrate up the trachea and down the esophagus. In the gastrointestinal tract they mature into adults and adhere to the small intestinal walls to feed through blood meals and reproduce. The eggs are passed through the feces and the life cycle repeats. (Adapted and modified from Camberis et. al, Curr Protoc Immunol, 2003).

Immune Responses to Helminthic Parasites

The immune response to helminth infection includes polarization of Th0 cells to a Th2 phenotype, eosinophilia, basophilia, mastocytosis, and elevated levels of serum IgE and IgG1 (158). The polarization of Th0 cells toward a Th2 phenotype is characterized

by increases in anti-inflammatory cytokines, such as IL-4, IL-13, IL-9, and IL-5 (153-157). Production of these anti-inflammatory cytokines leads to the alternative activation of macrophages. M2 macrophages during helminth infection control underlying Th1 pathogenesis, contribute to fibrosis and wound healing, and are important for worm expulsion and developing resistance (158). M2 macrophages control Th1 pathogenesis by propagating a Th2 cytokine response and through suppressive effects on T cell proliferation (158). With regards to fibrosis and wound healing; M2 macrophages highly express Fizz-1 which has been implicated in wound healing (158). Additionally, in a fibrotic response model of schitosomasis, polarization toward a Th2 response increased genes involved in tissue remodeling including matrix metalloproteinases, tissue inhibitors of matrix metalloproteinases, and several types of collagen (158). Finally, during *N.brasiliensis* infection, M2 macrophages recruit eosinophils to the lungs and peritoneum to contribute to worm expulsion (158). Therefore, M2 macrophages have been shown to promote resolution and are key components in immunity to parasitic helminths (141,156,158).

Heligmosomoides polygyrus (also referred to as *Heligosomoides bakeri*) is another commonly studied rodent parasitic nematode. An efficient immune response to and clearance of *H.polygyrus* is affected by host dietary Se levels (159,160). Interestingly, the course of primary infection was unaffected by diet. Instead, Se-deficient mice had a delayed worm clearance and increased fecundity during a secondary challenge (160). Se-deficiency was associated with a reduced local Th2 response and reduced M2 macrophages (160). Discovering novel strategies for the treatment of STHs is a global health issue that needs to be addressed, particularly in light of increasing development of

parasitic resistance to current anthelmintic drugs (151). Therapy with Se supplementation in combination with current anthelmintic regimens provides a novel treatment of STH infections, where regulation of intracellular pathways of resolution in innate immune cells is key to driving robust host immune responses.

Research Hypothesis

In this dissertation, the mechanism by which IL-4 and selenoprotein(s) simultaneously drive eicosanoid class switching to enhance M2 macrophage polarization will be examined through the use of chemical inhibition and genetic modification. These studies are based on the central hypothesis that ***selenoprotein(s) drive IL-4-dependent eicosanoid class switching to produce 15d-PGJ$_2$ which is important for M2 macrophage polarization and enhanced clearance during helminth infection.*** This hypothesis will be addressed by utilizing an *in vitro* bone marrow-derived macrophage culture system as well as an *in vivo* model of helminth *Nippostrongylus brasiliensis* model, which simulates the human infections *Necator Americanus* and *Ancylostoma duodenale*.

Three major questions will be addressed:

1. Does selenium enhance M2 macrophage polarization during a Th2 biased parasitic infection?

   a. Mice will be fed Se-Def, Se-Ade, and Se-Supp diets while infected with the helminth *Nippostrongylus brasiliensis* in order to characterize macrophages and examine clearance.

2. Does IL-4 regulate Cox-1 expression, and if so how?
   a. Various downstream pathways from the IL-4 receptor will be chemically and genetically downregulated and its effect on Cox-1 expression will be examined. The implications of altering Cox-1 expression will be elucidated using the *Nippostrongylus brasiliensis* infection model.
3. Which selenoprotein(s) are important for M2 macrophage polarization?
   a. Selenoproteins upregulated during IL-4 stimulation will be determined using a macrophage specific Sbp-2 knockout mouse model and proteomics. Those upregulated selenoproteins will be individually knocked out in BMDMs using CRISPR/Cas-9 genomic editing technology and examined for the ability to polarize toward an M2 macrophage phenotype.

References

1. Boyd, R. (2011) Selenium stories. *Nat Chem* **3**, 570
2. Wessjohann, L. A., Schneider, A., Abbas, M., and Brandt, W. (2007) Selenium in chemistry and biochemistry in comparison to sulfur. *Biol Chem* **388**, 997-1006
3. Hondal, R. J., Marino, S. M., and Gladyshev, V. N. (2013) Selenocysteine in thiol/disulfide-like exchange reactions. *Antioxid Redox Signal* **18**, 1675-1689
4. Steinmann, D., Nauser, T., and Koppenol, W. H. (2010) Selenium and sulfur in exchange reactions: a comparative study. *J Org Chem* **75**, 6696-6699
5. Beld, J., Woycechowsky, K. J., and Hilvert, D. (2008) Catalysis of oxidative protein folding by small-molecule diselenides. *Biochemistry* **47**, 6985-6987
6. Beld, J., Woycechowsky, K. J., and Hilvert, D. (2010) Small-molecule diselenides catalyze oxidative protein folding in vivo. *ACS Chem Biol* **5**, 177-182

7. Hidekazu Yamada, Y. K., Tomonori Aso, Hiroshi Uesugi, Tomokazu Fujimura and Koyo Yonebayashi. (1998) Chemical Forms and Stability of Selenium in Soil. *Soil Science and Plant Nutrition* **44**, 385-391
8. Fairweather-Tait, S. J., Collings, R., and Hurst, R. (2010) Selenium bioavailability: current knowledge and future research requirements. *Am J Clin Nutr* **91**, 1484S-1491S
9. Cubadda, F., Aureli, F., Ciardullo, S., D'Amato, M., Raggi, A., Acharya, R., Reddy, R. A., and Prakash, N. T. (2010) Changes in selenium speciation associated with increasing tissue concentrations of selenium in wheat grain. *J Agric Food Chem* **58**, 2295-2301
10. Driscoll, D. M., and Copeland, P. R. (2003) Mechanism and regulation of selenoprotein synthesis. *Annu Rev Nutr* **23**, 17-40
11. X. Dauchy, P.-G., A. Astruc, and M. Astruc. (1994) Analytical methods for the speciation of selenium compounds: a review. *Fresenius' Journal of Analytical Chemistry* **348**, 792-805
12. Steven P. Brimmer, W. R. F., and Kurt A. Kulhavy. (1987) Quantitative reduction of selenate ion to selenite in aqueous samples. *Analytical Chemistry* **59**, 1470-1471
13. Cupp-Sutton, K. A., and Ashby, M. T. (2016) Biological Chemistry of Hydrogen Selenide. *Antioxidants (Basel)* **5**
14. Stathopoulou, M. G., Kanoni, S., Papanikolaou, G., Antonopoulou, S., Nomikos, T., and Dedoussis, G. (2012) Mineral intake. *Prog Mol Biol Transl Sci* **108**, 201-236
15. Hatfield, D. L., and Gladyshev, V. N. (2002) How selenium has altered our understanding of the genetic code. *Mol Cell Biol* **22**, 3565-3576
16. Xu, X. M., Turanov, A. A., Carlson, B. A., Yoo, M. H., Everley, R. A., Nandakumar, R., Sorokina, I., Gygi, S. P., Gladyshev, V. N., and Hatfield, D. L. (2010) Targeted insertion of cysteine by decoding UGA codons with mammalian selenocysteine machinery. *Proc Natl Acad Sci U S A* **107**, 21430-21434
17. Kim, J. Y., Carlson, B. A., Xu, X. M., Zeng, Y., Chen, S., Gladyshev, V. N., Lee, B. J., and Hatfield, D. L. (2011) Inhibition of selenocysteine tRNA[Ser]Sec aminoacylation provides evidence that aminoacylation is required for regulatory methylation of this tRNA. *Biochem Biophys Res Commun* **409**, 814-819
18. Labunskyy, V. M., Hatfield, D. L., and Gladyshev, V. N. (2014) Selenoproteins: molecular pathways and physiological roles. *Physiol Rev* **94**, 739-777
19. Stoytcheva, Z., Tujebajeva, R. M., Harney, J. W., and Berry, M. J. (2006) Efficient incorporation of multiple selenocysteines involves an inefficient decoding step serving as a potential translational checkpoint and ribosome bottleneck. *Mol Cell Biol* **26**, 9177-9184
20. Berry, M. J., Banu, L., Chen, Y. Y., Mandel, S. J., Kieffer, J. D., Harney, J. W., and Larsen, P. R. (1991) Recognition of UGA as a selenocysteine codon in type I deiodinase requires sequences in the 3' untranslated region. *Nature* **353**, 273-276
21. Kryukov, G. V., Castellano, S., Novoselov, S. V., Lobanov, A. V., Zehtab, O., Guigo, R., and Gladyshev, V. N. (2003) Characterization of mammalian selenoproteomes. *Science* **300**, 1439-1443

22. Gonzalez-Flores, J. N., Gupta, N., DeMong, L. W., and Copeland, P. R. (2012) The selenocysteine-specific elongation factor contains a novel and multi-functional domain. *J Biol Chem* **287**, 38936-38945
23. Copeland, P. R., Stepanik, V. A., and Driscoll, D. M. (2001) Insight into mammalian selenocysteine insertion: domain structure and ribosome binding properties of Sec insertion sequence binding protein 2. *Mol Cell Biol* **21**, 1491-1498
24. Howard, M. T., Moyle, M. W., Aggarwal, G., Carlson, B. A., and Anderson, C. B. (2007) A recoding element that stimulates decoding of UGA codons by Sec tRNA[Ser]Sec. *RNA* **13**, 912-920
25. Foster, C. B. (2005) Selenoproteins and the metabolic features of the archaeal ancestor of eukaryotes. *Mol Biol Evol* **22**, 383-386
26. Mix, H., Lobanov, A. V., and Gladyshev, V. N. (2007) SECIS elements in the coding regions of selenoprotein transcripts are functional in higher eukaryotes. *Nucleic Acids Res* **35**, 414-423
27. Diamond, A. M. (2015) The subcellular location of selenoproteins and the impact on their function. *Nutrients* **7**, 3938-3948
28. Lubos, E., Loscalzo, J., and Handy, D. E. (2011) Glutathione peroxidase-1 in health and disease: from molecular mechanisms to therapeutic opportunities. *Antioxid Redox Signal* **15**, 1957-1997
29. Arthur, J. R. (2000) The glutathione peroxidases. *Cell Mol Life Sci* **57**, 1825-1835
30. Gijon, M. A., and Leslie, C. C. (1999) Regulation of arachidonic acid release and cytosolic phospholipase A2 activation. *J Leukoc Biol* **65**, 330-336
31. Papp, L. V., Lu, J., Holmgren, A., and Khanna, K. K. (2007) From selenium to selenoproteins: synthesis, identity, and their role in human health. *Antioxid Redox Signal* **9**, 775-806
32. Banning, A., Florian, S., Deubel, S., Thalmann, S., Muller-Schmehl, K., Jacobasch, G., and Brigelius-Flohe, R. (2008) GPx2 counteracts PGE2 production by dampening COX-2 and mPGES-1 expression in human colon cancer cells. *Antioxid Redox Signal* **10**, 1491-1500
33. Emmink, B. L., Laoukili, J., Kipp, A. P., Koster, J., Govaert, K. M., Fatrai, S., Verheem, A., Steller, E. J., Brigelius-Flohe, R., Jimenez, C. R., Borel Rinkes, I. H., and Kranenburg, O. (2014) GPx2 suppression of H2O2 stress links the formation of differentiated tumor mass to metastatic capacity in colorectal cancer. *Cancer Res* **74**, 6717-6730
34. Olson, G. E., Whitin, J. C., Hill, K. E., Winfrey, V. P., Motley, A. K., Austin, L. M., Deal, J., Cohen, H. J., and Burk, R. F. (2010) Extracellular glutathione peroxidase (Gpx3) binds specifically to basement membranes of mouse renal cortex tubule cells. *Am J Physiol Renal Physiol* **298**, F1244-1253
35. Zmorzynski, S., Swiderska-Kolacz, G., Koczkodaj, D., and Filip, A. A. (2015) Significance of Polymorphisms and Expression of Enzyme-Encoding Genes Related to Glutathione in Hematopoietic Cancers and Solid Tumors. *Biomed Res Int* **2015**, 853573
36. Ingold, I., Aichler, M., Yefremova, E., Roveri, A., Buday, K., Doll, S., Tasdemir, A., Hoffard, N., Wurst, W., Walch, A., Ursini, F., Friedmann Angeli, J. P., and

Conrad, M. (2015) Expression of a Catalytically Inactive Mutant Form of Glutathione Peroxidase 4 (Gpx4) Confers a Dominant-negative Effect in Male Fertility. *J Biol Chem* **290**, 14668-14678

37. Smith, A. C., Mears, A. J., Bunker, R., Ahmed, A., MacKenzie, M., Schwartzentruber, J. A., Beaulieu, C. L., Ferretti, E., Consortium, F. C., Majewski, J., Bulman, D. E., Celik, F. C., Boycott, K. M., and Graham, G. E. (2014) Mutations in the enzyme glutathione peroxidase 4 cause Sedaghatian-type spondylometaphyseal dysplasia. *J Med Genet* **51**, 470-474
38. R.F. Burk, a. K. E. K. (2010) Glutathione Peroxidases. *Comprehensive Toxicology* **4**, 229-242
39. Jakupoglu, C., Przemeck, G. K., Schneider, M., Moreno, S. G., Mayr, N., Hatzopoulos, A. K., de Angelis, M. H., Wurst, W., Bornkamm, G. W., Brielmeier, M., and Conrad, M. (2005) Cytoplasmic thioredoxin reductase is essential for embryogenesis but dispensable for cardiac development. *Mol Cell Biol* **25**, 1980-1988
40. Marcus Conrad, G. W. B., and Markus Brielmeier. (2006) *Mitochondrial and cytosolic thioredoxin reductase knockout mice.* , 2 ed., Springer, Boston, MA
41. Su, D., Novoselov, S. V., Sun, Q. A., Moustafa, M. E., Zhou, Y., Oko, R., Hatfield, D. L., and Gladyshev, V. N. (2005) Mammalian selenoprotein thioredoxin-glutathione reductase. Roles in disulfide bond formation and sperm maturation. *J Biol Chem* **280**, 26491-26498
42. Panicker, V. (2011) Genetics of thyroid function and disease. *Clin Biochem Rev* **32**, 165-175
43. Williams, G. R., and Bassett, J. H. (2011) Deiodinases: the balance of thyroid hormone: local control of thyroid hormone action: role of type 2 deiodinase. *J Endocrinol* **209**, 261-272
44. Salvatore, D., Tu, H., Harney, J. W., and Larsen, P. R. (1996) Type 2 iodothyronine deiodinase is highly expressed in human thyroid. *J Clin Invest* **98**, 962-968
45. Peeters, R. P., and Visser, T. J. (2000) Metabolism of Thyroid Hormone. in *Endotext* (De Groot, L. J., Chrousos, G., Dungan, K., Feingold, K. R., Grossman, A., Hershman, J. M., Koch, C., Korbonits, M., McLachlan, R., New, M., Purnell, J., Rebar, R., Singer, F., and Vinik, A. eds.), South Dartmouth (MA). pp
46. Shchedrina, V. A., Everley, R. A., Zhang, Y., Gygi, S. P., Hatfield, D. L., and Gladyshev, V. N. (2011) Selenoprotein K binds multiprotein complexes and is involved in the regulation of endoplasmic reticulum homeostasis. *J Biol Chem* **286**, 42937-42948
47. Meiler, S., Baumer, Y., Huang, Z., Hoffmann, F. W., Fredericks, G. J., Rose, A. H., Norton, R. L., Hoffmann, P. R., and Boisvert, W. A. (2013) Selenoprotein K is required for palmitoylation of CD36 in macrophages: implications in foam cell formation and atherogenesis. *J Leukoc Biol* **93**, 771-780
48. Fredericks, G. J., Hoffmann, F. W., Rose, A. H., Osterheld, H. J., Hess, F. M., Mercier, F., and Hoffmann, P. R. (2014) Stable expression and function of the inositol 1,4,5-triphosphate receptor requires palmitoylation by a DHHC6/selenoprotein K complex. *Proc Natl Acad Sci U S A* **111**, 16478-16483

49. Norton, R. L., Fredericks, G. J., Huang, Z., Fay, J. D., Hoffmann, F. W., and Hoffmann, P. R. (2017) Selenoprotein K regulation of palmitoylation and calpain cleavage of ASAP2 is required for efficient FcgammaR-mediated phagocytosis. *J Leukoc Biol* **101**, 439-448
50. Huang, S. C., Everts, B., Ivanova, Y., O'Sullivan, D., Nascimento, M., Smith, A. M., Beatty, W., Love-Gregory, L., Lam, W. Y., O'Neill, C. M., Yan, C., Du, H., Abumrad, N. A., Urban, J. F., Jr., Artyomov, M. N., Pearce, E. L., and Pearce, E. J. (2014) Cell-intrinsic lysosomal lipolysis is essential for alternative activation of macrophages. *Nat Immunol* **15**, 846-855
51. Korotkov, K. V., Kumaraswamy, E., Zhou, Y., Hatfield, D. L., and Gladyshev, V. N. (2001) Association between the 15-kDa selenoprotein and UDP-glucose:glycoprotein glucosyltransferase in the endoplasmic reticulum of mammalian cells. *J Biol Chem* **276**, 15330-15336
52. Reeves, M. A., Bellinger, F. P., and Berry, M. J. (2010) The neuroprotective functions of selenoprotein M and its role in cytosolic calcium regulation. *Antioxid Redox Signal* **12**, 809-818
53. Castets, P., Lescure, A., Guicheney, P., and Allamand, V. (2012) Selenoprotein N in skeletal muscle: from diseases to function. *J Mol Med (Berl)* **90**, 1095-1107
54. Dikiy, A., Novoselov, S. V., Fomenko, D. E., Sengupta, A., Carlson, B. A., Cerny, R. L., Ginalski, K., Grishin, N. V., Hatfield, D. L., and Gladyshev, V. N. (2007) SelT, SelW, SelH, and Rdx12: genomics and molecular insights into the functions of selenoproteins of a novel thioredoxin-like family. *Biochemistry* **46**, 6871-6882
55. Whanger, P. D. (2009) Selenoprotein expression and function-selenoprotein W. *Biochim Biophys Acta* **1790**, 1448-1452
56. Raman, A. V., Pitts, M. W., Seyedali, A., Hashimoto, A. C., Bellinger, F. P., and Berry, M. J. (2013) Selenoprotein W expression and regulation in mouse brain and neurons. *Brain Behav* **3**, 562-574
57. Jeon, Y. H., Park, Y. H., Lee, J. H., Hong, J. H., and Kim, I. Y. (2014) Selenoprotein W enhances skeletal muscle differentiation by inhibiting TAZ binding to 14-3-3 protein. *Biochim Biophys Acta* **1843**, 1356-1364
58. Loflin, J., Lopez, N., Whanger, P. D., and Kioussi, C. (2006) Selenoprotein W during development and oxidative stress. *J Inorg Biochem* **100**, 1679-1684
59. Novoselov, S. V., Kryukov, G. V., Xu, X. M., Carlson, B. A., Hatfield, D. L., and Gladyshev, V. N. (2007) Selenoprotein H is a nucleolar thioredoxin-like protein with a unique expression pattern. *J Biol Chem* **282**, 11960-11968
60. Cox, A. G., Tsomides, A., Kim, A. J., Saunders, D., Hwang, K. L., Evason, K. J., Heidel, J., Brown, K. K., Yuan, M., Lien, E. C., Lee, B. C., Nissim, S., Dickinson, B., Chhangawala, S., Chang, C. J., Asara, J. M., Houvras, Y., Gladyshev, V. N., and Goessling, W. (2016) Selenoprotein H is an essential regulator of redox homeostasis that cooperates with p53 in development and tumorigenesis. *Proc Natl Acad Sci U S A* **113**, E5562-5571
61. Wu, R. T., Cao, L., Chen, B. P., and Cheng, W. H. (2014) Selenoprotein H suppresses cellular senescence through genome maintenance and redox regulation. *J Biol Chem* **289**, 34378-34388

62. Prevost, G., Arabo, A., Jian, L., Quelennec, E., Cartier, D., Hassan, S., Falluel-Morel, A., Tanguy, Y., Gargani, S., Lihrmann, I., Kerr-Conte, J., Lefebvre, H., Pattou, F., and Anouar, Y. (2013) The PACAP-regulated gene selenoprotein T is abundantly expressed in mouse and human beta-cells and its targeted inactivation impairs glucose tolerance. *Endocrinology* **154**, 3796-3806
63. Boukhzar, L., Hamieh, A., Cartier, D., Tanguy, Y., Alsharif, I., Castex, M., Arabo, A., El Hajji, S., Bonnet, J. J., Errami, M., Falluel-Morel, A., Chagraoui, A., Lihrmann, I., and Anouar, Y. (2016) Selenoprotein T Exerts an Essential Oxidoreductase Activity That Protects Dopaminergic Neurons in Mouse Models of Parkinson's Disease. *Antioxid Redox Signal* **24**, 557-574
64. Saito, Y., Hayashi, T., Tanaka, A., Watanabe, Y., Suzuki, M., Saito, E., and Takahashi, K. (1999) Selenoprotein P in human plasma as an extracellular phospholipid hydroperoxide glutathione peroxidase. Isolation and enzymatic characterization of human selenoprotein p. *J Biol Chem* **274**, 2866-2871
65. Horibata, Y., and Hirabayashi, Y. (2007) Identification and characterization of human ethanolaminephosphotransferase1. *J Lipid Res* **48**, 503-508
66. Kryukov, G. V., Kumar, R. A., Koc, A., Sun, Z., and Gladyshev, V. N. (2002) Selenoprotein R is a zinc-containing stereo-specific methionine sulfoxide reductase. *Proc Natl Acad Sci U S A* **99**, 4245-4250
67. Kasaikina, M. V., Hatfield, D. L., and Gladyshev, V. N. (2012) Understanding selenoprotein function and regulation through the use of rodent models. *Biochim Biophys Acta* **1823**, 1633-1642
68. Han, S. J., Lee, B. C., Yim, S. H., Gladyshev, V. N., and Lee, S. R. (2014) Characterization of mammalian selenoprotein o: a redox-active mitochondrial protein. *PLoS One* **9**, e95518
69. Schomburg, L., and Schweizer, U. (2009) Hierarchical regulation of selenoprotein expression and sex-specific effects of selenium. *Biochim Biophys Acta* **1790**, 1453-1462
70. Berry, M. J. (2005) Insights into the hierarchy of selenium incorporation. *Nat Genet* **37**, 1162-1163
71. Bellinger, F. P., Raman, A. V., Reeves, M. A., and Berry, M. J. (2009) Regulation and function of selenoproteins in human disease. *Biochem J* **422**, 11-22
72. Bermano, G., Arthur, J. R., and Hesketh, J. E. (1996) Role of the 3' untranslated region in the regulation of cytosolic glutathione peroxidase and phospholipid-hydroperoxide glutathione peroxidase gene expression by selenium supply. *Biochem J* **320 (Pt 3)**, 891-895
73. Tsuji, P. A., Carlson, B. A., Anderson, C. B., Seifried, H. E., Hatfield, D. L., and Howard, M. T. (2015) Dietary Selenium Levels Affect Selenoprotein Expression and Support the Interferon-gamma and IL-6 Immune Response Pathways in Mice. *Nutrients* **7**, 6529-6549
74. Howard, M. T., Carlson, B. A., Anderson, C. B., and Hatfield, D. L. (2013) Translational redefinition of UGA codons is regulated by selenium availability. *J Biol Chem* **288**, 19401-19413

75. Berry, M. J., Banu, L., Harney, J. W., and Larsen, P. R. (1993) Functional characterization of the eukaryotic SECIS elements which direct selenocysteine insertion at UGA codons. *EMBO J* **12**, 3315-3322
76. Bubenik, J. L., Miniard, A. C., and Driscoll, D. M. (2014) Characterization of the UGA-recoding and SECIS-binding activities of SECIS-binding protein 2. *RNA Biol* **11**, 1402-1413
77. Martin, G. W., 3rd, Harney, J. W., and Berry, M. J. (1998) Functionality of mutations at conserved nucleotides in eukaryotic SECIS elements is determined by the identity of a single nonconserved nucleotide. *RNA* **4**, 65-73
78. Jones, G. D., Droz, B., Greve, P., Gottschalk, P., Poffet, D., McGrath, S. P., Seneviratne, S. I., Smith, P., and Winkel, L. H. (2017) Selenium deficiency risk predicted to increase under future climate change. *Proc Natl Acad Sci U S A* **114**, 2848-2853
79. Haug, A., Graham, R. D., Christophersen, O. A., and Lyons, G. H. (2007) How to use the world's scarce selenium resources efficiently to increase the selenium concentration in food. *Microb Ecol Health Dis* **19**, 209-228
80. https://ods.od.nih.gov/factsheets/Selenium-HealthProfessional/
81. Chen, J. (2012) An original discovery: selenium deficiency and Keshan disease (an endemic heart disease). *Asia Pac J Clin Nutr* **21**, 320-326
82. Liu, Y., Chiba, M., Inaba, Y., and Kondo, M. (2002) [Keshan disease--a review from the aspect of history and etiology]. *Nihon Eiseigaku Zasshi* **56**, 641-648
83. Thomson, C. D., and Robinson, M. F. (1980) Selenium in human health and disease with emphasis on those aspects peculiar to New Zealand. *Am J Clin Nutr* **33**, 303-323
84. Salonen, J. T., Alfthan, G., Huttunen, J. K., Pikkarainen, J., and Puska, P. (1982) Association between cardiovascular death and myocardial infarction and serum selenium in a matched-pair longitudinal study. *Lancet* **2**, 175-179
85. Yao, Y. F., Pei, F. X., Li, X. B., Yang, J., Shen, B., Zhou, Z. K., Li, L., and Kang, P. D. (2012) Preventive effects of supplemental selenium and selenium plus iodine on bone and cartilage development in rats fed with diet from Kashin-Beck disease endemic area. *Biol Trace Elem Res* **146**, 199-206
86. Yao, Y., Pei, F., and Kang, P. (2011) Selenium, iodine, and the relation with Kashin-Beck disease. *Nutrition* **27**, 1095-1100
87. Sudre, P., and Mathieu, F. (2001) Kashin-Beck disease: from etiology to prevention or from prevention to etiology? *Int Orthop* **25**, 175-179
88. Sun, G. X., Meharg, A. A., Li, G., Chen, Z., Yang, L., Chen, S. C., and Zhu, Y. G. (2016) Distribution of soil selenium in China is potentially controlled by deposition and volatilization? *Sci Rep* **6**, 20953
89. Tan, J., Zhu, W., Wang, W., Li, R., Hou, S., Wang, D., and Yang, L. (2002) Selenium in soil and endemic diseases in China. *Sci Total Environ* **284**, 227-235
90. Baum, M. K., Shor-Posner, G., Lai, S., Zhang, G., Lai, H., Fletcher, M. A., Sauberlich, H., and Page, J. B. (1997) High risk of HIV-related mortality is associated with selenium deficiency. *J Acquir Immune Defic Syndr Hum Retrovirol* **15**, 370-374

91. Beck, M. A., Levander, O. A., and Handy, J. (2003) Selenium deficiency and viral infection. *J Nutr* **133**, 1463S-1467S
92. Barrett, C. W., Singh, K., Motley, A. K., Lintel, M. K., Matafonova, E., Bradley, A. M., Ning, W., Poindexter, S. V., Parang, B., Reddy, V. K., Chaturvedi, R., Fingleton, B. M., Washington, M. K., Wilson, K. T., Davies, S. S., Hill, K. E., Burk, R. F., and Williams, C. S. (2013) Dietary selenium deficiency exacerbates DSS-induced epithelial injury and AOM/DSS-induced tumorigenesis. *PLoS One* **8**, e67845
93. Bamshad, M., and Wooding, S. P. (2003) Signatures of natural selection in the human genome. *Nat Rev Genet* **4**, 99-111
94. Voight, B. F., Kudaravalli, S., Wen, X., and Pritchard, J. K. (2006) A map of recent positive selection in the human genome. *PLoS Biol* **4**, e72
95. Romagne, F., Santesmasses, D., White, L., Sarangi, G. K., Mariotti, M., Hubler, R., Weihmann, A., Parra, G., Gladyshev, V. N., Guigo, R., and Castellano, S. (2014) SelenoDB 2.0: annotation of selenoprotein genes in animals and their genetic diversity in humans. *Nucleic Acids Res* **42**, D437-443
96. Meplan, C., Hughes, D. J., Pardini, B., Naccarati, A., Soucek, P., Vodickova, L., Hlavata, I., Vrana, D., Vodicka, P., and Hesketh, J. E. (2010) Genetic variants in selenoprotein genes increase risk of colorectal cancer. *Carcinogenesis* **31**, 1074-1079
97. Meplan, C., and Hesketh, J. (2012) The influence of selenium and selenoprotein gene variants on colorectal cancer risk. *Mutagenesis* **27**, 177-186
98. Haug, U., Poole, E. M., Xiao, L., Curtin, K., Duggan, D., Hsu, L., Makar, K. W., Peters, U., Kulmacz, R. J., Potter, J. D., Koepl, L., Caan, B. J., Slattery, M. L., and Ulrich, C. M. (2012) Glutathione peroxidase tagSNPs: associations with rectal cancer but not with colon cancer. *Genes Chromosomes Cancer* **51**, 598-605
99. Meplan, C., Crosley, L. K., Nicol, F., Beckett, G. J., Howie, A. F., Hill, K. E., Horgan, G., Mathers, J. C., Arthur, J. R., and Hesketh, J. E. (2007) Genetic polymorphisms in the human selenoprotein P gene determine the response of selenoprotein markers to selenium supplementation in a gender-specific manner (the SELGEN study). *FASEB J* **21**, 3063-3074
100. Meplan, C., Rohrmann, S., Steinbrecher, A., Schomburg, L., Jansen, E., Linseisen, J., and Hesketh, J. (2012) Polymorphisms in thioredoxin reductase and selenoprotein K genes and selenium status modulate risk of prostate cancer. *PLoS One* **7**, e48709
101. Meplan, C., Nicol, F., Burtle, B. T., Crosley, L. K., Arthur, J. R., Mathers, J. C., and Hesketh, J. E. (2009) Relative abundance of selenoprotein P isoforms in human plasma depends on genotype, se intake, and cancer status. *Antioxid Redox Signal* **11**, 2631-2640
102. Strauss, E., Oszkinis, G., and Staniszewski, R. (2014) SEPP1 gene variants and abdominal aortic aneurysm: gene association in relation to metabolic risk factors and peripheral arterial disease coexistence. *Sci Rep* **4**, 7061
103. Gentschew, L., Bishop, K. S., Han, D. Y., Morgan, A. R., Fraser, A. G., Lam, W. J., Karunasinghe, N., Campbell, B., and Ferguson, L. R. (2012) Selenium,

selenoprotein genes and Crohn's disease in a case-control population from Auckland, New Zealand. *Nutrients* **4**, 1247-1259

104. Schoenmakers, E., Agostini, M., Mitchell, C., Schoenmakers, N., Papp, L., Rajanayagam, O., Padidela, R., Ceron-Gutierrez, L., Doffinger, R., Prevosto, C., Luan, J., Montano, S., Lu, J., Castanet, M., Clemons, N., Groeneveld, M., Castets, P., Karbaschi, M., Aitken, S., Dixon, A., Williams, J., Campi, I., Blount, M., Burton, H., Muntoni, F., O'Donovan, D., Dean, A., Warren, A., Brierley, C., Baguley, D., Guicheney, P., Fitzgerald, R., Coles, A., Gaston, H., Todd, P., Holmgren, A., Khanna, K. K., Cooke, M., Semple, R., Halsall, D., Wareham, N., Schwabe, J., Grasso, L., Beck-Peccoz, P., Ogunko, A., Dattani, M., Gurnell, M., and Chatterjee, K. (2010) Mutations in the selenocysteine insertion sequence-binding protein 2 gene lead to a multisystem selenoprotein deficiency disorder in humans. *J Clin Invest* **120**, 4220-4235
105. Astudillo, A. M., Pérez-Chacón, G., Balboa, M. A., and Balsinde, J. (2009) Arachidonic acid mobilization by stimuli of the innate immune response. *Inmunología* **28**, 182-192
106. Gandhi, U. H., Kaushal, N., Ravindra, K. C., Hegde, S., Nelson, S. M., Narayan, V., Vunta, H., Paulson, R. F., and Prabhu, K. S. (2011) Selenoprotein-dependent up-regulation of hematopoietic prostaglandin D2 synthase in macrophages is mediated through the activation of peroxisome proliferator-activated receptor (PPAR) gamma. *J Biol Chem* **286**, 27471-27482
107. Vunta, H., Davis, F., Palempalli, U. D., Bhat, D., Arner, R. J., Thompson, J. T., Peterson, D. G., Reddy, C. C., and Prabhu, K. S. (2007) The anti-inflammatory effects of selenium are mediated through 15-deoxy-Delta12,14-prostaglandin J2 in macrophages. *J Biol Chem* **282**, 17964-17973
108. Narayan, V., Ravindra, K. C., Liao, C., Kaushal, N., Carlson, B. A., and Prabhu, K. S. (2015) Epigenetic regulation of inflammatory gene expression in macrophages by selenium. *J Nutr Biochem* **26**, 138-145
109. Ravindra, K. C., Narayan, V., Lushington, G. H., Peterson, B. R., and Prabhu, K. S. (2012) Targeting of histone acetyltransferase p300 by cyclopentenone prostaglandin Delta(12)-PGJ(2) through covalent binding to Cys(1438). *Chem Res Toxicol* **25**, 337-347
110. Rajakariar, R., Hilliard, M., Lawrence, T., Trivedi, S., Colville-Nash, P., Bellingan, G., Fitzgerald, D., Yaqoob, M. M., and Gilroy, D. W. (2007) Hematopoietic prostaglandin D2 synthase controls the onset and resolution of acute inflammation through PGD2 and 15-deoxyDelta12 14 PGJ2. *Proc Natl Acad Sci U S A* **104**, 20979-20984
111. Ruckrich, M. F., Schlegel, W., and Jung, A. (1976) Prostaglandin endoperoxide analogues and prostaglandid D2 as substrates of human placental 15-hydroxy prostaglandin dehydrogenase. *FEBS Lett* **68**, 59-62
112. Sun, F. F., Armour, S. B., Bockstanz, V. R., and McGuire, J. C. (1976) Studies on 15-hydroxyprostaglandin dehydrogenase from monkey lung. *Adv Prostaglandin Thromboxane Res* **1**, 163-169

113. Kaushal, N., Kudva, A. K., Patterson, A. D., Chiaro, C., Kennett, M. J., Desai, D., Amin, S., Carlson, B. A., Cantorna, M. T., and Prabhu, K. S. (2014) Crucial role of macrophage selenoproteins in experimental colitis. *J Immunol* **193**, 3683-3692
114. Langenbach, R., Loftin, C., Lee, C., and Tiano, H. (1999) Cyclooxygenase knockout mice: models for elucidating isoform-specific functions. *Biochem Pharmacol* **58**, 1237-1246
115. Fitzpatrick, F. A. (2004) Cyclooxygenase enzymes: regulation and function. *Curr Pharm Des* **10**, 577-588
116. Morita, I. (2002) Distinct functions of COX-1 and COX-2. *Prostaglandins Other Lipid Mediat* **68-69**, 165-175
117. Kang, Y. J., Mbonye, U. R., DeLong, C. J., Wada, M., and Smith, W. L. (2007) Regulation of intracellular cyclooxygenase levels by gene transcription and protein degradation. *Prog Lipid Res* **46**, 108-125
118. Williams, C. S., Mann, M., and DuBois, R. N. (1999) The role of cyclooxygenases in inflammation, cancer, and development. *Oncogene* **18**, 7908-7916
119. Mbonye, U. R., Wada, M., Rieke, C. J., Tang, H. Y., Dewitt, D. L., and Smith, W. L. (2006) The 19-amino acid cassette of cyclooxygenase-2 mediates entry of the protein into the endoplasmic reticulum-associated degradation system. *J Biol Chem* **281**, 35770-35778
120. Jiang, H., Harris, M. B., and Rothman, P. (2000) IL-4/IL-13 signaling beyond JAK/STAT. *J Allergy Clin Immunol* **105**, 1063-1070
121. Shuai, K., and Liu, B. (2003) Regulation of JAK-STAT signalling in the immune system. *Nat Rev Immunol* **3**, 900-911
122. Izuhara, K., Feldman, R. A., Greer, P., and Harada, N. (1994) Interaction of the c-fes proto-oncogene product with the interleukin-4 receptor. *J Biol Chem* **269**, 18623-18629
123. Jiang, H., Foltenyi, K., Kashiwada, M., Donahue, L., Vuong, B., Hehn, B., and Rothman, P. (2001) Fes mediates the IL-4 activation of insulin receptor substrate-2 and cellular proliferation. *J Immunol* **166**, 2627-2634
124. Izuhara, K., Feldman, R. A., Greer, P., and Harada, N. (1996) Interleukin-4 induces association of the c-fes proto-oncogene product with phosphatidylinositol-3 kinase. *Blood* **88**, 3910-3918
125. Byles, V., Covarrubias, A. J., Ben-Sahra, I., Lamming, D. W., Sabatini, D. M., Manning, B. D., and Horng, T. (2013) The TSC-mTOR pathway regulates macrophage polarization. *Nat Commun* **4**, 2834
126. Zhu, L., Yang, T., Li, L., Sun, L., Hou, Y., Hu, X., Zhang, L., Tian, H., Zhao, Q., Peng, J., Zhang, H., Wang, R., Yang, Z., Zhang, L., and Zhao, Y. (2014) TSC1 controls macrophage polarization to prevent inflammatory disease. *Nat Commun* **5**, 4696
127. Tyagi, S., Gupta, P., Saini, A. S., Kaushal, C., and Sharma, S. (2011) The peroxisome proliferator-activated receptor: A family of nuclear receptors role in various diseases. *J Adv Pharm Technol Res* **2**, 236-240
128. Adamson, R. (2009) Role of macrophages in normal wound healing: an overview. *J Wound Care* **18**, 349-351

129. Yang, J., Zhang, L., Yu, C., Yang, X. F., and Wang, H. (2014) Monocyte and macrophage differentiation: circulation inflammatory monocyte as biomarker for inflammatory diseases. *Biomark Res* **2**, 1
130. Sica, A., and Mantovani, A. (2012) Macrophage plasticity and polarization: in vivo veritas. *J Clin Invest* **122**, 787-795
131. Davies, L. C., Jenkins, S. J., Allen, J. E., and Taylor, P. R. (2013) Tissue-resident macrophages. *Nat Immunol* **14**, 986-995
132. Davies, L. C., and Taylor, P. R. (2015) Tissue-resident macrophages: then and now. *Immunology* **144**, 541-548
133. Yona, S., Kim, K. W., Wolf, Y., Mildner, A., Varol, D., Breker, M., Strauss-Ayali, D., Viukov, S., Guilliams, M., Misharin, A., Hume, D. A., Perlman, H., Malissen, B., Zelzer, E., and Jung, S. (2013) Fate mapping reveals origins and dynamics of monocytes and tissue macrophages under homeostasis. *Immunity* **38**, 79-91
134. Sheng, J., Ruedl, C., and Karjalainen, K. (2015) Most Tissue-Resident Macrophages Except Microglia Are Derived from Fetal Hematopoietic Stem Cells. *Immunity* **43**, 382-393
135. Haldar, M., and Murphy, K. M. (2014) Origin, development, and homeostasis of tissue-resident macrophages. *Immunol Rev* **262**, 25-35
136. Hashimoto, D., Chow, A., Noizat, C., Teo, P., Beasley, M. B., Leboeuf, M., Becker, C. D., See, P., Price, J., Lucas, D., Greter, M., Mortha, A., Boyer, S. W., Forsberg, E. C., Tanaka, M., van Rooijen, N., Garcia-Sastre, A., Stanley, E. R., Ginhoux, F., Frenette, P. S., and Merad, M. (2013) Tissue-resident macrophages self-maintain locally throughout adult life with minimal contribution from circulating monocytes. *Immunity* **38**, 792-804
137. Medzhitov, R. (2008) Origin and physiological roles of inflammation. *Nature* **454**, 428-435
138. Davies, L. C., Rosas, M., Jenkins, S. J., Liao, C. T., Scurr, M. J., Brombacher, F., Fraser, D. J., Allen, J. E., Jones, S. A., and Taylor, P. R. (2013) Distinct bone marrow-derived and tissue-resident macrophage lineages proliferate at key stages during inflammation. *Nat Commun* **4**, 1886
139. Gundra, U. M., Girgis, N. M., Ruckerl, D., Jenkins, S., Ward, L. N., Kurtz, Z. D., Wiens, K. E., Tang, M. S., Basu-Roy, U., Mansukhani, A., Allen, J. E., and Loke, P. (2014) Alternatively activated macrophages derived from monocytes and tissue macrophages are phenotypically and functionally distinct. *Blood* **123**, e110-122
140. Martinez, F. O., and Gordon, S. (2014) The M1 and M2 paradigm of macrophage activation: time for reassessment. *F1000Prime Rep* **6**, 13
141. Martinez, F. O., Helming, L., and Gordon, S. (2009) Alternative activation of macrophages: an immunologic functional perspective. *Annu Rev Immunol* **27**, 451-483
142. Arango Duque, G., and Descoteaux, A. (2014) Macrophage cytokines: involvement in immunity and infectious diseases. *Front Immunol* **5**, 491
143. Allavena, P., Sica, A., Solinas, G., Porta, C., and Mantovani, A. (2008) The inflammatory micro-environment in tumor progression: the role of tumor-associated macrophages. *Crit Rev Oncol Hematol* **66**, 1-9

144. Nelson, S. M., Lei, X., and Prabhu, K. S. (2011) Selenium levels affect the IL-4-induced expression of alternative activation markers in murine macrophages. *J Nutr* **141**, 1754-1761
145. Tang, D., Kang, R., Coyne, C. B., Zeh, H. J., and Lotze, M. T. (2012) PAMPs and DAMPs: signal 0s that spur autophagy and immunity. *Immunol Rev* **249**, 158-175
146. Serhan, C. N., Yacoubian, S., and Yang, R. (2008) Anti-inflammatory and proresolving lipid mediators. *Annu Rev Pathol* **3**, 279-312
147. Buckley, C. D., Gilroy, D. W., Serhan, C. N., Stockinger, B., and Tak, P. P. (2013) The resolution of inflammation. *Nat Rev Immunol* **13**, 59-66
148. Serhan, C. N., Brain, S. D., Buckley, C. D., Gilroy, D. W., Haslett, C., O'Neill, L. A., Perretti, M., Rossi, A. G., and Wallace, J. L. (2007) Resolution of inflammation: state of the art, definitions and terms. *FASEB J* **21**, 325-332
149. Serhan, C. N. (2014) Novel Pro-Resolving Lipid Mediators in Inflammation Are Leads for Resolution Physiology. *Nature* **510**, 92-101
150. http://www.who.int/mediacentre/factsheets/fs366/en/
151. Geerts, S., and Gryseels, B. (2000) Drug resistance in human helminths: current situation and lessons from livestock. *Clin Microbiol Rev* **13**, 207-222
152. Camberis, M., Le Gros, G., and Urban, J., Jr. (2003) Animal model of Nippostrongylus brasiliensis and Heligmosomoides polygyrus. *Curr Protoc Immunol* **Chapter 19**, Unit 19 12
153. Allen, J. E., and Maizels, R. M. (2011) Diversity and dialogue in immunity to helminths. *Nat Rev Immunol* **11**, 375-388
154. Chen, F., Liu, Z., Wu, W., Rozo, C., Bowdridge, S., Millman, A., Van Rooijen, N., Urban, J. F., Jr., Wynn, T. A., and Gause, W. C. (2012) An essential role for TH2-type responses in limiting acute tissue damage during experimental helminth infection. *Nat Med* **18**, 260-266
155. Jenkins, S. J., Ruckerl, D., Cook, P. C., Jones, L. H., Finkelman, F. D., van Rooijen, N., MacDonald, A. S., and Allen, J. E. (2011) Local macrophage proliferation, rather than recruitment from the blood, is a signature of TH2 inflammation. *Science* **332**, 1284-1288
156. Reece, J. J., Siracusa, M. C., and Scott, A. L. (2006) Innate immune responses to lung-stage helminth infection induce alternatively activated alveolar macrophages. *Infect Immun* **74**, 4970-4981
157. Stein, M., Keshav, S., Harris, N., and Gordon, S. (1992) Interleukin 4 potently enhances murine macrophage mannose receptor activity: a marker of alternative immunologic macrophage activation. *J Exp Med* **176**, 287-292
158. Kreider, T., Anthony, R. M., Urban, J. F., Jr., and Gause, W. C. (2007) Alternatively activated macrophages in helminth infections. *Curr Opin Immunol* **19**, 448-453
159. Smith, A., Madden, K. B., Yeung, K. J., Zhao, A., Elfrey, J., Finkelman, F., Levander, O., Shea-Donohue, T., and Urban, J. F., Jr. (2005) Deficiencies in selenium and/or vitamin E lower the resistance of mice to Heligmosomoides polygyrus infections. *J Nutr* **135**, 830-836

160. Smith, A. D., Cheung, L., Beshah, E., Shea-Donohue, T., and Urban, J. F., Jr. (2013) Selenium status alters the immune response and expulsion of adult Heligmosomoides bakeri worms in mice. *Infect Immun* **81**, 2546-2553

Chapter 2

Selenoprotein expression in macrophages is critical for optimal clearance of parasitic helminth *Nippostrongylus brasiliensis*

Published in The Journal of Biological Chemistry.

J Biol Chem. 2016 Feb 5;291(6):2787-98. Doi: 10.1074/jbc.M115.684738 [Epub 2015 Dec 7.]

Shakira M. Nelson[1,2*], Ashley E. Shay[1*], Jamaal L. James[1], Bradley A. Carlson[3], Joseph F. Urban Jr.[4], and K. Sandeep Prabhu[1].

* Both authors contributed equally.

Affiliations: [1]Center for Molecular Immunology and Infectious Disease and Center for Molecular Toxicology and Carcinogenesis, Department of Veterinary and Biomedical Sciences, The Pennsylvania State University, University Park, Pennsylvania 16802. [2]Division of Cancer Epidemiology and Genetics, NCI, National Institutes of Health, Rockville, Maryland 20850, [3]Molecular Biology of Selenium Section, Mouse Cancer Genetics Program, NCI, National Institutes of Health, Bethesda, Maryland 20892, and [4]United States Department of Agriculture, Agriculture Research Service, Beltsville Human Nutrition Research Center, Diet, Genomics, and Immunology Laboratory, Beltsville, Maryland 20705

Contributions: SMN and KSP conceived and coordinated the study and wrote the manuscript. SMN designed, performed, and analyzed the data shown in Figs 2.1 to 2.6. AES contributed to the preparation of the manuscript, examined gene expression in Fig 2.1F and Fig 2.3F to Fig 2.3I, and performed and analyzed the data shown in Fig 2.4A, Fig 2.4G, Fig 2.4H, Fig 2.5B to Fig 2.5F, and Fig 2.6E, LC-MS/MS analysis of Δ^{12}-PGJ_2, and *in vivo* treatment with 16,16-dimethyl-prostaglandin E_2. JLJ provided technical assistance with Fig 2.2. BAC provided mice and contributed to the preparation of the manuscript. JFU provided L3 helminth larvae and contributed to the preparation of the manuscript. All authors reviewed the results and approved the final version of the manuscript.

Abstract

The plasticity of macrophages is evident in helminthic parasite infections, providing protection from inflammation. Previously we demonstrated that the micronutrient selenium induces a phenotypic switch in macrophage activation from a classically activated (pro-inflammatory; M1) toward an alternatively activated (anti-inflammatory; M2) phenotype, where cyclooxygenase (Cox)-dependent cyclopentenone prostaglandin J_2 (15d-PGJ_2) plays a key role. Here, we hypothesize that dietary selenium modulates macrophage polarization toward a M2 phenotype to assist in the increasing clearance of adult *Nippostrongylus brasiliensis*, a gastrointestinal nematode parasite. Mice on a selenium-adequate (0.08 ppm) diet significantly augmented intestinal M2 presence while decreasing adult worms and fecal egg production when compared with infection of mice on selenium-deficient (<0.01 ppm) diet. Further increase in dietary selenium to supraphysiological levels (0.4 ppm) had very little or no impact on worm expulsion. Normal adult worm clearance and enhanced M2 gene expression were observed in the selenium-supplemented $Trsp^{fl/fl}LysM^{WT}$ mice that express selenoproteins driven by $tRNA^{Sec}$ (*Trsp*), whereas *N.brasiliensis*-infected $Trsp^{fl/fl}LysM^{Cre}$ selenium-supplemented mice showed a decreased clearance, with lowered intestinal expression of several M2 genes. Inhibition of the Cox pathway with indomethacin resulted in delayed worm expulsion in selenium-adequate mice. This was rescued with 15d-PGJ_2, which partially recapitulated the effect of selenium supplementation on fecal egg output in addition to increasing markers of M2 in the small intestine. Antagonism of Ppar-γ blocked the effect of selenium. These results suggest that optimal expression of

selenoproteins and selenium-dependent production of Cox-derived endogenous prostanoids, such as Δ^{12}-PGJ_2 and 15d-PGJ_2, may regulate M2 activation to enhance anti-helminthic parasite responses.

Introduction

The gastrointestinal nematode parasite *Nippostrongylus brasiliensis*, whose life cycle closely resembles that of human hookworm *Ancylostoma duodenale*, has a short infection cycle, with infective larvae invading through the skin followed by migration to the lungs and small intestine where they mature into adult worms, after which they are cleared from the body (1). In general, gastrointestinal parasites infect over 3.5 billion people worldwide, with severe infections often affecting children in underdeveloped and developing countries, leading to developmental and cognitive impairment. Recent studies have indicated dietary selenium deficiency exacerbates parasite pathogenesis and prolongs infection and disease (2, 3); however, the underlying mechanisms have not been elucidated.

The trace element selenium is a key component in immune responses to helminth infections (4). Selenium is an essential micronutrient that exists in the form of diverse metabolites and selenoproteins within the body (5-8). Selenoproteins exhibit disulfide oxidoreductase, peroxidase, and deiodinase activities in addition to other functions such as regulation of intracellular calcium flux and protein palmitoylation (9). Previous studies have shown that selenium exerts an anti-inflammatory effect by down-regulating the expression of pro-inflammatory mediators (10). Selenoprotein synthesis involves

enzymatic incorporation of selenium as the 21st amino acid, selenocysteine (Sec), by a complex process that is driven by *Trsp* that encodes $tRNA^{Sec}$ (8,11). Targeted deletion of the floxed *Trsp* allele by a tissue/cell-specific promoter-driven Cre recombinase markedly diminished expression of all selenoproteins (12). Substitution of Sec residue with Cys in some selenoproteins has been observed during selenium deficiency, which also markedly reduces their enzymatic activity (13,14).

Infections with intestinal parasites such as *N.brasiliensis* are characterized by a rapid and biased Th2-type response, producing elevated levels of interleukin (IL)-4 and IL-13 (15-18). These cytokines are thought to play a major role in intestinal physiology, causing rapid expulsion of parasites from the intestine (17,19-22). Interestingly, a robust Th2 response inhibits the generation of a Th1 response, protecting the host from excess inflammation (23-25) as well as priming the intestine for increased infiltration of macrophages, basophils, and eosinophils (17,26). As one of the most abundant immune cells in the gut mucosa, macrophages play a fundamental role in host defense to helminthic parasites (17,19,20,27).

Based on gene expression patterns, macrophages are often classified to belong to classically activated (M1) or alternatively activated (M2) phenotype, which represent two ends of a spectrum with poorly defined intermediate stages (17,28,29). As seen in a variety of helminthic parasite infections, M2 macrophages are induced by IL-4 and IL-13 (15,18,29). These cells express high levels of Fizz1, Arg1, and Ym1 (15,30). Of particular interest is the synergistic relationship between selenium and IL-4 to skew macrophage activation toward an M2-like phenotype, where selenoprotein expression was pivotal (7).

Herbert *et al.* (21) have reported that IL-4 and IL-13 can also induce the expression of Relm-β (resistin-like molecule-β) by goblet cells upon differentiation from intestinal epithelial cells to cause expulsion of *N.brasiliensis* and *Heligmosomoides polygyrus*. Although this report suggests a minimal role for macrophages, recent studies suggest that neutrophils are differentially activated in the context of a Th2 response to prime long-lived macrophages that effect rapid clearance of *N.brasiliensis* (31). Thus, it is clear that macrophages do have a role in optimal clearance of infection. Although the underlying mechanism of M2 macrophages in resistance to *N.brasiliensis* is not completely understood, studies have identified possible pathways involved. In the absence of Stat6, *N.brasiliensis* adult worms are not cleared effectively (24) due to a decrease in mucous secretion (19) and changes to intestinal physiology (17,32). In fact, Stat6 is well known to facilitate nuclear hormone receptor Ppar-γ-regulated gene expression in macrophages (33) that also plays a major role in M2 activation and resolution of inflammation (34-36). Along these lines, previous studies from our laboratory have established a significant deficit in selenium-dependent M2 polarization in the absence of Ppar-γ and Stat6 (7). Although a functional relationship between IL-4, IL-13, and Ppar-γ has yet to be established in *N.brasiliensis* infection, studies have demonstrated that increased activation of Ppar-γ via the production of its endogenous ligand in the form of cyclopentenone prostaglandins, Δ^{12}-PGJ_2 and 15d-PGJ_2, through selenium supplementation (37,38) polarizes macrophages toward an alternative phenotype (7). Interestingly, complete abrogation of the Cox-hematopoietic prostaglandin D_2 synthase (Hpgds) pathway inhibited endogenous cyclopentenone prostaglandins and consequent polarization of macrophages (7).

Although M2-dependent mechanisms of helminth clearance have been previously reported, there is limited mechanistic data on the relationship between selenoprotein expression and macrophages during helminth infections. Here we demonstrate that macrophage expression of selenoproteins regulate the arachidonic acid (AA)-Cox pathway to affect their polarization toward functional M2 macrophages that are associated with reduced number of adult nematode worms in the small intestine.

Materials and Methods

Mice

Three-week-old C57Bl/6 male mice were purchased from Charles River (Wilmington, MA) or Taconic Laboratories (Hudson, NY). Breeding pairs of IL-4 reporter mice (4Get mice) on a Balb/c background were generated by Dr. Richard M. Locksley (University of California, San Francisco, CA) and generously provided by Dr. Avery August (Cornell University, Ithaca, NY) (39,40). A transgenic C57BL/6 line carrying a lysozyme M Cre ($LysM^{Cre}$) transgene was crossed to a C57BL/6 mouse with a floxed *Trsp* ($Trsp^{fl/fl}$) allele, both generously provided by Dr. Dolph Hatfield (NIH, Bethesda, MD). These lines were crossed to obtain $Trsp^{fl/fl}LysM^{Cre}$ mice, as previously described (12). Targeted removal of the floxed *Trsp* allele by a Cre recombinase driven by the lysozyme M promoter disabled the expression of all selenoproteins in macrophages, monocytes, and some granulocytes (12). All mice were maintained on selenium-deficient (<0.01 ppm), selenium-adequate (0.08 ppm), or selenium-

supplemented diets (0.4 ppm) purchased from Harlan Teklad, Madison, WI, for at least 12 weeks before use in experiments. Selenium in the form of sodium selenite was used in selenium-adequate and selenium-supplemented diets. Studies were preapproved by the Institutional Animal Care and Use Committee and the Institutional Biosafety Committee at Penn State University.

Genotyping

The extent of *Trsp* deletion was determined by PCR analysis of the floxed region of the gene. Tail snips were taken from all mice. A mixture of 250 µl of lysis buffer and 5 µl of proteinase K (20 mg/ml, New England BioLabs, Ipswich, MA) was added to each tail snip and incubated overnight in a 65 °C water bath. Lysed tail snips were centrifuged at 20,800 × *g* for 5 min at 25 °C. Supernatants were collected and diluted (1:11) with diethyl pyrocarbonate water. PCR was carried out using 0.2 µM concentrations of primers, 2.5 mM $MgCl_2$, 0.2 mM concentrations of each deoxyribonucleotide triphosphate, 1.25 units of GoTaq DNA polymerase (Promega, Madison, WI), GoTaq buffer, and 1 µl of diluted DNA. To detect the transgene, two sets of primers were used as follows: primer set 1, CKNO2 (5′-GCAACGGCAGGTGTCGCTCTGCG-3′) and 8RP (5′-CGTGCTCTCTCCACTGGCTCA-3′) and primer set 2, Cre 8 (5′-CCCAGAAATGCCAGATTACG-3′), Mlys1 (5′-CTTGGGCTGGCCAGAATTTCTC-3′), and Mlys2 (5′-TTACAGTCGGCCAGGCTGAC-3′). The PCR products (*Trsp*$^{fl/fl}$, 1.1 kb; *Trsp*$^{fl/fl}$*LysM*^{Cre}, 700 bp; *Trsp*$^{fl/fl}$*LysM*^{WT}, 350 bp) were separated by electrophoresis on a 2% agarose gel and visualized by UV transillumination.

Infection of Mice with N.brasiliensis

Infective third stage larvae (L3) were maintained in a mixture of charcoal and lightly dampened *Sphagnum* moss and stored in plastic Petri dishes (1). Mice were subcutaneously inoculated with 500 L3 larvae in ~250 µl of PBS after collection from cultures using a modified Baermann's technique (1,24,41) and were studied on days 7, 8, 9, 11, and 14 post-infection. The timing of the studies correlated with the maximum effects of the parasite on gut function and coincided with ascending and descending egg production and worm expulsion (1,41). Fecal egg production was quantified using a modified McMaster technique (42), and adult worms were detected quantitatively by dissecting the intestine (below the stomach to above the cecum) lengthwise and submerging the tissue in a beaker of warm PBS using a tea strainer. The beaker was placed in a 37 °C water bath for 45 min. Remaining worms in the intestine tissue were counted using a microscope. Worms in suspension were counted on a gridded Petri plate.

Treatments

Indomethacin (Cayman Chemicals) was administered to mice in drinking water (containing 0.1% (v/v) ethanol) at a concentration of 0.00325% (w/v) (37) for two weeks before *N.brasiliensis* infection until two weeks post-infection, when the animals were euthanized. As a vehicle control, 0.1% ethanol (v/v) was used. Lipid extraction was performed from the jejunal tissue of indomethacin or vehicle-treated infected mice on day 8 post-infection, and LC-MS/MS was performed with multiple reaction monitoring (*m*/*z* 332.72 to 271.2) to quantify Δ^{12}-PGJ_2 as described earlier (37). Indomethacin

inhibited the production of Δ^{12}-PGJ_2 in the jejunum of infected mice day-8 post-infection, as indicated by LC-MS/MS (data not shown). 15d-PGJ_2 was administered daily at a concentration of 0.050 mg/kg/day (dissolved in sterile PBS) by intraperitoneal injection (~0.5 ml) for 7 days. Ppar-γ antagonist, GW9662 (Cayman Chemicals), was administered at 1 mg/kg body weight. GW9662 was dissolved in ethanol and diluted in sterile PBS (to 4% v/v) and intraperitoneally administered to selenium-adequate mice starting a day before infection with 500 larvae and continued each day during the 9-day period. Diluted ethanol in PBS was used as a vehicle control for comparison. The effect of GW9662 treatment on the jejunal expression of Ppar-γ target genes, *Arg1* and *Mrc1* (*Cd206*), was assessed using quantitative real time-PCR (qPCR) on day-8 post-infection as a measure of its *in vivo* efficacy. 16,16-dimethyl-prostaglandin E_2 (Cayman Chemicals) was formulated similarly in 4% (v/v) ethanol in PBS and injected at (10 μg/kg/day) starting simultaneously as infection with 500 larvae. The effect of indomethacin (2.5 μM) or GW9662 (1 μM) on the viability of L3 stage larvae as well as the viability and fecundity of adult worms was assessed after 12 hours of treatment in RPMI-1640 medium containing 10% FBS, 400 IU of penicillin, and 400 μg/ml streptomycin as described earlier (4,31). ATP levels were measured as an indicator of viability (metabolic activity) using the Promega CellTiter-Glo luminescent cell viability assay as described earlier (4,31).

qPCR

Total RNA was isolated from 1-mg sections of jejunum using Isol-RNA lysis reagent (5 Prime; Gaithersburg, MD). RNA concentrations were determined by UV spectroscopy. Briefly, 2 μg total RNA was reverse-transcribed into cDNA as previously described (7). TaqMan probes for *Arg1*, *Fizz1*, *Ym1*, *Mrc1* (*Cd206*), *Tnfa*, *Il1*β, *Inos*, and *Il-13* (from Applied Biosystems) were used to quantitate cDNA. As an internal control, a *Gapdh* probe was used to normalize the data. Amplifications were performed using PerfeCTa qPCR SuperMix Master Mix (Quanta Biosciences) in a 7300 Real time PCR system (Applied Biosystems). ΔC_t ($Ct_{Gene} - Ct_{GAPDH}$) was calculated for each sample and used for analysis of transcript abundance with respect to the untreated negative control.

Isolation of Epithelial Layer and Lamina Propria Lymphocytes from Small Intestine Tissue

Lymphocytes from the intestinal intra-epithelial lymphocyte and lamina propria were isolated as described (43). Briefly, small intestines were taken from mice nine days post-infection, and all Peyer's patches were removed. To isolate intra-epithelial lymphocytes, 20 ml of Hanks' buffer (Sigma) containing 1 mM DTT and 5 mM EDTA and one drop of 1 M HCl was added to tissues for 30 min and shaken at 250 rpm at 37 °C. This step was repeated until the supernatant became clear, each time collecting the supernatant and keeping it on ice. After the last wash, tissue pieces were rinsed in RPMI media to remove EDTA. To isolate lymphocytes from the lamina propria, tissues were

incubated in 30 ml of RPMI containing 300 mg of collagenase (300 units/ml) (Worthington Biochemical Corp., Lakewood, NJ) and 0.09 g of dispase (Sigma) for 1 h at 250 × *g* at 37 °C. After incubation, the supernatants were filtered using a mesh strainer (Fisher) into a fresh tube and centrifuged at 500 × *g* for 5 min at 4 °C. Lymphocyte pellets were resuspended in 40% Percoll and placed over an 80% Percoll mixture, creating a 40% (v/v)–80% (v/v) gradient. Tubes were centrifuged at 800 × *g* for 20 min at room temperature with the brake off. The lymphocyte interface between the gradients was collected into a new tube, and the cells were rinsed twice in flow buffer (pH 7.2; 50 ml of 10× PBS, 25 ml of FBS, and 2.5 ml sodium azide in a final volume of 500 ml with deionized water). A total of 500,000 cells were used for flow cytometric analysis.

Flow Cytometry

Cells isolated from the small intestine were washed in 1 ml of flow buffer (pH 7.2) and pelleted by centrifuging at 250 × *g* for 5 min at 4 °C. Pellets were resuspended in 100 μl of flow buffer containing F_c block (BD Biosciences) and stained with the following antibodies: PE-conjugated rabbit anti-mouse CD3, PE-Cy7™-conjugated anti-mouse CD11b (encoding integrin αM, Itgam), PE-conjugated rabbit anti-mouse Siglec-F antibodies (BD Pharmingen), rabbit anti-mouse Fizz1(Retlna1; Relmα) and rabbit anti-mouse Relmβ (Fizz2) (Peprotech, Rocky Hill, NJ), FITC-conjugated rat anti-mouse F4/80 (AbD Serotec, Raleigh, NC), PE-conjugated anti-mouse arginase-1, or FITC-conjugated anti-mouse CCR3 (R&D Systems) for 30 min at 4 °C in the dark. Cells were washed with 1 ml of flow buffer and centrifuged at 250 × *g* for 5 min. Unconjugated

primary antibody samples were stained with AF-647 goat anti-rabbit IgG secondary for 30 min at room temperature in the dark. For intracellular staining (Arg-1 or Fizz1), cells were fixed with 2% paraformaldehyde for 20 min and permeabilized for 15 min followed by staining. Stained cells were analyzed on a BD Accuri C6 Benchtop Cytometer using BD Accuri and FlowJo data analysis software programs (FlowJo, LLC, Ashland, OR). All data shown are compared with their respective isotype controls.

Myeloperoxidase Assay

Jejunum was homogenized in 50 mM potassium phosphate buffer (pH 6.0) and centrifuged. The pellet was resuspended in 50 mM potassium phosphate buffer containing 50 mM hexadecyltrimethylammonium bromide followed by sonication and centrifugation. 50 µl of supernatant was incubated with 1.45 ml of potassium phosphate buffer (pH 6.0) containing 0.167 mg/ml *o*-dianisidine dihydrochloride and 0.0005% hydrogen peroxide. Absorbance was measured at 460 nm every 30 s for 10 min. Activity of myeloperoxidase was calculated using the change in absorbance over time and the molar extinction coefficient of *o*-dianisidine.

Statistical Analysis

Results are presented as the mean ± S.E. To compare means, groups were analyzed using two-way ANOVA on GraphPad® Prism followed by appropriate post hoc

tests. Results were considered significantly different at p value ≤ 0.05. All experiments were performed in triplicate using at least three mice per experiment, for a total of $n = 9$.

Results

Effects of Dietary Selenium on Adult Worm Burden and Fecal Egg Production in N.brasiliensis-infected Mice

To determine the effects of dietary selenium on parasite clearance, mice fed either a selenium-deficient, selenium-adequate or selenium-supplemented diet were inoculated subcutaneously with 500 *N.brasiliensis* third-stage larvae (L3). Fecal eggs were isolated and quantified (1,24) on days 7, 8, 10, 11, and 14 post-infection. Compared with selenium-adequate- and selenium-supplemented mice, selenium-deficient mice had a significant increase in the number of eggs (**Fig 2.1A**). There was no significant difference in fecal eggs or number of adult worms between selenium-adequate- and selenium-supplemented mice throughout the infection (**Fig 2.1A-B**). However, selenium-deficient mice showed a significantly increased number of worms on days 7 and 8 post-infection (**Fig 2.1B**). Worm counts, however, began decreasing after day 8 post-infection, supporting previously published data (1,24).

Selenium Increases Intestinal M2 Macrophages in Response to Infection

The selenium-dependent mechanisms underlying increased anti-parasite effects were examined. It has been previously shown that mice utilize a biased Th2 response to

clear the *N.brasiliensis* infection from the intestine (15). Moreover, our previous data indicated a synergistic relationship between IL-4 and selenium as a key-contributing factor in the polarization of macrophages toward the M2 phenotype (7). To examine if selenium-dependent changes in M2 polarization were associated with a change in worm burden, we examined the expression of characteristic M2 genes *Arg1*, *Ym1*, and *Fizz1* in the jejunum of *N.brasiliensis*-infected mice as a function of dietary selenium. Jejunal tissue was collected on days 7, 8, and 11 post-infection (17). Expression of all three M2-associated genes were significantly higher in selenium-adequate- and selenium-supplemented mice compared with selenium-deficient mice starting on day 7 post-infection and increased further by day 8 post-infection followed by a significant decrease by day 11 post-infection, possibly related to worm clearance (**Fig 2.1C-E**). As expected, the expression of M1 genes, such as *Tnf*α, (**Fig 2.1F**) *Ifn*γ, and *Il1*β (not shown), were much lower than expression of M2 genes. The expression of all three M2 genes were significantly higher in all three diet groups in the *N.brasiliensis*-infected mice compared with their uninfected counterparts (**Fig 2.1G-I**), where *Arg1* and *Fizz1* increased with the selenium-adequate diet (*versus* selenium-deficient diet) but decreased with the selenium-supplemented diet, whereas *Ym1* increased with selenium-supplemented (*versus* selenium-deficient and selenium-adequate).

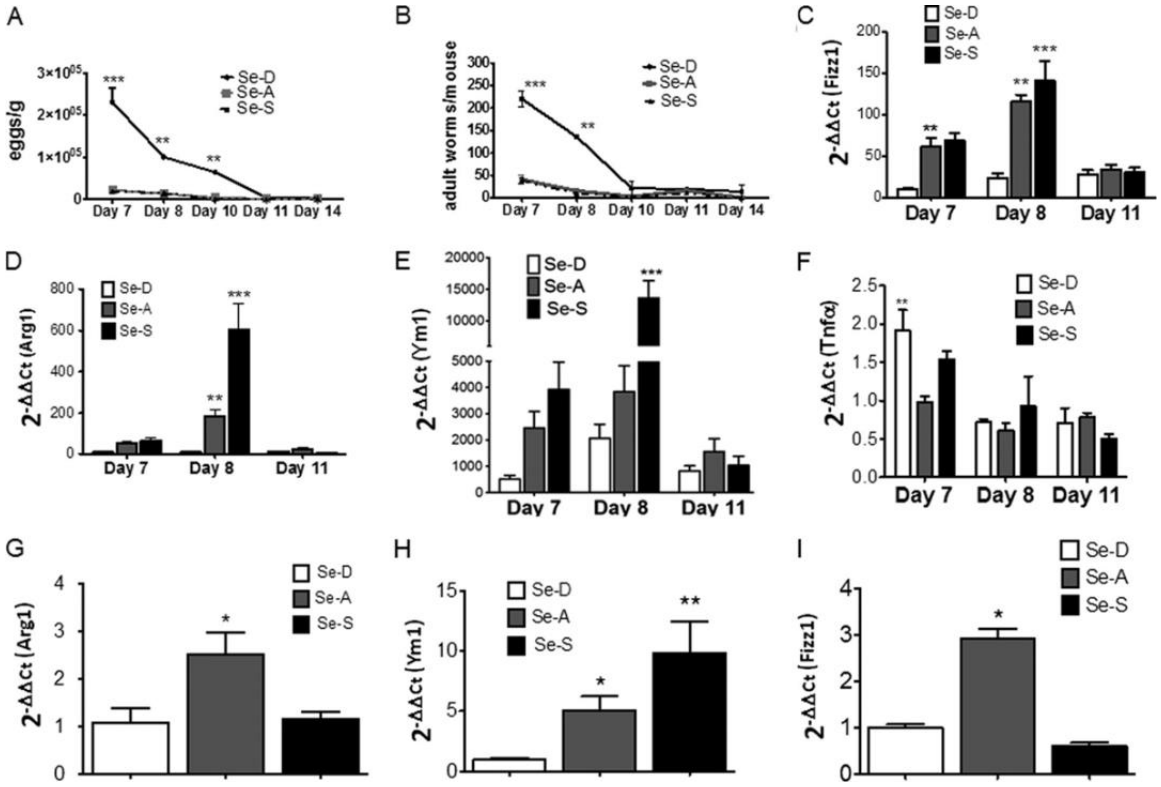

Figure 2.1: Effect of selenium on adult worm burden and M2 macrophage gene expression in *N.brasiliensis*-infected mice

*500 infective larvae were injected into selenium-deficient (Se-D), selenium-adequate (Se-A), and selenium-supplemented (Se-S) mice. In each panel, selenium-deficient mice are statistically compared with selenium-adequate and selenium-supplemented mice within each day. (**A**) Number of N.brasiliensis eggs per gram of feces from each mouse. (**B**) Number of adult worms per mouse in the whole small intestine (below the stomach to above the cecum) upon extraction. (**C-E**) qPCR analysis of the expression of Fizz1 (**C**), Arg1 (**D**), and Ym1 (**E**), and a M1 macrophage gene Tnfα (**F**) in the jejunum. (**G-I**), qPCR analysis of the expression of M2 macrophage genes Arg-I (**G**), Ym1 (**H**), and Fizz1 (**I**) in non-infected mice on selenium diets. Selenium-deficient mice are compared with selenium-adequate and selenium-supplemented mice. All data shown are the mean ± S.E., with a total of n = 9 mice used. Asterisks represent differences within days between diets. *, <0.05; **, <0.01; ***, <0.001 and were analysed using two-way ANOVA.*

To verify that the selenium-dependent increases in expression of M2 macrophage genes were associated with increased numbers of intestinal M2 macrophages after

infection, cells in the lamina propria were isolated at day 9 post-infection and analyzed by flow cytometry for F4/80^{+}and Fizz1^{+}-expressing cells, which mark M2 macrophages. Compared with non-infected mice, *N.brasiliensis* infection induced a significant increase in percentage of double positive M2 macrophages in all diet groups (**Fig 2.2A**). Moreover, the number of double-positive cells also increased when compared with non-infected cells (**Fig 2.2B**). Furthermore, selenium-adequate- and selenium-supplemented mice infected with *N.brasiliensis* led to a significantly greater percentage of double-positive cells when compared with selenium-deficient mice (**Fig 2.2A**). Taken together, these results suggest that selenium status increases in the presence of M2 macrophages in the intestine of infected mice.

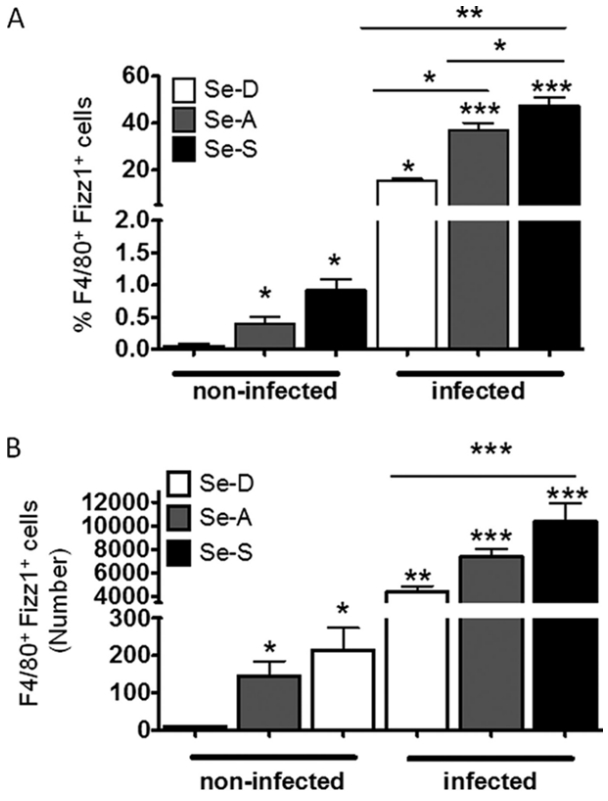

Figure 2.2: Increase in M2 macrophages in the lamina propria by selenium supplementation

*(**A-B**). Quantitation of F4/80^{+}Fizz1^{+} cells in the jejunum of N.brasiliensis-infected and uninfected control mice on the three diets. Bar graph percentages shown were calculated by averaging cell expression of F4/80 and Fizz1 from three separate flow cytometric experiments. All data shown are compared with isotype controls. Values are the mean ± S.E. with a total of n = 9 mice used. Across all groups mice are compared with non-infected selenium-deficient (Se-D) mice. Within the infected group, selenium-deficient mice were compared with both selenium-adequate (Se-A) and selenium-supplemented (Se-S) mice, indicated by the lines above each diet. Asterisks represent significant differences between groups. *, <0.05; **, <0.01; ***, <0.001 and were determined using two-way ANOVA with Tukey's post hoc testing.*

Selenoproteins Are Required for Optimal M2 Macrophage-induced Parasite Clearance

Recent studies from our laboratory have indicated a pivotal role for selenoproteins in the polarization of macrophage phenotypes (7). To determine the link between dietary selenium and cellular selenoproteins in parasite clearance, *Trsp$^{fl/fl}$LysM^{Cre}* mice were infected with *N.brasiliensis*. *Trsp$^{fl/fl}$LysM^{Cre}* mice fed a selenium-supplemented diet showed a significant increase in the amount of fecal eggs when compared with control *Trsp$^{fl/fl}$LysM^{WT}* mice at day 7 post-infection (**Fig 2.3A**). A similar pattern was also seen in the number of adult worms in the small intestine (**Fig 2.3B**). Fecal egg and adult worm burdens were diminished by day 11 post-infection in both strains of mice (**Fig 2.3A-B**). To determine the effect of *Trsp* deletion on M2 macrophage gene expression, we used qPCR to examine the modulation of M2 macrophage gene expression in the jejunum. A significant abrogation in the expression of *Arg1*, *Fizz1*, and *Ym1* was observed in *Trsp$^{fl/fl}$LysM^{Cre}* mice compared with *Trsp$^{fl/fl}$LysM^{WT}* mice at days 7, 8, and 11 post-infection (**Fig 2.3C-E**). Interestingly, expression of M1 macrophage genes, *Tnfα*, *Inos*, *Il-1β*, and *Ifnγ* were increased in the *Trsp$^{fl/fl}$LysM^{Cre}* mice, particularly on days 7 and 8 post-

infection compared with their *Trsp*$^{fl/fl}$*LysM*^{WT} counterparts (**Fig 2.3F-I**). Taken together, these data illustrate the essential role of selenoproteins in the optimal clearance of *N.brasiliensis*.

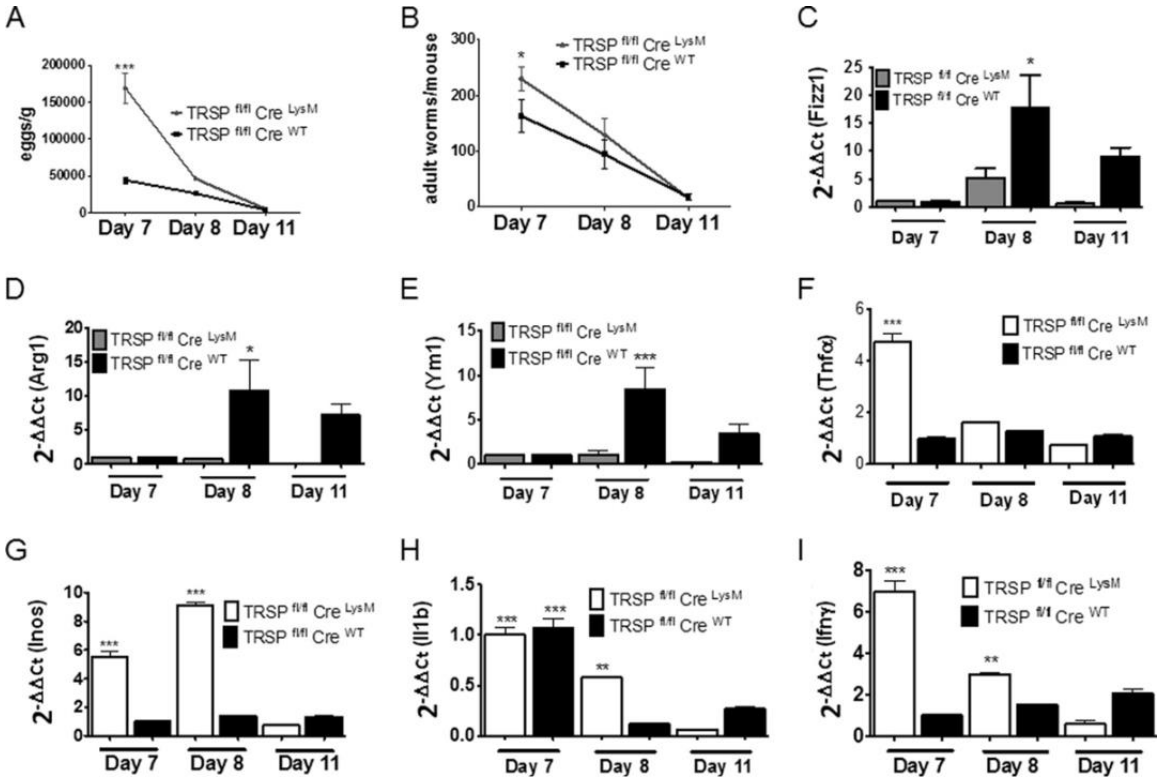

Figure 2.3: Selenoproteins are required for M2 macrophage gene expression and optimal *N.brasiliensis* clearance

Trsp$^{fl/fl}$*LysM*^{Cre} *and Trsp*$^{fl/fl}$*LysM*^{WT} *mice maintained on selenium-supplemented (Se-S) diets for 8–10 weeks were infected with 500 infective larvae. (**A**) Number of N.brasiliensis eggs per gram of feces from each mouse. (**B**) Worm burden in the whole small intestine upon extraction to count adult worms in the lumen of Trsp*$^{fl/fl}$*LysM*^{Cre} *and Trsp*$^{fl/fl}$*LysM*^{WT} *mice. (**C-E**) qPCR analysis of the expression of Fizz1 (**C**), Arg1 (**D**), and Ym1 (**E**). (**F-I**) expression of Tnfα (**F**), Inos (**G**), Il1β (**H**), and Ifnγ (**I**) in the jejunum of N.brasiliensis-infected Trsp*$^{fl/fl}$*LysM*^{Cre} *and Trsp*$^{fl/fl}$*LysM*^{WT} *mice. Values are the mean ± S.E., with a total of n = 9 mice used. Within each day Trsp*$^{fl/fl}$*LysM*^{Cre} *are statistically compared with Trsp*$^{fl/fl}$*LysM*^{WT} *mice. Asterisks represent significant differences between groups. *, <0.05; ***, < 0.001. Statistical differences were analysed using ANOVA with post hoc test.*

Essential Role of the Cyclooxygenase Pathway in Selenium-dependent Macrophage Polarization and Helminth Infection

Previous studies from our laboratory have demonstrated a selenium-dependent production of anti-inflammatory prostaglandin Δ^{12}-PGJ_2 and its dehydration product, 15d-PGJ_2, that serve as endogenous ligands for Ppar-γ in macrophages leading to the increase in M2 macrophage genes (38). Along these lines, qPCR analysis of the jejunal tissue on day 8 post-infection indicated a selenium-dependent increase in the expression of *Ptgs2* (Cox-2) and *Hpgds*, two critical enzymes required for the endogenous production of PGD_2-derived cyclopentenone prostaglandins, Δ^{12}-PGJ_2 and 15d-PGJ_2 (**Fig 2.4A**). To examine if selenium functions through a Cox-dependent pathway to modulate *N.brasiliensis* infection, we used indomethacin, a non-steroidal anti-inflammatory drug that inhibits Cox-derived biosynthesis of prostaglandins, including Δ^{12}-PGJ_2 and 15d-PGJ_2. LC-MS/MS analysis of jejunal extracts indicated a 6.6-fold decrease in the endogenous levels of Δ^{12}-PGJ_2 in selenium-adequate mice on day 8 post-infection upon treatment with indomethacin (data not shown). Inhibition of the Cox pathway significantly increased fecal eggs and adult worm burden on days 7 and 8 post-infection in selenium-adequate and selenium-supplemented mice compared with infected vehicle-treated mice (**Fig 2.4B-C**). However, incubation of L3 stage larvae or adult worms with indomethacin for 12 hours had no impact on the viability as seen in the form of ATP levels in addition to not affecting their fecundity (**Fig 2.4H**). Together, these results suggest the importance of the Cox-Hpgds pathway in selenium-dependent parasite clearance.

qPCR analysis was used to measure the effects of indomethacin on M2 and M1 macrophage gene expression in the jejunum of these mice. The selenium-dependent increases in *Fizz1*, *Arg1*, and *Ym1* expression in *N.brasiliensis*-infected mice on days 7 and 8 post-infection were blocked by treatment with indomethacin (**Fig 2.4D-F**). Conversely, the selenium-dependent inhibition of *Tnf*α expression (**Fig 2.4G**) was reversed with indomethacin treatment showing a significant increase in its expression on days 7, 8, and 11 post-infection. These data further demonstrate the importance of the Cox pathway in mediating the effects of selenium on the expression of M2 macrophage genes in the jejunum.

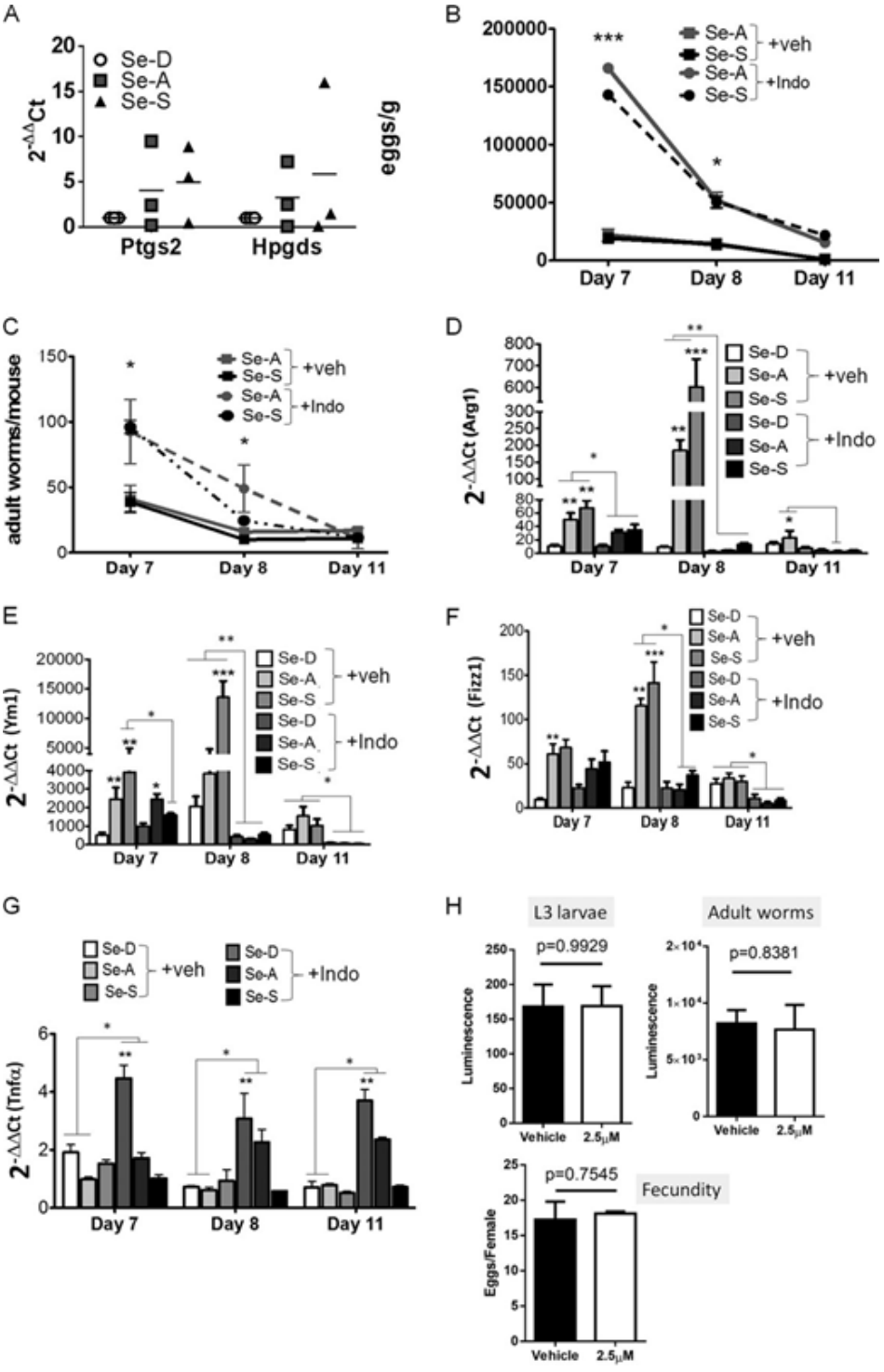

Figure 2.4: Involvement of the Cox pathway in *N.brasiliensis* clearance by selenium and its effect on the expression of M2 and M1 macrophage genes

*(**A**) Expression of Ptgs2 and Hpgds in the jejunum of selenium-deficient (Se-D), selenium-adequate (Se-A), and selenium-supplemented (Se-S) mice on day 8 post-infection by qPCR. Values are mean of n = 3 independent experiments from each diet group performed in triplicate. (**B-C**) Indomethacin (Indo) was administered to selenium-adequate and selenium-supplemented mice through drinking water (0.00325% w/v) for two weeks before infection through two weeks post-infection. Fecal eggs (**B**) and adult worms (**C**) were counted on days 7, 8, and 11 post-infection. All data are compared with vehicle-treated mice. Statistical differences comparing selenium-adequate and selenium-supplemented mice within each day were analysed using two-way ANOVA with Bonferroni (**B-C**). (**D-G**) qPCR was used to analyse expression of Arg1 (**D**), Ym1 (**E**), Fizz1 (**F**), and Tnfα (**G**) from the jejunum of N.brasiliensis-infected mice treated with 0.00325% (w/v) indomethacin for two weeks before infection and two weeks thereafter. Values are the mean ± S.E. with a total of n = 9 mice used. Two-way ANOVA with post hoc Bonferroni method was used to control for multiple comparisons between diet groups from vehicle- or indomethacin-treated mice as well as statistical differences comparing vehicle selenium-deficient mice to diet combinations within each day were analysed using Tukey's post hoc test. (**H**) Approximately five adult worms isolated from the small intestine of three infected C57BL/6 mice were plated per well in 0.2 ml of RPMI-1640 medium with 10% FBS and antibiotics and incubated overnight with indomethacin (2.5 μm) or vehicle at 37 °C. After incubation, female worms and eggs in the media were counted to assess the effect of indomethacin on fecundity. The number of eggs was normalized to the number of females per well. Similarly, 10 larvae were incubated as described above with indomethacin or vehicle. Adult worms and larvae were processed and used for chemiluminescence-based viability assay to detect ATP levels. As a negative control, adult worms or larvae in media were incubated at 80 °C for 5 min and homogenized with reagent after cooling. n = 3 per group. Unpaired two-tailed t test. Asterisks represent significant differences between groups. *, <0.05; **, <0.01.*

15-deoxy-prostaglandin J_2 Reduces Fecal Egg Shedding in N.brasiliensis-infected Mice

Based on the above data that demonstrated the selenium induction of macrophage polarization to be dependent on the Cox pathway, presumably mediated by 15d-PGJ_2-dependent mechanisms, we examined if exogenous treatment of selenium-deficient mice with 15d-PGJ_2 would recapitulate the protective effect of selenium. Indomethacin-treated selenium-deficient mice were administered 15d-PGJ_2 intraperitoneally (at 0.050 mg/kg/day) ~12 hours before infection with *N.brasiliensis*, and the treatment was

continued daily with 15d-PGJ_2 for a total of 7 days post-infection. As shown in **Fig 2.5A**, 15d-PGJ_2 treatment of selenium-deficient mice reduced fecal egg shedding on days 7 and 8 post-infection to levels below those seen in the untreated selenium-deficient control mice also on indomethacin (**Fig 2.5A**). Similar experiments were performed in selenium-adequate mice on indomethacin followed by treatment with 15d-PGJ_2 and infection (as above). Flow cytometric analyses of small intestinal tissue on days 7 and 8 post-infection indicated significantly increased $CD11b^+Arg\text{-}1^+$ cells in 15d-PGJ_2-treated groups on both days compared with the PBS control (**Fig 2.5B-C**). Furthermore, qPCR of prototypical genes (*Arg1*, *Ym1*, and *Fizz1*) in the small intestine were significantly increased by exogenous 15d-PGJ_2 treatment (data not shown). Given that 15d-PGJ_2 could partly mediate effects through Ppar-γ, we tested the role of a Ppar-γ antagonist, GW9662, in this model. Interestingly GW9662 treatment greatly increased the worm load in the jejunum (on day 8 post-infection) when compared with the vehicle control (**Fig 2.5D**). Although treatment of selenium-adequate mice with GW9662 reduced the expression of Ppar-γ target genes, *Mrc1* and *Arg1* (**Fig 2.5E**), *in vitro* studies showed that GW9662 had no effect on the viability of L3 stage larvae or adult worm or fecundity (**Fig 2.5F**). However, treatment of selenium-adequate mice with 16,16-dimethyl-prostaglandin E_2 had no affect the clearance of adult worms (data not shown).Together, these data suggest the importance of the Cox-Hpgds pathway in modulating parasite egg shedding, where Ppar-γ-dependent modulation of M2 macrophages is likely involved.

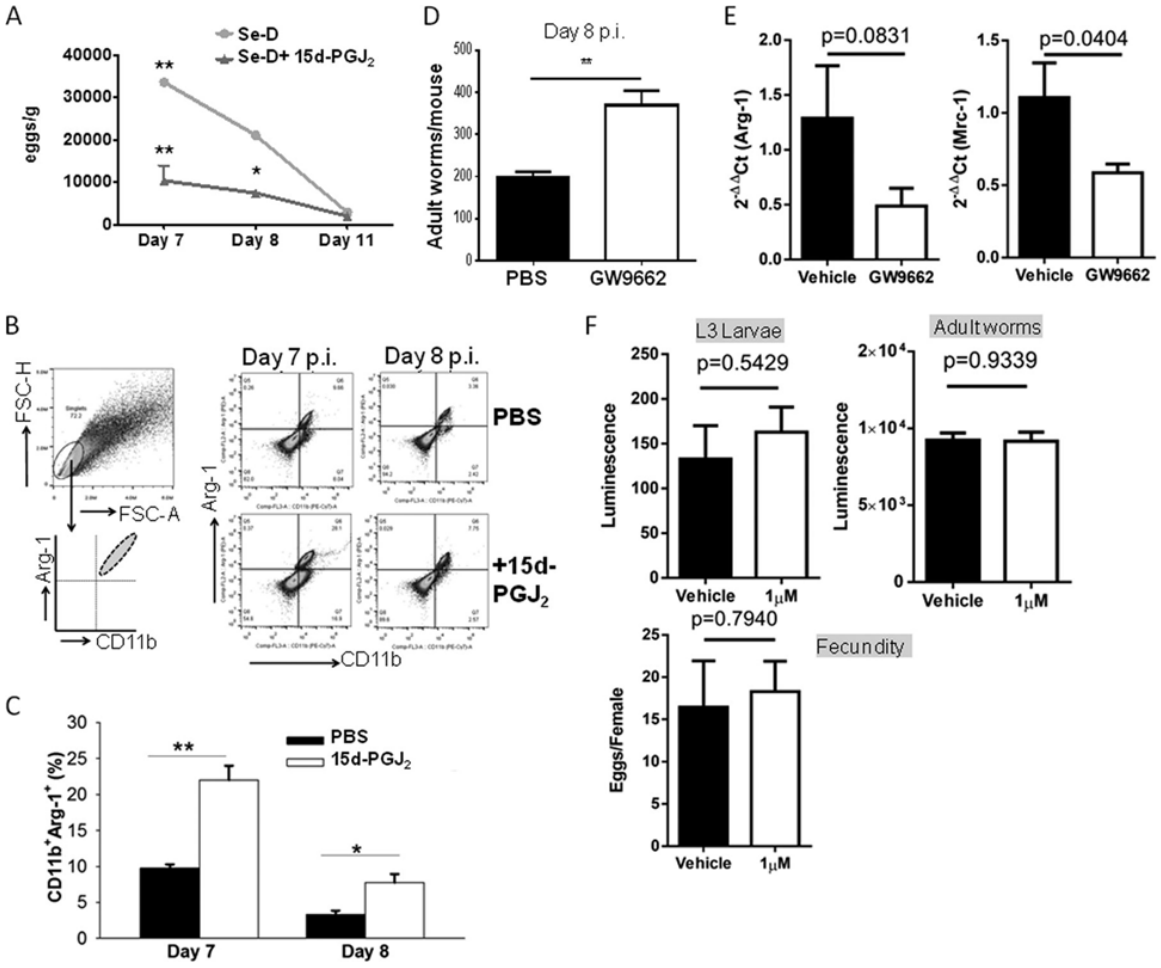

Figure 2.5: Effect of 15d-PGJ_2 and GW9662 on selenium-dependent adult worm clearance in *N.brasiliensis*-infected mice

(A) *Fecal eggs were counted in selenium-deficient mice treated with 0.00325% (w/v) indomethacin for two weeks before infection and two weeks thereafter. 12 hours before infection with N.brasiliensis, selenium-deficient (Se-D) mice were injected intraperitoneally with 0.050 mg/kg 15d-PGJ_2 or sterile PBS once daily for 7 days. Values are the mean ± S.E. of n = 4 per group. Asterisks represent significant differences between the selenium-deficient and selenium-deficient with 15d-PGJ_2 groups. *, <0.05; **, < 0.01; ***, < 0.001. Statistical differences were analysed using two-way ANOVA with Tukey's post hoc testing. (**B-C**) Indomethacin-treated mice on selenium-adequate (Se-A) diet (as above) received sterile PBS or 15d-PGJ_2 injections (0.05 mg/kg/day) starting 12 hours before infection. Single cell suspensions from the small intestine were prepared on days 7 and 8 post-infection, and cells were stained for CD11b (PE-Cy7) and Arg-1 (PE). Gating strategy and representative flow cytometry plots are shown in panels **B** and **C**, respectively. FSC-H and FSC-A represent forward scatter-height and forward scatter-area, respectively. (**D**) Mice on selenium-adequate diet received either vehicle*

*(ethanol in sterile PBS; 4% v/v) or GW9662 (formulated in 1 mg/kg/day) in vehicle injections starting 1 day before infection that were continued to up to 8 days post-infection. The number of adult worms per mouse was counted in the whole small intestine (below the stomach to above the cecum). n = 4 per group. Unpaired two-tailed t-test. *, p < 0.05; **, p < 0.01. (**E**) Expression of Arg1 and Mrc1 in the jejunum of selenium-adequate mice treated with GW9662 or vehicle on day 8 post-infection as above. n = 4 per group. Unpaired two-tailed t-test. (**F**) Effect of GW9662 on the viability of L3 stage larvae, adult worms, and fecundity of adult worms. L3 stage larvae and adult worms were treated with GW9662 or vehicle for 12 hours followed by an ATP assay in the larvae and adult worms and number of eggs per female worm. Boiled larvae and worms were used as negative controls. Data shown is n = 3 per group. Unpaired two-tailed t-test.*

Selenium Affects Th2 Cells

It is known that the clearance of *N.brasiliensis* is Th2-dependent (19, 20). To determine if selenium increases the presence of IL-4 producing Th2 cells in the small intestine to facilitate a type 2 response, we used flow cytometry to determine the number of $CD3^+$IL-4-producing Th2 cells. IL-4 GFP reporter mice (IL-4/GFP-enhanced transcript, 4Get, knock-in mice) on selenium-deficient, selenium-adequate, and selenium-supplemented diets were injected with 500 L3 larvae subcutaneously as described earlier. On day 8 post-infection, $CD3^+GFP^+$ lymphocytes from the lamina propria of small intestine were collected from *N.brasiliensis*-infected and non-infected mice. Interestingly, increase in dietary selenium levels led to a corresponding increase in $CD3^+$IL-4 producing (GFP^+) cells in the small intestine (**Fig 2.6A**). However, only selenium-adequate mice showed a statistically significant increase in $CD3^+GFP^+$ cells upon infection compared with their corresponding selenium-deficient control mice.

Selenium Status Affects IL-13 Expression

In addition to IL-4, IL-13 is also highly expressed in *N.brasiliensis* infection (15, 24) and is important in the clearance of adult worms (15, 17, 31). We determined if expression of *Il13* in *N.brasiliensis*-infected mice was selenium-dependent. qPCR was used to examine expression of *Il13* in jejunal tissue collected on days 7, 8, and 11 post-infection. Expression of *Il13* was highest on days 7 and 8 post-infection in mice fed selenium-supplemented and selenium-adequate diets, respectively, compared with mice fed selenium-deficient diet, decreasing on day 11 post-infection in all three groups (**Fig 2.6B**). These data strongly suggested that selenium status was an important factor in the regulation of *Il-13* expression in the gut in response to infection (**Fig 2.6B**). *N.brasiliensis* infection is known to induce intestinal eosinophilia that could contribute to local production of IL-13 (44). To determine if intestinal eosinophilia was selenium-dependent, leukocytes were isolated from the lamina propria of *N.brasiliensis*-infected mice and examined by flow cytometry. Cells were stained for surface Siglec F and CCR3 to detect the presence of eosinophils. Compared with uninfected mice, the percentage of Siglec-F^+/$CCR3^+$ cells detected in *N.brasiliensis*-infected mice fed selenium-deficient, selenium-adequate, and selenium-supplemented diets were significantly increased (**Fig 2.6C**). However, the percentage of Siglec F^+/$CCR3^+$ cells was not significantly different between mice fed different levels of selenium (**Fig 2.6D**). Further analysis of the jejunal extracts on day 8 post-infection was associated with an increase in myeloperoxidase activity in selenium-adequate and selenium-supplemented

mice when compared with the selenium-deficient mice, suggesting the role of neutrophils in worm clearance (**Fig 2.6E**).

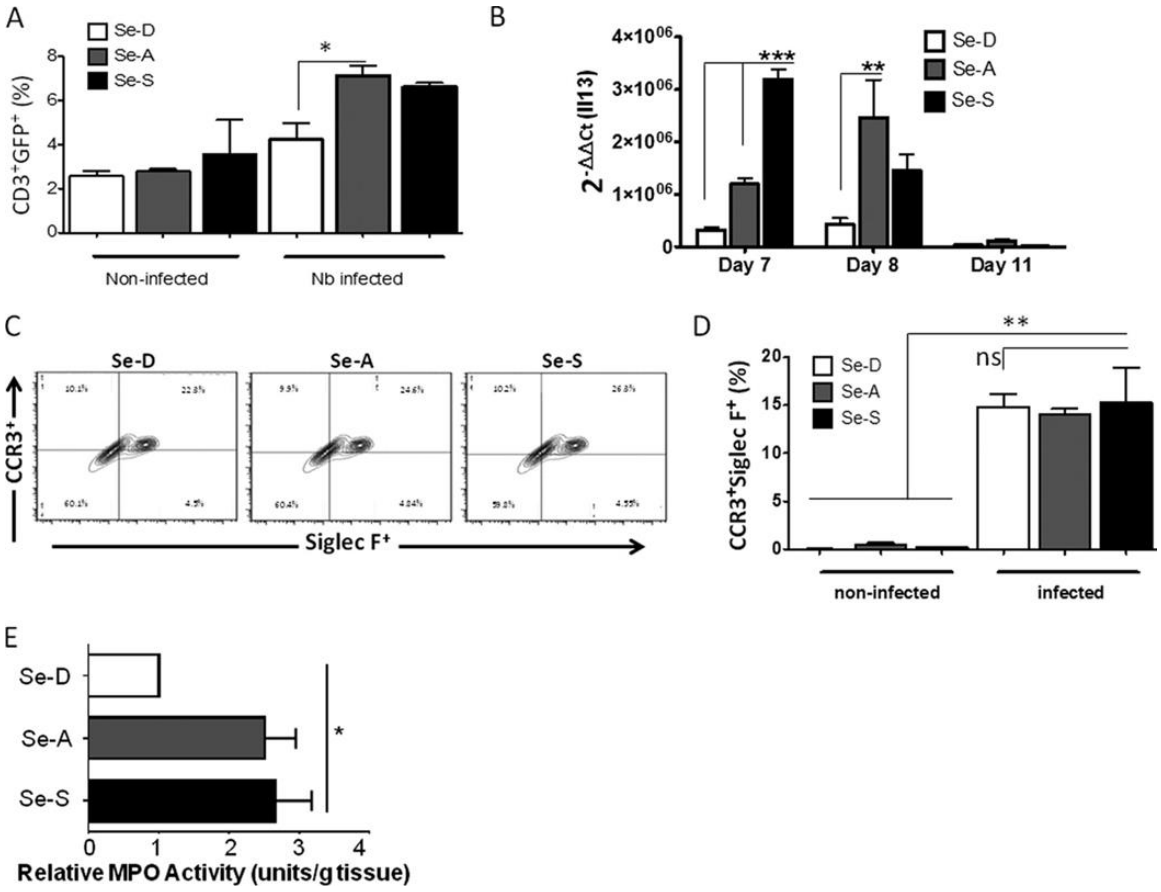

Figure 2.6: Effect of dietary selenium on the expression of IL-4 and IL-13

*(**A**) Quantitation of the $CD3^+GFP^+$ T cells in uninfected 4Get mice were compared with N.brasiliensis-infected mice on the three diets on day 8 post-infection selenium-deficient (Se-D) mice were compared with selenium-adequate (Se-A) and selenium-supplemented (Se-S) mice within each infection group. (**B**) Selenium-dependent increase in the expression of Il13 in the jejunal tissue from N.brasiliensis-infected C57BL/6 mice on selenium-deficient, selenium-adequate, and selenium-supplemented diets. Selenium-deficient mice were compared with selenium-adequate and selenium-supplemented mice within each day. (**C**) Representative scatter plots showing the $SiglecF^+CCR3^+$ cells in the lamina propria isolated from the small intestines of N.brasiliensis-infected C57BL/6 mice day 8 post-infection. (**D**) Comparison of $SiglecF^+CCR3^+$ cells in the lamina propria of uninfected and N.brasiliensis-infected C57BL/6 mice on selenium-deficient, selenium-adequate, and selenium-supplemented diets day 8 post-infection. Values are the mean ± S.E., with a total of n = 9 mice used. Selenium-deficient, selenium-adequate, and selenium-supplemented were compared with each other within each infection group.*

*Asterisks represent significant differences between groups. *, <0.05; **, <0.01. Statistical differences were analysed using two-way ANOVA with Tukey's post hoc testing. (**E**) Myeloperoxidase (MPO) activity in N.brasiliensis-infected jejunum of mice maintained on selenium-deficient, selenium-adequate, and selenium-supplemented diets. 500 infective larvae were inoculated into selenium-deficient, selenium-adequate, and selenium-supplemented mice, and jejunal tissue on day 8 post-infection was used for the assay. Values are the mean ± S.E. of n = 3 mice per group and are calculated relative to selenium-deficient group. *, p < 0.05 analysed by one-way ANOVA.*

Discussion

Studies have identified altered intestinal smooth muscle contractility, development of M2 macrophages, and IL-4Rα- and Stat6-dependent Th2 cell polarization as effectors against gastrointestinal infections (1,17,20,24). Although the beneficial effects of selenium on the clearance of gastrointestinal parasites have been reported (2,4), there is little information on the mechanistic relationship that ties selenium status of the host in a helminth-infected gut.

Clearance of adult *N.brasiliensis* from the intestine between days 7 and 8 post-infection was associated with a reduction in parasite egg shedding in selenium-adequate- and selenium-supplemented mice. We assessed the effects of increasing concentrations of dietary selenium on the expression of macrophage polarization genes in the jejunum during infection with *N.brasiliensis*. Expression of *Fizz1* and *Ym1* increased on days 7 and 8 post-infection, whereas expression of *Arg1* increased 7 days post-infection with a significantly high expression on day 8 post-infection. Our data demonstrate that all three genes are associated with increasing levels of selenium in the diet, corroborating the relationship between dietary selenium and optimal worm clearance. Previous studies have demonstrated delays in worm expulsion in *N.brasiliensis*-infected mice that lack IL-4Rα

on non-bone marrow-derived cells (45). This suggests that selenium-dependent effects may be more important to the pathway the larvae take to the small intestines without affecting the kinetics of worm expulsion itself, but the effects on adult worm fecundity in the intestine would argue for a local selenium-dependent mechanism.

Previous studies have shown the expulsion of a related gastrointestinal nematode parasite (*H. polygyrus bakeri*) during a secondary memory response was delayed in selenium-deficient-fed mice despite increased smooth muscle contractility (2). This suggests that the effect of selenium on smooth muscle function during a memory response in nematode infection may be absent or less critical to result in a multifaceted protective immune response against the nematode. Recent evidence has demonstrated a link between dietary selenium and Relmβ/Fizz2 expression in the intestine (4) during the memory response to *H. polygyrus bakeri* that could explain the reduced clearance of adult worms in selenium-deficient mice (2,21). Even though the differences in host responses vary with helminths, further studies are necessary to directly implicate the role of M2 macrophages in the small intestine in helminth clearance. It is also important to determine if selenium status affects infiltration and/or development of M2 macrophages in the small intestine. In addition, direct measurement of smooth muscle contractility as a function of selenium concentration would help in elucidating the underlying mechanisms.

To address whether the selenoproteome as a whole had an effect on pathogenesis and M2 macrophage polarization, we utilized a macrophage-specific deletion of the *Trsp* allele ($Trsp^{fl/fl}LysM^{Cre}$) (12). Compared with WT mice, $Trsp^{fl/fl}LysM^{Cre}$ mice displayed a significant delay in adult worm clearance despite being fed diets supplemented with selenium (0.4 ppm). These data demonstrate that the ability to

increase selenoprotein expression in monocytes/macrophages via dietary supplementation with selenium can be potentially harnessed to impact host-pathogen interaction. Comparative proteomic analysis of infective larval (L3) and adult worm stages of *N.brasiliensis* indicated the expression of a group of antioxidant enzymes, including the protein disulfide oxidoreductase (most likely a thioredoxin reductase), protein disulfide isomerase, peroxiredoxin, superoxide dismutase (Cu/Zn), and thioredoxin-like proteins (46). Thus, it appears that the larvae and/or adult worms may be well positioned to maintain infectivity and fecundity even under selenium-deficient conditions. However, systematic knockdown studies could provide further evidence once the complete genome sequence of *N.brasiliensis* becomes available.

Although worm clearance from the intestine requires Stat6 (17,24), the nuclear receptor Ppar-γ has also been shown to play a role in clearance (34). Infection of selenium-adequate and selenium-supplemented mice increased the expression of Cox-2 and Hpgds complementing our previous data that demonstrated the ability of selenium to shunt the AA-Cox pathway from pro-inflammatory prostaglandin E_2 and thromboxane A_2 toward anti-inflammatory and endogenous Ppar-γ agonist, 15d-PGJ_2(7,37,38), in macrophages. Inhibition of the Cox pathway by indomethacin significantly delayed adult worm clearance in selenium-adequate and selenium-supplemented mice, whereas GW9662 decreased the expression of *Mrc1* and *Arg1*, two downstream Ppar-γ target genes (47,48), increased adult worm burden in selenium-adequate mice. *In vitro* treatment of L3 stage larvae and adult worms with indomethacin or GW9662 had no impact on the viability of the L3 stage larvae or viability and fecundity of adult worm *per se*. Taken together these results suggest that the selenium status of the host is a key factor

in the clearance of *N.brasiliensis* that involves Ppar-γ. Similarly, administration of 15d-PGJ_2 (0.050 mg/kg) to selenium-deficient mice treated with indomethacin significantly decreased fecal egg shedding from days 7 to 11 post-infection, whereas 16,16-dimethyl-prostaglandin E_2 had no effect. In agreement with the qPCR results of expression of prototypical M2 macrophage genes, 15d-PGJ_2 treatment also increased $CD11b^+Arg\text{-}1^+$ cells in the small intestine, suggesting that selenium effects are mediated in part through the endogenously produced prostanoids, such as 15d-PGJ_2, to modulate M2 macrophage gene expression. More importantly, the role of Cox-derived metabolites in helminth clearance also begs an important question regarding the likely role of nonsteroidal anti-inflammatory drugs as a potential confounder in selenium-dependent anti-helminth-protective mechanisms, which is currently unknown.

Previous studies have shown clearance of *N.brasiliensis* to be sensitive to the effects of IL-13 (15,18,24). Interestingly, selenium-dependent increase in the expression of IL-13 in the jejunum of infected mice perhaps serves as a key mediator of helminth clearance. This is likely because IL-13 has also been reported to increase the endogenous production of 15d-PGJ_2 in macrophages (49). Thus, it is possible that selenoprotein expression is critical in the IL-13-dependent induction of 15d-PGJ_2 by macrophages. An additional question that is equally important is the source of IL-13. Based on our data (**Fig 2.6E**), it appears that neutrophils, in addition to ILC2 cells (16), could serve as a potential source of IL-13, which has been demonstrated recently (31), but the role of selenium in this process is intriguing and needs to be further examined.

In conclusion, our results suggest that increases in dietary selenium decreases the number of eggs per gram feces and lower numbers of adult *N.brasiliensis* in the intestine.

This is likely achieved through an increased activity of selenoprotein expressing M2 macrophages in the small intestine. Further studies are required to establish the exact mechanisms of clearance, particularly the role of selenoproteins in innate immune cells, such as neutrophils. The role of nonsteroidal anti-inflammatory drugs and Ppar-γ agonists in macrophage polarization needs to be elucidated to examine if exogenous factors (therapeutic drugs) impact host-pathogen interactions. Little is known about the dynamics of these therapies in gastrointestinal helminth infections, and a better understanding of these processes may help develop more effective regimens to cure such infections. Our study suggests that the protective effect of Se is mediated through the production of 15d-PGJ_2 by arachidonic acid metabolism. Interestingly, Cox-2, the inducible isoform which is highly associated with inflammation, is downregulated by IL-4. In order to determine the mechanism by which 15d-PGJ_2 is being produced during an IL-4 biased infection, Cox-1 expression will be examined. Additionally, to determine which selenoprotein(s) is playing a role in altering arachidonic acid metabolism to increase the production of PGJ_2 metabolites, a murine macrophage-specific knockout model will be employed to narrow down the list of selenoproteins.

References

1. Gause, W. C., Urban, J. F., Jr., and Stadecker, M. J. (2003) The immune response to parasitic helminths: insights from murine models. *Trends Immunol* **24**, 269-277
2. Au Yeung, K. J., Smith, A., Zhao, A., Madden, K. B., Elfrey, J., Sullivan, C., Levander, O., Urban, J. F., and Shea-Donohue, T. (2005) Impact of vitamin E or selenium deficiency on nematode-induced alterations in murine intestinal function. *Exp Parasitol* **109**, 201-208
3. de Souza, A. P., Sieberg, R., Li, H., Cahill, H. R., Zhao, D., Araújo-Jorge, T. C., Tanowitz, H. B., and Jelicks, L. A. (2010) The role of selenium in intestinal

motility and morphology in a murine model of Trypanosoma cruzi infection. *Parasitol Res* **106**, 1293-1298

4. Smith, A. D., Cheung, L., Beshah, E., Shea-Donohue, T., and Urban, J. F., Jr. (2013) Selenium status alters the immune response and expulsion of adult Heligmosomoides bakeri worms in mice. *Infect Immun* **81**, 2546-2553
5. Arthur, J. R., McKenzie, R. C., and Beckett, G. J. (2003) Selenium in the immune system. *J Nutr* **133**, 1457S-1459S
6. Bellinger, F. P., Raman, A. V., Reeves, M. A., and Berry, M. J. (2009) Regulation and function of selenoproteins in human disease. *Biochem J* **422**, 11-22
7. Nelson, S. M., Lei, X., and Prabhu, K. S. (2011) Selenium levels affect the IL-4-induced expression of alternative activation markers in murine macrophages. *J Nutr* **141**, 1754-1761
8. Papp, L. V., Lu, J., Holmgren, A., and Khanna, K. K. (2007) From selenium to selenoproteins: synthesis, identity, and their role in human health. *Antioxid Redox Signal* **9**, 775-806
9. Fredericks, G. J., and Hoffmann, P. R. (2015) Selenoprotein K and Protein Palmitoylation. *Antioxid Redox Signal* **23**, 854-862
10. Prabhu, K. S., Zamamiri-Davis, F., Stewart, J. B., Thompson, J. T., Sordillo, L. M., and Reddy, C. C. (2002) Selenium deficiency increases the expression of inducible nitric oxide synthase in RAW 264.7 macrophages: role of nuclear factor-B in up-regulation. *Biochem J* **366**, 203-209
11. Hatfield, D. L., and Gladyshev, V. N. (2002) How selenium has altered our understanding of the genetic code. *Mol Cell Biol* **22**, 3565-3576
12. Carlson, B. A., Yoo, M. H., Sano, Y., Sengupta, A., Kim, J. Y., Irons, R., Gladyshev, V. N., Hatfield, D. L., and Park, J. M. (2009) Selenoproteins regulate macrophage invasiveness and extracellular matrix-related gene expression. *BMC Immunol* **10**, 57
13. Turanov, A. A., Everley, R. A., Hybsier, S., Renko, K., Schomburg, L., Gygi, S. P., Hatfield, D. L., and Gladyshev, V. N. (2015) Regulation of selenocysteine content of human selenoprotein P by dietary selenium and insertion of cysteine in place of selenocysteine. *PLoS ONE* **10**, e0140353
14. Lu, J., Zhong, L., Lönn, M. E., Burk, R. F., Hill, K. E., and Holmgren, A. (2009) Penultimate selenocysteine residue replaced by cysteine in thioredoxin reductase from selenium-deficient rat liver. *FASEB J* **23**, 2394-2402
15. Kreider, T., Anthony, R. M., Urban, J. F., Jr., and Gause, W. C. (2007) Alternatively activated macrophages in helminth infections. *Curr Opin Immunol* **19**, 448-453
16. Huang, Y., Guo, L., Qiu, J., Chen, X., Hu-Li, J., Siebenlist, U., Williamson, P. R., Urban, J. F., Jr., and Paul, W. E. (2015) IL-25-responsive, lineage negative KLRG1(hi) cells are multipotential "inflammatory" type 2 innate lymphoid cells. *Nat Immunol* **16**, 161-169
17. Zhao, A., Urban, J. F., Jr., Anthony, R. M., Sun, R., Stiltz, J., van Rooijen, N., Wynn, T. A., Gause, W. C., and Shea-Donohue, T. (2008) Th2 cytokine induced alterations in intestinal smooth muscle function depend on alternatively activated macrophages. *Gastroenterology* **135**, 217-225

18. Zhao, A., McDermott, J., Urban, J. F., Jr., Gause, W., Madden, K. B., Yeung, K. A., Morris, S. C., Finkelman, F. D., and Shea-Donohue, T. (2003) Dependence of IL-4, IL-13, and nematode-induced alterations in murine small intestinal smooth muscle contractility on Stat6 and enteric nerves. *J Immunol* **171**, 948-954
19. Anthony, R. M., Rutitzky, L. I., Urban, J. F., Jr., Stadecker, M. J., and Gause, W. C. (2007) Protective immune mechanisms in helminth infection. *Nat Rev Immunol* **7**, 975-987
20. Anthony, R. M., Urban, J. F., Jr., Alem, F., Hamed, H. A., Rozo, C. T., Boucher, J. L., Van Rooijen, N., and Gause,W. C. (2006) Memory Th2 cells induce alternatively activated macrophages to mediate protection against nematode parasites. *Nat Med* **12**, 955-960
21. Herbert, D. R., Yang, J. Q., Hogan, S. P., Groschwitz, K., Khodoun, M., Munitz, A., Orekov, T., Perkins, C.,Wang, Q., Brombacher, F., Urban, J. F., Jr., Rothenberg, M. E., and Finkelman, F. D. (2009) Intestinal epithelial cell secretion of RELM-beta protects against gastrointestinal worm infection. *J Exp Med* **206**, 2947-2957
22. Horsnell, W. G., and Brombacher, F. (2010) Genes associated with alternatively activated macrophages discretely regulate helminth infection and pathogenesis in experimental mouse models. *Immunobiology* **215**, 704-708
23. Reyes, J. L., and Terrazas, L. I. (2007) The divergent roles of alternatively activated macrophages in helminthic infections. *Parasite Immunol* **29**, 609-619
24. Urban, J. F., Jr., Noben-Trauth, N., Donaldson, D. D., Madden, K. B., Morris, S. C., Collins, M., and Finkelman, F. D. (1998) IL-13, IL-4Ralpha, and Stat6 are required for the expulsion of the gastrointestinal nematode parasite Nippostrongylus brasiliensis. *Immunity* **8**, 255-264
25. Panzer, M., Sitte, S., Wirth, S., Drexler, I., Sparwasser, T., and Voehringer, D. (2012) Rapid in vivo conversion of effector T cells into Th2 cells during helminth infection. *J Immunol* **188**, 615-623
26. Schmid-Grendelmeier, P., Altznauer, F., Fischer, B., Bizer, C., Straumann, A., Menz, G., Blaser, K., Wüthrich, B., and Simon, H. U. (2002) Eosinophils express functional IL-13 in eosinophilic inflammatory diseases. *J Immunol* **169**, 1021-1027
27. Maizels, R. M., Pearce, E. J., Artis, D., Yazdanbakhsh, M., and Wynn, T. A. (2009) Regulation of pathogenesis and immunity in helminth infections. *J Exp Med* **206**, 2059-2066
28. Laskin, D. L. (2009) Macrophages and inflammatory mediators in chemical toxicity: a battle of forces. *Chem Res Toxicol* **22**, 1376-1385
29. Lawrence, T., and Natoli, G. (2011) Transcriptional regulation of macrophage polarization: enabling diversity with identity. *Nat Rev Immunol* **11**, 750-761
30. Nair, M. G., Gallagher, I. J., Taylor, M. D., Loke, P., Coulson, P. S., Wilson, R. A., Maizels, R. M., and Allen, J. E. (2005) Chitinase and Fizz family members are a generalized feature of nematode infection with selective upregulation of Ym1 and Fizz1 by antigen-presenting cells. *Infect Immun* **73**, 385-394
31. Chen, F., Wu, W., Millman, A., Craft, J. F., Chen, E., Patel, N., Boucher, J. L., Urban, J. F., Jr., Kim, C. C., and Gause, W. C. (2014) Neutrophils prime a long-

lived effector macrophage phenotype that mediates accelerated helminth expulsion. *Nat Immunol* **15**, 938-946

32. Madden, K. B., Whitman, L., Sullivan, C., Gause, W. C., Urban, J. F., Jr., Katona, I. M., Finkelman, F. D., and Shea-Donohue, T. (2002) Role of STAT6 and mast cells in IL-4- and IL-13-induced alterations in murine intestinal epithelial cell function. *J Immunol* **169**, 4417-4422
33. Szanto, A., Balint, B. L., Nagy, Z. S., Barta, E., Dezso, B., Pap, A., Szeles, L., Poliska, S., Oros, M., Evans, R. M., Barak, Y., Schwabe, J., and Nagy, L. (2010) STAT6 transcription factor is a facilitator of the nuclear receptor PPAR-regulated gene expression in macrophages and dendritic cells. *Immunity* **33**, 699-712
34. Anthony, B. J., Allen, J. T., Li, Y. S., and McManus, D. P. (2012) A role for peroxisome proliferator-activated receptors in the immunopathology of schistosomiasis? *PPAR Res* **2012**, 128068
35. Chawla, A., Barak, Y., Nagy, L., Liao, D., Tontonoz, P., and Evans, R. M. (2001) PPAR- dependent and independent effects on macrophage-gene expression in lipid metabolism and inflammation. *Nat Med* **7**, 48-52
36. Odegaard, J. I., Ricardo-Gonzalez, R. R., Goforth, M. H., Morel, C. R., Subramanian, V., Mukundan, L., Red Eagle, A., Vats, D., Brombacher, F., Ferrante, A. W., and Chawla, A. (2007) Macrophage-specific PPAR controls alternative activation and improves insulin resistance. *Nature* **447**, 1116-1120
37. Gandhi, U. H., Kaushal, N., Ravindra, K. C., Hegde, S., Nelson, S. M., Narayan, V., Vunta, H., Paulson, R. F., and Prabhu, K. S. (2011) Selenoprotein-dependent up-regulation of hematopoietic prostaglandin D2 synthase in macrophages is mediated through the activation of peroxisome proliferator-activated receptor (PPAR) gamma. *J Biol Chem* **286**, 27471-27482
38. Vunta, H., Davis, F., Palempalli, U. D., Bhat, D., Arner, R. J., Thompson, J. T., Peterson, D. G., Reddy, C. C., and Prabhu, K. S. (2007) The antiinflammatory effects of selenium are mediated through 15-deoxy-12,14- prostaglandin J2 in macrophages. *J Biol Chem* **282**, 17964-17973
39. Mohrs, M., Shinkai, K., Mohrs, K., and Locksley, R. M. (2001) Analysis of type 2 immunity in vivo with a bicistronic IL-4 reporter. *Immunity* **15**, 303-311
40. Voehringer, D., van Rooijen, N., and Locksley, R. M. (2007) Eosinophils develop in distinct stages and are recruited to peripheral sites by alternatively activated macrophages. *J Leukoc Biol* **81**, 1434-1444
41. Camberis, M., Le Gros, G., and Urban, J., Jr. (2003) Animal model of Nippostrongylus brasiliensis and Heligmosomoides polygyrus. *Curr Protoc Immunol* Chapter 19, Unit 19.12
42. Dunn, A., and Keymer, A. (1986) Factors affecting the reliability of the McMaster technique. *J Helminthol* **60**, 260-262
43. Lefrancois, L., and Lycke, N. (2001) Isolation of mouse small intestinal intraepithelial lymphocytes, Peyer's patch, and lamina propria cells. *Curr Protoc Immunol* Chapter 3, Unit 3.19
44. Allen, J. E., and Maizels, R. M. (2011) Diversity and dialogue in immunity to helminths. *Nat Rev Immunol* **11**, 375-388

45. Urban, J. F., Jr., Noben-Trauth, N., Schopf, L., Madden, K. B., and Finkelman, F. D. (2001) Cutting edge: IL-4 receptor expression by non-bone marrow-derived cells is required to expel gastrointestinal nematode parasites. *J Immunol* **167**, 6078-6081
46. Sotillo, J., Sanchez-Flores, A., Cantacessi, C., Harcus, Y., Pickering, D., Bouchery, T., Camberis, M., Tang, S. C., Giacomin, P., Mulvenna, J., Mitreva, M., Berriman, M., LeGros, G., Maizels, R. M., and Loukas, A. (2014) Secreted proteomes of different developmental stages of the gastrointestinal nematode Nippostrongylus brasiliensis. *Mol Cell Proteomics* **13**, 2736-2751
47. Chawla, A. (2010) Control of macrophage activation and function by *PPARs Circ Res* **106**, 1559-1569
48. Coste, A., Dubourdeau, M., Linas, M. D., Cassaing, S., Lepert, J. C., Balard, P., Chalmeton, S., Bernad, J., Orfila, C., Séguéla, J. P., and Pipy, B. (2003) PPAR promotes mannose receptor gene expression in murine macrophages and contributes to the induction of this receptor by IL-13. *Immunity* **19**, 329-339
49. Berry, A., Balard, P., Coste, A., Olagnier, D., Lagane, C., Authier, H., Benoit-Vical, F., Lepert, J. C., Séguéla, J. P., Magnaval, J. F., Chambon, P., Metzger, D., Desvergne, B., Wahli, W., Auwerx, J., and Pipy, B. (2007) IL-13 induces expression of CD36 in human monocytes through PPAR activation. *Eur J Immunol* **37**, 1642-1652

Chapter 3

IL-4 upregulates cyclooxygenase-1 expression in macrophages

Published in The Journal of Biological Chemistry.

J Biol Chem. 2017 Sept 1; 292(35): 14544-14555. Doi: 10.1074/jbc.M117.785014

[Epub 2017 Jul 6]

Ashley E. Shay[1], Bastihalli T. Diwakar[1], Bo-Jhih Guan[2], Vivek Narayan[3], Joseph F. Urban Jr[4], and K. Sandeep Prabhu[1].

Affiliations: [1]Center for Molecular Immunology and Infectious Disease and Center for Molecular Toxicology and Carcinogenesis, Department of Veterinary and Biomedical Sciences, 115 Henning Building, The Pennsylvania State University, University Park, PA 16802; [2]Department of Genetics and Genome Sciences, Case Western Reserve University, Cleveland, OH 44106; [3]Department of Cellular and Molecular Medicine, Lerner Research Institute, Cleveland Clinic, Cleveland, OH, 44195; [4]U.S. Department of Agriculture, Agriculture Research Service, Beltsville Human Nutrition Research Center, Diet, Genomics, and Immunology Laboratory, Beltsville, MD, 20705

Contributions: AES and KSP conceived and coordinated the study as well as wrote the manuscript and created the schematic. AES designed, performed, and analyzed the data shown in Figs 3.1 to 3.11. DBT performed and analyzed the data shown in Fig 3.2A to Fig 3.2C, Fig 3.2E, Fig 3.7B-C and Fig 3.9B. BJG performed and analyzed the data

shown in Fig 3.4F and assisted with manuscript preparation. VN cultured, stimulated, and harvested the BMDMs required for the polysome assay in Fig 3.4F and assisted with manuscript preparation. JFU provided L3 stage *N.brasiliensis* larvae and assisted with manuscript preparation. All authors reviewed the results and approved the final version of the manuscript.

Abstract

Macrophages use various cell-surface receptors to sense their environment and undergo polarized responses. The cytokines IL-4 and IL-13, released from T-helper type 2 (Th2) cells, drive macrophage polarization toward an alternatively activated phenotype (M2). This phenotype is associated with the expression of potent pro-resolving mediators, such as the prostaglandin (PG) D_2–derived cyclopentenone metabolite, 15d-PGJ_2, produced by the cyclooxygenase (*Ptgs*; Cox) pathway. Interestingly, IL-4 treatment of bone marrow–derived macrophages significantly downregulates Cox-2 protein expression, while Cox-1 levels are significantly increased. This phenomenon not only challenges the dogma that Cox-1 is only developmentally regulated, but also demonstrates a novel mechanism in which IL-4–dependent regulation of Cox-1 involves the activation of the mechanistic target of rapamycin complex (mTORC). Using specific chemical inhibitors, we demonstrate here that IL-4–dependent Cox-1 upregulation occurs at the post-transcriptional level via the Fes-Akt-mTOR axis. Activation of AMP-activated protein kinase (Ampk) by metformin, inhibition of mTORC by torin 1, or CRISPR/Cas9-mediated genetic knockout of tuberous sclerosis-2 (Tsc2) blocked the IL-4–dependent expression of Cox-1 and the ability of macrophages to polarize to M2. However, use of 15d-PGJ_2 partially rescued the effects of Ampk activation, suggesting the importance of Cox-1 in macrophage polarization as also observed in a model of gastrointestinal helminth clearance. In summary, these findings suggest a new paradigm where IL-4–dependent upregulation of Cox-1 expression may play a key role in tissue homeostasis and wound healing during Th2-mediated immune responses, such as parasitic infections.

Introduction

Macrophages utilize various cell surface receptors to sense their environment and elicit a polarized response. Based on the stimuli, macrophages can be polarized to either a M1 (classically-activated) pro-inflammatory phenotype or a M2 (alternatively-activated) anti-inflammatory phenotype that corresponds to two ends of a spectrum with many intermediate phenotypes (1,2). Interleukin (IL)-4 or IL-13 released by T-helper type 2 (Th2) cell responses during allergies, asthma, or parasitic infection (as seen during helminth *Nippostrongylus brasiliensis* infection), activate the IL-4 receptor on macrophages to drive M2 polarization (3-6). Binding of IL-4 to its receptor leads to the recruitment of various tyrosine kinases, such as Janus kinases (Jak1-3) and Feline sarcoma oncogene kinase (Fes). Jak-1 and Jak-3 activation of Signal Transducer and Activator of Transcription-6 (Stat6) leads to nuclear translocation and transcriptional activation of M2 macrophage genes including *peroxisome proliferator-activated receptor gamma* (*Ppar-γ*), *arginase-1*, *mannose receptor-1* (*Mrc-1*; *CD206*), and *Il10* (7).

In addition to signaling through the Jak/Stat pathway, IL-4 receptor engagement also upregulates protein translation through the recruitment of Fes (8). Fes activates phosphatidylinositide 3-kinase leading to the generation of phosphatidylinositol (3,4,5)-triphosphate. 3-phosphoinositide-dependent protein kinase-1 is activated by membrane phospholipids and is a major regulator of protein kinase B/Akt signaling (9,10). Additionally, mTORC activity increases the phosphorylation of Akt. Akt inhibits tuberous sclerosis complex (Tsc), activating mTORC. mTORC increases translation by activating ribosomal protein S6 kinase β-1 (p70S6K) and releasing elongation factor

eIF4E from its inhibitor 4EBP. S6 kinase negatively feeds back to inhibit phosphatidylinositide 3-kinase activity (11). Therefore Akt is both regulated and regulates mTORC signaling pathways. Finally, mTORC has been shown to play a critical role in M2 macrophage polarization in both peritoneal macrophages and bone marrow-derived macrophages (BMDMs) with IL-4 stimulation increasing the expression of Tsc1 and Tsc2 protein in stimulated macrophages (12).

Metformin, a commonly used anti-diabetic drug, increases Ampk activity, which upregulates the Tsc1/2 complex (13,14). Treatment with metformin has been shown to significantly reduce the IL-13 induced expression of M2 macrophage markers, such as CD206(14). However, little is known about how metformin treatment affects the production of endogenous ligands, Δ^{12}-prostaglandin (PG) J_2 and 15-deoxy-Δ-^{12,14}-PGJ_2 (15d-PGJ_2) that are known to activate Ppar-γ and affect polarization of macrophages (15-18). This is particularly interesting since IL-4/IL-13 significantly downregulate the expression of Cox-2 (19,20). IL-4 receptor signaling converges with arachidonic acid metabolism during an inflammatory stimulus at Ppar-γ signaling to drive M2 macrophage polarization (21). Upon stimulation, arachidonic acid is metabolized by Cox-1 and Cox-2 in a two-step conversion to PGH_2. PGH_2 is converted to PGE_2, PGI_2, $PGF_{2\alpha}$, PGD_2, and TXA_2 by specific synthases that play various roles in pathophysiology (22-24). While PGE_2 and TXA_2 exacerbate inflammation, PGD_2, a product of hematopoietic type PGD_2 synthase (Hpgds) and lipocalin-type PGD_2 synthase, mediates resolution of inflammation, primarily through two metabolites, Δ^{12}-PGJ_2 and 15d-PGJ_2. More importantly, Cox-1 functionally couples with Hpgds to form PGD_2 and its downstream products (25,26). Treatment with indomethacin, a non-selective Cox inhibitor, led to

decreased M2 macrophage markers *in vivo* as well as increased *N.brasiliensis* burden, which was reversed by exogenous treatment with 15d-PGJ_2 (17).

Even though Cox-1 (*Ptgs-1*) and Cox-2 (*Ptgs-2*) have a high-degree of sequence homology (~ 63%), they differ in many respects from gene structure to enzymatic activity. Cox-1 has been generally considered as a constitutive enzyme, with some exceptions such as upregulation of transcription in fibroblasts by TGFβ and IL-1β and during cellular differentiation of monocytes with phorbol ester in THP-1 cells (27). Cox-2 is subjected to transcriptional and post-translational regulation by diverse stimuli (28-31). While *Ptgs-2* promoter contains many regulatory elements present in "early immediate genes", the *Ptgs-1* promoter is more reminiscent of "house-keeping" genes lacking TATA and CAAT boxes, high GC content, and multiple transcriptional start sites (28-31). Additionally, *Ptgs*-2 mRNA, as well as protein, has a short half-life of two to seven hours, while *Ptgs*-1 mRNA and protein is relatively stable (29). The instability of Cox-2 protein is due to a 27 amino acid cassette at the C-terminus, not present in Cox-1, which targets it for degradation through the endoplasmic-reticulum-associated protein degradation system followed by ubiquitination and proteolysis by 26S proteasome (29,32).

Here we describe for the first time the post-transcriptional regulation of Cox-1 expression by IL-4 in primary macrophages (both human and mouse) to be mediated through the Fes-Akt-mTORC axis rather than the Jak/Stat pathway. Activation of Ampk or direct inhibition of mTORC by torin 1 blocked the IL-4-dependent expression of Cox-1 and affected macrophage polarization towards the M2 phenotype. Use of 15d-PGJ_2 partially rescued the effects of Ampk activation in mice infected with *N.brasiliensis*,

suggesting the importance of Cox-1 in the polarization of macrophages. This is in agreement with our previous findings demonstrating that loss of 15d-PGJ_2 by indomethacin treatment lead to a significant decrease in M2 macrophages and increase in parasite burden which was rescued by exogenous 15d-PGJ_2 treatment (17). In summary, these studies suggest a novel paradigm where IL-4-dependent post-transcriptional control of Cox-1 expression may play a key role in tissue homeostasis and wound healing during Th2-mediated immune responses, such as parasitic infections.

Materials and Methods

Mice

C57BL/6 male age-matched mice were purchased from Taconic Biosciences, Inc. (Hudson, NY) and maintained on an AIN-76-based semi-purified diet from Harlan-Teklad (Madison, WI). All studies were pre-approved by the Institutional Animal Care and Use Committee and the Institutional Biosafety Committee at Penn State University.

Bone Marrow-Derived Macrophage Culture

Femurs were harvested and bone marrow was collected from C57BL/6 male age-matched mice. Bone marrow was separated into a single cell suspension. Cells were plated in DMEM media (Life Technologies) with 5% (v/v) fetal bovine serum (Atlanta Biologicals), 2mM L-glutamine (Corning), 100I.U. penicillin (Corning), 100µg/mL

streptomycin (Corning), and 10% (v/v) L929 fibroblast conditioned DMEM media. L929 fibroblasts were purchased from American Type Culture Collection (Manassas, VA).

Treatments

Various compounds were used at the following concentrations: 7.5μM herbimycin A (Santa Cruz), 10μM Ly294002 (Cayman), 10μM Akt inhibitor VIII (Cayman), 250nM torin 1 (Selleck Chemicals), 80nM actinomycin D (Sigma), 10μM cycloheximide (gift from Dr. Gary Perdew, Penn State University), 50nM Jak inhibitor I (Santa Cruz), 20μM metformin (Sigma), and 30nM ozagrel (thromboxane synthase inhibitor; Cayman). Metformin was reconstituted in cell culture grade water while all other compounds were reconstituted in cell culture grade DMSO (Sigma) and added to cells at concentrations not exceeding 0.1% (v/v). Above mentioned compounds were added to BMDM cultures four hours prior to IL-4 stimulation, except for actinomycin D which was added 30 minutes prior to IL-4 stimulation due to impact on cell viability. IL-4 (10ng/ml; R&D Systems) was added for 20 hours, unless described otherwise in text, and cells were collected for analysis as described below. Cell viability was confirmed by trypan blue staining.

RNA Extraction and Real-Time PCR

Cell pellets were stored in 1mL of Tri-reagent (Thermo) at -80°C until RNA extraction. RNA extraction was performed according to the manufacturer's protocol as

described previously (21). RNA was reversed transcribed to cDNA using a high capacity cDNA reverse transcription kit (Life Technologies). cDNA was used in quantitative PCR with specific taqman probes for *Ptgs-1*, *Ptgs-2*, *Arg-1*, *Cd36*, *mPges-1*, *Txas-1*, or *Gapdh* (Life Technologies) in a StepOnePlus-Real Time PCR System (Thermo Applied Biosystems). Gene abundance was analyzed and $2^{-\Delta\Delta Ct}$ was calculated to represent change in gene expression relative to controls (49).

Western Immunoblot

Mammalian protein extraction reagent (Thermo) or tissue protein extraction reagent (Thermo) containing protease inhibitor cocktail (Roche) and 5mM sodium orthovanadate (Sigma) was added to cell pellets or tissue samples, respectively, and incubated on ice for 20 minutes and vortexed every five minutes. Cell debris was pelleted by centrifugation at 20,817*g* for ten minutes. Protein concentration in the supernatant was measured using a BCA protein assay kit (Thermo). Protein was loaded onto a discontinuous SDS-PAGE gel (t=12.5%). Nitrocellulose blotting membranes were blocked with a 5% (w/v) skim milk solution made with Tris buffered saline containing 0.1% Tween-20 (Sigma) for one hour prior to the addition of primary antibodies. Primary antibodies were added to the blots for 12 hours at 4^{o}C at the following dilutions: 1:2,000 Cox-1 (Cayman), 1:2,000 Cox-2 (Cayman), 1:2,000 Fes (Abcam), 1:1,000 phospho-S6K (R&D Systems), 1:1,000 total S6K (R&D Systems), 1:20,000 β-actin (Fitzgerald), and 1:600,000 Gapdh (Fitzgerald). Appropriate secondary antibodies conjugated to horseradish peroxidase were used at dilutions: 1:2,000 goat anti-rabbit (Thermo), or

1:5,000 goat anti-mouse (Thermo) and developed using West Pico reagent (Thermo). Autoradiograms densities were evaluated using Image-J (National Institutes of Health).

Flow Cytometry

Cells were enumerated by trypan blue staining using a hemocytometer. 100,000-200,000 cells were resuspended in 100µL flow buffer (phosphate buffered saline (Life Technologies) containing 100I.U. penicillin (Corning), 100µg/mL streptomycin (Corning), and 2% (v/v) fetal bovine serum (Atlanta)). Extracellular staining was performed by incubating cells with 0.25µg F_c block (BD Biosciences) for ten minutes followed 30 minutes at 4°C with the following antibodies: 0.25µg FITC-conjugated CD206 (Biolegend), 0.10µg PE-Cy7-conjugated CD11b (BD Biosciences), and 0.15µg APC-conjugated F4/80 (Miltenyi). Cells were then fixed by adding 2% formaldehyde solution (Sigma), and incubated for 20 minutes at room temperature. To perform intracellular staining, cells were resuspended in a permeability buffer (48.5mL phosphate buffered saline containing 1.5mL fetal bovine serum (Atlanta), 50mg saponin (Sigma), and 45mg sodium azide (J.T. Baker)) and incubated at room temperature for 15 minutes. Cells were resuspended in 100µL permeability buffer and 0.125µg PE-conjugated Arginase-1 (R&D Systems) antibody or 2.5µL AlexaFluor647-conjugated CD68 (BD Biosciences) and incubated for 30 minutes at room temperature. Cells were collected on the C6 Accuri Flow Cytometer (BD Biosciences) in addition to the following controls: unstained, OneComp eBeads (eBioscience) single stained, and fluorescence minus one

(FMO). Data was analyzed using FlowJo. Gating was based on fluorescence minus one staining controls.

Lipid Extraction and Liquid Chromatography-Mass Spectrometry

Endogenous lipids were extracted from cell culture media samples using C-18 Sep-pak cartridges (Waters, Milford, MA). Briefly, cell-free culture supernatants were acidified with 6N HCl and loaded on to the Sep-Pak cartridge, bound lipids were eluted with methanol, evaporated, and stored in ethyl acetate, until analysed at -80˚C. Lipids were suspended in 70% methanol and analysed by LC-MS/MS on an API 2000 LC-MS/MS system with Turbo V source and an electrospray ionization probe in negative ion mode (15). Quantitative analysis of 15d-$PGJ_{2,}$ was performed using a calibration curve generated by respective standards in multiple reaction monitoring mode using three transitions for 15d-PGJ_2 (315.1/271.1; 315.1/203.0; 315.1/158.0 *m/z*). Quantitative analysis of $PGE_{2,}$ was performed as described above using transitions for PGE_2 (351.2/315.0; 351.2/271.0; 351.2/189.0 *m/z*). Quantitative analysis of $TxB_{2,}$ was performed as described above using transitions for TxB_2 (369.0/195.1 and 369.0/168.9 *m/z*). Data acquisition and analysis was performed using Analyst software (AB Sciex; version 1.5).

Polysome Profile Assay

Polysome profiling and mRNA distribution analysis was performed as described previously (50). Briefly, BMDMs were seeded in 150mm petri plates and grown up to 70% confluence (~1.5×10^7 cells). Following DMSO or IL-4 treatment for 20 hours, cycloheximide (CHX) was added to cells in 100μg/mL for ten minutes at 37°C. Cells were collected at 1,500*g* for ten minutes and washed twice with cold PBS containing 100μg/mL CHX. The cell pellets were suspended in 300μL of lysis buffer (10mM HEPES-KOH (pH 7.5), 2.5mM $MgCl_2$, 100mM KCl, 0.25% NP-40, 100μg/mL CHX, 1mM DTT, 200unit/mL RNase inhibitor (RNaseOUT, Invitrogen) and EDTA-free protease inhibitor (Roche)), kept on ice for 20 minutes and then passed 15 times through a 23-gauge needle. Lysates were cleared by centrifugation at 16,000*g* for 20 minutes and supernatants (cytosolic cell extracts) were collected and measured in absorbance of 260nm. Approximately seven absorbance units (at 260nm) of lysates were layered over 15-54% cold sucrose gradients in buffer (10mM HEPES-KOH (pH 7.5), 2.5mM $MgCl_2$, and 100mM KCl). Gradients were centrifuged at 121,000*g* in a Beckman SW28 rotor for four hours at 4°C. After centrifugation, 12 equal-size fractions (1.2mL/fraction) were collected using a fraction collector. RNA from each fraction was isolated using TRIzol LS reagent (Invitrogen) and equal volume of RNA from each fraction was used for cDNA synthesis with SuperScript III First-Strand Synthesis Supermix (Invitrogen). The relative quantities of specific mRNAs were measured by qPCR using the VeriQuest SYBR Green qPCR master Mix (Affymetrix) on a StepOnePlus Real-Time PCR system (Applied Biosystem).

Infection with N.brasiliensis

Mice were pretreated with sterile PBS or 0.05mg/kg/day of 15d-PGJ_2 (formulated in sterile PBS) intraperitoneally and administered metformin (300mg/kg in Milli-Q water) or Milli-Q water alone starting one day prior to subcutaneous infection with 500 third stage *N.brasiliensis* larvae (L3)(17,51). Metformin water was made fresh and changed every other day throughout infection. Mice received intraperitoneal injections daily. Treatment was continued throughout the infection until sacrifice on day eight post-infection when adult worms in the jejunum were enumerated (52).

Human Macrophage Culture

Frozen human peripheral blood mononuclear cells (PBMC) were purchased from AllCells (Alameda, CA) from donors. Upon arrival, cells were thawed in a 37°C water and enumerated with trypan blue staining using a hemocytometer to determine cell viability. Cells were transferred to a 50mL tube and 20mL of RPMI-1640 (Corning) containing 2mM L-glutamine (Corning), 10% (v/v) fetal bovine serum (Atlanta), 100 I.U. penicillin (Corning), and 100µg/mL streptomycin (Corning) was added dropwise. Cells were centrifuged at 200x*g* for 15 min at room temperature. This was repeated and PBMCs were finally resuspended in 2mL media and enumerated by trypan blue using a hemocytometer. PBMCs were brought to a concentration of $3.0x10^6$ cells/mL and plated in a 6-well culture plate. Cells were cultured with 10ng/mL recombinant human macrophage colony-stimulating factor (M-CSF) (GoldBio) for 24 hours, then at 25ng/mL for remaining culturing period. Media was changed every three days for eight days

adding fresh M-CSF with each change (33). Adherent cells (comprising of 95% macrophages) were pre-treated with either DMSO or 250nM torin 1 followed by 20 hours with or without recombinant human IL-4 (R&D Systems) stimulation. Cells were harvested and analyzed by flow cytometry and western immunoblot as described above.

Transfection and Transduction

HEK293TN cells (System Biosciences; 350,000 cells/2 ml) were plated in DMEM media (Life Technologies) with 1mM sodium pyruvate (Life Technologies), 2mM L-glutamine (Corning), 100I.U./mL penicillin (Corning), 100µg/mL streptomycin (Corning), and 10% (v/v) fetal bovine serum (Atlanta Biologicals) in a 6-well plate and allowed to adhere overnight. Cells were then transfected three times, once every 24 hours with 2.45µg pMD2.G (Addgene), 4.9µg psPAX-2 (Addgene), 4.9µg lentiviral CRISPR gRNA plasmid (Amp^r/Pur^r) expressing mCherry (Vector Builder), 26.6µL TransIT 293 transfection reagent (Mirus), and 700µL serum free DMEM (Life Technologies). The gRNA sequences for non-targeting control and Tsc2 were GCACTACCAGAGCTAACTCA and CAGGAGGACCTGCGCGCGAA, respectively. Viruses were harvested and passed through a 0.45µM filter. Bone marrow was harvested from Cas9 GFP^+ mice and incubated with 1 part viral supernatant to 1 part BMDM media. After 48 hours of viral transduction, bone marrow cells were centrifuged at 100*g* for 5 min at 4°C and resuspended in DMEM media containing 2µg/mL puromycin (GoldBio) and continued for four days with puromycin, changing media every two days. Cells were imaged by fluorescent microscopy to detect GFP^+ and $mCherry^+$. After four

days of puromycin selection, cells were cultured in media without puromycin for an additional two days. BMDMs were stimulated with or without 10 ng/mL recombinant murine IL-4 (R&D Systems) for 20 hours and analyzed for Tsc2 knockout and Cox-1 expression by surveyor assay and western immunoblot, respectively.

Surveyor Assay

PCR was carried out using 0.2µM primers, the Takara Ex Taq PCR kit [0.25mM deoxyribonucleotide triphosphates, 1.25 units Ex Taq DNA polymerase, Ex Taq buffer], and 50ng DNA. Primer sequences are as follows: Tsc2 FWD= CACACAAACCATCGCAAC and Tsc2 REV= AACGCAAATAGTCAGCAAAG to create a 179 bp PCR product. After amplification, equal parts of non-targeting control and Tsc2 PCR products were mixed together and subjected to hybridization. As controls, non-targeting control only PCR products and Tsc2 only PCR products were also subjected to hybridization. Duplexes were subjected to Surveyor nuclease according to manufacturer instructions (Integrated DNA Technologies) to analysis heteroduplex formation. The PCR products were separated by electrophoresis on a 3% 1:3 agarose (Nuseive) gel and visualized by UV transillumination. PCR product bands at 121 bp and 58 bp after nuclease incubation represents successful genomic mutation in Tsc2 gene.

Bioinformatics and Statistics

The transcription start sites of murine and human *PTGS-1* were analyzed with Promoter 2.0 (cbs.dtu.dk) and DBTSS (dbtss.hgc.jp) that predict transcription start sites of vertebrate PolII promoters in DNA sequences (35,53). The most common transcription start site in *PTGS-1* that was predicted by Promoter 2.0 corroborated with consensus sequences defined by earlier studies (GeneBank: AF440204.1 and AH015269.2). All experimental data are expressed as mean ± SEM. Outliers were removed using ROUT method (Q=5.0%), where appropriate (**Fig 3.10**). Either an unpaired one-tailed t-test, an unpaired two-tailed t-test, a one-way ANOVA with Fisher's LSD test, or a two-way ANOVA with Fisher's LSD test was used, where appropriate, to compare the mean of each treatment group with the mean of each other treatment group using GraphPad Prism (GraphPad Software). A linear regression analysis was also performed, where appropriate. P values ≤ 0.05 were considered statistically significant.

Results

IL-4 Stimulation Increases the Expression of Cox-1

To determine the effects of IL-4 stimulation on Cox expression, murine BMDMs were treated with or without recombinant IL-4 for 20 hours prior to collection. Cells were collected and analyzed by real-time PCR and western immunoblot for *Ptgs*-1 (Cox-1) and Ptgs-*2* (Cox-2) expression, and by flow cytometry to quantify M2 macrophages ($CD206^+Arg\text{-}1^+F480^+CD11b^+$). In addition, lipids were extracted from cell culture media

supernatants to quantify the production of 15d-PGJ_2. *Ptgs-1* transcript levels were unaffected by IL-4 treatment (**Fig 3.1A**). Cox-1 protein levels were increased 2.5 fold with IL-4 stimulation compared to untreated control BMDMs (**Fig 3.1B**). Interestingly, *Ptgs-2* transcript was unaffected (data not shown) and Cox-2 protein was not detected in either untreated control or IL-4 treated BMDMs by western immunoblot (**Fig 3.1C**). Additionally, there was no increase in *mPges-1* or *Txas-1* expression with IL-4 stimulation compared to untreated control BMDMs (**Fig 3.1D-E**).

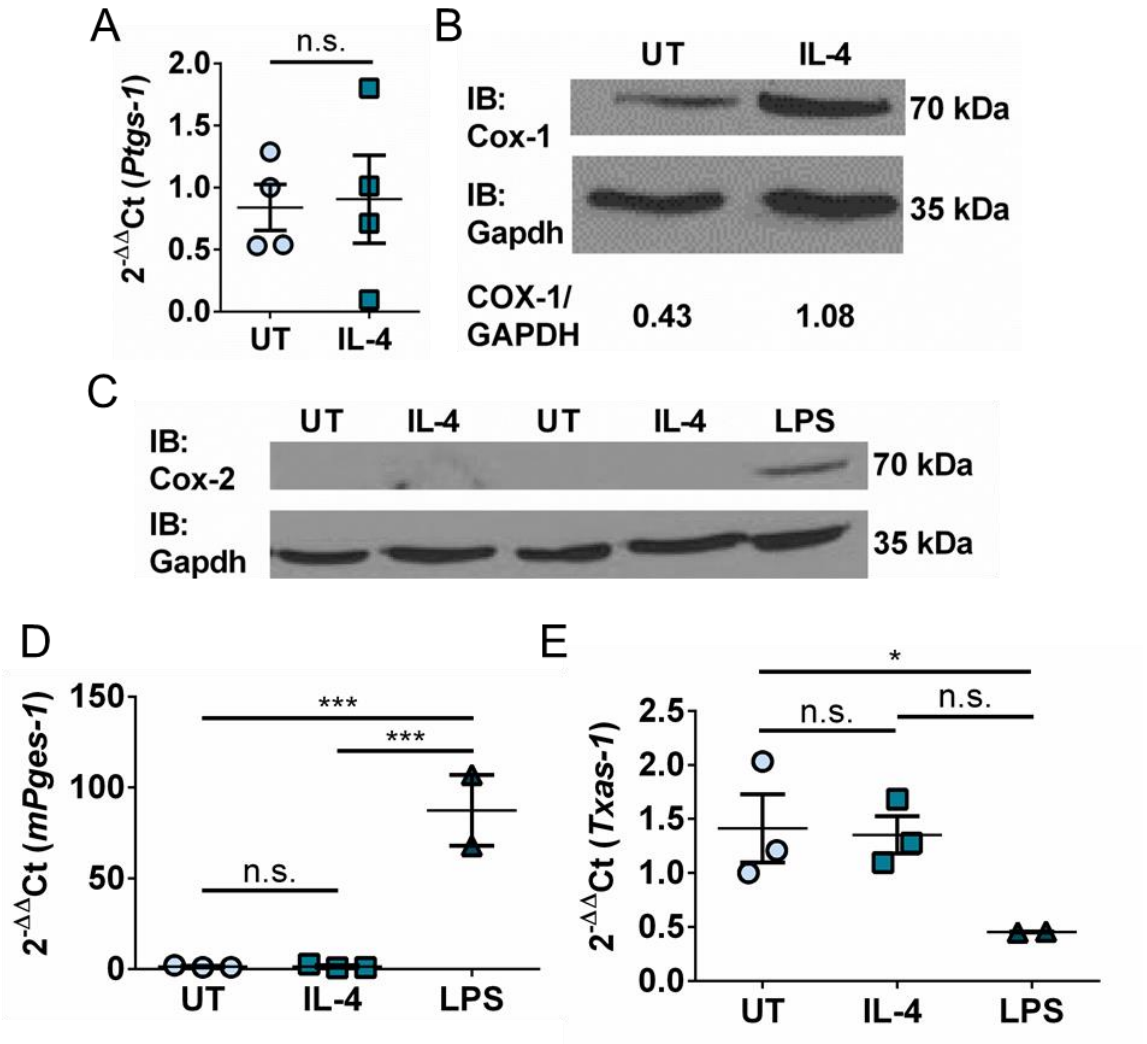

Figure 3.1: IL-4 stimulation increases Cox-1 protein expression but not other prostanoid synthases

*(**A**) Real-time PCR of Ptgs-1 expression in murine BMDMs stimulated with or without IL-4 and 0.1% DMSO for 20 hours. (**B**) Representative western immunoblot of Cox-1 and Gapdh expression in murine BMDMs stimulated with or without IL-4 for 20 hours. (**C**) Representative western immunoblot of Cox-2 and Gapdh expression in murine BMDMs stimulated with or without IL-4 or LPS for 20 hours. (N=1-2 biological replicates per group). (**D**) Real-time PCR on mPges-1 expression in murine BMDMs stimulated with or without IL-4 or LPS. (**E**) Real-time PCR on Txas-1 expression in murine BMDMs stimulated with or without IL-4 or LPS. Unpaired two-tailed t-test or One-way ANOVA with Fisher's LSD test. *p<0.05, ***p<0.001. N=2-4 biological replicates per group. All experimental data are expressed as mean ± SEM.*

LC-MS/MS analysis of BMDM culture media supernatants showed a statistically significant increase in the production of 15d-PGJ_2 20 hours post IL-4 treatment as compared to untreated control BMDMs (**Fig 3.2A**). IL-4 stimulation did not lead to an increase in the production of TxB_2 or PGE_2 compared to untreated control BMDMs (**Fig 3.2B-C**). BMDMs treated with the TXAS inhibitor, ozagrel, where able to polarize toward an M2 phenotype in response to IL-4 at similar levels to DMSO treated BMDMs (**Fig 3.2D**). Treatment with ozagrel, lead to a decrease in the production of TxB_2 (**Fig 3.2E**).

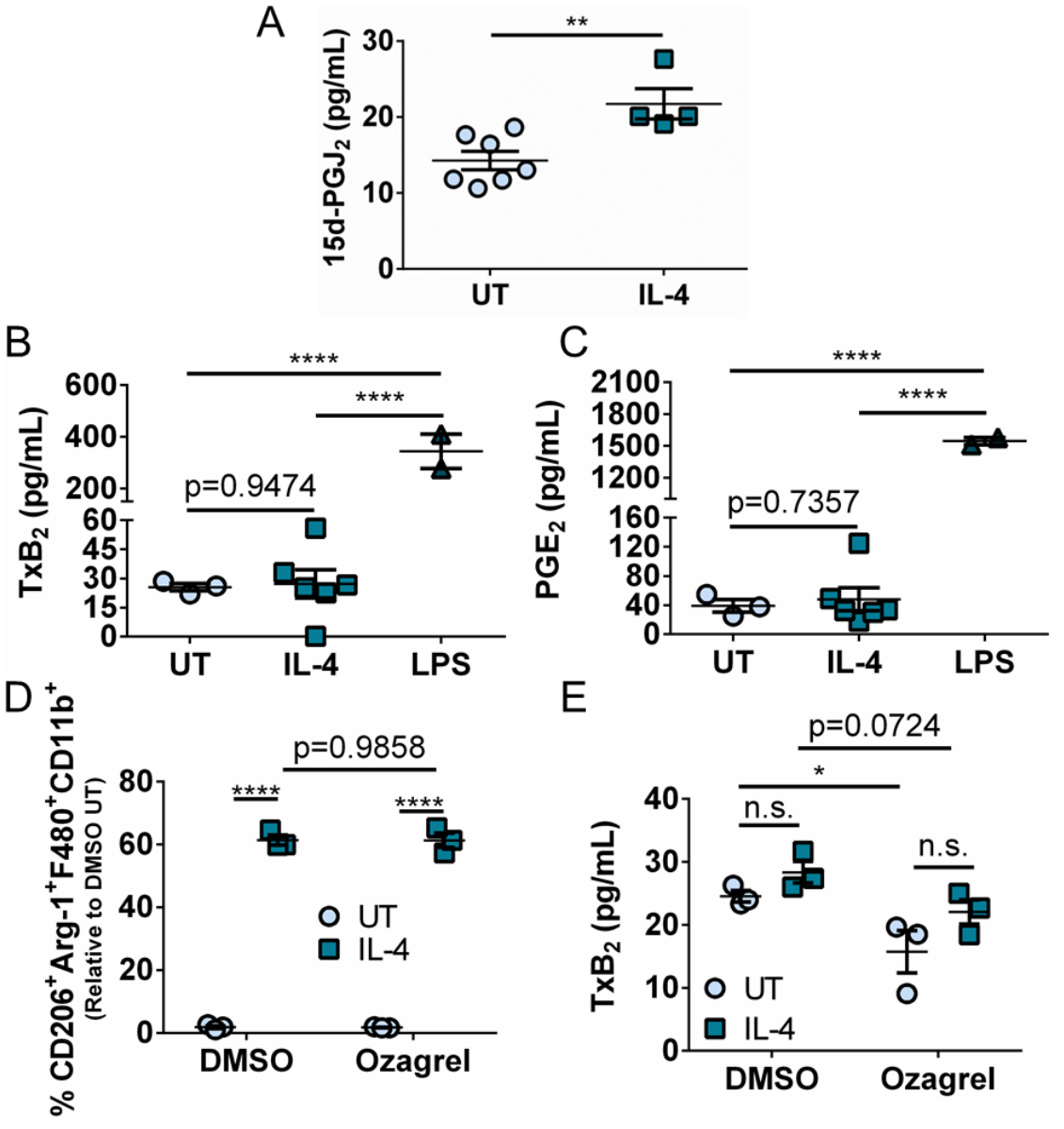

Figure 3.2: The effect of IL-4 stimulation on lipid mediator production

*(**A**) 15d-PGJ$_2$ production 20 hours post IL-4 stimulation. (**B**) TxB$_2$ in murine BMDM culture media supernatant stimulated with or without IL-4 or LPS. (**C**) PGE$_2$ in murine BMDM culture media supernatant stimulated with or without IL-4 or LPS. (**D**) Percentage CD206$^+$Arg-1$^+$F480$^+$CD11b$^+$ murine BMDMs stimulated with or without IL-4 or ozagrel relative to DMSO untreated control. (**E**) TxB$_2$ in murine BMDM culture media supernatant stimulated with or without IL-4 or ozagrel. Unpaired two-tailed t-test or One-way or Two-way ANOVA with Fisher's LSD test. *p<0.05, **p<0.01, ****p<0.0001. N=2-7 biological replicates per group. All experimental data are expressed as mean ± SEM.*

Finally, IL-4 stimulation led to approximately a 10-fold increase in the expression of M2 macrophages that was previously shown to be sensitive to indomethacin (**Fig 3.3A**) (17). Macrophages were first gated by their forward and side scatter characteristics followed by $CD11b^{+}F480^{+}$ cells, which consisted of ~98% of the macrophage population, and were further gated on $CD206^{+}$ and $Arg\text{-}1^{+}$ (**Fig 3.3B**). Furthermore, human macrophages differentiated from frozen PBMCs (33) also showed an increase in the expression of COX-1 protein upon treatment with IL-4 as with murine BMDMs. Differentiated human macrophages were confirmed by flow cytometry to be approximately 95% $CD68^{+}$ (**Fig 3.3C**). PBMCs from subject #1 and subject #2 had a 2.5-fold and 2.1-fold increase in COX-1 after IL-4 stimulation, respectively (**Fig 3.3D**). This data confirmed a previously reported increase in COX-1 expression after IL-4 stimulation (34).

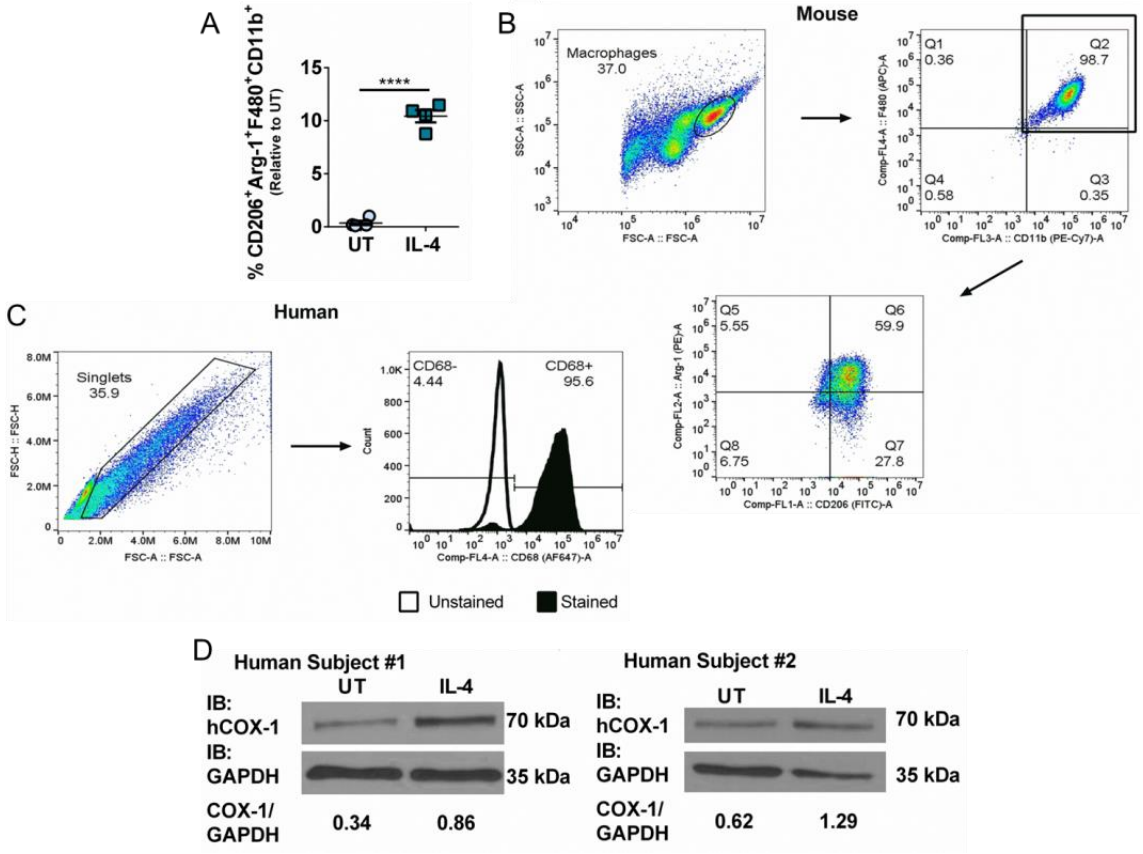

Figure 3.3: IL-4 drives M2 macrophage polarization and Cox-1 expression in humans

*(**A**) Percentage of $CD206^{+}Arg\text{-}1^{+}F480^{+}CD11b^{+}$ murine BMDMs stimulated with or without IL-4 relative to untreated control. (**B**) Representative images of murine BMDM flow cytometry gating strategy. (**C**) Representative images of human PBMC-derived macrophages flow cytometry gating strategy. (**D**) Western immunoblots of COX-1 and GAPDH from human PBMC-derived macrophages stimulated with or without human IL-4. Unpaired two-tailed t-test. ****p<0.0001. N=4 biological replicates per group. All experimental data are expressed as mean ± SEM.*

Cox-1 is Post-Transcriptionally Upregulated by IL-4 Stimulation

Based on the results above, to further examine whether regulation of Cox-1 expression was at the transcriptional or translational level, BMDMs were pre-treated with either actinomycin D or cycloheximide for 30 minutes or four hours, respectively, prior

to IL-4 stimulation. BMDMs treated with actinomycin D were collected two hours post-IL-4 stimulation due to impact on cell viability. BMDMs treated with cycloheximide were collected 20 hours post-IL-4 stimulation. *Arg-1* expression, which is known to be transcriptionally regulated by IL-4 stimulation, was evaluated to determine the efficacy of the actinomycin D treatment. BMDMs treated with actinomycin D had a 4-fold decrease in *Arg-1* expression compared to DMSO untreated control (**Fig 3.4A**). Cox-1 protein expression was not downregulated after actinomycin D treatment **(Fig 3.4B-C**). Strikingly, Cox-1 protein was completely absent in both untreated control and IL-4 treated cells compared to DMSO controls after cycloheximide treatment (**Fig 3.4D**). Since Cox-1 appears to be translationally regulated, we reasoned that *Ptgs-1* likely has a 5' terminal oligopyrimidine-like motif, which enables eIF4E to enhance translation. To this end, sequence analysis of *PTGS*-1 mRNA in both murine and human cells revealed the presence of 5' terminal oligopyrimidine sequences (**Fig 3.4E**). Interestingly, polysome profiling of murine BMDMs suggested that *Ptgs-1* translation is modulated by mTOR signaling, based on a loss of *Ptgs-1* mRNA from the heaviest polysome fractions (26% with IL-4 treatment) after torin 1 treatment (19% with IL-4 + torin 1 treatment), but is not mTOR exclusive (**Fig 3.4F**). As a comparison, *Rpl-13a*, a bona fide 5' terminal oligopyrimidine sequence containing mRNA (35), revealed a classical polysome profile for a typical mTOR-dependent mRNA, where all polysome fractions were sensitive to torin 1 treatment (30% with IL-4 treatment to 14% with IL-4 + torin 1 treatment) (**Fig 3.4F**).

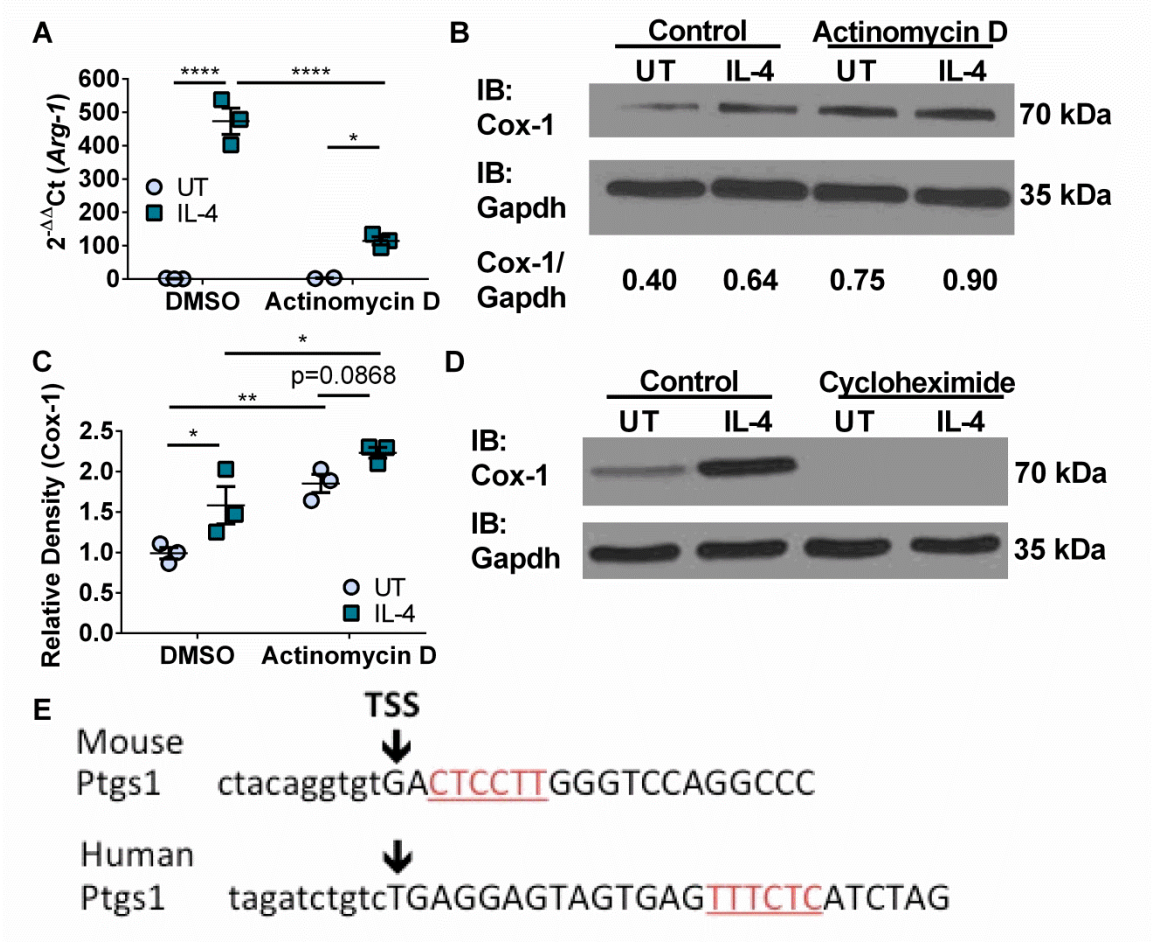
A
600
500
400
300
200
100
0
$2^{-\Delta\Delta}$Ct (*Arg-1*)
****
****
*
UT
IL-4
DMSO
Actinomycin D
B
Control
Actinomycin D
UT
IL-4
UT
IL-4
IB:
Cox-1
70 kDa
IB:
Gapdh
35 kDa
Cox-1/
Gapdh
0.40
0.64
0.75
0.90
C
Relative Density (Cox-1)
2.5
2.0
1.5
1.0
0.5
0.0
*
**
*
p=0.0868
UT
IL-4
DMSO
Actinomycin D
D
Control
Cycloheximide
UT
IL-4
UT
IL-4
IB:
Cox-1
70 kDa
IB:
Gapdh
35 kDa
E
TSS
Mouse
Ptgs1
ctacaggtgtGACTCCTTGGGTCCAGGCCC
Human
Ptgs1
tagatctgtcTGAGGAGTAGTGAGTTTCTCATCTAG

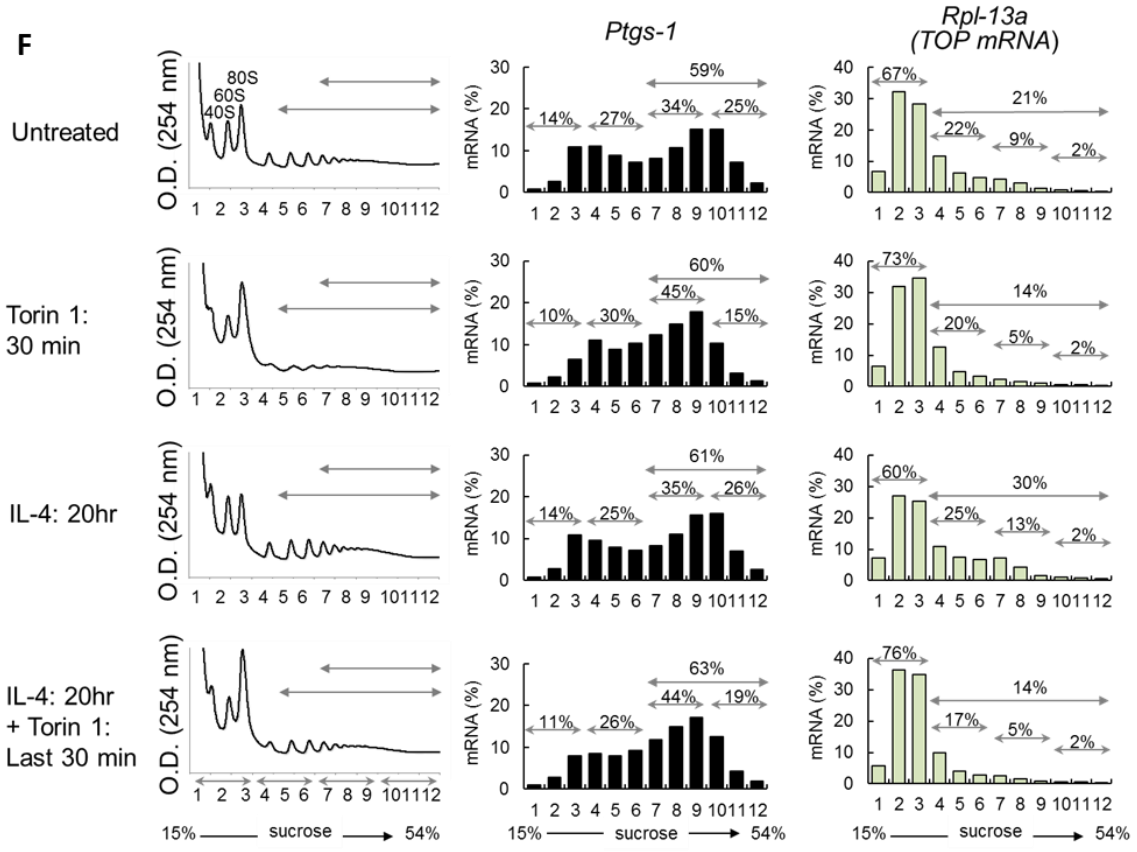

Figure 3.4: Cox-1 is post-transcriptionally upregulated by IL-4

*(**A**) Real-time PCR on Arg-1 expression in murine BMDMs stimulated with or without IL-4 and DMSO or actinomycin D. (**B**) Representative western immunoblot for Cox-1 and Gapdh expression in murine BMDMs stimulated with or without IL-4 and DMSO or actinomycin D. (**C**) Protein density of Cox-1 relative to DMSO untreated control. (**D**) Representative western immunoblot for Cox-1 and Gapdh expression in murine BMDMs stimulated with or without IL-4 and DMSO or cycloheximide. (**E**) Bioinformatic analysis of 5' terminal oligopyrimidine sequences in murine and human PTGS-1 mRNA. (**F**) Polysome profile on BMDMs stimulated with or without IL-4 and torin 1 for Ptgs-1 and Rpl-13a mRNA expression, N=1 per group. Two-way ANOVA with Fisher's LSD test. *p<0.05, **p<0.01 ****p<0.0001. N=2-4 biological replicates per group. All experimental data are expressed as mean ± SEM.*

The Role of Fes/Akt/mTOR Signaling Pathway in IL-4 Dependent Upregulation of Cox-1 Expression

The above data suggested that IL-4-treatment led to increased levels of Cox-1 protein. Therefore, we examined the underlying mechanisms downstream of the IL-4 receptor. BMDMs were treated with or without Jak inhibitor I four hours prior to IL-4 stimulation. Inhibitor efficacy was confirmed by the significant decrease in the expression of the Jak-dependent genes *Arg-1* and *Cd36* (**Fig 3.5A-B**). Surprisingly, Cox-1 was upregulated upon IL-4 treatment regardless of the presence or absence of Jak inhibitor I (**Fig 3.5C-D**). However, M2 macrophages were decreased by approximately 25-fold compared to untreated control BMDMs (**Fig 3.5E**).

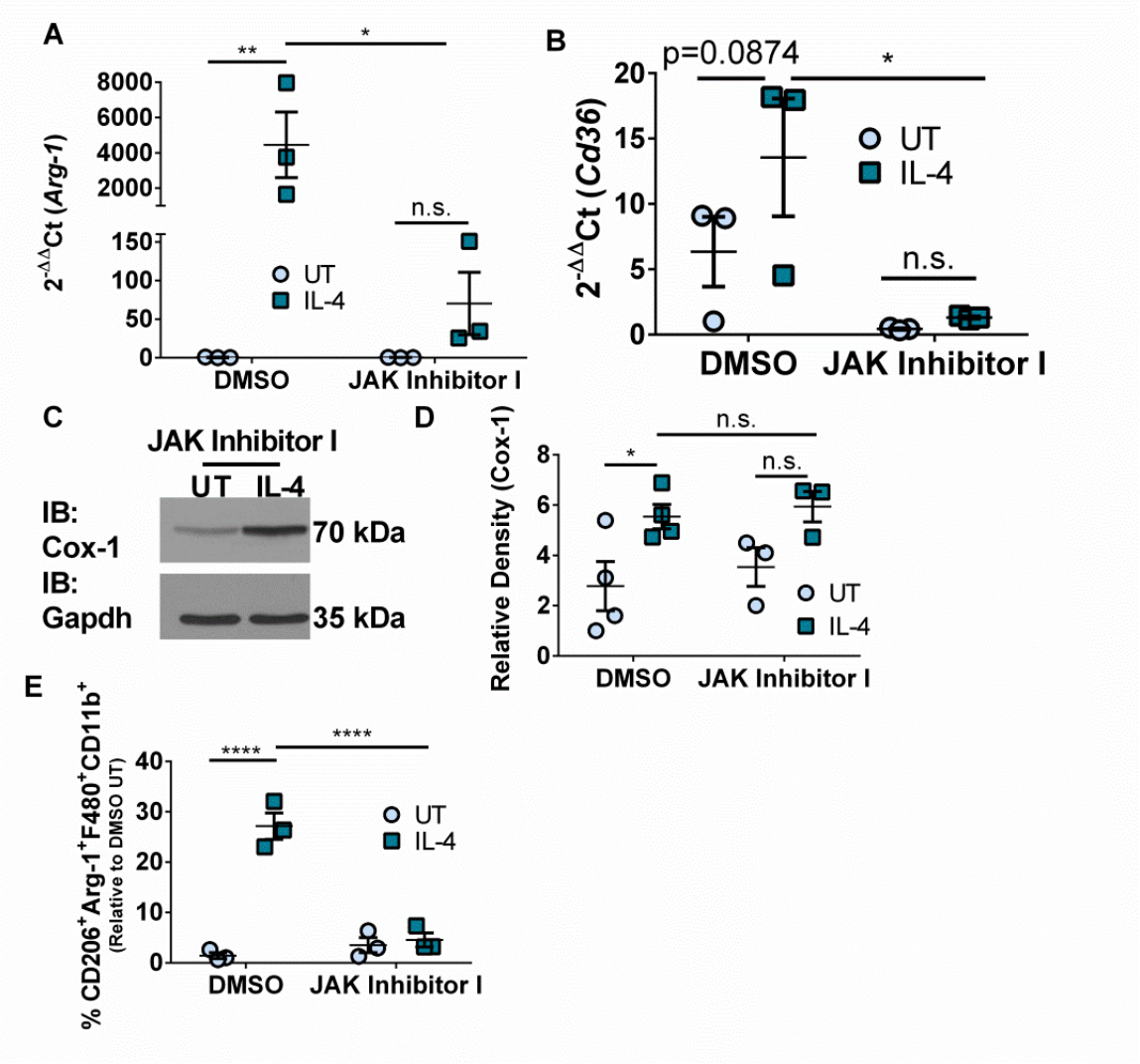

Figure 3.5: Inhibition of Jak signaling does not affect Cox-1 expression

*(**A**) Real-time PCR on Arg-1 expression in murine BMDMs stimulated with or without IL-4 and DMSO or Jak inhibitor I. (**B**) Real-time PCR on Cd36 expression in murine BMDMs stimulated with or without IL-4 and DMSO or Jak inhibitor I. (**C**) Representative western immunoblot for Cox-1 and Gapdh expression in murine BMDMs stimulated with or without IL-4 and Jak inhibitor I. (**D**) Protein density of Cox-1 relative to DMSO untreated control. (**E**) Percentage $CD206^{+}Arg\text{-}1^{+}F480^{+}CD11b^{+}$ murine BMDMs stimulated with or without IL-4 or Jak inhibitor I relative to DMSO untreated control. Two-way ANOVA with Fisher's LSD test. *p<0.05, **p<0.01, ****p<0.0001. N=3-4 biological replicates per group. All experimental data are expressed as mean ± SEM.*

Since IL-4-mediated expression of Cox-1 was not dependent on the Jak/Stat signaling pathway, we explored if the proto-oncogene protein tyrosine kinase Fes was key in transducing the signal downstream of the IL-4R to effect increased Cox-1 translation. Western immunoblot analysis of BMDMs confirmed the expression of Fes (**Fig 3.6A**). Incubation of BMDMs with the Fes inhibitor, herbimycin A, followed by treatment with IL-4 significantly decreased the expression of Cox-1 protein in BMDMs (**Fig 3.6B**).

Fes has been shown to signal through the Akt/mTOR pathway (8-10). In order to examine the activation of Akt/mTOR pathway, we first examined if phosphoinositide 3-kinase was involved upstream of Akt. BMDMs were pretreated with the phosphoinositide 3-kinase inhibitor, Ly294002, four hours prior to IL-4 stimulation. Treatment of BMDMs with Ly294002 and IL-4 did not decrease Cox-1 protein (**Fig 3.6C-D**). BMDMs were next pre-treated with Akt inhibitor VIII four hours prior to IL-4 stimulation. Western immunoblot analysis clearly showed that Akt inhibitor VIII significantly decreased the IL-4-dependent expression of Cox-1 protein (**Fig 3.6E**).

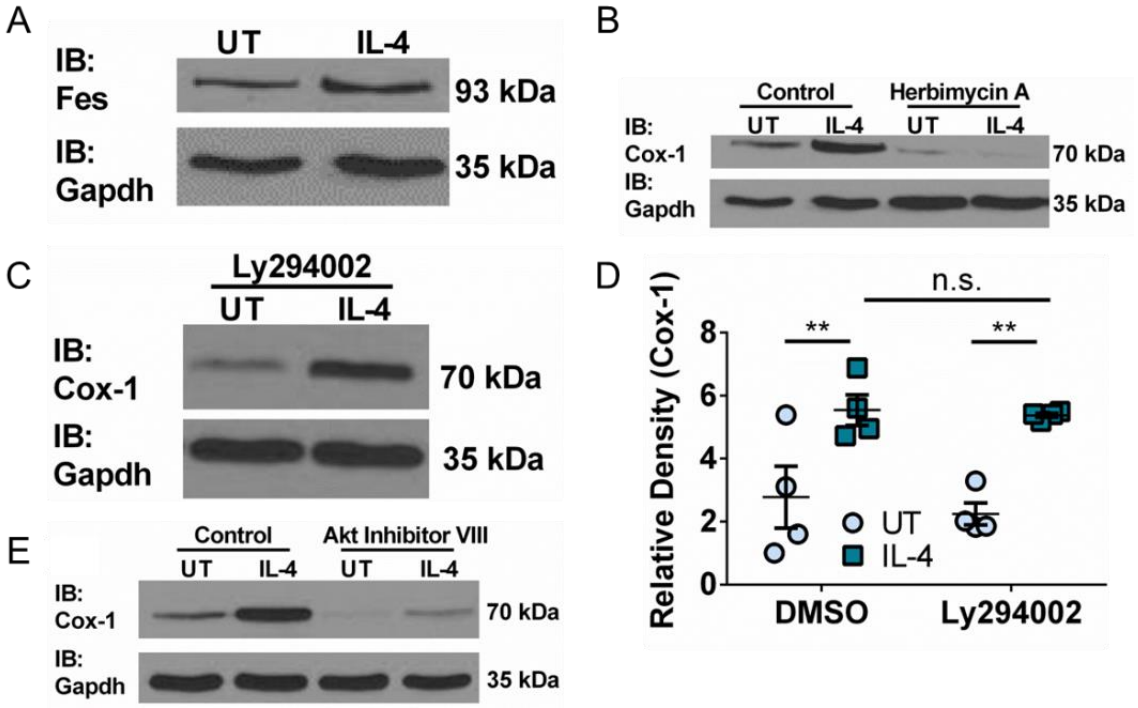

Figure 3.6: The role of Fes, phosphoinositide 3-kinase, and Akt in IL-4 dependent expression of Cox-1

(A) *Representative western immunoblot for Fes and Gapdh expression in murine BMDMs stimulated with or without IL-4. (N=1)* ***(B)*** *Representative western immunoblot for Cox-1 and Gapdh expression in murine BMDMs stimulated with or without IL-4 and DMSO or herbimycin A.* ***(C)*** *Representative western immunoblot for Cox-1 and Gapdh expression in murine BMDMs stimulated with or without IL-4 and Ly294002.* ***(D)*** *Protein density of Cox-1 relative to DMSO untreated control.* ***(E)*** *Representative western immunoblot for Cox-1 and Gapdh expression in murine BMDMs stimulated with or without IL-4 and DMSO or Akt inhibitor VIII. Two-way ANOVA with Fisher's LSD test. **p<0.01. N=3-4 biological replicates per group. All experimental data are expressed as mean ± SEM.*

Since polysome profiling suggested a loss of *Ptgs-1* mRNA from the heaviest polysome fractions following torin 1 treatment of IL-4 stimulated BMDMs, we examined if torin 1 treatment also impacted Cox-1 expression at the protein level. BMDMs were pretreated with torin 1 four hours prior to IL-4 stimulation. Torin 1, completely inhibited Cox-1 protein expression in both untreated control and IL-4 treated BMDMs (**Fig 3.7A**).

Treatment with torin 1 also significantly inhibited the phosphorylation of S6 kinase, which was slightly more phosphorylated in IL-4 treated BMDMs (**Fig 3.7B**). Torin 1 significantly decreased the production of 15d-PGJ_2 compared to DMSO + IL-4 treated cells (**Fig 3.7C**). Torin 1 treatment also led to a significant decrease in IL-4-dependent skewing of BMDMs towards an M2 phenotype (**Fig 3.7D**). Human PBMC-derived macrophages pre-treated with DMSO followed by IL-4 stimulation had a significant increase in COX-1, which was significantly decreased upon torin 1 pre-treatment (**Fig 3.7E**).

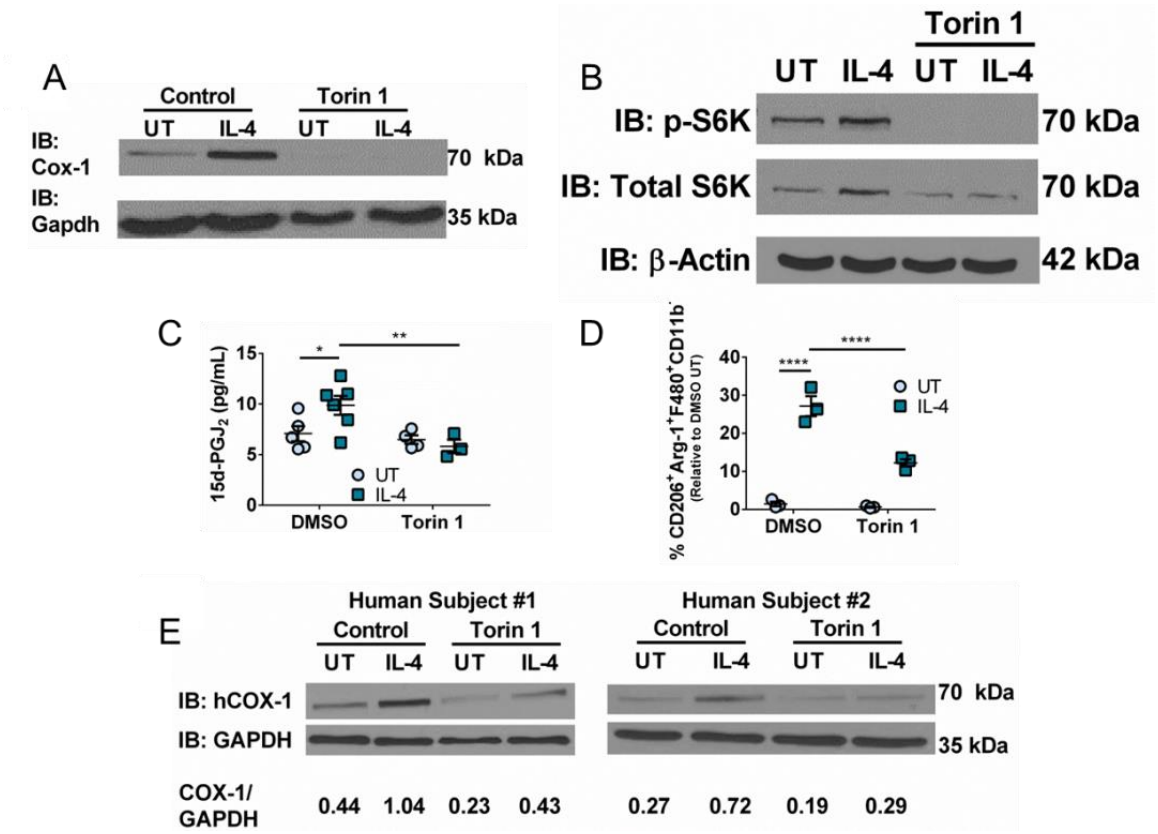

Figure 3.7: Cox-1 expression is controlled by the mTORC signaling pathway

*(**A**) Representative western immunoblot for Cox-1 and Gapdh expression in murine BMDMs stimulated with or without IL-4 and DMSO or torin 1. (**B**) Representative western immunoblot for p-S6K, total S6K, and β-actin expression in murine BMDMs stimulated with or without IL-4 and torin 1. (N=1) (**C**) Production of 15d-PGJ_2 from*

*murine BMDMs stimulated with or without IL-4 (20 hours) and DMSO or torin 1. (**D**) Percentage CD206$^+$Arg-1$^+$F480$^+$CD11b$^+$ murine BMDMs stimulated with or without IL-4 or torin 1 relative to DMSO untreated control. (**E**) Western immunoblots of COX-1 and GAPDH from human PBMC-derived macrophages stimulated with or without human IL-4 and DMSO or torin 1. Two-way ANOVA with Fisher's LSD test. *p<0.05, **p<0.01, ****p<0.0001. N=3-6 biological replicates per group. All experimental data are expressed as mean ± SEM.*

Fluorescent microscopy confirmed >70% population purity of the Ntc CRISPR gRNA and Tsc2 CRISPR gRNA (mCherry$^+$) into Cas9 GFP$^+$ bone marrow (**Fig 3.8A**). Tsc2 genomic mutation was confirmed by PCR followed by surveyor assay (**Fig 3.8B**). IL-4 stimulation of Ntc BMDMs led to a 2.8-fold increase in Cox-1 expression as seen throughout this study (**Fig 3.8C**). Knockout of Tsc2 in Cas9 BMDMs lead to a 2.4-fold decrease in Cox-1 expression compared to Ntc Cas9 BMDMs (**Fig 3.8C**). This further confirmed the role of mTOR signaling in Cox-1 protein expression through use of the CRISPR/Cas9 gene editing system.

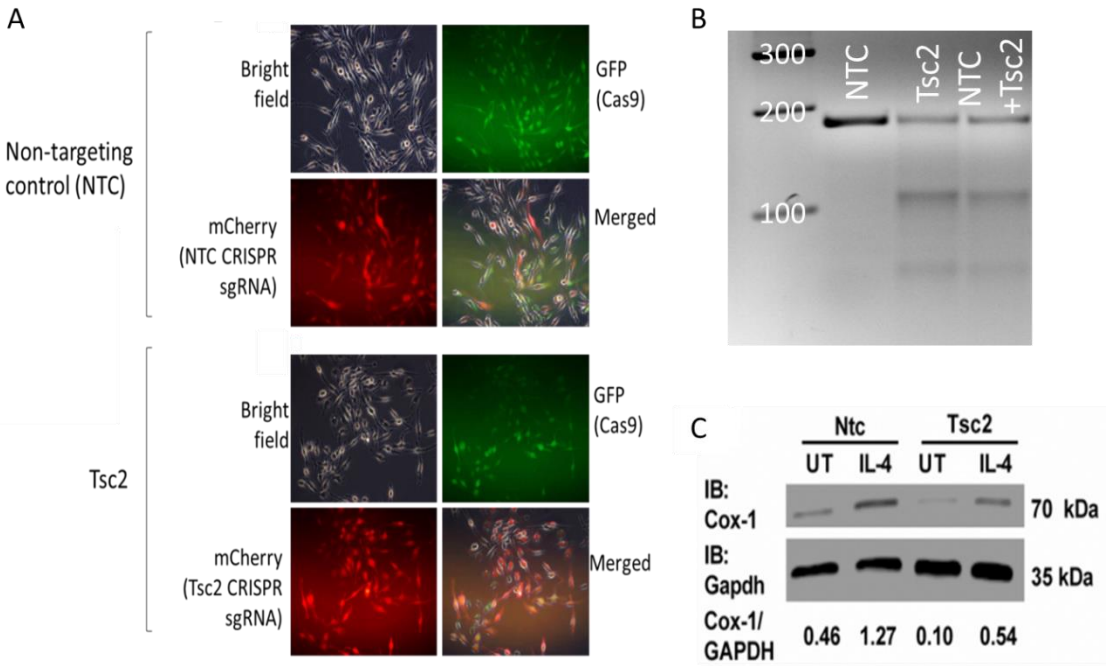

Figure 3.8: Genetic loss of mTORC regulatory protein, Tsc2, decreases Cox-1 expression upon IL-4 stimulation

*(**A**) 32X magnification of adherent cells. GFP=Cas9; mCherry=Non-targeting control (Ntc) or Tsc2 CRISPR gRNA. Images were merged as bright field, GFP and mCherry. (**B**) Representative DNA agarose gel for Ntc and Tsc2 transduced BMDMs processed by surveyor assay (**C**) Representative western immunoblot for Cox-1 and Gapdh expression in Cas9 murine BMDMs transduced with either Ntc or Tsc2-specific CRISPR gRNA and stimulated with or without IL-4 (N=1 per group).*

Activation of Amp-activated Protein Kinase Suppresses mTOR Signaling and Cox-1 Expression

We examined if metformin, a widely prescribed anti-diabetic drug that also activates Amp-activated protein kinase, which inhibits mTOR, affected Cox-1 expression in BMDMs. We reasoned that if metformin affected Cox-1 expression, it would translate to adversely affect the production of 15d-PGJ_2 and consequent polarization of macrophages. BMDMs were treated with or without metformin four hours prior to IL-4 stimulation (36). BMDMs treated with IL-4 following metformin pre-treatment had a decrease in Cox-1 expression (**Fig 3.9A**). LC-MS/MS analysis of the culture media supernatants showed decrease in 15d-PGJ_2 production upon metformin pre-treatment and IL-4 stimulation (**Fig 3.9B**). In addition, BMDMs treated with metformin and IL-4 had a slight but significantly decreased M2 macrophage phenotype compared to IL-4 stimulated BMDMs that were not treated with metformin (**Fig 3.9C**).

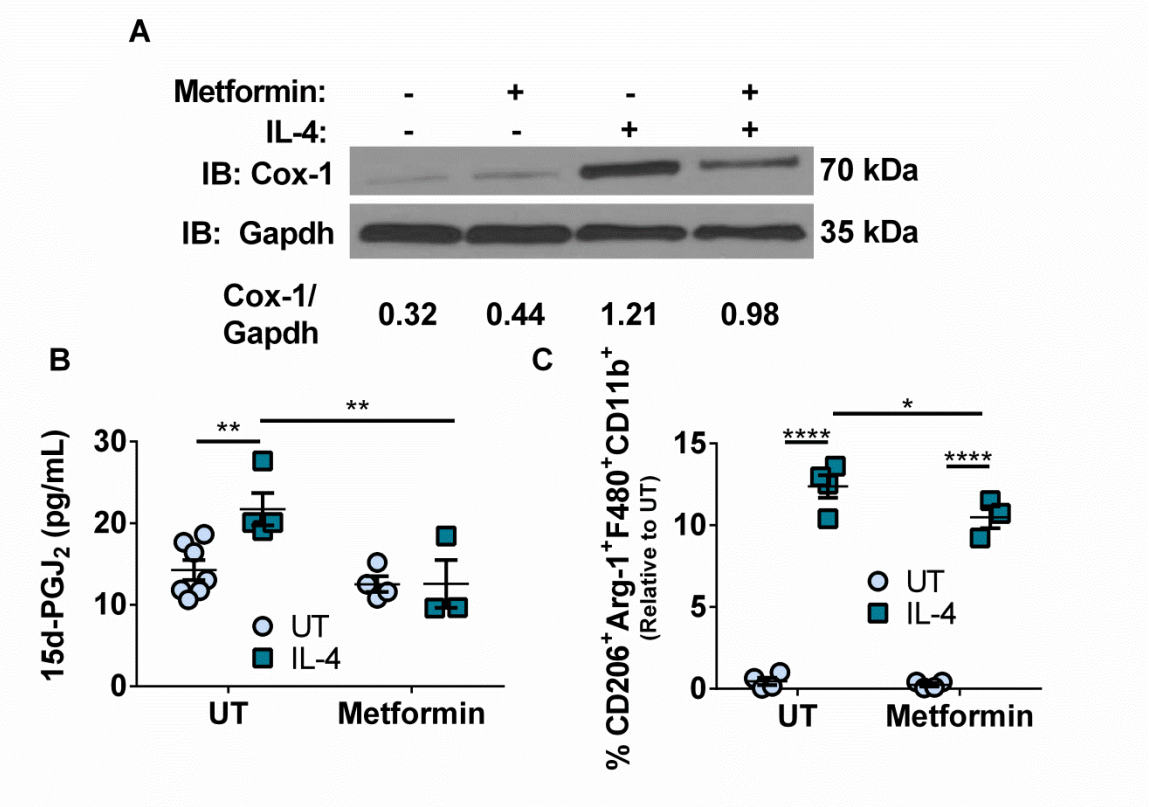

Figure 3.9: Amp-activated protein kinase activation *in vitro* reduced Cox-1 expression and M2 macrophages

*(**A**) Representative western immunoblot for Cox-1 and Gapdh expression in murine BMDMs stimulated with or without metformin or IL-4. (**B**) Production of 15d-PGJ$_2$ from murine BMDMs stimulated with or without metformin or IL-4 (20 hours). (**C**) Percentage CD206$^+$Arg-1$^+$F480$^+$CD11b$^+$ murine BMDMs stimulated with or without metformin or IL-4 relative to untreated control. Two-way ANOVA with Fisher's LSD test. *p<0.05, **p<0.01, ****p<0.0001. N=3-7 biological replicates per group. All experimental data are expressed as mean ± SEM.*

***In vivo* Amp-activated Protein Kinase Activation Exacerbates Parasitic Infection**

To examine if inhibition of mTOR through activation of Ampk by metformin treatment of mice impacted their ability to clear *N.brasiliensis* and if Cox-1-derived 15d-PGJ$_2$ played any role, mice were administered 300mg/kg metformin water with or without 0.05mg/kg/day 15d-PGJ$_2$ treatment one day prior to infection with infective

N.brasiliensis third-stage larvae (L3) and continued on treatment through day eight of the infection. Control mice either received Milli-Q water with sterile PBS intraperitoneal injections or metformin water with sterile PBS intraperitoneal injections. Immunoblot analysis of the jejunal extracts indicated a significant decrease in Cox-1 expression compared to the control jejunum (**Fig 3.10A**). Interestingly, jejunal extracts of mice revealed no Cox-2 expression in any of the treatment groups suggesting that Cox-1 was the predominant enzyme during a Th2 cytokine (IL-4/IL-13) response to infection with *N.brasiliensis* (**Fig 3.10B**) (37). Mice receiving Milli-Q water with sterile PBS intraperitoneal injections had the least parasitic burden as determined by number of adult *N.brasiliensis* worms in the small intestines (**Fig 3.10C**). However, metformin administration and sterile PBS intraperitoneal injections led to a three-fold higher adult worm burden compared to mice on Milli-Q water and sterile PBS intraperitoneal injections (**Fig 3.10C**). Further, mice on metformin water that were treated with exogenous 15d-PGJ_2 had a significant decrease in adult worm burden (**Fig 3.10C**). Interestingly, there was a strong negative correlation between the amount of Cox-1 protein expression and number of adult worms present in mice (**Fig 3.10D**). The expression of *Arg-1,* a M2 macrophage gene, was slightly decreased in the jejunum of mice treated with metformin; however treatment of mice with metformin and 15d-PGJ_2 restored the jejunal expression of *Arg-1* (**Fig 3.10E**).

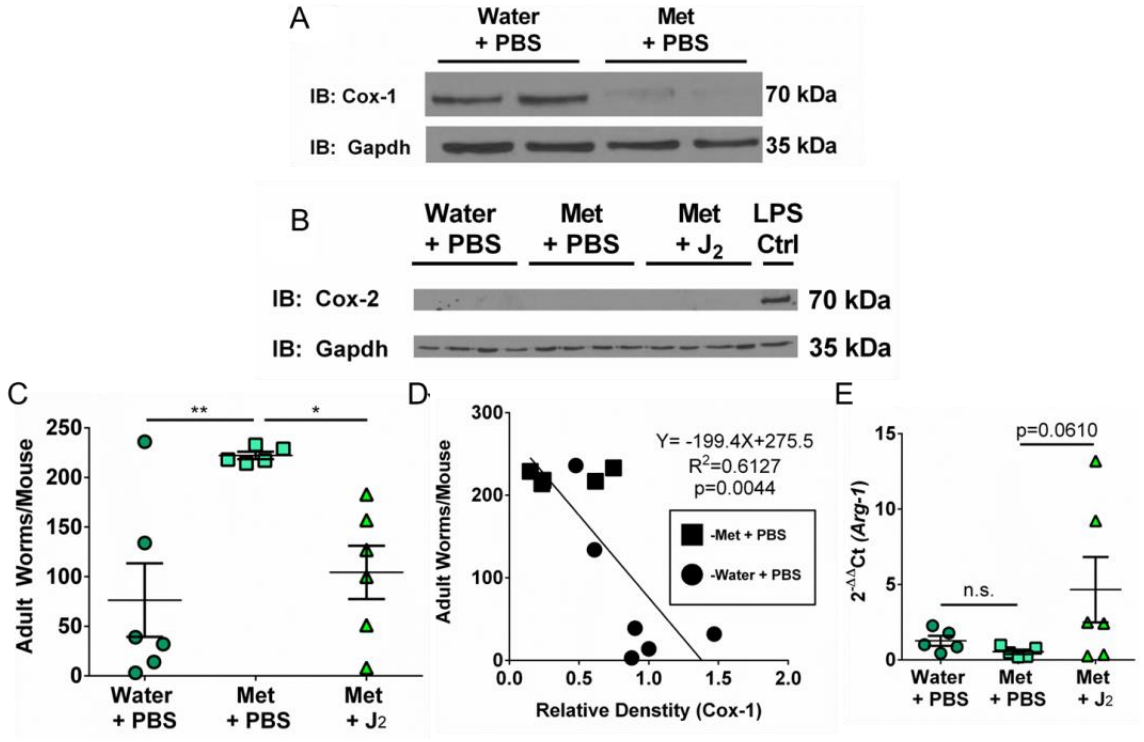

Figure 3.10: Amp-activated protein kinase activation *in vivo* delayed parasitic clearance

*(**A**) Representative western immunoblot for Cox-1 and Gapdh expression in the jejunum of mice treated with either water + PBS or metformin + PBS day eight post-infection with infective larvae. (**B**) Representative western immunoblot for Cox-2 and Gapdh expression in the jejunum of mice treated with either water + PBS, metformin + PBS, or metformin + 15d-PGJ$_2$ day eight post-infection with infective L3 and a LPS positive control. N= 1 (LPS) or 4 biological replicates per group. (**C**) Number of adult worms per mouse based on treatment day eight post-infection. (**D**) Correlation between Cox-1 protein expression and number of adult worms per mouse based on treatment day eight post-infection. (**E**) Real-time PCR on Arg-1 expression in the jejunum of infected mice based on treatment day eight post-infection. ROUT method (Q=5.0%). One-way ANOVA with Fisher's LSD test. Linear regression. *p<0.05, **p<0.01. N=5-6 biological replicates per group. All experimental data are expressed as mean ± SEM.*

Discussion

Cyclooxygenase-1 has been generally regarded as a constitutive enzyme regulated developmentally and key in the production of prostanoids, which effect homeostasis in

the kidney, stomach, and intestine. Previous studies have shown that various stimuli including TNFα, IL-1β, and LPS leads to the production of TxA_2/TxB_2 in monocytes/macrophages as well as human umbilical vein cells (HUVEC) (38,39). In unstimulated HUVECs, COX-1 is the predominant isoform leading to the production of TxA_2, however, upon IL-1β stimulation, COX-2 is significantly increased with a corresponding increase in PGE_2 and PGI_2 (38). IL-4 treatment has been shown in other studies to decrease pro-inflammatory mediators such as TxB_2 and PGE_2, which is also decreased in our study compared to LPS treatment. Additionally, we have shown that resting and IL-4 stimulated BMDMs produce baseline levels of TxB_2 and PGE_2, which appear to not play a significant role in M2 macrophage polarization. Our study describes a novel mechanism of upregulation of Cox-1 expression by a Th2 cytokine, IL-4, in macrophages. Interestingly, Cox-2, which is a highly inducible gene regulated by diverse stimuli via mechanisms involving transcriptional and translational control of expression, was significantly downregulated by IL-4, highlighting the importance of Cox-1 in a Th2 environment, such as during helminth infection.

Furthermore, the Akt-mTOR axis was involved in increased translation of *Ptgs-1* mRNA upon IL-4 treatment. The presence of 5' terminal oligopyrimidine sequences in the vicinity of the transcription start site in the 5' untranslated region of both murine and human *PTGS-1* mRNA further supported the involvement of mTOR. Surprisingly, *Ptgs-1* appears to not be exclusively regulated by mTOR in the same manner as traditional 5' terminal oligopyrimidine mRNA sequences. The use of CRISPR/Cas9 to knockout Tsc2 led to a decrease in Cox-1 expression. It is known that mTOR complex 1 is negatively regulated by Tsc complex while mTOR complex 2 is positively regulated by Tsc

complex. Additionally, mTORC2 is not sensitive to rapamycin treatment (data not shown) but is torin 1 sensitive. Finally, since Cox-1 does not behave as a *bona fide* 5' terminal oligopyrimidine sequence in regards to the polysome data, it is likely that mTORC2 may affect Cox-1 protein expression. However, the downstream targets of mTORC2 are unknown and further work is needed to delineate the functional differences between mTORC1 and mTORC2 in regulating Cox-1 protein expression. That being said mTOR signaling appears to play a role in the accumulation of Cox-1 protein over the course of IL-4 stimulation suggesting other mechanisms potentially involving protein stability.

Interestingly, when monocytes differentiate into macrophages various heat shock protein molecular chaperones are differentially expressed and vary depending on the macrophage polarization state (40,41). IL-4 treated (M2) macrophages differentially express five HSPs ($DNAJB_5$, $HSPA_{13}$, $HSPBAP_1$, $HSPH_1$, and $HSPB_1$) compared to unpolarized macrophages (41). Additionally, HSP27 ($HSPB_1$) has been shown to have anti-inflammatory and "anti-danger signal" activities (40). There are a few studies that have examined a relationship between Cox-2 and HSP27 during myofibroblast migration (42,43). Additionally, a recent study reported that HSP90 inhibition decreased Cox-2 mRNA expression and protein level in a colorectal cancer cell line (44). In light of the fact that IL-4 treatment of macrophages increases the expression of these chaperones, while significantly downregulating Cox-2 protein and increasing Cox-1 protein, it is plausible that Cox-1 interacts with HSPs, due to high structural similarities between Cox-1 and Cox-2, leading to the stabilization of Cox-1 protein. Further work is warranted to

investigate this phenomenon in macrophages and its overall impact on the pathophysiology of IL-4/IL-13-dependent intestinal clearance of *N.brasiliensis*.

The canonical pathway of signaling downstream of IL-4Rα typically involves Jak/Stat signaling and the phosphoinositide 3-kinase /Akt/mTOR pathway (7,11). While treatment of BMDMs with either herbimycin A, Akt inhibitor VIII, or torin 1 blocked Cox-1 protein expression; treatment with Ly294002 (phosphoinositide 3-kinase inhibitor), had no effect on Cox-1 expression implicating an alternate pathway of activation of Akt that involves Fes, as in T-cells and early myeloid progenitor cells (**Fig 3.11**) (8-10). Further work is warranted to characterize the under-appreciated interaction between IL-4Rα, Fes, and Akt in the context of mTOR activation. To extend the analysis of mTOR signaling and Cox-1 in macrophages, we showed that the production of 15d-PGJ_2 was significantly increased with IL-4 stimulation, which was inhibited upon loss of Cox-1 expression by torin 1 as well as metformin. Our data suggested that Cox-1 functionally couples with Hpgds to likely provide the ligand (15d-PGJ_2) to Ppar-γ, which acts in concert with Stat6 to activate transcription of Ppar-γ target genes to aid in macrophage (M2) polarization (15-17,45). More importantly, inhibition of mTOR by metformin, which negatively impacted M2 macrophage polarization, through decrease in Cox-1 expression, was rescued by exogenous treatment with 15d-PGJ_2 suggesting the importance of Cox-1 activity in macrophage function.

We utilized a helminth model to induce Th2 type inflammation to test the role of Cox-1 and metformin in helminth clearance. Mice treated with metformin had a significantly higher adult parasite burden compared to control mice, which was partially rescued with exogenous administration of 15d-PGJ_2. As in the helminth model, Cox-1

could also play a critical role in asthma and airway function. Cox-$1^{-/-}$ mice are hyper-responsive to bronchial constrictors and non-selective Cox inhibitors increased bronchial constriction in wildtype mice; while rofecoxib (a Cox-2 selective inhibitor) had no effect on airway hyper-responsiveness despite the expression of Cox-2 in epithelial tissue (46,47). This clearly suggested Cox-1, and not Cox-2, activity regulated airway function. However, metformin administration in asthmatics has proven to be beneficial (13) perhaps given its ability to impact a large set of mTOR targets, in addition to COX-1. In light of our studies demonstrating the regulation of Cox-1 by IL-4 in macrophage polarization, it is necessary to revisit the role of Cox-1 in the context of Th2 diseases in an effort to reconcile such apparent differences.

In conclusion, our studies provide evidence for a novel mechanism involving post-transcriptional regulation of Cox-1 expression upon IL-4 stimulation in human and murine macrophages (**Fig 3.11**). This is relevant because Cox activity is required to generate bioactive prostanoids, particularly PGJ_2 metabolites that serve as endogenous ligands for Ppar-γ and drive macrophage polarization (15-17,48). As shown here, only Cox-1, and not Cox-2, was expressed both *in vitro* and *in vivo* during a Th2-mediated response emphasizing the need to better understand the role of Cox-1 to enable development of new and more specific therapeutic regimens in addition to understanding how current drugs, such as metformin, may have unintentional effects on Cox regulation. Specifically, since inhibition of Cox-1 with indomethacin (17) or metformin was rescued by exogenous treatment with 15d-PGJ_2 to significantly alleviate nematode burden, it is clear that further studies are necessary to unravel the role of Cox-1 in promoting resolution in Th2-mediated inflammation.

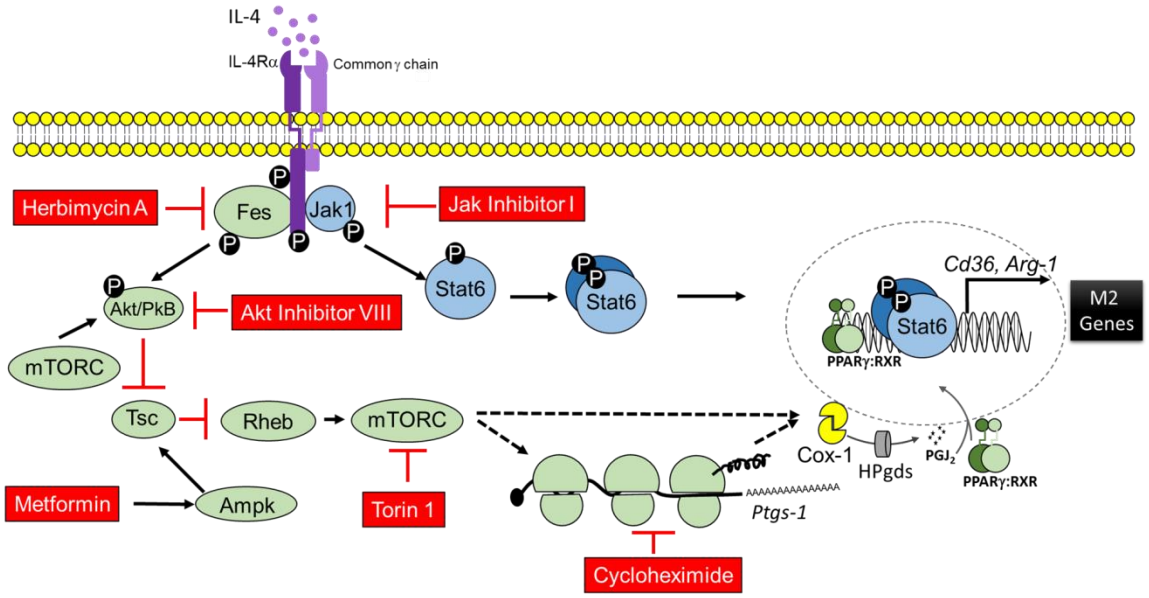

Figure 3.11: Schematic illustration of IL-4 mediated post-transcriptional control of Cox-1

In addition to the previously identified Jak/Stat6 pathway that is downstream of IL-4R, our studies suggested translational control of Cox-1 expression through the IL-4R, Fes, Akt, and mTOR axis to effect M2 polarization and resolution of helminth infection. Metformin-dependent activation of Ampk inhibited mTOR to decrease M2 macrophages in addition to Cox-1 translation which reduced 15d-PGJ$_2$ and subsequent Ppar-γ activation. Dotted lines represent post-transcriptional mechanisms of Cox-1 regulation downstream of mTOR complex that is yet to be identified.

References

1. Martinez, F. O., and Gordon, S. (2014) The M1 and M2 paradigm of macrophage activation: time for reassessment. *F1000Prime* Rep **6**, 13
2. Das, A., Sinha, M., Datta, S., Abas, M., Chaffee, S., Sen, C. K., and Roy, S. (2015) Monocyte and macrophage plasticity in tissue repair and regeneration. *Am J Pathol* **185**, 2596-2606
3. Gordon, S. (2003) Alternative activation of macrophages. *Nat Rev Immunol* **3**, 23-35
4. Martinez, F. O., Helming, L., and Gordon, S. (2009) Alternative activation of macrophages: an immunologic functional perspective. *Annu Rev Immunol* **27**, 451-483
5. Kreider, T., Anthony, R. M., Urban, J. F., Jr., and Gause, W. C. (2007) Alternatively activated macrophages in helminth infections. *Curr Opin Immunol* **19**, 448-453

6. Reece, J. J., Siracusa, M. C., and Scott, A. L. (2006) Innate immune responses to lung stage helminth infection induce alternatively activated alveolar macrophages. *Infect Immun* **74**, 4970-4981
7. Jiang, H., Harris, M. B., and Rothman, P. (2000) IL-4/IL-13 signaling beyond JAK/STAT. *J Allergy Clin Immunol* **105**, 1063-1070
8. Izuhara, K., Feldman, R. A., Greer, P., and Harada, N. (1994) Interaction of the c-fes proto-oncogene product with the interleukin-4 receptor. J Biol Chem 269, 18623-18629
9. Izuhara, K., Feldman, R. A., Greer, P., and Harada, N. (1996) Interleukin-4 induces association of the c-fes proto-oncogene product with phosphatidylinositol-3 kinase. *Blood* **88**, 3910-3918
10. Jiang, H., Foltenyi, K., Kashiwada, M., Donahue, L., Vuong, B., Hehn, B., and Rothman, P. (2001) Fes mediates the IL-4 activation of insulin receptor substrate-2 and cellular proliferation. *J Immunol* **166**, 2627-2634
11. Byles, V., Covarrubias, A. J., Ben-Sahra, I., Lamming, D. W., Sabatini, D. M., Manning, B. D., and Horng, T. (2013) The TSC-mTOR pathway regulates macrophage polarization. *Nat Commun* **4**, 2834
12. Zhu, L., Yang, T., Li, L., Sun, L., Hou, Y., Hu, X., Zhang, L., Tian, H., Zhao, Q., Peng, J., Zhang, H., Wang, R., Yang, Z., Zhang, L., and Zhao, Y. (2014) TSC1 controls macrophage polarization to prevent inflammatory disease. *Nat Commun* **5**, 4696
13. Park, C. S., Bang, B. R., Kwon, H. S., Moon, K. A., Kim, T. B., Lee, K. Y., Moon, H. B., and Cho, Y. S. (2012) Metformin reduces airway inflammation and remodeling via activation of AMP-activated protein kinase. *Biochem Pharmacol* **84**, 1660-1670
14. Ding, L., Liang, G., Yao, Z., Zhang, J., Liu, R., Chen, H., Zhou, Y., Wu, H., Yang, B., and He, Q. (2015) Metformin prevents cancer metastasis by inhibiting M2-like polarization of tumor associated macrophages. *Oncotarget* **6**, 36441-36455
15. Gandhi, U. H., Kaushal, N., Ravindra, K. C., Hegde, S., Nelson, S. M., Narayan, V., Vunta, H., Paulson, R. F., and Prabhu, K. S. (2011) Selenoprotein-dependent up-regulation of hematopoietic prostaglandin D2 synthase in macrophages is mediated through the activation of peroxisome proliferator-activated receptor (PPAR) gamma. *J Biol Chem* **286**, 27471-27482
16. Vunta, H., Davis, F., Palempalli, U. D., Bhat, D., Arner, R. J., Thompson, J. T., Peterson, D. G., Reddy, C. C., and Prabhu, K. S. (2007) The anti-inflammatory effects of selenium are mediated through 15-deoxy-Delta12,14-prostaglandin J2 in macrophages. *J Biol Chem* **282**, 17964-17973
17. Nelson, S. M., Shay, A. E., James, J. L., Carlson, B. A., Urban, J. F., Jr., and Prabhu, K. S. (2016) Selenoprotein Expression in Macrophages Is Critical for Optimal Clearance of Parasitic Helminth Nippostrongylus brasiliensis. *J Biol Chem* **291**, 2787-2798
18. Huang, J. T., Welch, J. S., Ricote, M., Binder, C. J., Willson, T. M., Kelly, C., Witztum, J. L., Funk, C. D., Conrad, D., and Glass, C. K. (1999) Interleukin-4-

dependent production of PPAR-gamma ligands in macrophages by 12/15-lipoxygenase. *Nature* **400**, 378-382

19. Cho, W., Kim, Y., Jeoung, D. I., Kim, Y. M., and Choe, J. (2011) IL-4 and IL-13 suppress prostaglandins production in human follicular dendritic cells by repressing COX-2 and mPGES-1 expression through JAK1 and STAT6. *Mol Immunol* **48**, 966-972
20. Vane, J. R., Bakhle, Y. S., and Botting, R. M. (1998) Cyclooxygenases 1 and 2. *Annu Rev Pharmacol Toxicol* **38**, 97-120
21. Nelson, S. M., Lei, X., and Prabhu, K. S. (2011) Selenium levels affect the IL-4-induced expression of alternative activation markers in murine macrophages. *J Nutr* **141**, 1754-1761
22. Lawrence, T., Willoughby, D. A., and Gilroy, D. W. (2002) Anti-inflammatory lipid mediators and insights into the resolution of inflammation. Nat Rev Immunol 2, 787-795
23. Serhan, C. N. (2014) Pro-resolving lipid mediators are leads for resolution physiology. *Nature* **510**, 92-101
24. Serhan, C. N., Chiang, N., and Van Dyke, T. E. (2008) Resolving inflammation: dual antiinflammatory and pro-resolution lipid mediators. *Nat Rev Immunol* **8**, 349-361
25. Ueno, N., Murakami, M., Tanioka, T., Fujimori, K., Tanabe, T., Urade, Y., and Kudo, I. (2001) Coupling between cyclooxygenase, terminal prostanoid synthase, and phospholipase A2. *J Biol Chem* **276**, 34918-34927
26. Kihara, Y., Gupta, S., Maurya, M. R., Armando, A., Shah, I., Quehenberger, O., Glass, C. K., Dennis, E. A., and Subramaniam, S. (2014) Modeling of eicosanoid fluxes reveals functional coupling between cyclooxygenases and terminal synthases. *Biophys J* **106**, 966- 975
27. Langenbach, R., Loftin, C., Lee, C., and Tiano, H. (1999) Cyclooxygenase knockout mice: models for elucidating isoform-specific functions. *Biochem Pharmacol* **58**, 1237-1246
28. Fitzpatrick, F. A. (2004) Cyclooxygenase enzymes: regulation and function. *Curr Pharm Des* **10**, 577-588
29. Kang, Y. J., Mbonye, U. R., DeLong, C. J., Wada, M., and Smith, W. L. (2007) Regulation of intracellular cyclooxygenase levels by gene transcription and protein degradation. *Prog Lipid Res* **46**, 108-125
30. Williams, C. S., Mann, M., and DuBois, R. N. (1999) The role of cyclooxygenases in inflammation, cancer, and development. Oncogene 18, 7908-7916
31. Morita, I. (2002) Distinct functions of COX-1 and COX-2. *Prostaglandins Other Lipid Mediat* **68-69**, 165-175
32. Mbonye, U. R., Wada, M., Rieke, C. J., Tang, H. Y., Dewitt, D. L., and Smith, W. L. (2006) The 19-amino acid cassette of cyclooxygenase-2 mediates entry of the protein into the endoplasmic reticulum-associated degradation system. *J Biol Chem* **281**, 35770-35778
33. Ramos, P., Casu, C., Gardenghi, S., Breda, L., Crielaard, B. J., Guy, E., Marongiu, M. F., Gupta, R., Levine, R. L., Abdel-Wahab, O., Ebert, B. L., Van

Rooijen, N., Ghaffari, S., Grady, R. W., Giardina, P. J., and Rivella, S. (2013) Macrophages support pathological erythropoiesis in polycythemia vera and beta-thalassemia. *Nat Med* **19**, 437-445

34. Martinez, F. O., Gordon, S., Locati, M., and Mantovani, A. (2006) Transcriptional profiling of the human monocyte-to-macrophage differentiation and polarization: new molecules and patterns of gene expression. *J Immunol* **177**, 7303-7311
35. Thoreen, C. C., Chantranupong, L., Keys, H. R., Wang, T., Gray, N. S., and Sabatini, D. M. (2012) A unifying model for mTORC1-mediated regulation of mRNA translation. *Nature* **485**, 109-113
36. Erices, R., Bravo, M. L., Gonzalez, P., Oliva, B., Racordon, D., Garrido, M., Ibanez, C., Kato, S., Branes, J., Pizarro, J., Barriga, M. I., Barra, A., Bravo, E., Alonso, C., Bustamente, E., Cuello, M. A., and Owen, G. I. (2013) Metformin, at concentrations corresponding to the treatment of diabetes, potentiates the cytotoxic effects of carboplatin in cultures of ovarian cancer cells. *Reprod Sci* **20**, 1433-1446
37. Oeser, K., Schwartz, C., and Voehringer, D. (2015) Conditional IL-4/IL-13-deficient mice reveal a critical role of innate immune cells for protective immunity against gastrointestinal helminths. *Mucosal Immunol* **8**, 672-682
38. Caughey, G. E., Cleland, L. G., Penglis, P. S., Gamble, J. R., and James, M. J. (2001) Roles of cyclooxygenase (COX)-1 and COX-2 in prostanoid production by human endothelial cells: selective up-regulation of prostacyclin synthesis by COX-2. *J Immunol* **167**, 2831- 2838
39. Kabashima, K., Murata, T., Tanaka, H., Matsuoka, T., Sakata, D., Yoshida, N., Katagiri, K., Kinashi, T., Tanaka, T., Miyasaka, M., Nagai, H., Ushikubi, F., and Narumiya, S. (2003) Thromboxane A2 modulates interaction of dendritic cells and T cells and regulates acquired immunity. *Nat Immunol* **4**, 694-701
40. Miller-Graziano, C. L., De, A., Laudanski, K., Herrmann, T., and Bandyopadhyay, S. (2008) HSP27: an anti-inflammatory and immunomodulatory stress protein acting to dampen immune function. *Novartis Found Symp* **291**, 196-208
41. Fagone, P., Di Rosa, M., Palumbo, M., De Gregorio, C., Nicoletti, F., and Malaguarnera, L. (2012) Modulation of heat shock proteins during macrophage differentiation. *Inflamm Res* **61**, 1131-1139
42. Saini, S., Liu, T., and Yoo, J. (2016) TNF-alpha stimulates colonic myofibroblast migration via COX-2 and Hsp27. *J Surg Res* **204**, 145-152
43. Chu, E., Saini, S., Liu, T., and Yoo, J. (2016) Bradykinin stimulates protein kinase D-mediated colonic myofibroblast migration via cyclooxygenase-2 and heat shock protein 27. *J Surg Res* **209**, 191-198
44. Mohammadi, A., Yaghoobi, M. M., Gholamhoseinian Najar, A., Kalantari-Khandani, B., Sharifi, H., and Saravani, M. (2016) HSP90 Inhibition Suppresses PGE2 Production via Modulating COX-2 and 15-PGDH Expression in HT-29 Colorectal Cancer Cells. *Inflammation* **39**, 1116-1123
45. Szanto, A., Balint, B. L., Nagy, Z. S., Barta, E., Dezso, B., Pap, A., Szeles, L., Poliska, S., Oros, M., Evans, R. M., Barak, Y., Schwabe, J., and Nagy, L. (2010) STAT6 transcription factor is a facilitator of the nuclear receptor PPARgamma-

regulated gene expression in macrophages and dendritic cells. *Immunity* **33**, 699-712

46. Harrington, L. S., Lucas, R., McMaster, S. K., Moreno, L., Scadding, G., Warner, T. D., and Mitchell, J. A. (2008) COX-1, and not COX-2 activity, regulates airway function: relevance to aspirin-sensitive asthma. *FASEB J* **22**, 4005-4010
47. Peebles, R. S., Jr., Hashimoto, K., Morrow, J. D., Dworski, R., Collins, R. D., Hashimoto, Y., Christman, J. W., Kang, K. H., Jarzecka, K., Furlong, J., Mitchell, D. B., Talati, M., Graham, B. S., and Sheller, J. R. (2002) Selective cyclooxygenase-1 and -2 inhibitors each increase allergic inflammation and airway hyperresponsiveness in mice. *Am J Respir Crit Care Med* **165**, 1154-1160
48. Odegaard, J. I., Ricardo-Gonzalez, R. R., Goforth, M. H., Morel, C. R., Subramanian, V., Mukundan, L., Red Eagle, A., Vats, D., Brombacher, F., Ferrante, A. W., and Chawla, A. (2007) Macrophage-specific PPARgamma controls alternative activation and improves insulin resistance. *Nature* **447**, 1116-1120
49. Livak, K. J., and Schmittgen, T. D. (2001) Analysis of relative gene expression data using real-time quantitative PCR and the 2(-Delta Delta C(T)) Method. *Methods* **25**, 402-408
50. Guan, B. J., Krokowski, D., Majumder, M., Schmotzer, C. L., Kimball, S. R., Merrick, W. C., Koromilas, A. E., and Hatzoglou, M. (2014) Translational control during endoplasmic reticulum stress beyond phosphorylation of the translation initiation factor eIF2alpha. *J Biol Chem* **289**, 12593-12611
51. Incio, J., Suboj, P., Chin, S. M., Vardam-Kaur, T., Liu, H., Hato, T., Babykutty, S., Chen, I., Deshpande, V., Jain, R. K., and Fukumura, D. (2015) Metformin Reduces Desmoplasia in Pancreatic Cancer by Reprogramming Stellate Cells and Tumor-Associated Macrophages. *PLoS One* **10**, e0141392
52. Camberis, M., Le Gros, G., and Urban, J., Jr. (2003) Animal model of Nippostrongylus brasiliensis and Heligmosomoides polygyrus. *Curr Protoc Immunol* Chapter 19, Unit 19 12
53. Knudsen, S. (1999) Promoter2.0: for the recognition of PolII promoter sequences. *Bioinformatics* **15**, 356-361

Chapter 4

The effects of a limited selenoproteome on M2 macrophage polarization

Ashley E. Shay[1], Arvind M. Korwar[1], Paul R. Copeland[2], Mary J. Kennett[1], Avinash K. Kudva[1], Venkatesha Basrur[3], Joseph F. Urban Jr[4], Ulrich Schweizer[5], Bradley A. Carlson[6], and K. Sandeep Prabhu[1]

Affiliations: [1]Department of Veterinary and Biomedical Sciences, The Pennsylvania State University, University Park, PA 16802; [2]Department of Biochemistry and Molecular Biology, Rutgers, Piscataway, NJ 08854; [3]Department of Pathology, Proteomics Resource Facility, University of Michigan, Ann Arbor, MI 48109; [4]U.S. Department of Agriculture, Agriculture Research Service, Beltsville Human Nutrition Research Center, Diet, Genomics, and Immunology Laboratory, Beltsville, MD, 20705 [5]Institute for Biochemistry and Molecular Biology, University of Bonn, Bonn, Germany; [6]Molecular Biology of Selenium Section, Mouse Cancer Genetics Program, NCI, National Institutes of Health, Bethesda, MD 20892

Contributions: AES and KSP conceived and coordinated the study as well as wrote the manuscript. AES designed, performed, and analyzed the data shown in Figs 4.1 to 4.6. PRC performed and analyzed the data shown in Fig 4.3A-B. AMK performed and analyzed the data shown in Fig 4.3E. VK generated the data shown in Fig 4.3E. AKK performed and analyzed the data shown in Fig 4.4E and Fig 4.5. MJK performed and

analyzed the data shown in Fig 4.6A-D. US provided the *Sbp2*$^{fl/fl}$ mice. BAC provided the *Trsp*$^{fl/fl}$ and *LysM*^{Cre} mice. JFU provided L3 stage *N.brasiliensis* larvae.

Abstract

Selenoprotein biosynthesis relies on a unique translational mechanism requiring selenocysteine $tRNA^{[Ser]Sec}$ (*Trsp*), a 3' untranslated region stem-loop structure, and a specialized set of proteins needed for optimal incorporation. Sec insertion sequence element binding protein-2 (Sbp2) binds to the stem-loop structure present in the 3' untranslated region of selenoprotein mRNAs and plays a critical role in the recruitment of selenocysteine charged $tRNA^{[Ser]Sec}$ to the translating ribosome for insertion at the UGA codon. Previous studies have shown that selenoproteins play a role in skewing arachidonic acid metabolism towards the production of Δ^{12}-prostaglandin J_2 (Δ^{12}-PGJ_2), which down-regulates inflammation. This increase in PGJ_2 production is important for increased M2 macrophage polarization needed for efficient *Nippostrongylus brasiliensis* infection clearance. Genetic deletion of *Trsp* in macrophages negatively affected the production of the entire selenoproteome which decreased Δ^{12}-PGJ_2 production and correlated with less efficient clearance of *N.brasiliensis*. However, genetic deletion of *Sbp-2* in macrophages led to a partial loss of the selenoproteome, reminiscent of a hierarchical control of expression. $Sbp2LysM^{Cre}$ bone marrow-derived macrophages (BMDMs), with a select few selenoproteins upregulated by IL-4 stimulation (*Seleno-I, Seleno-K, Txnrd-1*, and *Gpx-2*), were able to produce Δ^{12}-PGJ_2 at levels similar to those in $Sbp2LysM^{WT}$ BMDMs. Normal production of Δ^{12}-PGJ_2 led to unaltered M2 macrophage polarization and efficient *N.brasiliensis* clearance in $Sbp2LysM^{Cre}$ mice. These results suggest that these select few selenoproteins may regulate eicosanoid class

switching upon IL-4 stimulation to increase M2 macrophages to effectively clear *N.brasiliensis* infection.

Introduction

Selenium (Se) is a unique and essential micronutrient in that, unlike other minerals, it acts through the incorporation of the 21st amino acid, selenocysteine (Sec), into the growing polypeptide chain through a highly coordinated mechanism (1). Various forms of Se (selenite, selenate, Sec, and selenomethionine) are converted to hydrogen selenide. Hydrogen selenide is acted upon by the selenoprotein, selenophosphate synthetase-2 to generate selenophosphate and is charged to seryl-tRNA$^{[Ser]Sec}$ by a Sec transferase to form Sec-tRNA$^{[Ser]Sec}$ (*Trsp*). Sec-tRNA$^{[Ser]Sec}$ is recognized by a Sec specific elongation factor and ribosomal L30 protein through binding interactions with Sec insertion sequence (SECIS) element binding protein-2 (Sbp2) (2,3). Sbp2 binds to a unique stem-loop structure at the 3' untranslated region of mRNA destined to incorporate Sec at UGA codons instead of premature termination (2). Bioinformatic analysis scanning for SECIS elements has identified 25 selenoproteins in humans and 24 in mice (4). A majority of selenoproteins play critical roles in redox homeostasis (thioredoxin reductases [Txnrd], glutathione peroxidases [Gpx], and methionine-R-sulfoxide reductase [Msrb]) as well as thyroid metabolism (iodothyronine deiodinases [Dio]), and Se transport (selenoprotein P [Seleno-P]) (5). Txnrd-1 functions as homodimers containing a FAD prosthetic group and a NADPH binding domain to reduce thioredoxin which in turn reduces hydrogen peroxide, and lipid hydroperoxides (6). The Gpx family uses

glutathione (GSH) as a reductant to reduce hydrogen peroxide into water and lipid peroxides into alcohols generating oxidized glutathione (GSSG). Additionally, recent work has shown the importance of selenoprotein K (Seleno-K) in the activation and function of macrophages (8,9). Seleno-K is a 11kDa selenoprotein with a single transmembrane helix in its N-terminal that targets it to the ER membrane (10). Seleno-K has been shown to associate with the protein acetyltransferase, DHHC6, to palmitoylate cysteine residues on CD36, which is required for its clustered expression on the plasma membrane (11). However, many selenoproteins remain uncharacterized and new roles of already characterized selenoproteins need to be examined further.

Recent studies have revealed a novel role for selenoproteins in the switching of eicosanoids during arachidonic acid metabolism (12,13). Upon stimulation, arachidonic acid is released from the cell membrane by phospholipase A_2 and acted on by the cyclooxygenase (Cox) enzymes. Both the constitutively active form of Cox, Cox-1, and the inducible form, Cox-2, are able to enzymatically convert arachidonic acid to prostaglandin (PG) H_2. PGH_2 is metabolized by various prostaglandin synthases, in particular, hematopoietic prostaglandin D synthase (Hpgds), which converts PGH_2 to PGD_2. PGD_2 is unstable and readily undergoes non-enzymatic dehydration to form the cyclopentenone derivative, Δ^{13}-PGJ_2. Δ^{13}-PGJ_2 isomerizes to Δ^{12}-PGJ_2 followed by dehydration to form the end metabolite, 15-deoxy-$\Delta^{12,14}$-PGJ_2 (15d-PGJ_2) (14). These cyclopentenone prostaglandins (CyPGs) have been shown to have anti-inflammatory properties (15). Se supplementation, through selenoproteins, increases the expression of Hpgds through the production of CyPGs, which act as ligands for the peroxisome proliferator activated receptor (Ppar)-γ, in addition to inhibiting NK-κB (13,16). The

increase in CyPGs creates a positive feedback loop to further increase the expression of Hpgds through the binding of Ppar-γ to peroxisome proliferator activated receptor response element present in the promoter of *Hpgds* (13).

Macrophages can be classified by their activation states as M1 macrophages representing pro-inflammatory at one end of the spectrum and M2 representing anti-inflammatory at the other end of the spectrum with many poorly characterized intermediate phenotypes in between (17,18). The Se-dependent increase in Hpgds and endogenous CyPG production has been shown to increase M2 macrophage genes downstream of Ppar-γ activation (13,19). Additionally, Se works synergistically with IL-4 signaling to increase the polarization of macrophages to a M2 phenotype (20). Pharmacological inhibition of either arachidonic acid metabolism or IL-4 signaling decreased the Se-dependent expression of M2 macrophage genes (19,20).

Here we show that mice with macrophage-specific deletion of *Sbp2* express a partial selenoproteome compared to the total loss of selenoprotein expression as seen in macrophages from *Trsp* knockout mice. However, screening of all 25 known selenoproteins indicated only a select few (*Seleno-I*, *Seleno-K*, *Txnrd-1*, and *Gpx-2*) were upregulated under macrophage polarizing conditions in *Sbp2* knockout bone BMDMs compared to *Sbp2* wild-type BMDMs. These few selenoproteins were sufficient to facilitate arachidonic acid metabolism and macrophage polarization. As a result, expression of a subset of selenoproteins was sufficient to impart the protective effects of dietary Se against parasitic infection. This study provides evidence that a subset of selenoproteins are involved in arachidonic acid metabolism to increase M2 macrophages, which assist in resolving inflammatory challenges.

Materials and Methods

Mice

A C57BL/6 transgenic mouse with a floxed *Sbp2* (*Sbp2*$^{fl/fl}$) allele, generously provided by Dr. Ulrich Schweizer (University of Bonn), was crossed to a transgenic mouse containing Cre recombinase driven by the lysozyme M promoter (LysM^{Cre}), generously provided by Dr. Dolph Hatfield (NCI-NIH). Deletion of *Sbp2* creates an altered selenoprotein expression in macrophages, monocytes, and other granulocytes (21-23); while deletion of *Trsp* completely ablates the selenoproteome as shown earlier (24). Mice were maintained on either a Se-deficient (<0.01 ppm) or Se-supplemented diet (0.4 ppm sodium selenite) (Harlan Teklad), for at least 12 weeks before use in experiments. Studies were preapproved by the Institutional Animal Care and Use Committee and the Institutional Biosafety Committee at Penn State University.

Genotyping

Sbp2 deletion was confirmed by PCR analysis of the floxed region of the gene and the presence of LysM^{Cre}. Tail snips were incubated overnight at 65°C in 250µl of lysis buffer (100mM Tris-HCl, pH 8.8, 5mM EDTA, pH 8.0, 0.2% SDS, and 200mM NaCl) and 5µl of proteinase K (800 units/ml, New England BioLabs, Ipswich, MA). Lysed tail snips were centrifuged at 14,000rpm for five min at room temperature. Supernatants were collected and diluted (1:10) with nuclease free water. PCR was carried out using 0.4µM primers, 0.2mM deoxyribonucleotide triphosphates, 1.25 units GoTaq

DNA polymerase (Promega, Madison, WI), GoTaq buffer, and 1µl diluted DNA. Two sets of primers were used as follows: primer set 1: Sbp2fwd= TGTTTCTATTCTCATCTACTCTGCTCA and Sbp2rev= TAACTCCCCCTTTCCATCTG, and primer set 2: Cre-ER1= TCTGGCAGTAAAAACTATC, Cre-ER2= GTGAAACAGCATTGCTGTCACTT, Internal-1= CTAGGCCAGAGAATTGAAAGATCT and Internal-2= GTAGGTGGAAATTCTAGCATCATCC. The PCR products (floxed=379bp, non-floxed=210bp, non-specific band=672bp, cre=101bp, internal cre control=~320bp) were separated by electrophoresis on a 2% agarose gel and visualized by UV transillumination. *Sbp2* mice were considered wild-type if they either had no flox sequences or were heterozygous for flox sequences with Cre-recombinase under the LysM promoter present. *Trsp* mice were maintained and genotyped as previously described (19).

Cell Culture

Femurs were harvested and each were flushed with 5mL DMEM media (Life Tech) containing 2 mM L-glutamine (Corning), 100 I.U. penicillin (Corning), 100 µg/mL streptomycin (Corning), 5% Se-deficient fetal bovine serum (Atlanta), and 10% L929 supplemented media plated in 10cm plates and collected on the seventh day. Sodium selenite (Sigma) was added at 250nM for last five days. BMDM cultures were kept at 5% carbon dioxide and 37°C. Recombinant murine IL-4 (R&D systems) was added 20 hours prior to cell collection at a concentration of 10 ng/mL. Cell pellets were used in assays as described below.

RNA Extraction and Real-Time PCR

BMDMs were harvested and RNA was extracted using trizol according to the manufacturer's instructions (5 prime). Briefly, BMDMs were collected and homogenized with 1mL Trizol followed by room temperature incubation to aid in membrane dissociation. 200µL chloroform was added followed by agitation and centrifugation at 12,000g for 15 minutes. The upper aqueous layer was collected and RNA was precipitated by adding 500µL isopropanol and incubating at room temperature for ten minutes followed by centrifuging at 12,000g for ten minutes. Pellets were washed with 1mL 75% ethanol and centrifuged at 7,600g for five minutes. RNA pellets were dried and reconstituted with nuclease free water. Concentration and RNA quality was measured by spectrophotometry. 2µg RNA was used to reverse transcribe cDNA using a kit (Life technologies). 2µL cDNA was used in a 10µL reaction containing qPCR master mix (Quanta), nuclease free water, and either macrophage polarization specific taqman probes (Life technologies) or Sybr Green selenoprotein primers (Eurofins). Gene abundance was analyzed and $2^{-\Delta\Delta Ct}$ was calculated to represent change in gene expression relative to *Gapdh*.

^{75}Se Radiolabeling

BMDMs were cultured as described above except 100nM radiolabeled ^{75}Se (University of Missouri Research Reactor) was added simultaneously with 10ng/mL recombinant murine IL-4 (R&D Systems) for 20 hours and then harvested for phosphorImaging (GE Healthcare). Media was removed and NP-40 lysis buffer (50mM

Tris pH 8.0, 150mM NaCl, 1% NP-40, 1mM dithiothreitol and 0.5mM phenylmethylsulfonyl fluoride) was added directly to culture dishes to lyse cells. Supernatant was cleared by centrifuging at 17,000*g* for 10 minutes. Supernatant was transferred to a new tube and a portion was combined with 4X SDS sample buffer, boiled, and frozen. Sample and ^{75}Se HepG2 marker was loaded onto a 12% SDS-polyacrylamide gel. The gels were Coomassie stained, dried, and phosphorimaged overnight. A scanned Coomassie gel was used to normalize samples. These experiments were performed at Rutgers University, Piscataway, NJ.

Proteomics

Cultured BMDMs treated with and without IL-4 were harvested, washed with PBS and protein was extracted in 50mM HEPES buffer containing 8M urea. Proteins were reduced and alkylated by 100mM DTT at 56°C for 15min and 200mM iodoacetamide in the dark for 15min, respectively followed by hydrolysis overnight 37°C by using proteomic grade trypsin (Sigma Aldrich) in 10:1 ratio. 400ng of tryptic digest was reconstituted in 5μL of 0.1% formic acid in 3% ACN and applied on to Easy nLC (Thermo Fisher Scientific) C18 column online coupled to HR/AM Q-Exactive Orbitrap MS (Thermo Fisher Scientific) at the University of Michigan Proteomic Resource Facility, Ann Arbor, MI, in collaboration with Dr. Venkatesha Basrur. The instrument parameters were fine-tuned and optimized for better results. The MS acquired data-set were processed by using Proteome Discoverer, Version 2.1 (Thermo Fisher Scientific). The SEQUEST HT (a computer algorithm for database search) was used for peptide

identification. The data-set were searched against Mouse database [*Mus musculus* (SwissProt TaxID=10090 (v2017-05-10)]. The search was performed using the following parameters: Peptide and fragment mass tolerance were 10 ppm, 0.5Da, respectively, with two missed cleavages and 1% false discovery rate. Search criteria included fixed and variable modifications as carbamidomethylation (Cysteine) and oxidation (Methionine), respectively.

Western Immunoblot

BMDMs were incubated with mammalian protein extraction reagent, 1mM phenylmethylsulfonyl fluoride, 5 µg/mL leupeptin, 5 µg/mL pepstatin, and 5 µg/mL aprotinin on ice for 20 minutes with vortexing every five minutes. Cellular debris was pelleted by centrifugation at maximum speed for ten minutes. Supernatant was collected and protein concentration was measured using a BCA protein assay kit (Thermo). Protein was loaded onto a discontinuous SDS-PAGE gel (t=12.5%). Proteins were transferred to a nitrocellulose blotting membrane and blocked with skim milk for 45 minutes and then incubated overnight with primary antibody in skim milk at the following dilutions: Txnrd-1, 1:769 (Abcam). Cox-1, 1:2,000 (Cayman). Cox-2, 1:2,000 (Cayman). Hpgds, 1:2,000 (Cayman). Gpx-1, 1:2,000 (Abcam). Gapdh, 1:600,000 (Fitzgerald). Secondary antibodies: goat anti-rabbit 1:2,000 (Gpx-1), 1:2,500 (Cox-1, Cox-2, Hpgds, and Txnrd-1) (Thermo), goat anti-mouse 1:5,000 (Gapdh) (Thermo). The western immunoblot was developed with the supersignal west pico chemiluminescent substrate (Thermo).

Lipid Extraction and Liquid Chromatography-Mass Spectrometry

Cell media was collected and acidified with hydrochloric acid (0.06N). Samples were passed through a Sep-pak classic C18 column (Waters) three times followed by a wash with hexane and elution with methanol. Extracts were dried under a constant stream of nitrogen gas and resuspended in 200uL 70% methanol. Δ^{12}-PGJ_2 was quantified by extracted ion chromatography and multiple reaction monitoring (transition from base ion peak of 332.8 m/z to 188.9, 314.9, and 271.3 daughter ions) on a liquid chromatograph-triple quadrupole mass spectrometer using a 70% isocratic gradient on ESI^- mode. Peaks were analyzed using ABSCIEX Analyst software as described earlier (25).

Nippostrongylus brasiliensis Infection

Sbp2LysM^{WT} and *Sbp2LysM*^{Cre} mice were subcutaneously infected with 500 third stage larvae (L3), generously provided by Dr. Joseph Urban Jr. (USDA), and euthanized day eight post-infection. L3 larvae, adult worms, and eggs were isolated and enumerated as previously described (26).

Histology

The left lobe of the lung was removed day eight post *N.brasiliensis* infection, fixed in 10% paraformaldehyde, sectioned, and stained with H&E for histopathology (The Pennsylvania State University Animal Diagnostic Laboratory). Histological analysis was performed blindly (Dr. Mary Kennett) and the slides were scored as follows: 0–4: 0:

within normal limits, 1: minimally affected, 2: mildly affected, 3: moderately affected, and 4: severely affected. Total score was the average of the scores for inflammation, necrosis, emphysema, consolidation, airway hyperplasia, and hemorrhage.

Statistics

All data are expressed as mean ± SEM. Two-way ANOVA with Fisher's LSD test was used to compare the mean of each treatment group to the mean of each other treatment group using GraphPad Prism (GraphPad Software). P values ≤ 0.05 were considered statistically significant.

Results

Macrophage-specific Sbp2 Knockout BMDMs have Incomplete Selenoprotein Transcriptome Expression

Previous work from our laboratory has shown that selenoproteins are important for the polarization of macrophages toward an M2 phenotype by generating anti-inflammatory CyPGs (13,19,20,27). However little is known about which of the 24 selenoproteins are important in macrophage polarization. To determine which selenoproteins are involved in macrophage polarization, *Sbp2*$^{fl/fl}$ mice were bred with *LysM*^{Cre} mice in order to selectively delete *Sbp2* in macrophages (**Fig 4.1A**). Excision of *Sbp2* by genetic recombination was determined by confirming the presence of both LoxP sites on both alleles and Cre recombinase by PCR (**Fig 4.1B-C**). All selenoprotein

mRNA expression levels were measured by real time-PCR in *Sbp2LysM*^{WT} and *Sbp2LysM*^{Cre} BMDMs treated with or without 250nM Se and IL-4 stimulation for 20 hours. Selenoproteins that showed an increase in expression with IL-4 stimulation and 250nM Se in *Sbp2LysM*^{Cre} BMDMs (*Gpx-2*, *Seleno-I*, *Seleno-K*, *Txnrd-1*, *Txnrd-3*, and *Seleno-M*) compared to *Sbp2LysM*^{WT} BMDMs with no Se added were examined further (**Fig 4.1D-H**). *Seleno-I, Seleno-K, Txnrd-1,* and *Gpx-2* were significantly increased in *Sbp2LysM*^{Cre} BMDMs treated with 250nM Se compared to *Sbp2LysM*^{WT} BMDMs with no Se addition (**Fig 4.2A-D**). *Seleno-M* expression was significantly increased in *Sbp2LysM*^{WT} BMDMs treated with 250nM Se compared to 0nM Se, but not in *Sbp2LysM*^{Cre} BMDMs (**Fig 4.2E**). There were no significant differences in expression of *Txnrd-3* for any treatment (**Fig 4.2F**). Therefore loss of the selenoprotein biosynthesis protein Sbp2 in macrophages downregulates the transcriptional expression of all selenoprotein mRNAs except *Seleno-I, Seleno-K, Txnrd-1,* and *Gpx-2* when treated with IL-4.

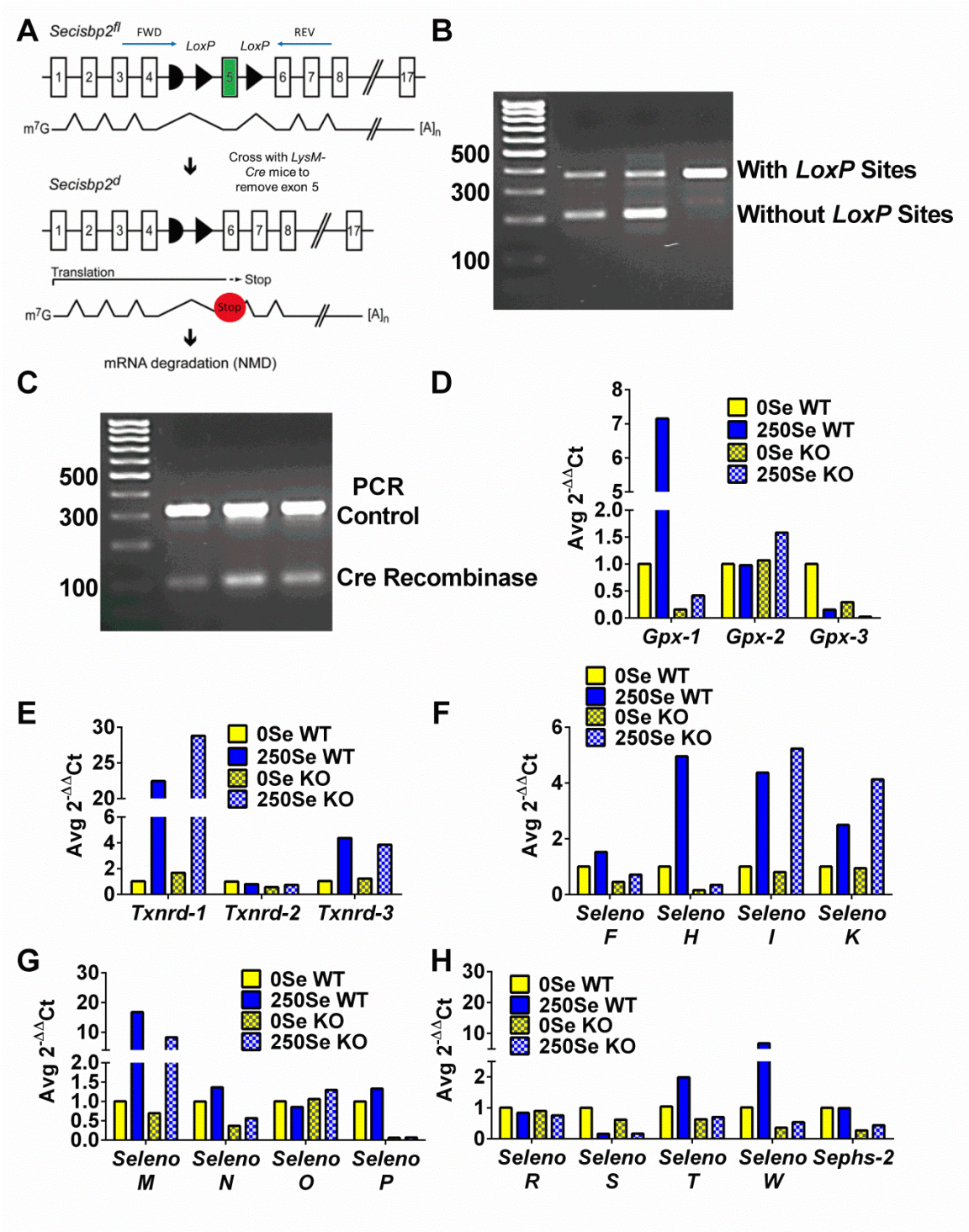

Figure 4.1: Selenotranscriptome screening

*(**A**) Schematic depicting the Sbp2 Lox-Cre breeding strategy. (**B**) PCR of murine genomic DNA to determine the presence of LoxP sequences in the Sbp2 gene. (**C**) PCR of murine*

*genomic DNA to determine the presence of Cre recombinase under the LysM promoter. (**D**) Real-time PCR on Gpx-1, Gpx-2, and Gpx-3 expression in Sbp2LysM^{WT} and Sbp2LysM^{Cre} BMDMs treated with or without 250nM Se and IL-4. (**E**) Real-time PCR on Txnrd-1, Txnrd-2, and Txnrd-3 expression in Sbp2LysM^{WT} and Sbp2LysM^{Cre} BMDMs treated with or without 250nM Se and IL-4. (**F**) Real-time PCR on Seleno-F, Seleno-H, Seleno-I, and Seleno-K expression in Sbp2LysM^{WT} and Sbp2LysM^{Cre} BMDMs treated with or without 250nM Se and IL-4. (**G**) Real-time PCR on Seleno-M, Seleno-N, Seleno-O, and Seleno-P expression in Sbp2LysM^{WT} and Sbp2LysM^{Cre} BMDMs treated with or without 250nM Se and IL-4. (**H**) Real-time PCR on Seleno-R, Seleno-S, Seleno-T, Seleno-V, Seleno-W, and Sephs-2 expression in Sbp2LysM^{WT} and Sbp2LysM^{Cre} BMDMs treated with or without 250nM Se and IL-4. N=1 individual mouse per group.*

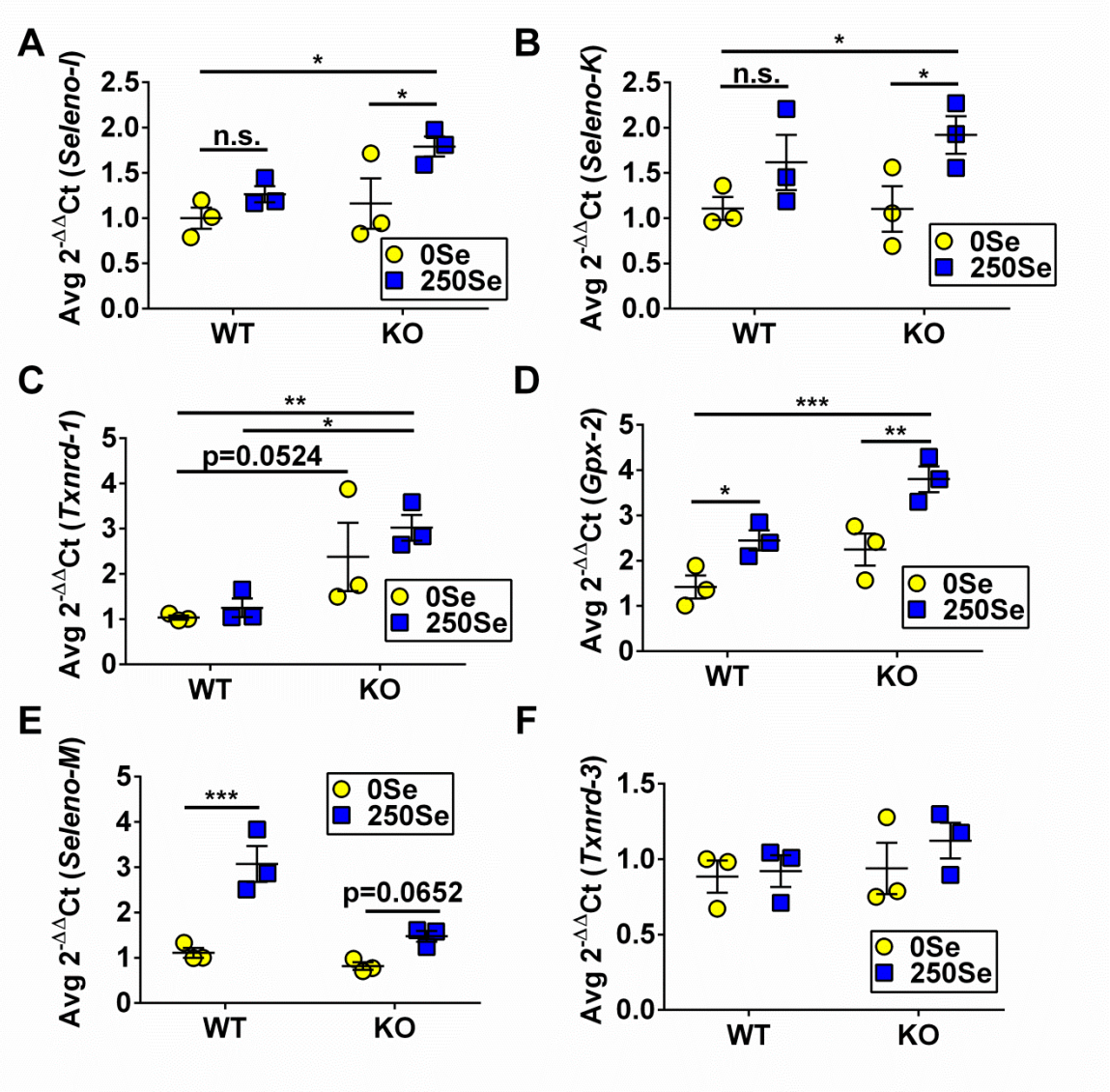

Figure 4.2: IL-4 upregulates a select few selenoproteins in *Sbp2$^{fl/fl}$LysM^{Cre}* BMDMs

*(**A**) Real-time PCR on Seleno-I expression in Sbp2LysM^{WT} and Sbp2LysM^{Cre} BMDMs treated with or without 250nM Se and IL-4. (**B**) Real-time PCR on Seleno-K expression in Sbp2LysM^{WT} and Sbp2LysM^{Cre} BMDMs treated with or without 250nM Se and IL-4. (**C**) Real-time PCR on Txnrd-1 expression in Sbp2LysM^{WT} and Sbp2LysM^{Cre} BMDMs treated with or without 250nM Se and IL-4. (**D**) Real-time PCR on Gpx-2 expression in Sbp2LysM^{WT} and Sbp2LysM^{Cre} BMDMs treated with or without 250nM Se and IL-4. (**E**) Real-time PCR on Seleno-M expression in Sbp2LysM^{WT} and Sbp2LysM^{Cre} BMDMs treated with or without 250nM Se and IL-4. (**F**) Real-time PCR on Txnrd-3 expression in Sbp2LysM^{WT} and Sbp2LysM^{Cre} BMDMs treated with or without 250nM Se and IL-4. Two-way ANOVA with Fisher's LSD test. *p<0.05, **p<0.01, ***p<0.001. N=3 individual mice per group. All experimental data are expressed as mean ± SEM.*

To compare the incorporation of Se into selenoproteins, BMDMs from *Sbp2LysM^{WT}*, *Sbp2LysM^{Cre}*, *TrspLysM^{Cre}*, and *TrspLysM^{WT}* were cultured with or without 250nM Se for five days and then stimulated with or without IL-4. Treatment with radiolabeled ^{75}Se revealed a decrease in overall selenoprotein expression in *Sbp2LysM^{Cre}* BMDMs compared to *Sbp2LysM^{WT}*, but only a partial ablation compared to *TrspLysM^{Cre}* BMDMs (**Fig 4.3A-B**). In order to confirm the ^{75}Se findings of a partial loss of selenoprotein expression, Gpx-1 and Txnrd-1 were detected by Western immunoblot as markers of selenoproteome expression. Due to both the poor resolving powers as well as the need to add Se, which leads to selenoprotein biosynthesis in deficient treatment groups, in ^{75}Se radiolabeling Western immunoblot and proteomic analysis were also employed to examine selenoproteome expression. Western immunoblot analysis revealed no significant difference in protein expression of Txnrd-1 between *Sbp2LysM^{WT}* BMDMs and *Sbp2LysM^{Cre}* BMDMs (**Fig 4.3C**). In contrast to Txnrd-1, Gpx-1 was not expressed in *Sbp2LysM^{Cre}* BMDMs treated with 250nM Se (**Fig 4.3D**). Gpx-1 expression in *Sbp2LysM^{WT}* BMDMs showed a strong Se dependence (**Fig 4.3D**). Additionally, proteomic analysis of wild-type BMDMs revealed seven selenoproteins were increased in

the presence of both 250nM Se and IL-4 stimulation, Txnrd-1, Gpx-1, Gpx-4, Seleno-F, Seleno-M, Seleno-O, and Seleno-T (**Fig 4.3E**). Therefore, deletion of *Sbp2* in macrophages led to only a partial ablation of selenoprotein expression. Deletion of *Sbp2* in macrophages creates a potential bottleneck in selenoprotein translation emphasizing a hierarchy in expression, particularly during Th2-biasing conditions.

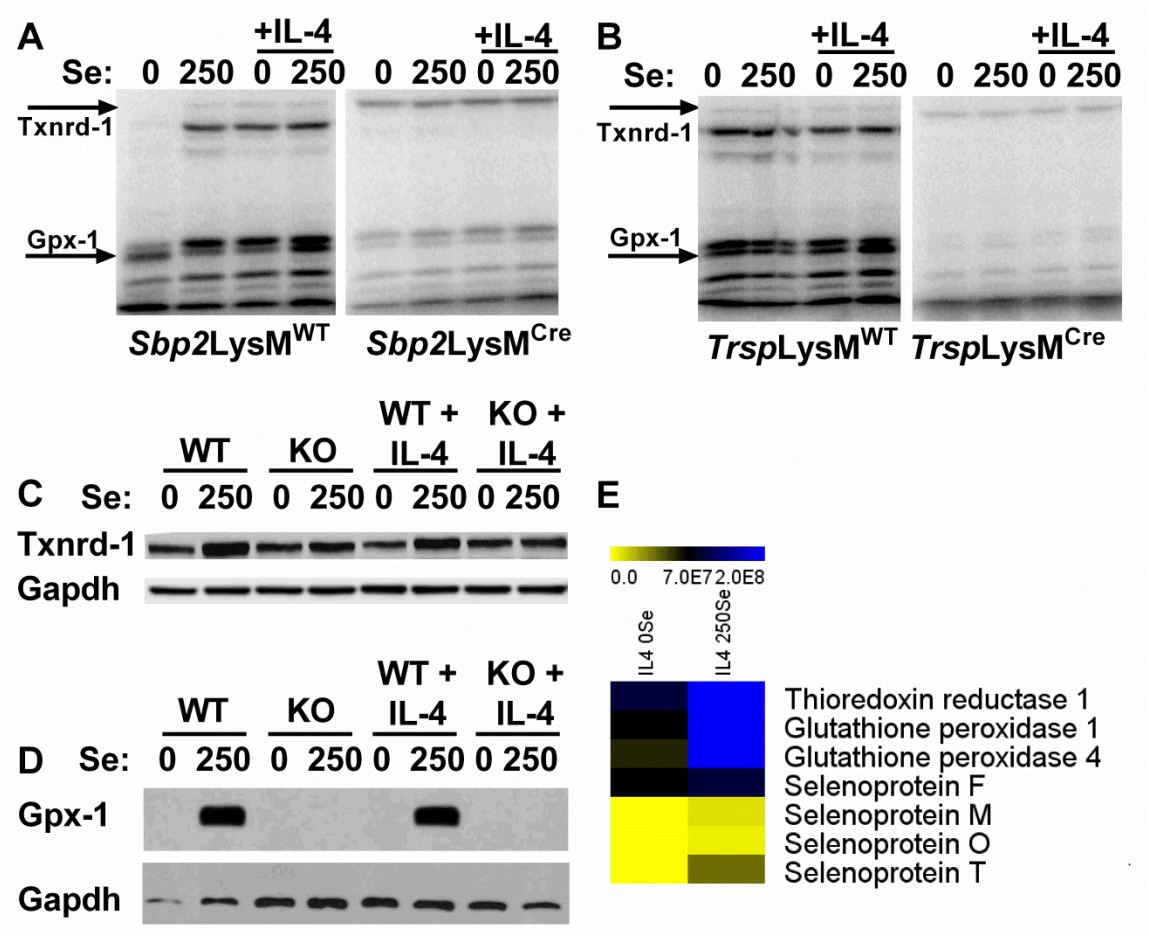

Figure 4.3: *Sbp2LysM*^{Cre} BMDMs have an incomplete selenoproteome

*(**A**) Representative phosphorimage of* ^{75}*Se radiolabeled selenoproteins in Sbp2LysM*^{WT} *and Sbp2LysM*^{Cre} *BMDMs treated with or without 250nM Se and IL-4. (**B**) Representative phosphorimage of* ^{75}*Se radiolabeled selenoproteins in TrspLysM*^{WT} *and TrspLysM*^{Cre} *BMDMs treated with or without 250nM Se and IL-4. (**C**) Representative western immunoblot of Txnrd-1 and Gapdh expression in Sbp2LysM*^{WT} *and Sbp2LysM*^{Cre} *BMDMs treated with or without 250nM Se and IL-4. (**D**) Representative western*

*immunoblot of Gpx-1 and Gapdh expression in Sbp2LysM^{WT} and Sbp2LysM^{Cre} BMDMs treated with or without 250nM and IL-4. (**E**) Proteomics heatmap of selenoproteins in C57BL/6 BMDMs treated with or without 250nM Se and IL-4. N=3 (**A-D**) individual mice per group, N=1 (**E**).*

Selenoproteins Influence Arachidonic Acid Metabolism

Previous research from our laboratory has shown that Se increases the expression of Hpgds to generate the Ppar-γ ligand Δ^{12}-PGJ_2, which increase the expression of M2 macrophage genes (13,19,20). Since *Sbp2LysM^{Cre}* BMDMs have a partial selenoproteome, we examined if arachidonic acid metabolism by the COX pathway was affected in the presence of a select few selenoproteins. BMDMs were analyzed by RT-PCT for *Ptgs-1* and *Ptgs-2* gene expression. *Ptgs-1* was significantly increased in both *Sbp2LysM^{WT}* BMDMs and *Sbp2LysM^{Cre}* BMDMs with IL-4 stimulation and 250nM Se (**Fig 4.4A**). *Ptgs-2* was significantly increased in *Sbp2LysM^{Cre}* BMDMs compared to *Sbp2LysM^{WT}* BMDMs in both unstimulated and IL-4 stimulated (**Fig 4.4B**). Cox-1, Cox-2, and Hpgds protein levels were quantified by western immunoblot. IL-4 stimulated BMDMs expressed higher levels of Cox-1 than unstimulated or LPS stimulated BMDMs (**Fig 4.4C**). Cox-2 was only expressed in LPS stimulated BMDMs (**Fig 4.4D**). Hpgds was present in both *Sbp2LysM^{WT}* BMDMs and *Sbp2LysM^{Cre}* BMDMs (**Fig 4.4C-D**). Δ^{12}-PGJ_2 was extracted from cell media and analyzed by LC-MS/MS. Both genotypes showed a Se dependent increase in Δ^{12}-PGJ_2 production with 250nM IL-4 stimulated with no significant differences between genotypes **(Fig 4.4E**). These data suggest that *Sbp2LysM^{Cre}* BMDMs, which express a select few selenoproteins are able to mediate the production of Δ^{12}-PGJ_2.

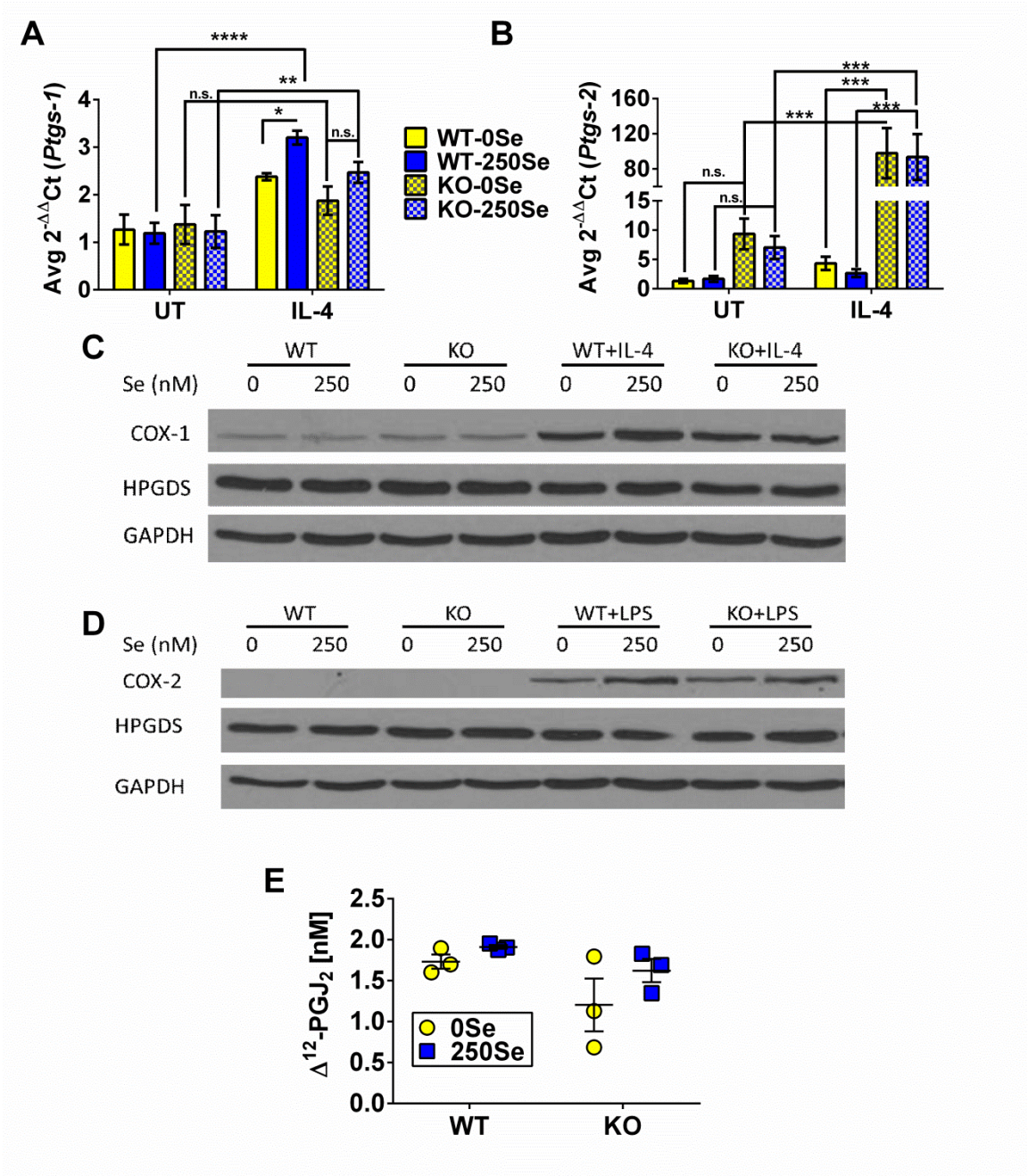

Figure 4.4: *Sbp2LysM*^{Cre} BMDMs have normal arachidonic acid metabolism

*(**A**) Real-time PCR of Ptgs-1 expression in Sbp2LysM*^{WT} *and Sbp2LysM*^{Cre} *BMDMs treated with or without 250nM Se and with or without IL-4. (**B**) Real-time PCR of Ptgs-2 expression in Sbp2LysM*^{WT} *and Sbp2LysM*^{Cre} *BMDMs treated with or without 250nM Se and with or without IL-4. (**C**) Representative western immunoblot of Cox-1, Hpgds, and Gapdh expression in Sbp2LysM*^{WT} *and Sbp2LysM*^{Cre} *BMDMs treated with or without 250nM and IL-4. (**D**) Representative western immunoblot of Cox-2, Hpgds, and Gapdh*

*expression in Sbp2LysM^{WT} and Sbp2LysM^{Cre} BMDMs treated with or without 250nM and LPS. (**E**) Δ^{12}-PGJ$_2$ in Sbp2LysM^{WT} and Sbp2LysM^{Cre} BMDM culture media supernatant treated with or without 250nM Se and IL-4. Two-way ANOVA with Fisher's LSD test. *p<0.05, **p<0.01, ***p<0.001, ****p<0.0001. N=3 individual mice per group. All experimental data are expressed as mean ± SEM.*

Limited Selenoproteome Expression Allows for Macrophage Polarization

Selenium works synergistically with IL-4 to increase the expression of M2 macrophage genes, such as *Arg-1*, *Fizz-1*, and *Ym-1* and decrease M1 macrophage genes, such as *IL-1β* and *Tnf-α* (19,20). Therefore, *Sbp2LysM^{Cre}* BMDMs were examined to determine the ability to polarize towards an M2 phenotype based on Se status and stimulus despite having an incomplete selenoproteome. *Sbp2LysM^{WT}* and *Sbp2LysM^{Cre}* BMDMs were treated with or without 250nM Se for five days and stimulated with or without IL-4 for 20 hours to induce M2 macrophage polarization. M2 genes (*Arg-1*, *Fizz-1*, and *Ym-1*) were significantly higher in IL-4 stimulated groups compared to unstimulated BMDMs regardless of genotype (**Fig 4.5A-C**). Therefore, macrophages are able to polarize toward an M2 phenotype when treated with IL-4 despite the loss of *Sbp2*.

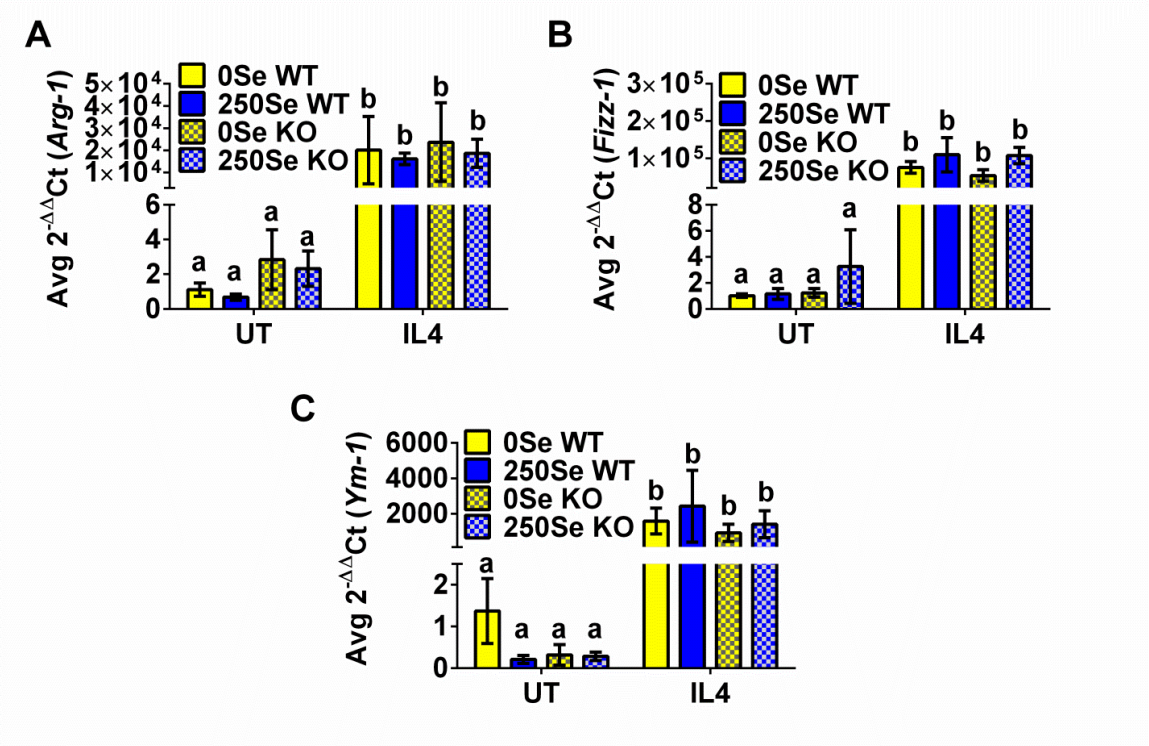

Figure 4.5: IL-4 upregulates M2 macrophage genes in both genotypes

*(**A**) Real-time PCR of Arg-1 expression in Sbp2LysM^{WT} and Sbp2LysM^{Cre} BMDMs treated with or without 250nM Se and with or without IL-4. (**B**) Real-time PCR of Fizz-1 expression in Sbp2LysM^{WT} and Sbp2LysM^{Cre} BMDMs treated with or without 250nM Se and with or without IL-4. (**C**) Real-time PCR of Ym-1 expression in Sbp2LysM^{WT} and Sbp2LysM^{Cre} BMDMs treated with or without 250nM Se and with or without IL-4. Two-way ANOVA with Fisher's LSD test. A different letter represents a significant difference between treatments. N=3 per group. All experimental data are expressed as mean ± SEM.*

Sbp2 Macrophage-specific Null Mice are Able to Mount a Sufficient Th2 Immune Response to Clear Nippostrongylus brasiliensis

In order to examine the effects of a limited selenoproteome *in vivo*, we utilized a soil-transmitted rodent helminth infection, *Nippostrongylus brasiliensis*. This infection is characterized by a strong Th2 cell response with high levels of IL-4 production (28,29). It has previously been shown that dietary Se is important for enhanced clearance of this

parasite (19). Additionally, inhibition of arachidonic acid metabolism in Se supplemented mice led to a significant decrease in M2 macrophages and increased parasite burden. The Se effect could be rescued with exogenous administration of 15d-PGJ_2 (19). To examine if expression of a select few selenoproteins in macrophages, as in the *Sbp2LysM*^{Cre} mice, would be sufficient for protection, *Sbp2LysM*^{WT} and *Sbp2LysM*^{Cre} were infected subcutaneously with 500 L3 larvae and euthanized day eight post-infection. Since the infection also passes through the lungs, lung tissue was harvested day eight post-infection for histology to measure of the resolution response. H&E staining revealed significantly decreased inflammation between dietary groups but no significant differences between genotypes (**Fig 4.6A-D**). There were no significant differences between *Sbp2LysM*^{WT} and *Sbp2LysM*^{Cre} upon enumerating adults worms in the small intestine of a mouse (**Fig 4.6E**) as well as by eggs/gram feces (**Fig 4.6F**). There were significant differences between dietary groups in both adult worms and eggs with Se supplemented mice having a lower parasite burden (**Fig 4.6E-F**). *Sbp2LysM*^{Cre} mice responded to Se-supplementation, despite having an altered selenoproteome in macrophages, to clear *N.brasiliensis* infection as efficiently as *Sbp2LysM*^{WT} mice.

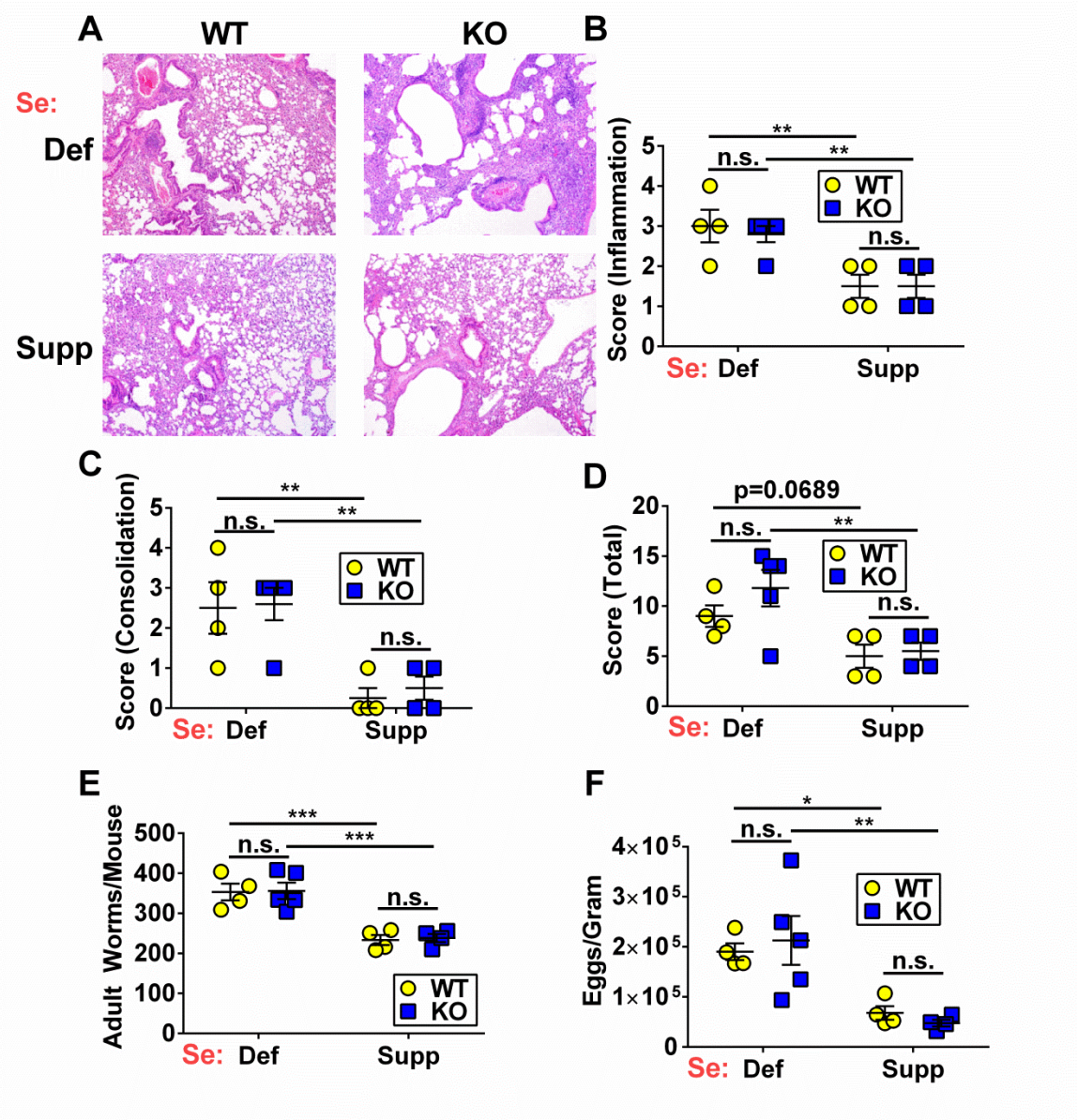

Figure 4.6: Dietary selenium supplementation reduces parasitic burden

*(**A**) Representative H&E sections of left lobe of lung from N.brasiliensis infected Sbp2LysM^{WT} and Sbp2LysM^{Cre} mice on either Se-Def or Se-Supp diet day eight post-infection. (**B**) Histopathological scoring of inflammation in the left lobe of the lungs of N.brasiliensis infected Sbp2LysM^{WT} and Sbp2LysM^{Cre} mice on either Se-Def or Se-Supp diet day eight post-infection. (**C**) Histopathological scoring of consolidation in the left lobe of the lungs of N.brasiliensis infected Sbp2LysM^{WT} and Sbp2LysM^{Cre} mice on either Se-Def or Se-Supp diet day eight post-infection. (**D**) Histopathological scoring of total in the left lobe of the lungs of N.brasiliensis infected Sbp2LysM^{WT} and Sbp2LysM^{Cre} mice on either Se-Def or Se-Supp diet day eight post-infection. (**E**) Number of adult worms per*

*mouse based on genotype and diet day eight post-infection. (**F**) Number of eggs per gram feces based on genotype and diet day eight post-infection. Two-way ANOVA with Fisher's LSD test. *p<0.05, **p<0.01, ***p<0.001. N=4-5 individual mice per group. All experimental data are expressed as mean ± SEM.*

Discussion

Selenoprotein biosynthesis requires specialized components in order to generate and incorporate Sec $tRNA^{[Ser]Sec}$ into polypeptide chains at UGA codons. Since all selenoprotein mRNAs compete for the same resources in order to be translated, changes in Se status, 3' untranslated region, and genetic variants drive preferential expression, hierarchy, of selenoproteins. At the gene level, expression of certain selenoproteins are resistant to changes in Se status, such as *Gpx-4* and *Txnrd-1*, while others are highly responsive to changes in Se status, such as *Gpx-1*, *Msrb-1*, and *Seleno-W* (30). Deletion of *Sbp2* in macrophages using Cre-Lox recombination exacerbated selenoprotein hierarchical expression demonstrating a transcriptional increase in *Seleno-I*, *Seleno-K*, *Txnrd-1*, and *Gpx-2* in $Sbp2LysM^{Cre}$ 250nM Se IL-4 treated BMDMs. The partial expression of selenoproteins in $Sbp2LysM^{Cre}$ BMDMs was confirmed by ^{75}Se radiolabeling and western immunoblot as seen with Gpx-1 and Txnrd-1 expression. Despite limited selenoprotein production, $Sbp2LysM^{Cre}$ BMDMs were able to produce Δ^{12}-PGJ_2 and polarize toward an M2 phenotype in the presence of 250nM Se and IL-4. To date, there is some indirect evidence supporting a role for *Seleno-K*, *Txnrd-1*, and *Gpx-2* in macrophage polarization, however little is known about the function of *Seleno-I.*

The main source of energy for M2 macrophages is oxidative phosphorylation fueled through fatty acid oxidation, while M1 macrophages use aerobic glycolysis (31). Inhibition of fatty acid oxidation prevents M2 polarization (32). CD36 is a fatty acid translocase and the principal receptor for oxLDL (33). Upon TNFα treatment, *Seleno-K*$^{-/-}$ BMDMs had a lower expression of CD36 compared to wild-type BMDMs, whereas SR-A levels remained the same between the two genotypes (11). CD36 expression was reduced in *Seleno-K*$^{-/-}$ BMDMs as a result of defective palmitoylation (11). This decrease in CD36 expression correlated with a decrease in LDL uptake compared to wild-type BMDMs (11). Since fatty acid oxidation is the major source of energy for M2 macrophages and *Seleno-K*$^{-/-}$ BMDMs have reduced LDL uptake through reduced CD36 expression, it is plausible *Seleno-K*$^{-/-}$ BMDMs have a reduced ability to polarize in response to IL-4, however this needs to be examined further.

In another study, exogenous treatment with thioredoxin-1 (Trx-1) has been shown to promote anti-inflammatory M2 macrophages and antagonize atherosclerosis (34). *In vitro* treatment with 1μg/mL Trx-1 and 15ng/mL IL-4 lead to increased expression of the M2 macrophage markers CD206 and IL-10 (34). Additionally, administration of Trx-1 during LPS stimulation led to a decrease in the M1 macrophage markers tumor necrosis factor-α and monocyte chemoattractant protein-1 (34). In a mouse model of atherosclerosis, where murine *ApoE* was replaced with human *APOE2*, these ApoE2 knockin (ApoE.Ki) mice developed hyperlipoproteinemia with elevated plasma cholesterol and triglyceride levels that spontaneously develop atherosclerotic plaques when on normal diet, which is further exacerbated by high fat diet. Treatment with Trx-1 and LPS challenge of ApoE2.Ki mice shifted macrophages within lesions from a M1 to a

M2 phenotype and significantly reduced the aortic lesion area compared to ApoE2.Ki mice not treated with Trx-1 (34). Finally, human atherosclerotic vessel specimens revealed Trx-1 to colocalize with M2, but not M1 macrophage markers (34). These studies lend credence to the idea that an increased expression of Txnrd-1, as seen in our model, could potentially lead to higher levels of its physiological substrate, Trx-1, to further promote M2 macrophage polarization.

Finally, it has been shown that changes in GSH/GSSG ratio affects CD36 expression in macrophages. Depletion of GSH pools and decreasing the GSH/GSSG ratio with L-buthionine-S,R-sulfoximine (BSO) increases the translational efficiency of the M2 marker and oxLDL receptor, CD36, in a concentration-dependent manner (35). In addition to treatment with BSO, siRNA inhibition of glutamate cysteine ligase (GCL), a rate-limiting enzyme in *de novo* glutathione synthesis, also led to a decrease in GSH, which correlated with an increase in CD36 protein expression levels (35). Oil Red O staining confirmed increased oxLDL uptake in macrophages treated with BSO that was decreased by blocking CD36 with anti-CD36 antibody (35). Since a decrease in GSH leads to an increase in CD36 expression and increased oxLDL uptake, which is the major source of energy for M2 macrophages, depletion of GSH may increase polarization in response to IL-4. Therefore, it stands to reason that an increase, as seen in our results, in Gpx-2 would also lead to a reduction of the cellular pool of GSH leading to an increase in CD36 to facilitate fatty acid oxidation and M2 macrophage polarization.

Seleno-I, also referred to as ethanolamine phosphotransferase-1, is a member of the CDP-alcohol phosphatidyltransferase class-I family (5). It catalyzes the transfer of phosphoethanolamine from CDP-ethanolamine to diacylglycerol to produce

phosphatidylethanolamine, which is involved in the formation and maintenance of vesicular membranes, regulation of lipid metabolism, and protein folding (36). Seleno-I's potential role in the regulation of lipid metabolism may include arachidonic acid metabolism in the generation of prostaglandins or potentially protein stability of M2 markers, however this remains to be investigated.

In addition to producing adequate levels of Δ^{12}-PGJ_2 and polarizing toward an M2 macrophage phenotype, *Sbp2LysM*^{Cre} mice are able to clear *N.brasiliensis* infection similarly to *Sbp2LysM*^{WT} mice when on Se-Supp diet when examining number of eggs per gram feces or number of adult worms per mouse. Histopathological examination of the lung, a major site of damage by *N.brasiliensis*, from day eight post infection mice, revealed decreased inflammation in Se-Supp mice compared to Se-Def mice regardless of genotype. Together this data suggests that either one or more of these select few selenoprotein(s) expressed in *Sbp2LysM*^{Cre} mice play an important role in macrophage polarization leading to effective resolution of infection.

References

1. Schmidt, R. L., and Simonovic, M. (2012) Synthesis and decoding of selenocysteine and human health. *Croat Med J* **53**, 535-550
2. Squires, J. E., and Berry, M. J. (2008) Eukaryotic selenoprotein synthesis: mechanistic insight incorporating new factors and new functions for old factors. *IUBMB Life* **60**, 232-235
3. Driscoll, D. M., and Copeland, P. R. (2003) Mechanism and regulation of selenoprotein synthesis. *Annu Rev Nutr* **23**, 17-40
4. Mix, H., Lobanov, A. V., and Gladyshev, V. N. (2007) SECIS elements in the coding regions of selenoprotein transcripts are functional in higher eukaryotes. *Nucleic Acids Res* **35**, 414-423
5. Labunskyy, V. M., Hatfield, D. L., and Gladyshev, V. N. (2014) Selenoproteins: molecular pathways and physiological roles. *Physiol Rev* **94**, 739-777

6. Arner, E. S., and Holmgren, A. (2000) Physiological functions of thioredoxin and thioredoxin reductase. *Eur J Biochem* **267**, 6102-6109
7. Lubos, E., Loscalzo, J., and Handy, D. E. (2011) Glutathione peroxidase-1 in health and disease: from molecular mechanisms to therapeutic opportunities. *Antioxid Redox Signal* **15**, 1957-1997
8. Huang, Z., Hoffmann, F. W., Norton, R. L., Hashimoto, A. C., and Hoffmann, P. R. (2011) Selenoprotein K is a novel target of m-calpain, and cleavage is regulated by Toll-like receptor-induced calpastatin in macrophages. *J Biol Chem* **286**, 34830-34838
9. Norton, R. L., Fredericks, G. J., Huang, Z., Fay, J. D., Hoffmann, F. W., and Hoffmann, P. R. (2017) Selenoprotein K regulation of palmitoylation and calpain cleavage of ASAP2 is required for efficient FcgammaR-mediated phagocytosis. *J Leukoc Biol* **101**, 439-448
10. Shchedrina, V. A., Everley, R. A., Zhang, Y., Gygi, S. P., Hatfield, D. L., and Gladyshev, V. N. (2011) Selenoprotein K binds multiprotein complexes and is involved in the regulation of endoplasmic reticulum homeostasis. *J Biol Chem* **286**, 42937-42948
11. Meiler, S., Baumer, Y., Huang, Z., Hoffmann, F. W., Fredericks, G. J., Rose, A. H., Norton, R. L., Hoffmann, P. R., and Boisvert, W. A. (2013) Selenoprotein K is required for palmitoylation of CD36 in macrophages: implications in foam cell formation and atherogenesis. *J Leukoc Biol* **93**, 771-780
12. Mattmiller, S. A., Carlson, B. A., and Sordillo, L. M. (2013) Regulation of inflammation by selenium and selenoproteins: impact on eicosanoid biosynthesis. *J Nutr Sci* **2**, e28
13. Gandhi, U. H., Kaushal, N., Ravindra, K. C., Hegde, S., Nelson, S. M., Narayan, V., Vunta, H., Paulson, R. F., and Prabhu, K. S. (2011) Selenoprotein-dependent up-regulation of hematopoietic prostaglandin D2 synthase in macrophages is mediated through the activation of peroxisome proliferator-activated receptor (PPAR) gamma. *J Biol Chem* **286**, 27471-27482
14. Shibata, T., Kondo, M., Osawa, T., Shibata, N., Kobayashi, M., and Uchida, K. (2002) 15-deoxy-delta 12,14-prostaglandin J2. A prostaglandin D2 metabolite generated during inflammatory processes. *J Biol Chem* **277**, 10459-10466
15. Straus, D. S., and Glass, C. K. (2001) Cyclopentenone prostaglandins: new insights on biological activities and cellular targets. *Med Res Rev* **21**, 185-210
16. Rossi, A., Kapahi, P., Natoli, G., Takahashi, T., Chen, Y., Karin, M., and Santoro, M. G. (2000) Anti-inflammatory cyclopentenone prostaglandins are direct inhibitors of IkappaB kinase. *Nature* **403**, 103-108
17. Italiani, P., and Boraschi, D. (2014) From Monocytes to M1/M2 Macrophages: Phenotypical vs. Functional Differentiation. *Front Immunol* **5**, 514
18. Martinez, F. O., and Gordon, S. (2014) The M1 and M2 paradigm of macrophage activation: time for reassessment. *F1000Prime Rep* **6**, 13
19. Nelson, S. M., Shay, A. E., James, J. L., Carlson, B. A., Urban, J. F., Jr., and Prabhu, K. S. (2016) Selenoprotein Expression in Macrophages Is Critical for Optimal Clearance of Parasitic Helminth Nippostrongylus brasiliensis. *J Biol Chem* **291**, 2787-2798

20. Nelson, S. M., Lei, X., and Prabhu, K. S. (2011) Selenium levels affect the IL-4-induced expression of alternative activation markers in murine macrophages. *J Nutr* **141**, 1754-1761
21. Fradejas-Villar, N., Seeher, S., Anderson, C. B., Doengi, M., Carlson, B. A., Hatfield, D. L., Schweizer, U., and Howard, M. T. (2017) The RNA-binding protein Secisbp2 differentially modulates UGA codon reassignment and RNA decay. *Nucleic Acids Res* **45**, 4094-4107
22. Seeher, S., Atassi, T., Mahdi, Y., Carlson, B. A., Braun, D., Wirth, E. K., Klein, M. O., Reix, N., Miniard, A. C., Schomburg, L., Hatfield, D. L., Driscoll, D. M., and Schweizer, U. (2014) Secisbp2 is essential for embryonic development and enhances selenoprotein expression. *Antioxid Redox Signal* **21**, 835-849
23. Seeher, S., and Schweizer, U. (2014) Targeted deletion of Secisbp2 reduces, but does not abrogate, selenoprotein expression and leads to striatal interneuron loss. *Free Radic Biol Med* **75 Suppl 1**, S9
24. Moustafa, M. E., Kumaraswamy, E., Zhong, N., Rao, M., Carlson, B. A., and Hatfield, D. L. (2003) Models for assessing the role of selenoproteins in health. *J Nutr* **133**, 2494S-2496S
25. Finch, E. R., Tukaramrao, D. B., Goodfield, L. L., Quickel, M. D., Paulson, R. F., and Prabhu, K. S. (2017) Activation of PPARgamma by endogenous prostaglandin J2 mediates the antileukemic effect of selenium in murine leukemia. *Blood* **129**, 1802-1810
26. Camberis, M., Le Gros, G., and Urban, J., Jr. (2003) Animal model of Nippostrongylus brasiliensis and Heligmosomoides polygyrus. *Curr Protoc Immunol* **Chapter 19**, Unit 19 12
27. Vunta, H., Davis, F., Palempalli, U. D., Bhat, D., Arner, R. J., Thompson, J. T., Peterson, D. G., Reddy, C. C., and Prabhu, K. S. (2007) The anti-inflammatory effects of selenium are mediated through 15-deoxy-Delta12,14-prostaglandin J2 in macrophages. *J Biol Chem* **282**, 17964-17973
28. Nair, M. G., and Herbert, D. R. (2016) Immune polarization by hookworms: taking cues from T helper type 2, type 2 innate lymphoid cells and alternatively activated macrophages. *Immunology* **148**, 115-124
29. Bouchery, T., Kyle, R., Camberis, M., Shepherd, A., Filbey, K., Smith, A., Harvie, M., Painter, G., Johnston, K., Ferguson, P., Jain, R., Roediger, B., Delahunt, B., Weninger, W., Forbes-Blom, E., and Le Gros, G. (2015) ILC2s and T cells cooperate to ensure maintenance of M2 macrophages for lung immunity against hookworms. *Nat Commun* **6**, 6970
30. Zhang, Q., Chen, L., Guo, K., Zheng, L., Liu, B., Yu, W., Guo, C., Liu, Z., Chen, Y., and Tang, Z. (2013) Effects of different selenium levels on gene expression of a subset of selenoproteins and antioxidative capacity in mice. *Biol Trace Elem Res* **154**, 255-261
31. Kelly, B., and O'Neill, L. A. (2015) Metabolic reprogramming in macrophages and dendritic cells in innate immunity. *Cell Res* **25**, 771-784
32. Huang, S. C., Everts, B., Ivanova, Y., O'Sullivan, D., Nascimento, M., Smith, A. M., Beatty, W., Love-Gregory, L., Lam, W. Y., O'Neill, C. M., Yan, C., Du, H., Abumrad, N. A., Urban, J. F., Jr., Artyomov, M. N., Pearce, E. L., and Pearce, E.

J. (2014) Cell-intrinsic lysosomal lipolysis is essential for alternative activation of macrophages. *Nat Immunol* **15**, 846-855

33. Pepino, M. Y., Kuda, O., Samovski, D., and Abumrad, N. A. (2014) Structure-function of CD36 and importance of fatty acid signal transduction in fat metabolism. *Annu Rev Nutr* **34**, 281-303
34. El Hadri, K., Mahmood, D. F., Couchie, D., Jguirim-Souissi, I., Genze, F., Diderot, V., Syrovets, T., Lunov, O., Simmet, T., and Rouis, M. (2012) Thioredoxin-1 promotes anti-inflammatory macrophages of the M2 phenotype and antagonizes atherosclerosis. *Arterioscler Thromb Vasc Biol* **32**, 1445-1452
35. Yang, X., Yao, H., Chen, Y., Sun, L., Li, Y., Ma, X., Duan, S., Li, X., Xiang, R., Han, J., and Duan, Y. (2015) Inhibition of Glutathione Production Induces Macrophage CD36 Expression and Enhances Cellular-oxidized Low Density Lipoprotein (oxLDL) Uptake. *J Biol Chem* **290**, 21788-21799
36. Horibata, Y., and Hirabayashi, Y. (2007) Identification and characterization of human ethanolaminephosphotransferase1. *J Lipid Res* **48**, 503-508

Chapter 5

Discussion

Three questions were addressed in this dissertation to examine the central hypothesis that ***selenoprotein(s) drive IL-4-dependent eicosanoid class switching to produce 15d-PGJ$_2$ which is important for M2 macrophage polarization and enhanced clearance during helminth infection.***

1. Does selenium enhance M2 macrophage polarization during a Th2 biased parasitic infection?
2. Does IL-4 regulate Cox-1 expression, and if so how?
3. Which selenoprotein(s) are important for M2 macrophage polarization?

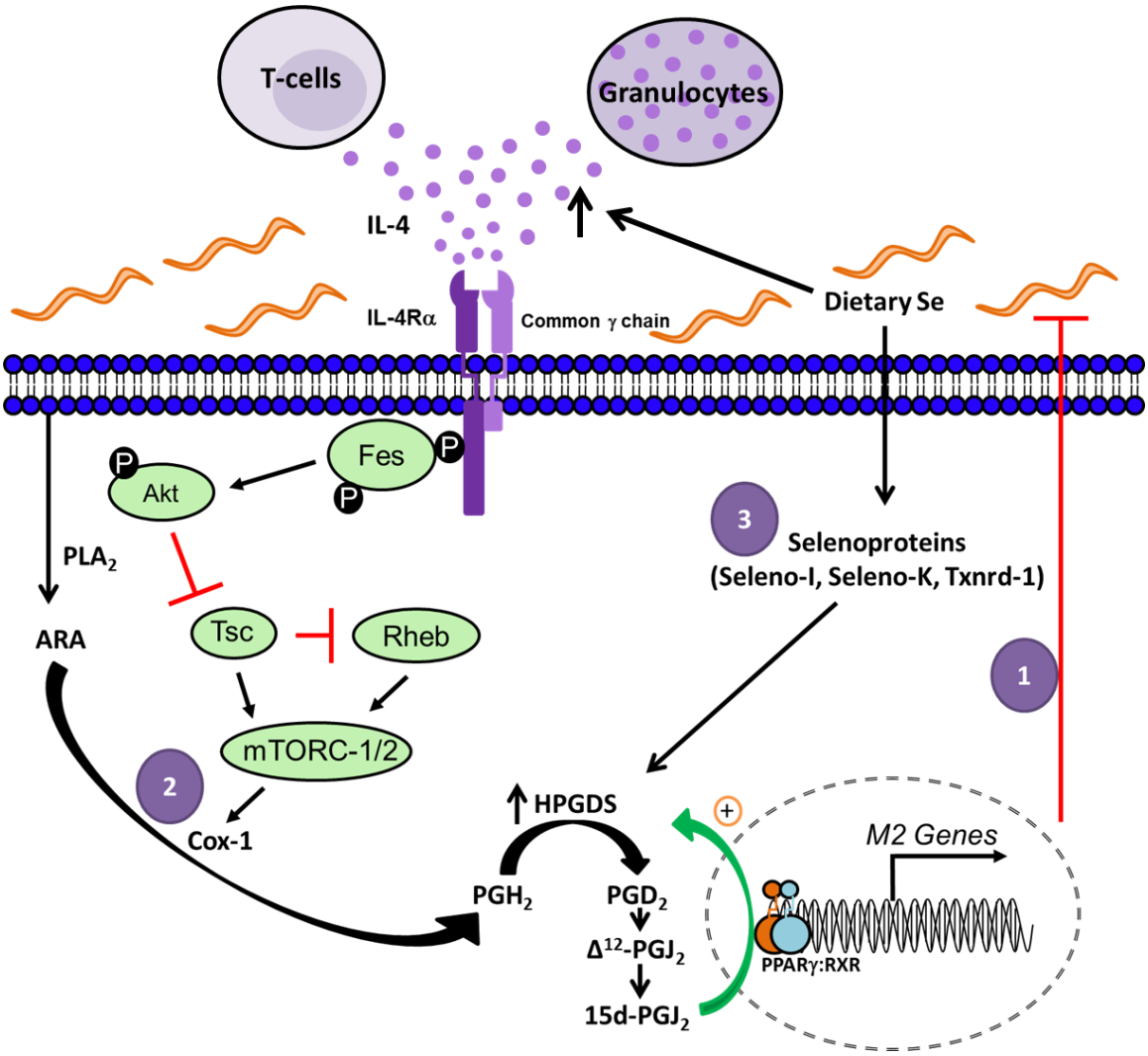

Figure 5.1: Schematic illustration of overall findings

Graphical summary of the overall findings from this dissertation. Purple circles with white number indicates which specific question is being addressed. Dietary selenium through a select subset of selenoproteins (Seleno-I, Seleno-K, and Txnrd-1) are enhancing both the production of IL-4 and IL-4-dependent M2 macrophage polarization during a Th2 biased parasitic infection. M2 macrophage polarization is enhanced through both the post-transcriptional upregulation of Cox-1 by IL-4 receptor signaling and through increased Hpgds expression by selenoproteins. Both mechanisms increase

Ppar-γ-dependent M2 macrophage gene expression through the increased production of 15d-PGJ$_2$.

Since it is known that a Th2 biased immune response is required to clear *Nippostrongylus brasiliensis* and previous data has indicated a synergistic relationship between IL-4 and Se during M2 macrophage polarization (1-5), the question was raised as to whether Se can increase M2 macrophages *in vivo* to enhance helminth clearance. Se-deficiency led to a significant increase in parasite burden compared Se-ade or Se-Supp as determined by number of eggs per gram feces and number of adult worms per mouse. Mice on Se-supp diet had increased expression of the M2 macrophage genes, *Arg-1*, *Fizz-1*, and *Ym-1* days seven and eight post-infection in the jejunum compared to mice on Se-def diet. Se-def mice had an increase expression in the M1 macrophage gene *Tnfα* compared to Se-supp mice day seven post-infection. These dietary findings where confirmed through the use of a genetically modified mice with a deletion in the gene required to generate Sec charged tRNA specifically in macrophages ($Trsp^{fl/fl}LysM^{Cre}$). Despite being fed a Se-supp diet, these knockout mice had significantly higher parasite burden, decreased M2 macrophage gene expression, and increased M1 macrophage gene expression compared to wild-type mice. In conclusion dietary Se enhances M2 macrophage polarization to efficiently clear a Th2 biased parasitic infection (Fig 5.1). These findings provide insight into an unexplored area of Se research examining selenoproteins' roles in macrophage polarization. This study also expands the knowledge of understanding macrophage polarization by providing novel and targetable mechanisms for promoting resolution and enhancing wound repair through M2 macrophages.

Previous studies have shown clearance of *N.brasiliensis* to be sensitive to the effects of IL-13 (1,4,6). Interestingly, there was a Se-dependent increase in the expression of *Il13* in the jejunum of infected mice. IL-13 has also been reported to increase the endogenous production of 15d-PGJ_2 in macrophages (7). Thus, it is possible that selenoprotein expression is critical in the IL-13-dependent induction of 15d-PGJ_2 by macrophages. An additional question that is equally important is the source of IL-13. Based on our data (Fig2.6E), it appears that neutrophils, in addition to ILC2 cells (2), could serve as a potential source of IL-13, which has been demonstrated recently (8), but the role of selenium in this process is intriguing and needs to be further examined.

In a recent study by Chen et.al, depletion of neutrophils led to a loss of M2 macrophage polarization and loss of accelerated clearance of a secondary *N.brasiliensis* infection (8). It was reported that neutrophils polarize toward an alternatively-activated "N2" phenotype (8). N2 neutrophils provide the helper functions necessary for the development of long-lived effector macrophages (8). These primed long-lived effector macrophages persistent in the lungs even after three months post-primary *N.brasiliensis* infection and contribute to the accelerated clearance following a secondary infection with *N.brasiliensis* (8). This presents and interesting questions as to whether the Se effects described in the studies above were macrophage-specific or first through the polarization of neutrophils and the subsequent activation of macrophages.

In order to examine the effects of selenium on neutrophils, mice will be kept on Se-Def, Se-Ade, and Se-Supp diets and infected with *N.brasiliensis*. Neutrophils will then be harvested from infected mice and characterized by flow cytometry to determine if Se has increased N2 neutrophils and decreased N1 neutrophils. Se-Supp mice will have

their neutrophils depleted through administration of Ly6G antibody and helminth clearance will be quantified to determine is Se is mediated its protective effects directly or indirectly through neutrophils. Additionally, S100 MRP neutrophil-specific Cre mice are available in our lab to breed with *Trsp*$^{fl/fl}$ mice to generate neutrophil-specific selenoprotein deficient mice. This study would explore a novel role for selenoproteins in the newly and poorly described field of neutrophil polarization and the role of neutrophils in macrophage activation. This will help separate our findings into a macrophage-specific or neutrophil-specific or mixture of the two phenomenon.

Our study suggests that the protective effect of Se is mediated through the production of 15d-PGJ_2 by arachidonic acid metabolism. Interestingly, Cox-2, the inducible isoform which is highly associated with inflammation, is downregulated by IL-4. In order to determine the mechanism by which 15d-PGJ_2 is being produced during an IL-4 biased infection, Cox-1 expression was examined. Post-transcriptional regulation of Cox-1 by IL-4 receptor signaling is a novel, paradigm shifting finding that challenges the existing dogma in the Cox field (Fig 5.1). By defining a regulatory mechanism for Cox-1 protein expression during inflammation this study has brought new light to the issue of the need to develop Cox isoform specific non-steroidal anti-inflammatory drugs and for the reevaluation of current on the market medications that inhibit mTORC signaling for potential unintended side effects due to the inhibition of Cox-1.

Inhibition of mTORC signaling through the activation of AMP-activated protein kinase by metformin led to a significant decrease in Cox-1 protein expression in the jejunum of *N.brasiliensis* mice compared to control (Fig 3.10A). Decrease is Cox-1 protein corresponded to a decrease in 15d-PGJ_2 and M2 macrophage markers (Fig 3.9B-

C). AMP-activated protein kinase is a master regulator of metabolism. Upon activation AMP-activated protein kinase increases pathways of catabolism including mitochondrial biogenesis, fatty-acid oxidation, glucose uptake, and glycolysis and decreases pathways of anabolism including fatty-acid synthesis, sterol synthesis, rRNA synthesis, and protein synthesis (9) (Fig 5.2). The overall effects on AMP-activated protein kinase activation on mammalian metabolism are the promotion of oxidative phosphorylation rather than glycolysis (9). However, it has been shown that AMP-activated protein kinase activation increases glycolysis through the phosphorylation of 6-phosphofructo-2-kinase isoform 3, which in turn increased the cellular concentration of the glycolytic activator fructose-2,6-bisphosphate (9). Since M1, pro-inflammatory, macrophages primarily use glycolysis to generate large amounts of ATP in a short amount of time in order to respond to the demands of an inflammatory challenge and M2, anti-inflammatory, macrophages rely on oxidative phosphorylation and fatty-acid oxidation for energy it is of relevance to examine the metabolic phenotypes in our studies to determine the effects of AMP-activated protein kinase activation on macrophage phenotype (9). In addition to the activation of AMP-activated protein kinase by a variety of anti-inflammatory drugs it is also regulated by exercise and glucose status (9). Therefore, AMP-activated protein kinase activation can affect the metabolism of immune cells and the response to inflammatory challenges in a variety of scenarios.

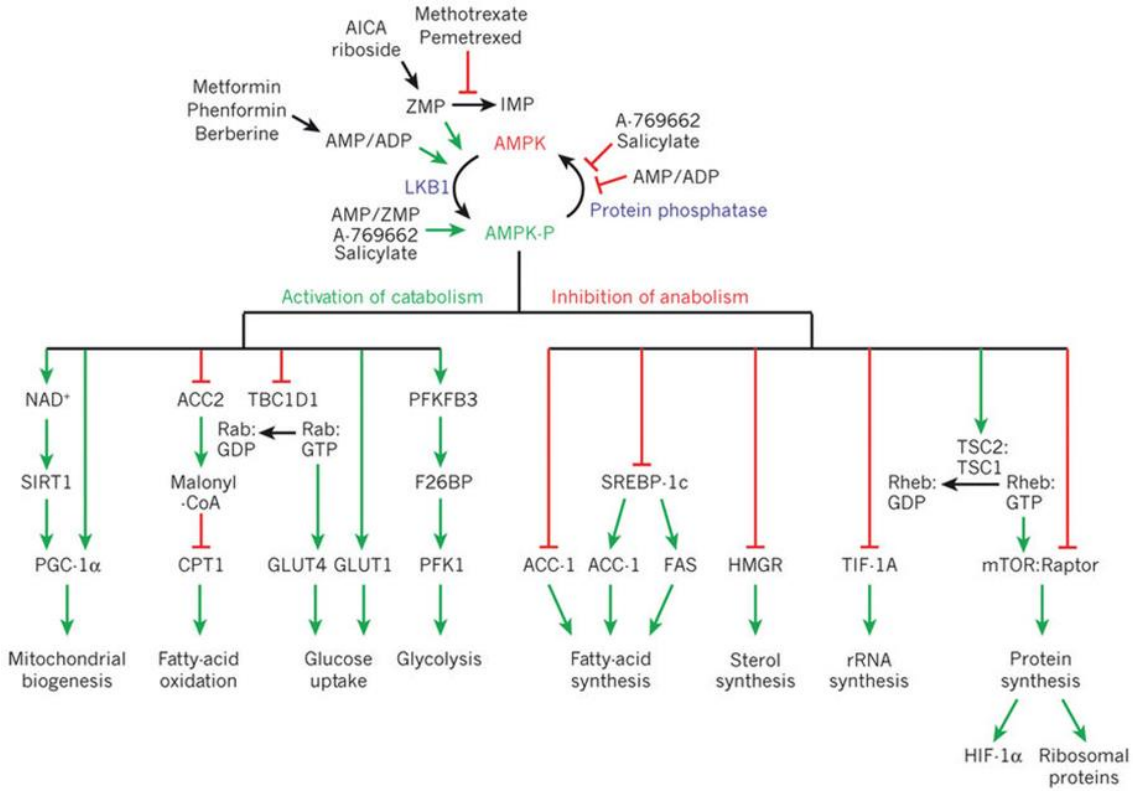

Figure 5.2: Regulation of AMP-activated protein kinase by various drugs and the principle metabolic pathways effected

AMPK is a master regulator of metabolism that has a variety of stimulus-dependent spatiotemporal downstream effects. AMPK can be activated by various drugs either through phosphorylation, inhibition of dephosphorylation, or by direct allosteric activation. AMPK activation has been shown to promote catabolic pathways including mitochondrial biogenesis, fatty-acid oxidation, glucose uptake, and glycolysis (shown on the left) while simultaneously downregulating anabolic pathways including fatty-acid synthesis, sterol synthesis, rRNA synthesis, and protein synthesis (shown on the right). (Adapted from O'Neill et. al, Nature 2013).

Finally, to determine which selenoprotein(s) is playing a role in altering arachidonic acid metabolism to increase the production of PGJ_2 metabolites, a murine macrophage-specific knockout model was employed to narrow down the list of selenoproteins. Loss of selenocysteine insertion sequence binding protein-2 (Sbp2) in macrophages, as confirmed by PCR, creates a bottleneck during selenoprotein biosynthesis that emphasizes a hierarchy of expression under various conditions, which was confirmed by ^{75}Se radiolabeling and western immunoblot. IL-4 stimulation with 250nM Se increases the transcriptional expression of *Seleno-I*, *Seleno-K*, *Txnrd-1*, and *Gpx-2* in $Sbp2^{fl/fl}LysM^{Cre}$ BMDMs (Fig 5.1). Proteomics analysis of wild-type BMDMs treated with or without 250nM Se and IL-4 revealed the upregulation of Txnrd-1, Gpx-1, Gpx-4, Seleno-F, Seleno-M, Seleno-O, and Seleno-T. This study provides novel insight into defining new immuno-regulatory functions for both previously characterized and uncharacterized selenoproteins.

In conclusion this dissertation defines a novel mechanism by which dietary Se is enhancing both the production of IL-4 and IL-4-dependent M2 macrophage polarization during a Th2 biased parasitic infection. M2 macrophage polarization is enhanced through both the post-transcriptional upregulation of Cox-1 by IL-4 receptor signaling and through increased Hpgds expression by selenoproteins. Both mechanisms increase Ppar-γ-dependent M2 macrophage gene expression through the increased production of 15d-PGJ_2. Increased M2 macrophage polarization through dietary Se administration enhances both the clearance of *N.brasiliensis* and the process of resolution.

References

1. Kreider, T., Anthony, R. M., Urban, J. F., Jr., and Gause, W. C. (2007) Alternatively activated macrophages in helminth infections. *Curr Opin Immunol* **19**, 448-453
2. Huang, Y., Guo, L., Qiu, J., Chen, X., Hu-Li, J., Siebenlist, U., Williamson, P. R., Urban, J. F., Jr., and Paul, W. E. (2015) IL-25-responsive, lineage negative KLRG1(hi) cells are multipotential "inflammatory" type 2 innate lymphoid cells. *Nat Immunol* **16**, 161-169
3. Zhao, A., Urban, J. F., Jr., Anthony, R. M., Sun, R., Stiltz, J., van Rooijen, N., Wynn, T. A., Gause, W. C., and Shea-Donohue, T. (2008) Th2 cytokine induced alterations in intestinal smooth muscle function depend on alternatively activated macrophages. *Gastroenterology* **135**, 217-225
4. Zhao, A., McDermott, J., Urban, J. F., Jr., Gause, W., Madden, K. B., Yeung, K. A., Morris, S. C., Finkelman, F. D., and Shea-Donohue, T. (2003) Dependence of IL-4, IL-13, and nematode-induced alterations in murine small intestinal smooth muscle contractility on Stat6 and enteric nerves. *J Immunol* **171**, 948-954
5. Nelson, S. M., Lei, X., and Prabhu, K. S. (2011) Selenium levels affect the IL-4-induced expression of alternative activation markers in murine macrophages. *J Nutr* **141**, 1754-1761
6. Urban, J. F., Jr., Noben-Trauth, N., Donaldson, D. D., Madden, K. B., Morris, S. C., Collins, M., and Finkelman, F. D. (1998) IL-13, IL-4Ralpha, and Stat6 are required for the expulsion of the gastrointestinal nematode parasite Nippostrongylus brasiliensis. *Immunity* **8**, 255-264
7. Berry, A., Balard, P., Coste, A., Olagnier, D., Lagane, C., Authier, H., Benoit-Vical, F., Lepert, J. C., Séguéla, J. P., Magnaval, J. F., Chambon, P., Metzger, D., Desvergne, B., Wahli, W., Auwerx, J., and Pipy, B. (2007) IL-13 induces expression of CD36 in human monocytes through PPAR activation. *Eur J Immunol* **37**, 1642-165
8. Chen, F., Wu, W., Millman, A., Craft, J. F., Chen, E., Patel, N., Boucher, J. L., Urban, J. F., Jr., Kim, C. C., and Gause, W. C. (2014) Neutrophils prime a long-lived effector macrophage phenotype that mediates accelerated helminth expulsion. *Nat Immunol* **15**, 938-946
9. O'Neill, L. A. J., and Hardie, D. G. (2013) Metabolism of inflammation limited by AMPK and pseudo-starvation. *Nature* **493**, 346-355

Ashley Elizabeth Shay

Education

INSTITUTION AND LOCATION	DEGREE	YEAR	FIELD OF STUDY
University of Delaware	B.Sc.	2008-2012	Biological Sciences; Concentration in Cellular, Molecular Biology, and Genetics. Minor in Biochemistry (Advisor: Dr. Vicky Funanage)
The Pennsylvania State University	Ph.D.	2012-2017	Molecular Medicine (Advisor: Dr. K. Sandeep Prabhu)

Positions:

2010-2012	Undergraduate student researcher at Nemours A.I. duPont Hospital for Children
2011-2012	Public Relations officer for University of Delaware's American Society for Biochemistry and Molecular Biology Undergraduate Affiliate Network (ASBMB-UAN) Chapter
2012-2017	Graduate research assistant at The Pennsylvania State University

Publications:

Manuscripts:

- **A.E. Shay***, A.K. Kudva*, and K.S. Prabhu. Selenium and Inflammatory Bowel Disease. *Am J Physiol Gastrointest Liver Physiol*. June 4, 2015. *Contributed equally
- **A.E. Shay***, S.M. Nelson*, J.L. James, N. Kaushal, A. Gunderson, B.A. Carlson, J.F. Urban Jr, and K.S. Prabhu. Selenoprotein Expression in Macrophages is Critical for Optimal Clearance of Parasitic Helminth *Nippostrongylus brasiliensis*. *J Biol Chem*. December 7, 2015. *Contributed equally
- **A.E.Shay**, B.T. Diwakar, B.J. Guan, V. Narayan, J.F. Urban and K.S. Prabhu. IL-4 upregulates cyclooxygenase-1 expression in macrophages. *J Biol Chem*. July 6, 2017.

Book Chapter:

- B.T. Diwakar*, E.R. Finch*, C. Liao*, **A.E. Shay***, and K.S. Prabhu. The Role of Selenoproteins in Resolution of Inflammation. Selenium Its Molecular Biology and Role in Human Health. *Springer*. September 16, 2016. *Contributed equally

Research Support:

2010	NIH Delaware INBRE Grant Recipient
2011	NIH Delaware INBRE Grant Recipient
2014	NIH 5T32AI074551-04 Animal Models of Inflammation Training Grant Recipient

Awards:

2010	Member of Tri-Beta Biological Honor Society
2011	Winner of an ASBMB-UAN Travel Award
2012	First place winner in category for poster presentation at University of Maryland, Baltimore County Undergraduate Research Symposium
2016	International Winter Eicosanoid Meeting Travel Award
2017	J. Lloyd and Dorothy Foehr Huck Endowment Travel Stipend
2017	Sahakian Family Endowment Travel Award
2017	Santosh Nigam Memorial Outstanding Young Scientist Award Nominee